FUNCTIONALLY NON-ADAPTIVE RETINAL PLASTICITY IN RAT MODELS OF HUMAN RETINAL DEGENERATIVE DISEASE

TREVOR MCGILL
Bachelor of Science, University of Lethbridge, 2002
Master of Science, University of Lethbridge, 2004

A Thesis
Submitted to the School of Graduate Studies
of the University of Lethbridge
in Partial Fulfillment of the
Requirements for the Degree

DOCTOR OF PHILOSOPHY

Neuroscience
University of Lethbridge
LETHBRIDGE, ALBERTA, CANADA

Abstract

The established model used for evaluating potential therapies for retinal disease has significant limitations. A new model is proposed to account for these limitations: the visual adaptation model. The visual adaptation model was developed to provide a novel approach for testing potential treatments for retinal disease, and the work in this thesis provides empirical support for this model. Specifically, we evaluated two potential therapies for retinal degenerative disease and examined their effects on vision and retinal anatomy. In addition, the profile of retinal reorganization and its functional correlates were examined in RCS rats and transgenic rats which express a rhodopsin mutation; however, immunohistological work targeted one specific line (S334ter-4). Collectively, these studies provide evidence that supports the retinal adaptation model. These studies also provide a novel view of retinal and visual function in retinal disease which should be considered when evaluating treatments involving retinal degeneration.

Acknowledgements

I need to thank the many people who were instrumental in the completion of this project. Firstly, I would like to thank my supervisor Dr. Glen Prusky. Throughout the last 6 years, Glen has taught me many things, most important of which is not specifically science related, but rather, that resiliency in all facets of life will undoubtedly help you to achieve your goals. With respect to academia, Glen has provided support, encouragement, and direction throughout my educational career. In particular, Glen's enthusiasm about science helped heighten my interest and enthusiasm as well, which has turned out to be very beneficial.

Another instrumental person in the development and completion of this project is Dr. Raymond Lund. Dr. Lund collaborated with Dr. Prusky and myself for the last 5 years and has been more than helpful and accommodating throughout that period. It is through this collaboration that the many of my publications have arisen. In addition, throughout the last few years, many people in Dr. Lund's lab have also been very helpful.

Similarly, Dr. Matthew Lavail has collaborated with Dr. Prusky and I for the last 3 years. During that time Dr. Lavail has been extremely generous to me including hosting visits to his lab, and providing me with all the necessary tools I needed to complete this large body of work. Specifically, Dr. Lavail has provided me with numerous animals, reagents, surgical supplies, and access to his lab including the very knowledgeable Dr. Micheal Mathes, and Mr. Doug Yasumura. In addition, a number of projects have arisen from the work done with Dr. Lavail, and has left the door open for many future opportunities for me.

Dr. Robert Douglas is a long time friend of Dr. Prusky's and has become a close acquaintance of mine throughout my career thus far. Dr. Douglas has been instrumental in the development of the behavioral tasks I used extensively throughout all of my projects. In addition, Dr. Douglas often helped with technical questions and provided a critical mind and eye when I was preparing manuscripts.

There is no question that one's parents are some of, if not, the most important people in anyone's lives; mine are no exception. My parents Robert (Bob) and Pamela (Pam) McGill have afforded me the opportunity to grow intellectually and individually as a person, while providing support for all of my endeavors. Because the list of reasons to thank my parents is extremely extensive, and far too long to describe here, I will suffice to say that I could not have done this without you.

My wife Charity, and my son Zachary are the reasons I am still a happy person, and likely the reason that I am still somewhat sane. Every day, I look forward to seeing them because they bring such joy to my life. They truly are my inspiration. I love you both.

Mrs. Christine Reinhart (Pohl) has been my closest academic friend for many years, and it is my intention to keep it that way. Throughout our careers at the University of Lethbridge, we have met many interesting and unique individuals, yet Christine and I have always found common ground and always enjoy one another's company. Being an officemate sometimes requires putting friendship before work which Christine is always willing and able to do. Ellie, as someone once nicknamed her, I want to thank you for the time we spent together, hopefully our friendship will endure.

Nazia Alam may very well be the most generous and giving person I have ever met. Nazia, not only helped me with virtually all of my experiments, she has been instrumental in the overall function of the Prusky lab from maintaining our breeding colonies, to surgical expertise, to a somewhat business administrative role. In addition to her extensive role in the lab, and her time consuming familial duties, Nazia always found time to recognize birthdays, organize parties, and the list goes on. Did I mention that she has done the majority of this while taking on a full undergraduate course load! Unbelievable! Nazia, you are truly a unique and special person and I am very fortunate to have someone like you in my life. Thank you for everything.

Last but not least, there are a host of people who either worked in the Prusky lab, or in the CCBN in general, who have in one form or another contributed to my work. Specifically, Valerie Lapointe, Byron Silver, Wayne Tschetter, have all helped me at one time or another and deserve my deepest gratitude. I wish you all the best in your future endeavors.

A group of people who often get overlooked are the people who work at the CCBN. Most notably: Naomi Cramer, Karen Dow-Cazal, and Charlotte Holmes. These people were also instrumental and I am truly thankful for all their help.

A final note – there are a number of people who I have not mentioned (family, friends, and co-workers alike) who also deserve recognition for their efforts in helping me, so to those unmentioned, I thank you.

Table of Contents

ABSTRACT iii
ACKNOWLEDGMENTS iv
TABLE OF CONTENTS vii
LIST OF ABBREVIATIONS xi
LIST OF FIGURES xiv
LIST OF TABLES xvii
CHAPTER I – Introduction
1. Introduction 1
1.1 The retina 1
1.2 RPE cells 3
1.3 Vision and visual function 4
1.4 RDD 6
1.5 Treatment of RDD 7
2. Animal models 9
2.1 Advantages of rodent models for vision research 11
2.2 Animal models used in these studies 13
2.2.1 Long Evans rat 13
2.2.2 RCS rat 14
2.2.3 Transgenic rhodopsin mutants 16
3. Photoreceptors equal vision model 17
3.1 Inconsistencies in Established Model 19
4. Visual Adaptation Model 20
4.1 Retinal Remodeling 21
4.2 Implications of Retinal Remodeling 22
5. Goal of Thesis 24
CHAPTER II – CNTF in Long-Evans rat
1. Introduction 28
2. Methods 30
2.1 Animals and Injections 30
2.2 Electroretinography 32
2.3 Virtual Optokinetic System (VOS) 33
2.4 Visual Water Task (VWT) 34
2.5 Luminance Thresholds Responses Recorded in the Superior Colliculus 35
2.6 Histology and Morphometric Analysis 35
2.7 Statistical Analysis 36
3. Results 36
3.1 Effects of Intravitreal CNTF Injections 36
3.1.1 Changes measured with ERG 36
3.1.2 OKR 37
3.1.3 Luminance Threshold Responses Measured in the superior colliculus 38
3.1.4 Morphological Changes 38
3.1.5 Dose Response Analysis of Transient Changes

Induced by Intravitreal Injection of CNTF....39
3.1.6 Dose Response Analysis of Protection of the Retina from Constant Light Damage by Intravitreal Injection of CNTF....40
3.2 Effects of Subretinal AAV-CTNF Injections....41
3.2.1 Functional Changes Measured with the ERG....41
3.2.2 OKR....41
3.2.3 Visual Acuity....41
3.2.4 Morphological Changes....42
4. Discussion....43
5. Summary....51
CHAPTER III – RCS rat in VOS
1. Introduction....53
2. Methods....55
2.1 Animals....55
2.2 Virtual Optokinetic System (VOS)....56
2.3 Visual Water Task (VWT)....57
2.4 Immunohistochemical preparation....58
2.4.1 Tissue preparation....58
2.4.2 Immunohistochemistry....59
3. Results....60
3.1 Spatial Frequency and Contrast Sensitivity Thresholds in Non-Dystrophic Rats....60
3.2 RCS rat Spatial Frequency Thresholds and Contrast Sensitivity....60
3.3 Task comparison....61
3.4 Immunohistochemical analysis....62
4. Discussion....62
5. Summary....67
CHAPTER IV – Schwann cell transplantation
1. Introduction....69
2. Methods....71
2.1 Animals....71
2.2 Donor cells....72
2.3 Transplantation....73
2.4 Behavioral Assessment of Vision....73
2.4.1 Virtual Optokinetic System....74
2.4.2 Visual Water Task....75
2.5 Anatomical analysis....76
2.6 Statistical analysis....77
3. Results....77
3.1 Effects of transplantation (VOS)....77
3.1.1 Spatial frequency thresholds....77
3.1.2 Contrast sensitivity....78
3.2 Effects of transplantation (VWT)....79
3.2.1 Training....79
3.2.2 Testing....79

3.3 Histological analysis 80
4. Discussion 81
5. Summary 86
CHAPTER V – Transgenic rats with a rhodopsin mutation
1. Introduction 87
2. Methods 90
2.1 Animals 90
2.2 Behavioral measurements of vision 90
2.3 Experimental design 91
3. Results 93
3.1 P23H-1 93
3.2 P23H-3 94
3.3 S334ter-3 94
3.4 S334ter-4 95
3.5 S334ter-9 95
3.6 Visual water task data 96
3.7 Comparison between measures 97
4. Discussion 97
5. Summary 100
CHAPTER VI – Immunohistochemical analysis of retinal remodeling
1. Introduction 101
2. Methods 103
2.1 Animals 103
2.2 Tissue preparation 103
2.3 Immunohistochemistry 104
3. Results 105
3.1 Photoreceptors 105
3.2 Inner retinal neurons 105
3.3 Muller glia and microglial cells 106
4. Discussion 106
5. Summary 109
CHAPTER VII – Discussion
1. General discussion 111
2. Established photoreceptor equals vision model 111
3. Visual adaptation model 112
3.1 Effects of CNTF 113
3.2 RCS rats 113
3.3 Transgenic rats with rhodopsin mutations 114
3.4 Retinal remodeling 115
3.5 Photoreceptors 116
3.6 Discontinuities in measurements of visual function 119
3.7 Potential mechanism of remodeling induced visual impairments 119
3.8 Neurotrophic factors 120
3.9 Cell transplantation 121
3.10 Growth factors versus Cells 123
3.11 Summary 125

4. Animal Model 126
5. Future directions and final thoughts 127
6. Summary 133
FIGURES 134
TABLES 187
REFERENCES 188
APPENDICIES
APPENDIX A – Published graduate work 204

List of Abbreviations

RDD = Retinal Degenerative Disease

RCS = Royal College of Surgeons

RPE = Retinal Pigment Epithelium

AMD = Age-related Macular Degeneration

RP = Retinitis Pigmentosa

VWT = Visual Water Task

CNS = Central Nervous System

c/d = cycles per degree

PETH = Pink Eye Tan Hooded

CCAC = Canadian Council on Animal Care

CCBN = Canadian Center for Behavioural Neuroscience

ERG = Electroretinogram

IACUC = Institutional Animal Care and Use Committee

NTF = Neurotrophic Factor

bFGF = basic Fibrillary Growth Factor

BDNF = Brain Derived Neurotrophic Factor

CNTF = Ciliary Neurotrophic Factor

GDNF = Glial Derived Neurotrophic Factor

rdy +, *p*+ = non dystrophic, pigmented

rdy -, *p*+ = dystrophic, pigmented

AAV = Adeno-Associated Virus

OS = Outer Segment

IS = Inner Segment

INL = Inner Nuclear Layer

ONL = Outer Nuclear Layer

IPL = Inner Plexiform Layer

OPL = Outer Plexiform Layer

OKR = Optokinetic Response

VOS = Virtual Optomotor System

P23H = Proline-23-Histidine (rhodopsin mutation)

S334ter = Serine-334-terminate (rhodopsin mutation)

ARVO = Association for Research in Vision and Ophthalmology

IOVS = Investigative Ophthalmology and Visual Science

SC = Superior Colliculus

SCN = Suprachiasmatic Nucleus

LGN = Lateral Geniculate Nucleus

MD = Monocular Deprivation

ARPE19 = human retinal pigment epithelial cell line

ECT = Encapsulated Cell Therapy

SFN = Society for Neuroscience

LE = Long-Evans

PR = Photoreceptor

RD = Retinal Degeneration

PI = Post-Injection

ANOVA = Analysis of Variance

NDRCS = Non Dystrophic RCS rats

SEM = Standard Error of the Mean

AOS = Accessory Optic System

NOT = Nucleus of the Optic Tract

DTN = Dorsal Terminal Nucleus

NIH = National Institutes of Health

PBS = Phosphate Buffered Saline

OCT = Optimal Cutting Temperature

DAPI = 4',6-diamidino-2-phenylindole

MHC = Major Histocompatibility Complex

GFAP = Glial Fibrillary Acidic Protein

Trk = Tyrosine Kinase

P347L = Proline 347 Leucine

List of Figures

Figure 1: The Visual Water Task....134

Figure 2: The Virtual Optomotor System – apparatus construction....135

Figure 3: The Virtual Optomotor System – apparatus function....136

Figure 4: Light micrographs of RCS rat retinal degeneration....137

Figure 5: ERG and OKR changes following injection of CNTF....138

Figure 6: Light micrographs of LE rat retina following injection of CNTF....140

Figure 7: ERG and OKR dose response analysis of CNTF injection....141

Figure 8: Dose response of CNTF protection from constant light damage....142

Figure 9: ERG changes following AAV-CNTF injection....143

Figure 10: OKR changes following AAV-CNTF injection....144

Figure 11: Visual acuity six months post AAV-CNTF injection....145

Figure 12: Light micrographs of AAV-CNTF injected LE retinas....146

Figure 13: Distribution of photoreceptor loss following AAV-CNTF injection....148

Figure 14: OKR spatial frequency thresholds of LE and ND-RCS rats....149

Figure 15: OKR contrast sensitivity thresholds of LE and ND-RCS rats....150

Figure 16: RCS rat OKR spatial frequency threshold degeneration....151

Figure 17: OKR contrast sensitivity curves of RCS rats....152

Figure 18: OKR contrast sensitivity of spatial frequency channels in RCS rats....153

Figure 19: VWT and VOS task comparison....154

Figure 20: VWT static and moving grating acuity comparison....155

Figure 21: Confocal images of RCS rat retinas – horizontal cell neurite sprouting....156

Figure 22: Confocal images of RCS rat retinas – Muller glia reactivity....157

Figure 23: Confocal images of RCS rat retinas – bipolar cell neurite sprouting.....158

Figure 24: Preservation of OKR with syngeneic Schwann cell transplants 159

Figure 25: Contrast sensitivity following syngeneic Schwann cell transplantation ...160

Figure 26: Spatial frequency channels of syngeneic transplanted animals 161

Figure 27: Spatial frequency channels of allogeneic transplanted animals.....162

Figure 28: Grating acuity of syngeneic and allogeneic transplanted animals 163

Figure 29: Light micrographs of syngeneic transplanted retina – 1 164

Figure 30: Light micrographs of syngeneic transplanted retina – 2 165

Figure 31: Confocal images of syngeneic transplanted retina near injection site 166

Figure 32: Light micrographs of syngeneic Schwann cells in RCS rat retina.....167

Figure 33: Visual system measurements of P23H-1 rats.....169

Figure 34: Contrast sensitivity function of P23H-1 rats.....170

Figure 35: Visual system measurements of P23H-3 rats.....171

Figure 36: Contrast sensitivity function of P23H-3 rats.....172

Figure 37: Visual system measurements of S334ter-3 rats.....173

Figure 38: Contrast sensitivity of spatial frequency channels in S334ter-3 rats 174

Figure 39: Visual system measurements of S334ter-4 rats.....175

Figure 40: Contrast sensitivity of spatial frequency channels in S334ter-4 rats 176

Figure 41: Visual system measurements of S334ter-9 rats.....177

Figure 42: OKR of P15 and P25 S334ter-9 rats 178

Figure 43: Spatial frequency channel contrast sensitivity in P15-S334ter-9 rats.....179

Figure 44: Spatial frequency channel contrast sensitivity in P25-S334ter-9 rats.....180

Figure 45: Static and moving grating acuity of P23H-1.....181

Figure 46: Confocal images of S334ter-4 rat retinas – horizontal & bipolar cells.....182

Figure 47: Confocal images of S334ter-4 rat retinas –cones.....183

Figure 48: Confocal images of S334ter-4 rat retinas –neurite sprouting.....184

Figure 49: Confocal images of S334ter-4 rat retinas – Muller glial scar formation...185

Figure 50: Confocal images of S334ter-4 rat retinas – micro glia activation.....186

List of Tables

Table 1: Antibodies..187

Chapter I - Introduction

1. Introduction

Age-related macular degeneration (AMD) and Retinitis Pigmentosa (RP) are the major constituents of a group of retinal degenerative diseases (RDDs) that affect millions of people worldwide. Currently, there are limited treatments for these diseases, and those that are available cater to a relatively small number of patients, often require repeated treatment applications, and have unsatisfactory rates of success. Although experimental treatments for RDD are on the horizon, there is reason to believe that these may also prove unsatisfactory because they are based on the established theoretical model of *photoreceptors equal vision*, which has significant limitations. To improve our understanding of retinal function, to improve the treatment of RDD, and to account for inconsistencies of the established model, a new model is proposed to direct future research: *the visual adaptation model*. The research presented in this thesis provides empirical support for the visual adaptation model and develops a framework to guide future studies into experimental therapies for RDD.

1.1 The Retina

The primary function of the retina is to capture light signals and convert them into neural signals to be transmitted to the visual cortex of the brain. The vertebrate retina, like other central nervous system tissue, contains several populations of neurons ensheathed by glial processes. The photoreceptor layer, which is primarily responsible for light capture, is the outermost layer of the retina and is apposed to the retinal pigment epithelium (RPE). There are two classes of photoreceptor neurons present in the

vertebrate retina: rod photoreceptor cells providing low-light vision and cone photoreceptor cells providing bright-light color vision. The photoreceptor outer-segments (OS) contain the photo- pigments for the absorption of light. Photoreceptor OS's lie interdigitated with RPE microvilli while the somata are positioned in a layer termed the outer nuclear layer (ONL).

The inner nuclear layer (INL) contains the somata of a number of second order neurons such as horizontal, bipolar, and amacrine cells. Horizontal cells are the laterally interconnecting neurons that help integrate and regulate the input from multiple photoreceptor cells. There are several types of bipolar cells that selectively synapse with cone photoreceptors. These include both on-and off- type bipolar cells. Bipolar cells that synapse with rod photoreceptors make contact with between 15 and 50 rods depending on the location within the retina, which allows convergence of synaptic signals from numerous rod photoreceptors to converge upon a single rod bipolar cell. Cone bipolar cells extend axons that synapse directly onto retinal ganglion cells, whereas rod bipolar cells extend a single axon with several terminal processes that synapse with amacrine cells but do not appear to synapse with retinal ganglion cells directly. Amacrine cells, like horizontal cells, work laterally affecting the output from bipolar cells, however, their tasks are often more specialized. Amacrine cells are the primary cells that provide input to retinal ganglion cells.

There are numerous forms of retinal ganglion cells including midget, parasol, and bistratified. Each class of retinal ganglion cell transmits trains of action potentials through their axons that exit the retina and form the optic nerve, transmitting neural

signals to the lateral geniculate nucleus (LGN) of the thalamus and then to areas of the visual cortex.

There are three main types of glial cells exist in the retina that include Muller cells, astrocytes, and microglial cells. Muller cells are a type of radial glial cell. Muller glial cells play an important role in the recovery of neurotransmitters such as glutamate after it is released from glutamatergic synapses. Astrocytes cells are closely associated with the blood vessels and are normally located at the vitreal surface of the retina except for the central foveal region in some retinas. Microglial cells are present in several layers of the retina, and during retinal degeneration they phagocytose debris from neuronal death.

1.2 RPE cells

The RPE is a monolayer of epithelial cells that lie adjacent to the photoreceptor outer segments and provide a structurally and metabolically supportive role to the photoreceptors. The RPE are tightly linked forming an important molecular barrier that is the basis of the blood retinal barrier. The RPE provides structural support for the photoreceptors by extending fingerlike projections that interdigitate with photoreceptor OS. These projections also assist with the normal phagocytosis of shed photoreceptor OS. As photons are absorbed by rhodopsin molecules embedded in discs within the photoreceptor OS, the chromophore 11-cis retinal is converted to 11-trans retinal resulting in the transduction of a neuronal signal emitted by the photoreceptor. Over time, these rhodopsin filled discs are shed by the photoreceptor and phagocytosed by the RPE. 11-trans retinal is then converted back to 11-cis retinal and transported back to the

photoreceptor. This forms the basis for the cyclic nature of the photoreceptor-RPE interaction.

Pigmentation of the RPE protects photoreceptors from the damaging effects of light (LaVail and Battelle, 1975). The lack of pigmentation has consequences for visual function. For example, if albino animals are exposed to large quantities of light, photoreceptor degeneration results. However, a thorough quantitative analysis of visual impairments using the light induced degeneration procedure has not yet been reported. The lack of pigmentation in the RPE of albino rats is also thought to allow stray photons to be reflected within the retina resulting in blurring of the visual image. This visual blur along with other abnormalities result in visual acuities of albino animals approximately half that of pigmented strains (Prusky et al., 2002).

1.3 Vision and Visual Function

Visual function has become a term in the literature that encompasses electroretinogram (ERG) wave recordings, superior colliculus (SC) recordings, visual cortex recordings, and the pupillary light reflex. In many reports, visual function is equated with functional vision, this is simply not true and as the experiments in this thesis show, often times visual function and functional vision do not directly compare to one another. Furthermore, because vision is defined as the perceptual experience of seeing, it necessarily requires that a behavioral evaluation is performed to assess it. Therefore, it is important to make a clear distinction between visual function and functional vision: Visual function is defined as the function of any component of the visual system and is typically measured using an electrophysiological technique such as ERG or luminance

thresholds from the SC, but may include a behavioral measure of vision. Conversely, functional vision is defined as vision measured through the system as a whole, which requires a behavioral assessment.

In the human retina, cone photoreceptors are associated with the ability to detect color at bright-light levels, otherwise known as photopic vision. Rod photoreceptors are optimal at low-light levels, which is referred to as scotopic vision. Scotopic vision provides the brain with information about light and dark, but lacks color information. Rod photoreceptors are rapidly saturated in bright-lighting conditions and do not respond in bright luminance ranges.

The studies in this thesis employ multiple methods of measuring the function of components of the visual system, as well as measuring the function of the system as a whole. For example, the ERG is an electrophysiological measure of the retina that is routinely performed using multiple lighting conditions. Low light (scotopic) ERG's are designed for the evaluation of rod photoreceptors, while high light (photopic) conditions are designed to examine cone photoreceptors. The output of an ERG provides an a- and b-wave. The a-wave is believed to be a measure of photoreceptor activity while the b-wave is thought to be an indicator of inner retinal and ganglion cells. Another measure of visual function employed in the studies done here is luminance threshold measurements from the SC. This is an electrophysiological technique that measures the minimum difference between the stimulus luminance and background illumination. Thresholds are typically measured at 16 points in the SC of each hemisphere. Because the SC is organized in a retinotopic fashion, this technique provides information as to the degree of function in relation to specific areas of the retina and of the visual field.

Vision will be measured using two behavioral tasks throughout the course of this thesis, both utilizing visual stimuli in the photopic range. The Visual Water Task (VWT) is a task in which animals are required to make a discrimination based upon visual perception. The visual thresholds obtained using the VWT are thought to be regulated by the visual cortex. Second, the Virtual Optomotor System (VOS) is a task that elicits an animal's reflexive optokinetic tracking response (OKR) to a moving visual stimulus, thought to be mediated by structures such as the SC and other accessory optic system nuclei. Finally, because human vision is cone dominated, and because many retinal and visual degenerative diseases result in the death of cones and cone mediated vision, the experiments in this thesis focus primarily on photopic measurements of vision.

1.4 RDD

Clinically, numerous forms of RDD exist that vary in age of onset, cellular and molecular abnormalities including those of genetic origin, and rate of progression. In some cases, the disease also carries with it vestibular or other sensory nervous system abnormalities. RDD generally goes unnoticed in the patient until significant visual problems are present, which is usually the reason the patient seeks medical attention. RDD's are characterized by visual dysfunction accompanied by progressive photoreceptor death. There are many animal models of human RDD each with a specific etiology, however, the general disease process in each model is essentially the same. The onset of disease usually begins with some form of insult such as a genetic mutation, extensive light damage, or age. From this, excessive stress to the photoreceptor occurs resulting in progressive irreversible cell death. As photoreceptor death progresses, ERG

wave amplitudes decrease, thresholds measured from the SC decline, and vision deteriorates.

1.5 Treatment of RDD

Unfortunately, there is currently no generally accepted clinical treatment for RDD. Currently, the most promising approaches are cell transplantation and neurotrophic factor delivery. Experimental approaches designed to replace lost retinal cells such as photoreceptors and thereby restore lost vision have proved largely unsuccessful, therefore much of the research effort has shifted into developing suitable and effective preventative treatments. Reports of early cell transplantation before significant photoreceptor death has occurred have utilized many different cells types including RPE cells (ARPE19) (Lund et al., 2001; McGill et al., 2004b; Wang et al., 2005b), human and rat Schwann cells (Hammarberg et al., 1996; Lawrence et al., 2000; Keegan et al., 2003; Lawrence et al., 2004; McGill et al., 2004b; Wang et al., 2005b; McGill et al., 2007a), human neural progenitor cells (Gamm et al., 2007), human embryonic stem cells (Lund et al., 2006; Gaillard and Sauve, 2007; Maclaren and Pearson, 2007), bone marrow mesenchymal stem cells (Arnhold et al., 2006; Inoue et al., 2007), oligodendrocyte progenitor cells (Laeng et al., 1996), and iris pigment epithelial cells (Schraermeyer et al., 1999; Schraermeyer et al., 2000). Most of these studies have focused on photoreceptor preservation and showed that cell transplantation can preserve photoreceptors (Lawrence et al., 2000; Lund et al., 2001; Coffey et al., 2002; Lawrence et al., 2004; Wang et al., 2005b). Select studies examined the beneficial effects of cell transplantation on electrophysiological responses (Lawrence et al., 2000; Lund et al., 2001; Coffey et al., 2002), and the duration of optokinetic tracking (Lawrence et al.,

2000; Lund et al., 2001; Coffey et al., 2002; Lawrence et al., 2004). Recently, McGill et al. (McGill et al., 2004b) reported that both the human retinal pigment epithelial cell line (ARPE19) and human Schwann cell transplants also delayed vision loss, the first report which focused on preventing the loss of vision as the primary goal.

Neurotrophic factors are a family of proteins that promote the survival of neurons and have been shown to play a role in signaling in the nervous system (Hasegawa et al., 2004), for differentiation of neural precursor cells (Hosomi et al., 2003), regulating axonal outgrowth (Yamashita et al., 1999), and supporting neuronal survival during development (Karlsson et al., 2001). The factors are produced by a number of sources including glial cells, fibroblasts, and epithelial cells. In the retina specifically, a number of growth factors including basic fibroblast growth factor (bFGF), glial derived neurotrophic factor (GDNF), and ciliary neurotrophic factor (CNTF) have been identified to be of protective benefit (Carwile et al., 1998). Injection of these growth factors into animal models of human retinal disease results in widespread preservation of photoreceptors when injected intravitreally, and a more local preservation when delivered sub-retinally (Faktorovich et al., 1990). Adenoviral transfection of retinal cells to express bFGF has also been shown to promote photoreceptor survival for up to 56 days in the same animals (Akimoto et al., 1999). GDNF is another neurotrophin that has been shown to be of benefit to photoreceptors in human (Carwile et al., 1998), mouse (Frasson et al., 1999; Keegan et al., 2003; Andrieu-Soler et al., 2005), and rat (McGee Sanftner et al., 2001; Lawrence et al., 2004) eyes. In addition, CNTF has been shown to slow photoreceptor degeneration in 12 different inherited retinal degenerations in mice (Cayouette and Gravel, 1997; LaVail et al., 1998; Liang et al., 2001a; Bok et al., 2002),

rats (Liang et al., 2001a; Wang et al., 2002), dogs (Pearce-Kelling et al., 1998; Tao et al., 2002), and cats (Chong et al., 1997; Chong et al., 1999), and protects photoreceptors from the damaging effects of light in rats (LaVail et al., 1992b) and mice (LaVail et al., 1998). However, few studies have examined closely the effects of neurotrophin delivery on vision in animals with a degenerating retina.

2. Animal models

The most important consideration in determining an appropriate animal model for the studies proposed here is that the model must be suitable for quantifiable visual capabilities that can be tested quickly, efficiently, and repeatedly. Previous studies of visual function have used electroretinograms or electrophysiological measurements in the CNS to determine how retinal cells respond to various visual stimuli. Using these methods, researchers have also been able to study retinal receptive fields, cortical receptive fields, and other visual functions such as contrast detection and square wave grating detection (Girman et al., 1999; Girman and Lund, 2007). Although much has been learned from these studies, few studies have provided quantitative measures of spatial vision. This is important as vision is a system-wide measure of function, loss of vision is what characterizes the disease, and rescue of vision is the true measure of success when employing a treatment to limit the loss of function in RDDs. A significant advantage to the use of rodents for these studies is that two behavioral tasks (Prusky et al., 2000a; Prusky et al., 2004a) have recently been developed which can be used to quantify visual thresholds quickly and repeatedly (Prusky et al., 2002; Douglas et al., 2005) even in rodents with a degenerating retina (McGill et al., 2004a; McGill et al., 2004b).

Second, it is important to use a model in which the gene mutation responsible for retinal degeneration has been identified. Identification of the mutation allows for further investigation into the cell biology and gene expression by knowing which cells are likely to be directly and indirectly affected by the mutation. Knowledge of the mutated gene will also allow for a more in-depth examination of the functional correlates of the mutated gene's phenotype. Clinically, once the mutated gene is identified in animal models, humans can then be screened for these mutations.

Third, similarity to forms of human retinal degenerative disease is an important criterion. The ultimate goal of vision research is to understand the structure and function of the human visual system and how to prevent or correct abnormalities. Retinitis Pigmentosa (RP) is the name given to a category of genetic eye diseases that cause gradual deterioration of the retina (Rivolta et al., 2002). The name itself refers to pigment changes in the retina that are usually caused by the movement of Retinal Pigment Epithelial (RPE) cells into the neural retina, a distinguishing feature used for diagnosis (Gartner and Henkind, 1982; Kalloniatis and Fletcher, 2004). In most cases of RP, a genetic defect causes the death of photoreceptor cells, followed by the detachment of RPE cells from Bruch's membrane and their migration into the inner retina where they accumulate around the thin-walled blood vessels (Milam et al., 1998). The majority of RP cases are primary photoreceptor defects such as rhodopsin mutations (eg. P23H, S334ter), although some forms exist in which the primary defect is located in the RPE cells (i.e. Mertk). Many animal models of human RDD exist such as transgenic rats with rhodopsin mutations (Steinberg et al., 1996), and the RCS rat (Gal et al., 2000). These are models of RP that express gene mutations with orthologues that have been identified

in the human population. Both models appear to follow a degenerative profile similar to that of human RP patients (Mullen and LaVail, 1976; Steinberg et al., 1996). The use of animals with clinically analogous retinal disease increases the applicability of the results from experiments evaluating potential therapies.

Finally, the animal model must also be available for testing treatment regimens for efficacy and safety which usually requires numerous trials. Rodents fulfill each of these requirements and therefore, for the purposes of this thesis, are the animal model of choice.

2.1 Advantages of Rodent models for vision research

A fortuitous advantage of rodents as a model for vision research is that they have had a great deal of anatomical and cell biological studies performed on them, and the visual capabilities of mice and rats can be and have been characterized behaviorally and is supported by ERG wave amplitudes, recordings from the superior colliculus, or single unit responses in the cortex. Rats specifically have been used for a number of studies in which their visual capabilities have been characterized in a fashion similar to that used in humans (Prusky et al., 2000b; Prusky et al., 2000a, c, d; Prusky et al., 2002; Prusky and Douglas, 2003; McGill et al., 2004a; McGill et al., 2004b; Prusky et al., 2004a; Prusky and Douglas, 2004; Prusky et al., 2004b; Douglas et al., 2005; Prusky et al., 2006; McGill et al., 2007a; Prusky et al., 2008). Despite previous misconceptions, rats have a mammalian visual system with visual functions similar to humans, and easily characterized using the Visual Water Task (Figure 1(Prusky et al., 2000a)) or the Virtual Optomotor System (Figures 2,3(Prusky et al., 2004a)). Rats have small eyes compared to those of humans, but technological advances have allowed researchers to modify a sub-

retinal transplantation procedure developed in rabbits (Lopez et al., 1987) for use in rats (Li and Turner, 1988). Although the rat retina appears to lack a fovea or area centralis, it is very similar to the human peripheral retina containing both rods and cones, which can provide quite detailed vision at close distances. In addition, the visual behavior of rats shows their tendency to foveate on objects, especially when required to discriminate between visual stimuli (TJM, unpublished observations). Finally, rats are also capable of using their relatively small number of cone photoreceptors for making color discriminations, suggesting that dichromatic vision does not imply a purely black and white visual field (Jacobs et al., 2001).

The rat visual system evolved to specialize in low light and low resolution vision, however, many of the psychophysical measurements that can be obtained in humans, such as acuity and contrast sensitivity, can also be quantified in rats. Normal laboratory rats have a visual acuity of approximately 1.0-1.2 cycles per degree (c/d) (Dean, 1981; Prusky et al., 2000a; McGill et al., 2004a), and although this is significantly lower than the acuity of humans, it is a quantifiable measurement of vision. Rats have the characteristic inverted "U" shaped contrast sensitivity function (Keller et al., 2000; McGill et al., 2004a; Douglas et al., 2005; McGill et al., 2007a) as found in humans, but with a lower peak sensitivity (Keller et al., 2000). It has also been shown that rats can discriminate between gratings that differ in orientation by as little as 3 degrees (Bowden et al., 2002, SFN abstract, online), and that motion coherence, thought to be an extra-striate property, can be measured in rats (Neve et al., 2002, SFN abstract, online;(Douglas et al., 2006). Although the rat's visual capabilities are not specialized for a high degree

of central vision, they have a visual system that is fundamentally similar to that of humans with similar measurable visual functions that can be assessed behaviorally.

Currently, rat models of RDD have the advantage of providing genetically manipulated animals targeting specific genes of choice, or animals in which the natural occurring mutation is known and has been stabilized. For these reasons, there are many more rodent models of RDD than all other species combined (Chader, 2002). In addition, some evidence suggests rats (non-dystrophic and dystrophic) have the capacity for retinal remodeling (Sullivan et al., 2003; Fisher et al., 2005; Gehlbach et al., 2006; Marc et al., 2007), promoting their utility as an appropriate animal model for the studies proposed here.

2.2 Animal Models used in these studies

2.2.1 Long-Evans rat

The Long-Evans rat was originally developed by Drs. Long and Evans in 1915 by crossing several Wistar Institute white female rats with a wild grey male rat. In 1978, Charles River laboratories received their first shipment of "Long-Evans" (LE) rats and established a breeding colony. Since then, LE rats have been used as a standard laboratory rat for a number of studies of visual system function. For example, using LE rats we have examined visual acuity using the visual water task (Prusky et al., 2000a; Prusky et al., 2002; McGill et al., 2004a), OKR thresholds (Prusky et al., 2004a; Douglas et al., 2005; McGill et al., 2007a; McGill et al., 2007b), plasticity in the visual system (Prusky et al., 2006), and visual motion (Douglas et al., 2006). In addition, LE rats have been used as visually-sighted controls in cell transplantation studies designed to prevent vision loss in rodent models of human retinal disease (McGill et al., 2004b; McGill et al.,

2007a). Finally, LE rats have also been used for examining the harmful effects of large doses of neurotrophic factors in a normal eye (McGill et al., 2007b).

2.2.2 RCS rat

The most popular rat model of RDD is the RCS rat. The RCS rat has a recessive mutation in the *Mertk* gene expressed in the RPE cells (D'Cruz et al., 2000). This mutation renders the RPE cells unable to perform their supportive role of phagocytosing photoreceptor outer-segments at a normal rate (Mullen and LaVail, 1976; Edwards and Szamier, 1977) which ultimately results in progressive photoreceptor death (Figure 4). The mutation in the Mertk gene also has an orthalogue mutation (*MERTK)* found in a small population of human patients with RP (Gal et al., 2000). Both rats and humans which express the mutation in the MERTK gene appear to following the same degenerative profile. Furthermore, because vision and photoreceptor loss in AMD may be attributable in many cases to RPE cell dysfunction, the RCS rat serves as an indirect model when contemplating non-genetic interventions such as cell transplantation to alleviate the condition.

The development of the Royal College of Surgeons rat model began in 1938, when Bourne and colleagues recognized a dystrophy in a pink-eyed tan hooded (PETH) rat (Bourne et al., 1938b, a; Bourne and Grüneberg, 1939). Dowling and Sidman (1962)(Dowling and Sidman, 1962) cross-bred the PETH strain to develop both pigmented and pink-eyed rats, both dubbed the Royal College of Surgeons (RCS) rat; the breeding pairs of which were originally housed at the Royal College of Surgeons in London. The strain has since been out-bred to produce a pigmented non-dystrophic line as well (LaVail et al., 1975; LaVail, 1981).

In 1975, Lavail et al.,(LaVail et al., 1975) discovered that pigmentation of the retina slows the degeneration of retinal cells and 1 year later, in 1976, Mullen and Lavail (Mullen and LaVail, 1976) reported that the primary defect is in the RPE cell layer as proven by using experimental rat chimeras (Mullen and LaVail, 1976), and subsequently confirmed in dish (Edwards and Szamier, 1977; Effron et al., 1981). The progressive degeneration of the retina is associated with a buildup of debris (Lolley and Farber, 1976) produced by shed rod outer segment discs (LaVail et al., 1981). In addition, Perlman (1978)(Perlman, 1978a, b) showed abnormalities in the regeneration of rhodopsin suggesting that light exposure could accelerate retinal abnormalities in these rats, confirming Farber and Lolley's (1977)(Farber and Lolley, 1977) previous findings. Subsequent anatomical studies in the RCS rat have shown that there is significant disruption of the outer segments (Lue, 1994; Sauve et al., 2001) by three weeks of age, and by one month of age this process is even more evident as well as thinning of the outer nuclear layer (ONL). By three months of age, the ONL has been reduced to a single layer of cell bodies with the debris zone occupying the former outer-segment area (Sauve et al., 2002). By six months the inner nuclear layer is in direct contact with the RPE cell layer with very few photoreceptors surviving (Sauve et al., 2002). Secondary changes in the inner retina, including the loss of retinal ganglion cells from whole quadrant segments of retina, as well as laminar disruption and changes in the inner plexiform layer have also been shown in animals more than 6 months old (Villegas-Perez et al., 1998; Jones et al., 2003; Marc et al., 2003; Jones and Marc, 2005; Marc et al., 2007).

Functional measurements of the retina measured by electroretinogram (ERG) showed progressive decline in b-wave amplitude and prolongation of the time to the peak

of the b-wave with age (Perlman, 1978a). In addition, the pupillary light reflex used as an indicator of retinal function showed a progressive decrease in sensitivity to light with age (Trejo and Cicerone, 1982). In 1986, Wecker et al. (Wecker and Ison, 1986) paired auditory and visual startle cues and presented these stimuli to RCS rats producing a reliable startle response. With age, the RCS rats showed an increase in response time to the visual stimuli which suggested a progressive deterioration of visual function. Since these studies, limited work has looked carefully at the decline in vision over time, but rather, compared experimental groups such as non-dystophics or those with cell transplants (Trejo and Cicerone, 1987; Lawrence et al., 2000) or used luminance discrimination for visual thresholds (DiLoreto et al., 1998). In 2004, however, McGill et al. (McGill et al., 2004a) characterized the visual perception of the RCS rat throughout the course of visual degeneration. This study (McGill et al., 2004a) showed that RCS rats had near normal visual acuity at 1 month of age which progressively declined until visual thresholds were no longer measureable at 11 months.

2.2.3 Transgenic rhodopsin mutants

Recently developed transgenic rats (Steinberg et al., 1996) which express rhodopsin mutations (P23H or S334ter) are gaining popularity due to their similarity to human RP, in which, P23H mutations represent the largest cohort. Animals that express P23H mutations have a proline to histidine amino acid substitution that causes an inappropriate tertiary structure of the rhodopsin protein. Rats with the S334ter mutation have a truncated rhodopsin protein which causes similar abnormalities as found in P23H rats. Limited studies have used these animals, however, they have been used for gene therapy treatment regimens (Green et al., 2001; Bok et al., 2002; Gorbatyuk et al., 2007),

light damage models (Green et al., 2001), and as models for cell transplant therapy evaluation (Seiler and Aramant, 1998; Sagdullaev et al., 2003). Although relatively little is known about these animals, it is apparent that retinal remodeling does occur in late stages of degeneration (Jones et al., 2005).

In summary, rat models contain each of the qualities, including retinal plasticity, which lend themselves to be used as suitable subjects for vision research. In addition, because much of what we know about how the visual system works came from loss-of-function studies, rat models of retinal dysfunction serve as a suitable model for the studies described in this thesis. Furthermore, many of the rat models of RDD have had the genetic mutation identified or have been developed (ie transgenics) to express known mutations, and these mutations have also been found in the human condition. Moreover, rodent models of RDD appear to be the most appropriate model for characterizing the effects of genetic mutations on vision because of the recent development of behavioral tasks (Prusky et al., 2004a; Douglas et al., 2005) that can be used to quantify visual thresholds. Finally, experimental treatments designed to prevent the progression of RDD, and the effects of these treatments on the visual system, can be systematically evaluated in these models.

3. Photoreceptors equal vision model.

The established photoreceptors equal vision model is a theoretical model based upon a linear relationship of the number of functional photoreceptors and the degree of functional vision. Prior to the development of the VWT and VOS, the ERG was used as the primary indicator of treatment success. Given that the a-wave of the ERG is derived from the activity of the photoreceptors, then rescuing photoreceptors in retinal disease

models would also rescue the ERG a-wave, and possibly b-wave as well, and usually in a linear fashion. This relationship formed the basis of the photoreceptors equal vision model. This theoretical model was born out of the results of many early studies on retinal disease mostly performed using the Royal College of Surgeons (RCS) rat. In the RCS rat, disruption of the normal phagocytotic function of the RPE is achieved through a gene mutation (*mertk*) in the tyrosine kinase receptor (Gal et al., 2000). This mutation drastically reduces the rate of OS phagocytosis by the RPE such that shed OS's from the photoreceptors accumulate in the subretinal space resulting in a "debris zone." This debris zone further toxifies photoreceptors and eventually causes their death. Early in life, the RCS rat appears to have a relatively normal ONL and near normal visual function and near normal vision. Even though the mutation is in the RPE cells in these animals, the established model appears to hold true because as the ONL degenerates so do ERG wave amplitudes (Pinilla et al., 2005a).

The established model also appears to hold true in other cases of retinal disease. For example, mutations in genes that affect proteins found specifically in photoreceptors often result in the progressive loss of photoreceptors and a corresponding loss of visual function. Specifically, mice that have been engineered to develop a coneless (Ying et al., 2000) retina have deficits in photopic ERG b-wave amplitudes (Williams et al., 2005), a likely indicator of cone function. Mice that express a gene mutation in rhodopsin (rd mice) undergo progressive rod photoreceptor degeneration resulting in progressively declining scotopic ERG a- and b-wave amplitudes (Chang et al., 2007). In clinical cases of RP, where the gene mutation is expressed primarily in the rod photoreceptors, the premature death of rods eventually leads to the decay of cone photoreceptors resulting in

night vision problems followed by a loss of central high acuity color vision. Furthermore, transgenic rats that express rhodopsin mutations also undergo progressive photoreceptor degeneration and exhibit visual deficits measured behaviorally and electrophysiologically (Thomas et al., 2004; Seiler et al., 2005; Seiler et al., 2007).

3.1 Inconsistencies in established model

Although the established photoreceptor equals function model appears consistent in many cases, there are a number of circumstances that are inconsistent with this model. For example, studies (Mullen and LaVail, 1976; Sauve et al., 2002) using the RCS rat have reported that ONL thickness and ERG waves were no longer quantifiable by 6-7 months of age, however, behavioral measures suggest that vision remains intact until ~10 months of age (McGill et al., 2004a). Sagdullaev et al. (2003) (Sagdullaev et al., 2003) reported a similar finding using the S334ter line-3 rat, a transgenic rhodopsin mutant model of human RP. In these animals, by post-natal day (P)60-100, photoreceptor cell death is near complete and multi-unit recordings from the superior colliculus are non-responsive, however, a complementary study by Thomas et al. (2004) (Thomas et al., 2004) reported OKR using the same strain of rats at both P135 and P205, long after photoreceptors have degenerated. Furthermore, in animals with non-degenerating retinas, the differences observed between visual acuity in multiple rat strains cannot simply be accounted for by photoreceptors alone (Prusky et al., 2002).

The likely reason for the inconsistencies with the established model is that the visual system is a *visual system*. That is, retinal function relies on the circuits that enable the establishment of receptive fields, which are necessary for the spatial construction of

the visual world. Visual processing in the brain downstream of the retina also requires spatially constructed information for interpretation. If the retinal circuits are changed, vision won't be normal, even with intact photoreceptors. Recent evidence from studies using the RCS rat, which is the most popular rodent model of RDD, have shown that along with progressive photoreceptor death inner retinal changes also occur. Examples of such changes are neurite outgrow from bipolar and horizontal cells, Muller glial cell growth and scar formation, and vascularization of the inner retina (Marc et al., 2003; Wang et al., 2003; Jones and Marc, 2005; Wang et al., 2005a). Currently, no study has addressed how these retinal changes affect behaviorally measured vision. These changes typically occur late in the degenerative profile at a time when significant photoreceptor and vision loss has already occurred, making it difficult to discern the effects on vision of photoreceptor loss versus retinal change.

4. Visual adaptation model

Due to the limitations of the established model, a new model is proposed for studying RDD's and their treatments: the visual adaptation model. The visual adaptation model suggests that: the retina is capable of significant neural remodeling, the retina undergoes these changes in models of RDD at many different stages of degeneration, these changes are likely non-adaptive in nature, visual performance is not dependent upon a linear relationship with photoreceptor survival, visual function is plastic and may not be directly affected by changes in retinal circuitry.

4.1 Retinal remodeling

Neuronal remodeling, in general, is not a new concept and has been extensively documented in epilepsy (Represa and Ben-Ari, 1992) and learning/memory (Chklovskii et al., 2004), and has been indicated in retinal detachment (Lewis et al., 2002; Fisher and Lewis, 2003; Fisher et al., 2005; Sethi et al., 2005), and in retinal degenerations (Kolb and Gouras, 1974). Using an animal model of retinal detachment, Fisher and Lewis (2005) (Fisher et al., 2005) have found many instances of retinal reorganization. For example, following extended retinal detachment there are changes in protein expression in photoreceptors, remodeling of rod bipolar cells, horizontal cells, ganglion cells, Muller glial cells, and astrocytes (Fisher et al., 2005). Interestingly, some of these changes such as rod and on-cone bipolar cell and horizontal cell dendritic reorganization have also been found in the aged human retina (Eliasieh et al., 2007) suggesting that these changes are not a species specific phenomenon.

Retinal reorganization was not afforded much support in the past until studies showed abnormal changes in the inner retina following photoreceptor degeneration, including the sprouting of photoreceptors and horizontal cells in the rd1 mouse (Strettoi and Pignatelli, 2000; Strettoi et al., 2002). More support arose when the pathological features in human RP correlated with those in the RCS rat (Milam et al., 1998; Fariss et al., 2000; Pavlidis et al., 2000; Wang et al., 2005a). Since the early indications of retinal plasticity, another group of researchers have examined further the reorganizational events which occur in the degenerating retina. Jones and Marc (Jones et al., 2003; Marc et al., 2003; Jones and Marc, 2005; Jones et al., 2005; Marc et al., 2007) have examined multiple models of RDD, including the RCS rat and rhodopsin transgenic rats, and

devised a classification system for the varying degrees of retinal reorganization. Phase 1 begins with the expression of a primary insult which may consist of the expression of a mutated gene, or a more easily noticed lack of function such as reduced ERG wave amplitudes or OKR thresholds. Phase 2 consists of photoreceptor cell death that typically begins with photoreceptor stress eventually resulting in cell death and often accompanied by bystander effects or loss of trophic support. Phase 3 begins with evidence of cone loss and a protracted period of global remodeling of the remnant neural retina. As death of rods and cones progresses, bipolar and horizontal cells are deafferented and retract most of their dendrites. In addition, horizontal cells develop anomalous axonal processes and dendritic stalks that enter the inner plexiform layer. Eventually, bipolar cell death is evident and, as remodeling progresses over months and years, more retinal neurons are lost and patches of the ganglion cell layer can become depleted. Remodeling activity peaks at mid-phase 3 when remaining retinal cells such as amacrine and bipolar cells relocate to various positions throughout the retina. Although no study has looked closely at the functional effects of retinal remodeling on vision, some studies have suggested that these changes are non-adaptive (Lewis et al., 2002; Fisher and Lewis, 2003; Jones et al., 2003; Marc et al., 2003; Fisher et al., 2005; Jones and Marc, 2005; Jones et al., 2005; Marc et al., 2007).

4.2 Implications of retinal remodeling

Retinal remodeling has serious implications visual system function. There are two possible effects retinal remodeling could have on visual function: adaptive or non-adaptive. Adaptive consequences would entail an improvement or maintenance of visual function. Non-adaptive consequences include a decline in visual function. In non

degenerating animals retinal remodeling appears to have only non-adaptive properties (Fisher et al., 2005). In retinal degenerative animals, retinal remodeling appears to also have non-adaptive consequences, although these are difficult to parse from the effects of photoreceptor degeneration. In animals with a degenerating retina, it remains unclear whether any functionally adaptive process is evident in either the retina or in other visual centers in the brain.

Retinal remodeling also has implications for the treatment of RDD. For example, RP patients who have a specific genetic mutation that causes the progressive degeneration of the retina are necessarily predisposed to premature retinal reorganization. This means that as the patient's disease progresses, the retina and the circuitry within it has changed and/or is changing. This suggests that the treatment for early stage RP may be different than the treatment for middle or late-stage RP. Furthermore, as cell transplantation, gene therapy, and other treatments gain popularity as suitable therapies for diseases such as RP, one must consider that these therapies are typically delivered via sub-retinal injection, causing a temporary yet significant retinal detachment. This detachment as describe above (Fisher et al., 2005), can promote reorganization of the retina complicating further the circumstances involved when treating patients with RDDs. Supposing a complete replacement of the photoreceptors for late stage retinal disease is possible, the inner retina has undoubtedly undergone significant remodeling suggesting that neural information in this circumstance would likely be corrupt, reducing the efficacy of such treatment.

It is currently unclear what the signal is that promotes reorganization in retinal degenerations, however, results of Wang et al. (Wang et al., 2005a) and Pinilla et al.

(Pinilla et al., 2007) showed that, when photoreceptors are preserved in the RCS rat through cell transplantation performed at an early stage of degeneration, reorganization of the retina is delayed. Therefore, the signal that promotes reorganization is likely either the loss of neural input due to the loss of photoreceptors themselves, or possibly a loss of neurotrophic support, which is then restored by the cell transplants (Faktorovich et al., 1990; McGill et al., 2004b; McGill et al., 2007a). In either case, it is suggested that reorganization of the retina is non-adaptive and preventing neuronal remodeling and the loss of photoreceptors is likely to be most effective for rescuing visual function.

5. Goal of thesis

The goal of this thesis is to provide empirical support for the visual adaptation model and to develop a framework to guide future studies of retinal and visual system function and experimental therapies for RDD. This will provide three primary benefits to retinal research: 1) this research will account for inconsistencies in other models while simultaneously providing a theoretical construct from which future research on retinal function will be based, 2) this work will also provide a clinically relevant model, and experiments to support it, to help guide the development of future treatments for RDD by improving our understanding of retinal disease and treatment efficacy, 3) and finally, this work will examine the relationship between two forms of treatment for RDD and their effects on retinal reorganization helping elucidate the mechanisms of such changes in the retina. In addition, these studies will attempt to address 2 fundamental questions about the visual adaptation model: 1) what causes the initiation of retinal remodeling, and 2) is retinal remodeling functionally non-adaptive.

The studies in this thesis were to undertaken to address a few important, yet specific, issues with respect to the visual adaptation model. The first issue addressed was whether growth factors, when administered from an exogenous source, could cause retinal remodeling, and if so, to examine the functional consequences of such change. This is an important issue as growth factor delivery into the retina remains one of the premier methods of treating RDD, and any negative consequences of such treatment could reflect negatively on itself. In addition, the current belief of how cell transplantation provides benefit to a degenerating retina is through the continuous secretion of such factors. Given that high doses of CNTF have been shown to cause transient reduction in the ERG (Wen et al., 2006), and some evidence exists for CNTF induced retinal changes (Rhee et al., 2007), it was important to examine whether the ERG reductions and retinal changes result in modified vision. The design of this experiment removed the complexity of retinal degeneration by using a non-retinal degenerating rat model, which clarified the effects of exogenous growth factors on normal retinal function. In addition, these effects were examined using a logarithmic dose dependant experimental design to determine if a concentration exists that does not cause visual impairments, but also could be beneficial in a diseased retina.

The second experiment addressed whether retinal remodeling occurs in the early stages of retinal degeneration in the RCS rat, and characterized the degenerative profile of OKR thresholds using a novel behavioral task. As the RCS rat is the most widely used model for studies of RDD, it was important to establish a baseline of visual performance throughout the degeneration of the retina, while also establishing the onset and course of

retinal remodeling. The results of this study provide the background information required when examining potential therapies for human RDD.

The third experiment examined the effects of cell transplantation on preserving vision and photoreceptor rescue, and how this treatment (and the potential preservation of retinal structure and visual function) affected retinal remodeling in the RCS rat. The primary goal of this study was to clarify whether cell transplantation, another premiere method of treating RDD, using cells that produce factors known to preserve photoreceptors, reduced remodeling of the retina in addition to preserving vision and photoreceptor cells while avoiding immune system suppression. Using this procedure, we expected to elicit a dichotomy between the effects of growth factors, in which, in the non-degenerating retina growth factors were detrimental to retinal and visual function, whereas, in the diseased retina growth factors helped rescue compromised function. The results of this study were also intended to assist in the understanding of normal retinal disease processes, as well as identify key issues that need to be addressed when developing a suitable treatment for RDD.

The fourth and fifth experiments were designed as a stepping stone to branch the above work into another model of RP, transgenic rats that express a mutation in the rhodopsin gene. As the background information about visual function in these animals is largely unknown, it was important to perform a longitudinal characterization of ERG wave amplitudes, ONL thickness, and OKR thresholds to examine the degree of correlation between standard measures of visual function. This was subsequently followed by examining retinal remodeling using one line of the transgenic rats in comparison with the functional testing results. The results of this experiment provided

critical information about how different measures of the retina, retinal function, and visual function relate in an animal model of RP other than the RCS rat. In addition, these two studies also provide empirical evidence that retinal remodeling is likely a non-adaptive process in animal models of RDD.

The work in this thesis places heavy emphasis on behaviorally measured vision, specifically OKR thresholds and visual acuity. This is of particular advantage for a number of reasons. First, retinal degenerative disease is partially characterized by the loss of vision, and in most cases, the visual problems are what initially prompted patients to seek medical attention. Second, vision is the most clinically relevant measure of disease progression and of treatment success. Third, using the top-down approach (measuring vision upfront) has prompted new insights into visual system and retinal function which could not be conceived while using a bottom-up approach (evaluating photoreceptor survival). Fourth, two widely accepted methods of measuring behavior dependent visual thresholds are now available which encouraged a more comprehensive examination of multiple forms of vision (Prusky et al., 2004a; Douglas et al., 2005). Finally, quantified visual profiles in animal models of human RDD will provide the necessary background to examine the efficacy of potential treatments for retinal disease.

Chapter II – CNTF in Long-Evans rat

1. Introduction

A number of neuroprotective agents slow photoreceptor (PR) cell loss in animal models of inherited retinal degenerations (RDs)(Faktorovich et al., 1990; Lavail et al., 1992a; Cayouette et al., 1999; Frasson et al., 1999; Liu et al., 1999; Lau et al., 2000; Ogilvie et al., 2000; Green et al., 2001; Liang et al., 2001b; Machida et al., 2001; Whiteley et al., 2001; Agarwal et al., 2002; Leveillard et al., 2004). Ciliary neurotrophic factor (CNTF) appears to be mutation-independent and the most universally effective, thus far, as it slows PR degeneration in 12 different inherited RDs in mice (Cayouette and Gravel, 1997; LaVail et al., 1998; Liang et al., 2001a; Bok et al., 2002), rats (Liang et al., 2001a; Wang et al., 2002), dogs (Pearce-Kelling et al., 1998; Tao et al., 2002), and cats (Chong et al., 1997; Chong et al., 1999), and protects PRs from the damaging effects of light in rats (LaVail et al., 1992b) and mice (LaVail et al., 1998). The relative lack of specificity of CNTF in its survival-promoting activity is potentially advantageous and has led, in part, to a recent Phase I (safety) clinical trial using implants of encapsulated cells releasing CNTF in patients with retinitis pigmentosa (Sieving et al., 2006) using encapsulated cell technology described previously in the *rcd1* canine model of retinitis pigmentosa (Tao et al., 2002).

A worrisome property of CNTF is that whereas it rescues PRs from degeneration when delivered continuously following adeno-associated virus (AAV) vector transduction, it reduces scotopic (rod-dominated) and photopic (cone-dominated) electroretinographic (ERG) amplitudes (Liang et al., 2001a; Bok et al., 2002), which are typically a measure of PR and retinal function. This appears to occur in a dose-dependent

manner (Bok et al., 2002). The continuous delivery of CNTF also results in a reduction of some or all ERG responses in normal mice (Schlichtenbrede et al., 2003), rabbits (Bush et al., 2004), and rats (Liang FQ, et al. *IOVS* 2003;44:ARVO E-Abstract 3585). Continuous delivery of CNTF has also been associated with structural changes in PRs (Bok et al., 2002; Bush et al., 2004; Zeiss et al., 2006) and inner retinal cells (Zeiss et al., 2006; Rhee et al., 2007), with outright loss of PR cells in some cases (Liang FQ, et al. *IOVS* 2003;44:ARVO E-Abstract 3585), and these changes also appear to occur in a dose-dependent manner in mice (LaVail MM et al., unpublished observations;(Zeiss et al., 2006)).

In contrast to continuous delivery, the intravitreal injection of CNTF or Axokine®, a mutant form of CNTF, has also been shown to reduce ERG amplitudes transiently in dogs with cone-rod dystrophy (Luthert, PJ, personal communication, 2001) and in normal rats (Wen et al., 2006). In both of these cases, the ERG suppression was evident by about 1-2 weeks after injection (rat and dog, respectively), but at 3-4 weeks after injection, the ERG amplitudes had returned to match those of the control eyes in the same animals. In the study with rats, transient changes in PR structure and PR phototransduction proteins also occurred (Wen et al., 2006).

An important unanswered question about the suppression of ERG responses by CNTF is whether it reflects functional change in vision. In most instances, the reduction of ERG amplitudes follows the loss of vision in patients with inherited RDs, so the suppression of ERG amplitudes by CNTF might be seen as a negative effect. In some cases, though, reduced or absent ERG amplitudes seem to have little effect on vision, such as in Duchenne muscular dystrophy (Cibis et al., 1993; Cibis and Fitzgerald, 2001).

Moreover, it is not clear that CNTF-induced ERG alterations are a negative effect, because the agent can, in fact, protect PRs from cell death at the same time as reducing ERG amplitudes (Liang et al., 2001b; Bok et al., 2002; Schlichtenbrede et al., 2003). To understand the effect of CNTF-induced reduction of ERG responses on vision in the normal, mature rat eye, we have used a virtual optokinetic system (VOS; OptoMotry ©(Prusky et al., 2004a; Douglas et al., 2005)) to quantify spatial frequency thresholds of the optokinetic response (OKR) before and after both intravitreal injection of CNTF that results in transient suppression of ERG responses, and subretinal injection of AAV-vectored CNTF that results in sustained suppression of ERG responses. In addition, we used the Visual Water Task (Prusky et al., 2000a) to evaluate the effects of the AAV-vectored CNTF on perceptual spatial vision. The central physiological consequences of CNTF injection were also examined by measurement of luminance thresholds in the superior colliculus. Following behavioral testing, the retinas were examined for the morphological phenotypic features some have found associated with the application of CNTF (Bok et al., 2002; Bush et al., 2004; Zeiss et al., 2006) and the behavioral findings were correlated with measurements of ERG amplitudes. Finally, the results of this study provided contrast between the established photoreceptor equals vision model and the visual adaptation model using a clinically relevant therapy for RDD.

2. Methods

2.1 Animals and Injections

All components of this study were conducted in accordance with the ARVO Statement for the Use of Animals in Ophthalmic and Vision Research and the guidelines of the institutional animal care committees at the University of Lethbridge, University of

Utah and University of California, San Francisco. The work presented in this study was the result of collaboration between Dr. Glen Prusky's and Dr. Matthew Lavail's laboratories as I took advantage of the strengths of each laboratory. Adult Long-Evans rats were maintained in a 12:12-hour light-dark cycle at an in-cage illuminance of <150 lux. Prior to injections, ERG measurements or physiological recording from the superior colliculus, rats were anesthetized with intramuscular mixture of ketamine (13 mg/kg) and xylazine (87 mg/kg). Corneas were anesthetized with 0.5% proparacaine, and pupils were dilated with 2.5% phenylephrine hydrochloride followed by 1.0% atropine.

To study transient effects of CNTF, intravitreal monocular injections of recombinant rat CNTF (R&D Systems, Minneapolis, MN) were made using a transscleral approach as described elsewhere (Paskowitz et al., 2004) and the dose of 10 µg (2 mg/ml in 5 µl of PBS) was injected to be consistent with that used previously by Wen and coworkers (Wen et al., 2006). Following our initial study, we carried out a dose-response analysis of the effects of intravitreally injected recombinant rat CNTF at doses of 1,000, 100, 10 and 1 ng, each in a volume of 2 µl.

For comparison of the dose-response analysis of rat CNTF effects on the ERG responses and OKR thresholds to therapeutic doses of CNTF, we have included the morphological results of a dose-response study of the protective effect of rat CNTF carried out several years ago by one of us (MML) using normal albino Sprague-Dawley rats at 3-4 months of age. The recombinant rat CNTF for this study was a gift of Regeneron Pharmaceuticals (Terrytown, NY) and was injected intravitreally into one eye of rats at doses of 400, 200, 100, 50, 25, 10, 2 and 0.2 ng, each in a volume of 1 µl. Two days after the injection of CNTF, the rats were exposed to constant fluorescent light for 7

days at an illuminance level of 125-175 ft-c, as described elsewhere (Faktorovich et al., 1992).

To study long-term effects of constitutively secreted CNTF, subretinal injections of AAV-vectored CNTF were made in the superior hemisphere of rat eyes as described (Bok et al., 2002). The AAV vector (serotype 2) with chicken beta actin promoter resulted in the expression of a secreted (DH) variant of human CNTF with an increased affinity towards CNTFRα (Saggio et al., 1995) which was the most potent survival promoting form of several AAV-CNTF types in rescuing photoreceptors in *rds*$^{+/-P216}$ mice (Bok et al., 2002). Two µl of the rAAV-CBA-sDH-CNTF vector (hereafter AAV-CNTF) with a titer of 10^{11} infectious particles per ml (Bok et al., 2002) were injected into one eye of each rat. In initial experiments, we found that both intravitreal and subretinal PBS-injected eyes gave indistinguishable results from uninjected eyes, as measured by histology, ERG and OKR testing, therefore, uninjected eyes served as controls for most of the experimental study.

2.2 Electroretinography

Rats were dark-adapted overnight and then in dim red light, were anesthetized as above. Bilateral, simultaneous full-field scotopic ERGs were elicited with 10-µsec flashes of white light, and responses were recorded using contact lens electrodes (Bayer et al., 1999) with a UTAS-E 3000 Visual Electrodiagnostic System (LKC Technologies, Inc., Gaithersburg, MD). Scotopic stimuli were presented at an intensity of 0.4 log cd-sec/m^2 at 2-minute intervals, and the response to 2 successive flashes was averaged. This was followed by a single stimulus at 2.4 log cd-sec/m^2. Rats were then exposed to a

background light of 29 cd/m^2 for 10 minutes before recording photopic responses to stimuli presented at a rate of 2 Hz at 0.4 log cd-sec/m^2, a total of 20 successive flashes were averaged. Responses were amplified at a gain of 4,000, filtered between 0.3 to 500 Hz and digitized at a rate of 2,000 Hz on 2 channels. The amplitude of the a-and b-waves was measured. Scotopic a-waves were measured from the baseline to the peak in the cornea-negative direction in response to a stimulus of +2.4 log cd-sec/m^2, and b-waves were measured from the cornea-negative peak to the major cornea-positive peak in response to a stimulus of +0.4 log cd-sec/m^2. ERG responses from the treated eye were compared to responses from the contralateral control eye for each animal.

2.3 Virtual Optokinetic System (VOS)

OKR spatial frequency thresholds were measured once prior to injection and repeatedly after injection. The VOS measures the threshold of optokinetic tracking response to moving gratings (Prusky et al., 2004a; Douglas et al., 2005). The apparatus consisted of four computer monitors positioned around a square testing arena. A sine wave grating was drawn on a virtual cylinder projected in 3D coordinate space on the monitors (Figure 2; OptoMotry©, CerebralMechanics, Lethbridge, Alberta, Canada), and the cylinder was rotated. In brief, an unrestrained rat was placed on a platform in the center of the arena. A video camera provided real-time video feedback from above, and the position of the head on each frame was used to continually center the hub of the cylinder at the rat's viewing position. The cylinder was rotated at a constant speed (12 °/s; Figure 3). On each trial an experimenter judged whether the rat made tracking movements with its head and neck to follow the drifting grating. The spatial frequency

threshold, the point at which animals no longer tracked, was obtained by incrementally increasing the spatial frequency of the grating at 100% contrast. Thresholds through each eye were measured separately by reversing the rotation of the cylinder (Douglas et al., 2005).

2.4 Visual Water Task (VWT)

The VWT is a visual perception task previously described in detail (Prusky et al., 2000a; Prusky et al., 2002; McGill et al., 2004a; McGill et al., 2004b). Briefly, the apparatus consisted of a trapezoidal-shaped pool with two computer monitors facing through a clear glass wall into the wide end of the pool, and a midline divider extended into the pool from between the monitors, creating a Y-maze with a stem and two arms. Animals were trained to discriminate between a sine wave grating and gray of the same mean luminance displayed on the screens using a computer program (Figure 1; Vista©, CerebralMechanics, Lethbridge, Alberta, Canada).

Training and testing followed the same procedure as described elsewhere (McGill et al., 2004a; McGill et al., 2004b) except animals were only tested once at approximately 180 days postinjection (PI) of AAV-CNTF. Animals were tested in blocks of trials at progressively incrementing spatial frequencies until they could no longer distinguish between the visual stimuli at a minimum of 7/10 correct. Grating acuity was calculated as the 70% correct point on a cumulative normal curve fit to the data. Monocular testing required placing a small occluder over one eye during each trial, which was removed immediately following that trial. All testing was done early in the light phase of the circadian cycle. Thresholds through each eye were obtained in sequence.

2.5 Luminance Threshold Responses Recorded in the Superior Colliculus

We measured luminance thresholds by recording multiunit neuronal responses in the superior colliculus contralateral to the tested eye, as described elsewhere (Sauve et al., 2002). In short, for each position recorded in the superior colliculus, a discrete receptive field was localized and the brightness of a flashing spot, 3˚ diameter projected on a hemisphere, was varied with neutral density filters until a response was obtained that was double the background activity. This was defined as the luminance threshold level. The measurements were performed 2 weeks after CNTF injection using the initial high dose of 10 μg (2 mg/ml in 5 μl of PBS). The luminance thresholds were measured separately in both colliculi, contralateral to treated and untreated eyes in the same animal in one recording session, in order to compare both eyes in the same individual rat.

2.6 Histology and Morphometric Analysis

Following behavioral testing, animals received a lethal dose of euthansol (sodium pentabarbitol, 0.3 ml/kg), and those sacrificed after ERG testing or constant light exposure were killed with an overdose of carbon dioxide and then were immediately perfusion fixed with a mixture of 2% paraformaldehyde and 2.5% glutaraldehyde in phosphate buffered saline. Eyes were marked for orientation, removed, and then bisected along the vertical meridian and embedded in an Epon-Araldite mixture, with sections cut at 1 μm thickness as described (LaVail and Battelle, 1975).

Measurements of the outer nuclear layer (ONL) thickness, taken as an index of photoreceptor number (Michon et al., 1991), and rod outer segment lengths were obtained from 54 locations around the retina as described (Faktorovich et al., 1990; Lewin et al.,

1998). These 54 measurements were either averaged to provide a single value for each retina to allow statistical comparison of treatment and control groups, or plotted as a distribution of thickness across the retina. For morphological assessment of the therapeutic dose-response of CNTF in the light damage experiments, the relative scale of 0-4+ rescue based on number of photoreceptors surviving and photoreceptor integrity was used as described (Lavail et al., 1992a; LaVail et al., 1997; LaVail et al., 1998).

2.7 Statistical Analysis

In most cases the data between CNTF-injected and contralateral control eyes were compared with a two-tailed paired Student's *t*-test. OKR spatial frequency thresholds were compared at each time point for each rat using repeated measures analysis of variance (ANOVA), with Bonferroni's post-test for ANOVA values ($p < 0.05$) to compare means at individual time points.

3. Results

3.1 Effects of Intravitreal CNTF Injection

The most thorough analysis of transient effects of intravitreally injected CNTF is that by Wen et al. (2006) (Wen et al., 2006). In order to compare our findings with that work, most of our studies described here used the same large dose of 10 µg used by Wen et al. (2006) (Wen et al., 2006). These findings are followed by dose-response analyses of CNTF injection.

3.1.1 Changes measured with ERG

A group of 11 rats monocularly injected with 10 µg of CNTF was initially followed for 28 days PI, since we anticipated an initial suppression of maximal ERG amplitudes at 6 days, with full recovery by 21 days PI (Wen et al., 2006). Indeed, at 6

days PI, the scotopic a-and b-waves and photopic b-wave amplitudes were 45-70% lower than those of their fellow control eyes (Figure 5A). However, at 21 and 28 days PI, while the scotopic a-waves had recovered to levels not significantly different from those of control eyes, the scotopic b-wave and photopic b-wave amplitudes unexpectedly had not yet fully recovered (Figure 5A).

A second group of 7 rats was then followed with weekly ERG recordings from 28-98 days PI. Remarkably, each of the ERG amplitudes was suppressed for an extended period (Figure 5A). Scotopic a-wave amplitudes remained below control levels throughout most of the test period, although they were significantly different only at 42 and 70 days PI (Figure 5A). Scotopic b-wave amplitudes remained below control values through 91 days PI, and were significantly different through 49 days and at 70 days PI (Figure 5A). Photopic b-waves were the most severely affected both in the degree and duration of suppression. These remained below control levels throughout the test period and were significantly different from those of controls through 84 days PI, except at 63 days PI. Thus, the first time all three ERG waves recovered from CNTF-induced suppression was at 91 days PI.

3.1.2 OKR

The spatial frequency threshold of the OKR averaged 0.53 cycles per degree (c/d) prior to injection (Figure 5B), which was comparable to previously published values from the same strain (Douglas et al., 2005). PI measures revealed that thresholds through CNTF-injected eyes dropped slightly to 0.51 c/d after 2 days, and by 3 days the thresholds had declined to 0.45 c/d (Figure 5B), the first PI interval at which the thresholds were significantly different from those of controls ($p < 0.001$). This decline

continued until day 8 when the threshold reached 0.21 c/d where they remained until PI day 56. Thereafter, the thresholds began to recover. The spatial frequency thresholds had recovered to near control values by 85 and 94 days PI, but still differed significantly ($p < 0.05$). Full recovery was seen at 105 days (Figure 5B) and beyond (data not shown).

3.1.3 Luminance Threshold Responses Measured in the Superior Colliculus.

Multiunit recordings were made in 5 animals 2 weeks following intravitreal injection of CNTF in the right eye using the same doses as those used for the ERG and behavioral testing in the initial high dose study, the left eye was an intact control. In each animal, the thresholds were measured at 4-6 points in each colliculus. In sum, we collected data from 29 points related to the injected eyes, and from 23 points related to the untreated eyes. The corresponding mean values (± SEM) of the thresholds were 0.64 ± 0.085 log units for the injected eyes, and 0.29 ± 0.023 log units for the untreated eyes. Thus, CNTF injection elevated the visual thresholds in treated eyes by 0.35 log units (approximately 2.2 times) in comparison with untreated eyes with a high level of statistical significance ($p < 10^{-6}$).

3.1.4 Morphological Changes

We examined the retinas of 3 or more rats before and 6, 21, 28 and 199 days after intravitreal injection of 10 μg of CNTF. At 6 days PI, the photoreceptor outer segments were clearly damaged, being irregular in caliber and somewhat tattered (Figure 6B) compared to the smooth profiles of normal outer segments (Figure 6A). The rod outer segments were also much shorter than normal, reduced to about 54% of their normal length (preinjection length, 23.6 ± 1.1 μm, mean ± SD; 6 days PI, 12.7 ± 0.8 μm; n=3; $p < 0.0005$). By 21 days PI (Figure 6C) and thereafter, the outer segments had returned to

their normal appearance and length (preinjection 23.6 ± 1.1 μm; 21 days PI, 23.8 ± 0.8 μm, n=3, p = 0.85). The outer segments were normal at the later ages, as well (data not shown). These changes are virtually identical to those seen previously by Wen et al. (2006) (Wen et al., 2006) at 6 and 21 days PI.

The rod photoreceptor nuclei appeared normal at all PI times (Figures 6B, C), and at no time did they have the dispersed heterochromatin giving a cone-like appearance such as that seen with continuous delivery of CNTF in mice (Bok et al., 2002) and rabbits (Bush et al., 2004).

3.1.5 Dose-Response Analysis of Transient Changes Induced by Intravitreal Injection of CNTF

Persistent suppression of ERG responses and reduction of spatial frequency thresholds of the OKR resulted from injection of 10 μg of CNTF. Because the doses being tested for potential therapeutic use in human patients are several orders of magnitude lower than the 10 μg used here and by Wen et al., (2006) (Wen et al., 2006) we carried out a log-unit step reduction dose-response analysis of ERG responses and OKR threshold measurements at 6 and 21 days PI.

As noted above, the 10 μg (10,000 ng) injection resulted in a large reduction in the OKR threshold and all ERG responses 6 days PI, most of which had not returned to normal values at 21 days PI (Figure 7A). Following a 1,000 ng dose (Figure 7B), all of the measured parameters were similarly affected at 6 days PI, but by 21 days PI, all three of the ERG responses had recovered to levels not statistically different from those of control eyes. The OKR threshold, while not as reduced as it was with the higher dose, nevertheless was still affected at 21 days PI (Figure 7B). At a dose of 100 ng (Figure 7C),

the ERG responses at 6 days PI appeared somewhat reduced, but were not statistically different from control values, and by 21 days PI, all of the ERG responses were at normal levels (Figure 7C). At doses of 10 ng (Figure 7D) and 1 ng (Figure 7E), the ERG responses were unaffected by the CNTF injection.

The OKR thresholds were reduced at lower doses of CNTF than those affecting the ERG responses. At a dose of 1,000 ng, for example, the OKR threshold was still reduced from normal at 21 days PI, whereas the ERG responses no longer were statistically different from controls. Similarly, at both PI intervals at a dose of 100 ng (Figure 7C) and after 6 days PI at a dose of 10 ng (Figure 7D), OKR thresholds were still reduced, whereas the ERG responses were not different from control values. Neither OKR thresholds nor ERG responses were affected by the dose of 1 ng (Figure 7E).

3.1.6 Dose-Response Analysis of Protection of the Retina from Constant Light Damage by Intravitreal Injection of CNTF

The injection of 100, 200 and 400 ng of CNTF gave maximal protection from the damaging effects of a 7-day constant light exposure (Figure 8). The dose of 50 ng was slightly less protective, but was still statistically indistinguishable from that produced by 400 ng. The dose of 25 ng provided statistically less protection than the maximal dose ($p < 0.005$) , but it gave a relative score of 2+ for the degree of protection (Figure 8), which is considered moderate protection (LaVail et al., 1997). Lower doses of 10, 2 and 0.2 ng gave progressively less rescue, but while the protection afforded by10-ng dose was minimal, it was significantly greater than that provided by the 0.2-ng dose ($p < 0.05$).

3.2 Effects of Subretinal AAV-CNTF Injection

3.2.1 Functional Changes Measured with the ERG

Rats injected subretinally with AAV-CNTF were examined by ERG at 42 and 95 days PI. As shown in Figure 9, all ERG amplitudes were about 20-40% lower than in contralateral control eyes at 42 days PI and about 20-50% lower at 95 days PI, although at the latter PI interval the scotopic a-waves were not statistically different from control values. As with the intravitreal CNTF injections, the photopic b-waves were the most significantly depressed of the different ERG responses (Figure 9).

3.2.2 OKR

Spatial frequency thresholds were obtained prior to injection and all eyes tested were of normal values (0.53 c/d , n=12; (Prusky et al., 2004a; Douglas et al., 2005)). Thresholds obtained following injection were very close to normal through 11 days PI (0.50 c/d; Figure 10) but were already statistically lower than normal by 11 days PI ($p < 0.01$). By 14 days PI, however, the thresholds had fallen rapidly to 0.390 c/d (Figure 9). The thresholds continued to decrease rapidly to 0.210 c/d by 18 days, less than 50% of normal ($p < 10^{-10}$), where they remained unchanged until at least 180 days PI, the longest PI interval examined (Figure 10).

A second group of animals with sub-retinal AAV-vectored CNTF was tested at 120 days PI and also showed a significant impairment in thresholds (0.300 c/d), although slightly less than the previous group (data not shown). Uninjected eyes of all rats had normal thresholds (0.53 c/d) at all points tested.

3.2.3 Visual Acuity

The perceptual visual acuity of 5 animals that received AAV-vectored CNTF was

measured binocularly and monocularly through each eye separately at 6 months PI using the VWT. All animals learned the task readily and had no obvious behavioral deficits in task performance. Acuity measured binocularly and monocularly from uninjected eyes was about 1.0 c/d (Figure 11), which is comparable to previous data generated in Long-Evans rats (Prusky et al., 2000a; Prusky et al., 2002; McGill et al., 2004a). However, acuity measured monocularly through the injected eye (Figure 11) was significantly lower (0.500 c/d, $p < 0.003$).

3.2.4 Morphological Changes

A group of 5 rats that had been injected subretinally in the superior hemisphere with AAV-CNTF and which showed suppressed ERG amplitudes (Figure 9) and reduced spatial frequency thresholds at 180 days PI (Figure 10) was examined histologically at 194 days PI. The retinas of 2 of the injected eyes appeared normal throughout the retinal section along the vertical meridian (cf. Figures 12A, 12B; Figure 13). However, 3 of the retinas showed loss of photoreceptors across at least half of the superior hemisphere (Figure 13), with reduction of the ONL to 1-3 rows of nuclei (Figures 12C, 12D). Despite the significant loss of photoreceptors in some regions near the subretinal injections, the overall ONL thickness of the 5 injected eyes (23.8 ± 2.6 μm, mean ± SEM) was only slightly less than that of uninjected controls (25.3 ± 0.6 μm) and did not differ significantly ($p = 0.16$).

Most of the photoreceptors in the severely depleted areas of the ONL showed dispersed heterochromatin giving them a cone-like appearance, and these cells were also present in the transition zones between the most degenerated and normal regions of retina (Figure 12D). However, none were present in regions of relatively normal retina such as

that shown in Figure 12B or at the far right of Figure 12C.

Since continuous delivery of CNTF resulted in an increased thickness of the inner retina in dogs (Zeiss et al., 2006), we measured the inner retina of the eyes injected with AAV-CNTF as we did for the ONL. The thickness of the inner retina in the eyes injected with AAV-CNTF was indistinguishable from that in the control eyes, regardless of whether the entire retina was compared from all 5 injected animals or from the 3 injected animals that showed loss of the ONL, measuring the INL only in the regions of the ONL loss (data not shown).

Using immunohistochemistry, Rhee et al. (2007) (Rhee et al., 2007) have found that the same AAV-CNTF vector used in the present study causes an increase in number and a change in the distribution of bipolar and Müller cell nuclei in the degenerating retinas of *rds*$^{+/-P216L}$ transgenic mice. While we could not use cell-specific staining with the plastic-embedded sections in the present study, we did find changes in the inner nuclear layer of the normal rats injected with AAV-CNTF that were consistent with those found by Rhee et al., at least for Müller cell nuclei which can be identified in plastic sections. Whereas most Müller cell nuclei in normal rat retinas are situated in the middle or middle-to-outer part of the inner nuclear layer (Figure 12A), many were found distributed throughout the inner nuclear layer, both in regions of otherwise normal retina (Figure 12B) and in partially degenerated regions (Figure 12C).

4. Discussion

We have found that intravitreal injection of a high dose of CNTF (10 μg) results not only in transient suppression of ERG responses, but also functional changes in vision in normal rats as demonstrated by transient reduction of OKR thresholds and reduction of

luminance threshold responses measured in the superior colliculus. In addition, continuous delivery of AAV-vectored CNTF results in sustained reduction in ERG responses and OKR thresholds for at least 6 months, as well as reduced visual acuity measured with the VWT.

The precision with which the decline in OKR thresholds paralleled the suppression of the ERG responses following CNTF injection (Figure 5) was remarkable, and although the ERG responses showed a more rapid partial recovery than did the spatial frequency thresholds, both returned to normal at about the same time, 91 (for all ERG responses) and 105 days following injection, respectively. The reduction in spatial frequency thresholds following subretinal AAVCNTF injection occurred between 11 and 18 days following injection, which is precisely the time required for full gene expression of AAV2-vectored markers such as green fluorescent protein (Bennett et al., 1997). Thus, the OKR can be used with high precision and sensitivity to rapidly and noninvasively assess the positive and negative effects of vision-based therapies.

CNTF signaling involves binding of the cytokine to receptor associated Jak kinases, leading to phosphorylation of members of the signal transducer and activator of transcription (STAT) family, STAT1 and STAT3, as well as the triggering of signal-related kinase (p42/44 ERK; (Peterson et al., 2000; Rhee et al., 2004)). When the same AAV-CNTF used in the present study was injected subretinally into transgenic *rds*$^{+/-}$ ^{P216L} mice, persistent cytokine signaling was seen 65 days later in the retina, as elevated levels of phospho-STAT1 and STAT3 and phospho-ERK1 and ERK2 were demonstrated by immunocytochemical staining and Western blot analyses (Rhee et al., 2007). Moreover, Bok et al. (2002) (Bok et al., 2002) have shown in these same mice

that all ERG responses were significantly and persistently reduced following AAV-CNTF injection. Thus, in the present study, it was not surprising to find persistent ERG and visual behavioral changes in the rats injected with AAV-CNTF. However, it was most unexpected to find an extremely long recovery time of 91-105 days following intravitreal injection of CNTF, particularly since previous studies have shown clearing of CNTF from the retina between 2-4 days (Cayouette et al., 1998; Peterson et al., 2000) and only transient elevation of relevant signaling molecules. Following intravitreal injection of CNTF, pERK is elevated for less than 6 hours (Wahlin et al., 2000), STAT1 and STAT3 phosphorylation signals are seen for only up to 4 days (Peterson et al., 2000), and phosphorylated MAPK (a member of the ras-MAPK signaling pathway) was only activated at 1 hour in rats (Peterson et al., 2000). With the same high dose (10 μg) of intravitreally injected CNTF that we used, Wen et al. (2006) (Wen et al., 2006) found an increase in STAT3 phosphorylation for as long as 6 days, with a gross reduction by 3 weeks, far less than the recovery time for the ERG and OKR (Figure 5). In each of these and other studies, and in studies showing that CNTF receptors are localized primarily on Müller cells and not on photoreceptors in rodents (Beltran et al., 2005), it is strongly suggested that Müller cells are the target of CNTF in the retina, and that these cells initiate neuroprotective signaling of undetermined nature (Peterson et al., 2000; Wen et al., 2006). This same undefined and perhaps long-lived signal may also mediate the suppression of ERG responses and spatial frequency thresholds, and be responsible for the long recovery time following CNTF injection, but this remains to be determined.

There is an apparent dose-dependence for the PR nuclear phenotypic changes

caused by subretinally injected AAV-CNTF. Only those regions near the injection site, which were presumably exposed to the highest concentration of continuous CNTF, showed rod PR nuclei with dispersed heterochromatin, which may signal structural modification of DNA during gene expression (Felsenfeld et al., 1996). Indeed, it was only in the areas where there was frank loss of some photoreceptor cells that the nuclear changes in the surviving cells were seen, yet we are fairly certain based on other studies with subretinal AAV injections that some secreted CNTF was available to all photoreceptors (Bok et al., 2002). Similar dose-dependence for CNTF-induced changes in nuclear phenotype and other features have been found in 1) *rds*$^{+/-P216L}$ mice by comparison of results from different vectors, promoters and routes of administration (Bok et al., 2002), and 2) normal rabbits (Bush et al., 2004) and normal and *rcd-1* dogs (Zeiss et al., 2006), where different concentrations of CNTF were delivered by encapsulated cell-based technology. Thus, in the normal Long-Evans rat, we see that AAV-vectored CNTF may cause PR cell death at the area of highest concentration, yet cause no structural damage to PRs adjacent to the area of highest concentration. Liang et al. (Liang F, et al. *IOVS* 2003;44:ARVO E-Abstract 3585) have made preliminary observations with intravitreal injections of AAV-CNTF in albino Sprague-Dawley rats, with some PR cell death in 5/9 rats, primarily in the retinal quadrant that was injected, again showing a dose-dependent negative effect. The exact cause of cell death is not known. We assume it is due to the highly localized and continuous release of CNTF following the subretinal injection of AAV-CNTF, and not to the AAV vector, itself. This same AAV vector has been injected subretinally to deliver DNA that encodes a number of different molecules without causing photoreceptor degeneration (Lewin et

al., 1998; Min et al., 2005; Pang et al., 2006). On the other hand, at very high doses greater than used here, highly localized PR damage has been reported (Jacobson et al., 2006b; Jacobson et al., 2006a). Moreover, we cannot exclude the possibility that the subretinal injection in some way changes the sensitivity of photoreceptors to the effects of AAV-vectored CNTF.

The effects of a high dose of CNTF on the ERG and behavioral responses are greater for the cone pathways, or the cones themselves, than for the rods. In the present study, behavioral testing with the VOS and VWT is in the photopic illuminance range (30-40 cd/m^2), and the photopic b-wave showed the greatest and longest suppression following a high-dose CNTF injection. The photopic b-wave ERG response reflects cone function, but is thought to be generated primarily by depolarizing bipolar cells in the rat (Xu et al., 2003). Consistent with our findings with the high CNTF dose, in normal rabbits the only suppressed ERG responses found with continuously released CNTF using encapsulated cell technology (Tao et al., 2002) were those of cone b-waves at dim flash intensities (Bush et al., 2004). The cones, themselves, may actually be affected by CNTF (albeit perhaps indirectly). In *rcd-1* and normal dog retinas, higher doses of CNTF released from encapsulated cells resulted in reduced immunohistochemical staining with antibody to human cone arrestin, and the effect was greater than that on rhodopsin (in rods; (Zeiss et al., 2006)). Similarly, in AAV-vectored CNTF in *rds*$^{+/-P216L}$ mouse retinas, both s-opsin and m-opsin normally expressed in cones was greatly reduced, but rhodopsin expression was not significantly affected (Rhee et al., 2007). It should be noted that AAV-vectored CNTF also results in the increase in number and distribution of bipolar and Müller cell nuclei in *rds*$^{+/-P216}$

mouse retinas (Rhee et al., 2007) and we found similar changes in the distribution of Müller cell nuclei in normal rat retinas in the present study with the same AAV-CNTF vector. Even single injections of CNTF can cause similar (or even more extensive) cellular changes in the immature retina of *XLPRA2* dogs (Beltran et al., 2007).

We have performed a formal dose-response study of intravitreally injected CNTF (Figure 7), and the results were instructive in several ways. First, unlike the high 10,000 ng dose, it was apparent that the ERG suppression was transient and short lived at a dose of 1,000 ng, and that none of the ERG waves was suppressed at doses of 100 ng or less. Second, it demonstrated a clear segregation of the effect of CNTF on the ERG and OKR. The OKR was more sensitive to the effects of CNTF than the ERG, with significant reduction in spatial frequency thresholds of the OKR at 1-2 log units lower dose than that affecting the ERG. This greater effect on the OKR in the dose-response study is consistent with that seen with the very high dose (Figure 5), in which the OKR thresholds remained at a very low level for a prolonged period, whereas the ERG responses partially recovered sooner. The separation of ERG responses and OKR thresholds following CNTF injection indicates that the two measures may not be tightly linked, but the mechanisms for this remain to be explored.

Third, the dose-response study provides a possible explanation of the prolonged recovery time following high-dose CNTF injection compared to the full recovery seen by 21 days by Wen et al. (Wen et al., 2006). We have used recombinant rat CNTF rather than recombinant human CNTF used by Wen et al.,(Wen et al., 2006) and rat CNTF has 4-5 times the potency in survival-promoting activity than the human form (Masiakowski et al., 1991). In our present study, reduction of CNTF dose by one log unit (to 1,000 ng)

resulted in full recovery of ERG responses at 21 days PI, just as seen by Wen et al. (Wen et al., 2006). It should be pointed out that structurally, our findings of rod outer segment recovery to normal length by 21 days PI are the same as those of Wen et al. (Wen et al., 2006).

Fourth, comparison of the dose-response findings with a dose-response study of light damage strongly suggest that therapeutic doses of CNTF exist that do not suppress ERG responses. In the light damage study, a dose of 10 µg provided minimal but significant protection, 25 µg gave moderate protection, 50 and 100 µg gave strong protection (Figure 8), and none of these doses suppressed the ERG responses (Figure 7). It should be noted that two different rat strains were compared, but this is unavoidable since albinos must be used for consistent light damage studies and pigmented rats must be used for precise analysis of the OKR (Prusky, unpublished observations). Our findings support the observation by Bush et al. (2004) (Bush et al., 2004) that doses of CNTF released by encapsulated cell technology that protect photoreceptors in a canine model do not adversely affect the ERG in normal rabbits. The only other dose-response study of any neurotrophic factor in the eye, as far as we are aware, was carried out in the rcd-1 dog with retinal degeneration (Tao et al., 2002) and in that case the most protective doses were accompanied by morphological changes in the retina (Zeiss et al., 2006). It should be noted that in the present study, the more sensitive OKR thresholds were still slightly reduced at therapeutic doses of 100 ng at 21 days PI and 10 ng at 6 days PI, but these effects were extremely small. The significance of these small reductions is unclear.

The fact that CNTF is neuroprotective in many forms of retinal degeneration in laboratory animals provided the impetus, in part, to a Phase I clinical trial of CNTF

delivered by encapsulated cell intraocular implants in patients with retinitis pigmentosa that was successfully completed recently (Sieving et al., 2006). What consequences do the present findings have for clinical application of CNTF? Precise applicability of our findings to human retinas must be qualified for several reasons. First, accurate dose comparisons are difficult to make. The doses released in the first human trial with encapsulated cell devices were about 109 ng/day (with a reduction to 0.28 ng/day at 6 months after implantation) with the lower-dose device, and 162 ng/day (with a reduction to 1.53 ng/day at 6 months) with the higher-dose device (Sieving et al., 2006). On the one hand, these doses are probably below the threshold for ERG suppression, even in the present study, but in addition, these doses in the human trials were diluted about 200 times more than in the rat eye due to differences in eye size (vitreous volume approximately 4 ml in human eye, 20 µl in rat eye). Moreover, rat CNTF was used in the present study, which is 4-5 times more potent than human CNTF (Masiakowski et al., 1991) in the clinical trial. On the other hand, the CNTF in the human trials is released continuously, and the consequences of even low-dose continuous release are difficult to assess. Second, there are species differences reported in the localization of CNTFRα to photoreceptor cells, and rodent retinas may differ from human retinas in this regard (Beltran et al., 2005). Third, it is probable that degenerating photoreceptor cells respond differently to various agents than do normal photoreceptors. Zeiss et al. (Zeiss et al., 2006) found that continuous application of CNTF had a more adverse affect on *rcd-1* dog retinas than on wild-type dog retinas. However, while AAV-vectored CNTF suppresses ERG responses in wild-type mouse retinas (Schlichtenbrede et al., 2003), we have found that the same AAVCNTF vector used in the present study can cause overt photoreceptor

degeneration in the same strain (C57BL/6) of wild-type mice in the region of injection (and presumably highest concentration of CNTF) (LaVail MM et al., unpublished observations). The same vector never resulted in this cell loss in *rds*$^{+/-P216L}$ mouse retinas (Bok et al., 2002) adding further to the idea that normal retinas may be more sensitive to the negative effects of high doses of CNTF than are degenerating retinas. Finally, it is clear that retinal function was affected adversely by the large dose of CNTF. CNTF can cause synaptic reorganization (Lowenstein et al., 1993) and that these changes may also be dose dependent.

Thus, there is still much to learn about the protective and possible negative actions of CNTF, and how they relate to retinas undergoing inherited retinal degenerations. It is clear that very high doses of CNTF applied to the retina can cause reduction in ERG response amplitudes, elevation of luminance thresholds as measured at the superior colliculus, reduction in visual acuity and behavioral tracking responses and, in some cases, outright loss of photoreceptors. Thus, therapeutic application of CNTF in retinal degenerations needs to be closely monitored to prevent these negative effects, should they occur in the human retina. However, our dose-response studies strongly support the notion that a therapeutic dose of CNTF exists that does not suppress ERG responses (Bush et al., 2004).

5. Summary

Growth factor delivery into the vitreous or sub-retinal space in high concentrations causes death of photoreceptors as well as decreases in ERG wave amplitudes and reductions in behaviorally measured visual thresholds. A single high dose of recombinant CNTF into the vitreous caused a temporary shortening of

photoreceptor outer segments but no inner retinal changes, however, visual thresholds were suppressed far longer than the time it took for ERG and ONL measurements to return to normal. Sub-retinal delivery of AAV-CNTF caused, in addition to the photoreceptor impairments, changes in Muller cells consistent with inner retinal changes seen in retinal degenerations (Jones and Marc, 2005), although not to such a dramatic extent. Furthermore, the changes in photoreceptors and Muller cells paralleled persistently decreased optokinetic visual thresholds and visual acuity impairments, however no other inner retinal neurons appear to be affected by the introduction of CNTF (Rhee et al., 2007). Although we cannot discount the potential effects of a small retinal detachment caused by the injection itself, the results suggest that changes in endogenous CNTF levels may trigger Muller cell activation and mobilization in retinal degenerations, and that reducing Muller cell activity will play a significant role in attempting to maintain normal function when treating degenerating retinas. Although in this particular portion of the study, the Muller cell changes could not be separated from the damaging effects seen on the photoreceptors themselves, the results appear to provide support for the visual adaptation model.

Chapter III – RCS rat in VOS

1. Introduction

A popular model for studying human retinal degenerative disease is the Royal College of Surgeons (RCS) rat. The RCS rat has a mutation in the gene *mertk*, which has a human orthalogue (D'Cruz et al., 2000) that results in the inability of retinal pigment epithelial (RPE) cells to perform their normal phagocytotic function on photoreceptor outersegments (Mullen and LaVail, 1976). Ultimately, this loss of function mutation results in the progressive death of photoreceptors (Mullen and LaVail, 1976), loss of ERG wave amplitudes (Sauve et al., 2004), and degeneration of behaviorally measured visual acuity (McGill et al., 2004a). In addition, recent studies have shown that changes in inner retinal neurons occur in late stages of degeneration, typically beginning around 6 months of age or later (Marc et al., 2003; Jones and Marc, 2005; Wang et al., 2005a; Marc et al., 2007; Pinilla et al., 2007). Subsequent studies have evaluated visual acuity following cell transplantation (McGill et al., 2004b; McGill et al., 2007a) in the RCS rat and showed that visual acuity can be preserved for up to at least 7 months, and that with successful transplantation, inner retinal changes can be significantly delayed (Wang et al., 2005a; Pinilla et al., 2007).

The use of the VWT in the behavioral studies described above were limited in that the training and testing procedures required by the task to quantify visual thresholds required a significant period of time, and therefore, limited the number of thresholds that could be generated to ~1 per month. More recently, Prusky et al., (Prusky et al., 2004a) developed a Virtual Optomotor System (VOS) which can be used to examine acuity

thresholds and generate contrast sensitivity curves through each eye independently on a daily basis. A further advantage of the VOS is that it does not require prior training of the animal to generate visual thresholds. Recently, Douglas et al. (Douglas et al., 2005) employed the VOS for the purpose of characterizing spatial frequency thresholds and contrast sensitivity curves of non-dystrophic pigmented mice and rats. The results of this study showed that using the VOS, spatial frequency thresholds were lower than in the VWT, however, contrast sensitivity thresholds were more highly sensitive at lower spatial frequencies. In addition, the study showed that thresholds generated in the VOS are not dependent on the visual cortex (Prusky et al., 2008), whereas visual thresholds measured in the VWT have been shown previously to be cortex dependent (Prusky et al., 2000d). Another difference between the tasks is the visual stimuli. Although nearly identical sinusoidal gratings are used, the VOS relies on moving gratings, whereas the gratings used in the VWT are static. Finally, the thresholds generated using the VOS are a reflexive based response to stabilize visual information on the retina rather than measuring a perceptual based choice between stimuli as in the VWT.

Due to the popularity of the VOS for use in screening animals with visual deficits, and for evaluating treatment success in the RCS rat, it was important to characterize the visual degeneration profile of the RCS rat in the VOS from an early age until thresholds can no longer be measured, similar to the procedure used in the VWT (McGill et al., 2004a). In addition, this provided an opportunity to examine whether early inner retinal changes occur in the RCS rat and if so, could these changes be linked to any deficits in visual function. The results of this study should yield 3 important findings: 1) a profile of visual deterioration which allows for comparison between cortical and sub-cortical based

visual thresholds as the retina degenerates 2) a timeline which elucidates more clearly when inner retinal changes begin and what specific changes occur, and 3) will provide a background for evaluating therapeutic interventions such as cell transplantation in an animal model of human retinal degenerative disease.

In this study, the established model would predict that visual thresholds should deteriorate in a relatively linear fashion with photoreceptor degeneration. That is, when 100% of photoreceptors are present, visual thresholds should be at normal values. When the retina has degenerated to 90% of photoreceptors surviving, visual thresholds should measure near 90% of normal, and so on. The visual adaptation model, on the other hand, suggests that visual thresholds may not decrease in a linear fashion with relation to photoreceptor survival, but rather, that changes to the circuitry within the retina may occur throughout the course of visual degeneration, and that these changes account, at least in part, for the visual decline.

2. Methods

2.1 Animals

All procedures used in this study conform to the University of Lethbridge's animal welfare protocols which are approved and governed by the Canadian Council on Animal Care (CCAC) and are also in accordance with the ARVO Statement on the Use of Animals in Ophthalmic and Vision Research.

Six Long Evans hooded rats, six non-dystrophic RCS rats (rdy^-, p^+), and six dystrophic RCS rats (rdy^+, p^+) were used in this study. Long Evans rats were bred from stock originally obtained from Charles River and raised in the Canadian Centre for

Behavioural Neuroscience (CCBN) vivarium. RCS breeding pairs were obtained from the Lund laboratory at the University of Utah and their offspring were born and raised at the CCBN. Long-Evans rats and non-dystrophic RCS rats of both sexes were tested as adults, 6-12 months of age. Dystrophic RCS rats of both sexes were tested monthly beginning around one month of age. For the duration of the experiment, all animals were housed in the same room with an ambient temperature of 21C°, 35% relative humidity, 12-hour light cycle, where food and water were available ad libitum. The housing consisted of transparent plexiglas cages (35cm L x 20cm W x 13cm H) hanging on a rack with other cages.

2.2 Virtual Optokinetic System (VOS)

The apparatus consists of four computer monitors positioned around a square testing arena. An unrestrained rat is placed on a platform in the center of the arena and a sine wave grating drawn on a virtual cylinder projected on the monitors in 3D coordinate space (Figure 2; OptoMotry©; CerebralMechanics). A video camera provides real-time video feedback from above, and the position of the head on each frame is used to continually center the hub of the cylinder at the rat's viewing position. On each trial the cylinder is rotated at a constant speed (12 °/s) and the experimenter judges whether the rat makes tracking movements with its head and neck to follow the drifting grating (Figure 3). The spatial frequency threshold, the point at which animals no longer tracked, was obtained by incrementally increasing the spatial frequency of the grating at 100% contrast. Contrast sensitivity thresholds were measured at up to eight different spatial frequencies by systematically decreasing the contrast until no tracking was observed. Thresholds through each eye were measured separately by reversing the rotation of the

cylinder (Douglas et al., 2005). Experimenters were blind to previously-recorded thresholds and treatment conditions whenever possible, and thresholds were regularly confirmed by more than one observer.

2.3 Visual Water Task (VWT)

The VWT is a visual perception task previously described in detail (Prusky et al., 2000b; Prusky et al., 2000a, c, d; Prusky et al., 2002; McGill et al., 2004a; McGill et al., 2004b; Prusky and Douglas, 2004; Prusky et al., 2004b). Briefly, a trapezoidal-shaped pool with a midline divider at the wide end is filled with water to submerge a hidden escape platform. Two computer monitors face into the wide end of the pool. The platform is always placed directly below the monitor displaying the positive (grating) stimulus, and nothing is placed below the monitor displaying the negative (gray) stimulus of the same luminance. The left/right positions of the stimuli are alternated randomly over trials (Figure 1; Vista©, CerebralMechanics).

Training and testing procedures were the same as described elsewhere (Prusky et al., 2000a; McGill et al., 2004a). Two sets of visual stimuli were used: the first set consisted of a sinusoidal grating and a grey screen of the same mean luminance, the second set consisted of sinusoidal gratings on both screens, however, one grating was moving rightward, and the other moving leftward. Moving gratings drifted at a rate of 12 degrees per second (d/s). Using both sets of stimuli, animals were tested in blocks of trials at progressively incrementing spatial frequencies until they could no longer distinguish between the stimuli at a minimum of 7/10 correct. Accuracy for a given frequency was measured in blocks of 10 trials when near threshold and shorter blocks at

the low spatial frequencies, thereby minimizing the number of trials far away from threshold. Acuity was calculated as the 70% correct point on a best-fit curve of the data. The same procedure was used for both static and moving discriminations.

2.4 Immunohistochemical preparation

To perform the immunohistochemical analysis of the RCS rat retinas, we established collaboration with Dr.'s Steve Fisher and Geoff Lewis at the University of California, Santa Barbara. Dr. Fisher and Dr. Lewis are experts in the field of retinal remodeling and have extensive knowledge and expertise in immunohistochemical evaluations of the retina.

2.4.1 Tissue preparation

Animals were euthanized by lethal dose of euthansol (sodium pentabarbitol, 0.3 ml/kg), eyes were marked for orientation, removed, and immediately immersion fixed using a mixture of 4% paraformaldehyde in phosphate buffered saline. The cornea and lens were then removed, and the eyecup was cut in half. One half of the eye was stored in the fixative solution. From this sample, small areas of retina were excised and embedded in low-melting-point agarose then sectioned at 100 μm. Sections were then labeled with various antibodies to photoreceptors, second and third order neurons, synaptic vesicles and ribbons, and glial and microglial proteins: Their distribution was determined using an Olympus FluoView confocal microscope.

2.4.2 Immunohistochemistry

For confocal analysis, 100-um-thick agarose-embedded sections were cut on a microtome (Vibratome, Technical Products International, Polysciences, Warrington, PA) and blocked overnight at 4°C in normal donkey serum (1:20) containing 0.1 M phosphate-buffered saline (PBS), 0.5% bovine serum albumin (BSA; Fisher Scientific, Pittsburgh, PA), 0.1% Triton X-100 (Roche Molecular Biochemicals, Indianapolis, IN), and 0.1% sodium azide (Sigma, St. Louis, MO), together referred to as PBTA. The next day, the sections were incubated in primary antibodies overnight at 4°C on a rotator. The sections were then rinsed in PBTA and incubated in donkey anti-mouse or anti-rabbit IgG conjugated to the fluorochrome Cy2, Cy3, or Cy5 (Jackson ImmunoResearch Laboratories, Inc., West Grove, PA) overnight at 4°C on a rotator. Finally, the sections were mounted in 5% n-propyl gallate in glycerol and viewed on a laser scanning confocal microscope (model 1024; Bio-Rad, Hercules, CA). All antibody solutions were made in PBTA.

The primary antibodies used in this study were a mouse monoclonal antibody to rod opsin (Rho4D2, 1:50; provided by Robert Molday, University of British Columbia, Vancouver, British Columbia, Canada),a mouse polyclonal antibody to Vimentin (1:100; Dako, Carpinteria, CA) a rabbit polyclonal antibody to synaptophysin (1:100; Dako, Carpinteria, CA), a rabbit polyclonal antibody to glial fibrillary acidic protein (GFAP, 1:400; Dako, Carpinteria, CA), a goat polyclonal antibody to Chat (1:50; Chemicon), a rabbit polyclonal antibody to PKC-beta (1:100; Biomol. Res. Labs). In addition, some sections were stained with biotinylated peanut agglutinin (PNA) lectin (400 g/mL; Vector

Laboratories, Burlingame, CA) and Isolectin B4 (0.5mg; Vector Laboratories, Burlingame, CA; 1:50).

3. Results

3.1 Spatial Frequency and Contrast Sensitivity thresholds in Non-dystrophic rats

Spatial frequency thresholds of both adult Long-Evans (LE) and non-dystrophic RCS (NDRCS) rats were ~0.530 c/d, comparable to that measured previously in the VOS (Douglas et al., 2005; Figure 14). These spatial frequency thresholds were substantially lower than visual acuity measured from the same strains of rats in the VWT (McGill et al., 2004a). Contrast sensitivity curves for Long-Evans and NDRCS rats were nearly identical to each other, and to previously published data (Douglas et al., 2005). Each curve had a typical inverted U-shape with peak sensitivity at ~0.1 c/d (Figure 15).

3.2 RCS rat Spatial Frequency thresholds and Contrast Sensitivity

Dystrophic RCS rats were tested from 4-41 weeks of age, over which time spatial frequency threshold dropped from 0.53 c/d to less than 0.08 c/d (Figure 16). Contrast sensitivity was measured weekly and was near normal at 4 weeks of age, but degenerated rapidly thereafter (Figure 17). Figure 18 displays the contrast sensitivity at spatial frequency throughout the course of visual deterioration. High spatial frequencies lost sensitivity to contrast first whereas low and peak spatial frequencies retained sensitivity longest. For both spatial frequency and contrast thresholds, there was a rapid decline in sensitivity until the 19th week, after which sensitivities declined more slowly (Figure 16, Figure 18).

3.3 Task comparison

Comparison of thresholds measured from the RCS rat in the Visual Water Task (McGill et al., 2004a) and the Virtual Optokinetic System yielded an interesting result that from 3 months of age onward, the visual thresholds measured in each task are not statistically different, however, thresholds measured early are higher in the VWT than in the VOS: 0.83 c/d and 0.53 c/d, respectively (Figure 19). These thresholds are near non-dystrophic values (1.0 and 0.53 c/d, respectively) and therefore, in part, prompted further investigation into the differences in measured thresholds between the VWT and the VOS. An obvious difference between the tasks is the static versus moving sine-wave gratings. Fortunately, the Vista software was capable of generating moving sine-wave gratings, leftward moving on one screen, and rightward on the other. Using Long-Evans rats, we first trained them to perform the static grating versus grey discrimination (Figure 20A). Once trained, all animals performed the task at near perfection up to a spatial frequency of ~0.8 c/d. Beyond that, animals made increasing numbers of errors but remained above the 70% criterion until about 0.95 c/d. The acuity was determined to be 0.965 c/d (SEM=0.068; n=6; Figure 20C), a value similar to those reported previously (Dean, 1978, 1981; Prusky et al., 2000a; McGill et al., 2004a). Subsequently, the same animals were trained to discriminate between a leftward and a rightward moving sine-wave grating which drifted at a constant rate of 12 degrees-per-second. Due to the previous training and static grating testing, animals quickly learned to discriminate between gratings moving in opposite directions (Figure 20B). The animals performed at near 100% until ~0.45 c/d, resulting in a motion acuity of ~0.512 c/d (SEM=0.021; Figure 20C).

Interestingly, this value closely resembles the spatial frequency thresholds obtained in the VOS.

3.4 Immunohistochemical analysis

Immunohistochemical staining of RCS rat retinas at P28 showed a near normal looking retina exhibiting proper lamination of the retina, rod opsin localized in the rod outer segments, and little evidence of abnormalities within horizontal or ganglion cells (Figure 20A). RCS rat retinas at P56, and P149 (Figures 20B and C) showed evidence of photoreceptor degeneration and ganglion cell activation. In addition, by P149 severe photoreceptor degeneration is obvious (Figure 20C), ganglion cell migration and filament growth are extending into the INL (Figure 20C) has begun, as well as growth of horizontal neurites are evident in the outer retina (Figure 20C).

In addition, at P28 (Figure 21A) and P56 (Figure 21B), Muller cells have mostly normal processes through the retina, however, some Muller cell changes are evident. Significant Muller cell sprouting into in the subretinal space becomes quite obvious by P149 (Figures C & D). In addition, by P149, RCS rats show significant bipolar cell neurite sprouting.

4. Discussion

This study is the first longitudinal description of OKR spatial frequency and contrast sensitivity thresholds in the RCS rat. Previously, we (McGill et al., 2004a) evaluated the spatial vision of the RCS rat in a visual perception task in order to provide a background for cell transplantation studies. We found that non-dystrophic animals had acuity and contrast sensitivity typical of a pigmented laboratory rat, and the dystrophic strain showed a progressive decline in visual acuity from ~80% of normal at P30 to

immeasurable levels in most animals by P330 (McGill et al., 2004a). Those results indicated that the mutation in *mertk* (D'Cruz et al., 2000) was responsible for the loss of vision in dystrophic RCS rats, and that no significant visual abnormalities were present in the background strain. The results of the present study, using measurements of OKR, confirm this conclusion by showing that the non-dystrophic RCS rats had normal OKR spatial frequency and contrast sensitivity, and dystrophic animals degenerated from normal values at 4 weeks of age, to no response by 41 weeks. Although spatial frequency thresholds in the two tasks differ in normal animals (i.e. VWT ~1.0 c/d; VOS ~0.53 c/d; Figure 19), after ~12 weeks of age in dystrophic RCS rats, thresholds measured in both tasks are essentially the same (Figure 19). This indicates that in the late stages of visual degeneration in the RCS rat, using the VOS is most practicable because the task requires no reinforcement training and multiple thresholds can be measured on a daily basis.

Another distinct advantage to using the VOS is that the task enables the repeated measurement of contrast sensitivity in animals with a degenerating retina, which is not feasible with the VWT. The contrast sensitivity curve of adult non-dystrophic RCS rats measured with the VOS displayed a typical inverted-U shape. (Birch and Jacobs, 1979; Keller et al., 2000; McGill et al., 2004a; Prusky et al., 2004a; Prusky and Douglas, 2004) However, sensitivity is generally higher than that measured in the VWT, and peak sensitivity is ~0.1 c/d, which is a lower spatial frequency than that obtained from the VWT (~0.2 c/d) (McGill et al., 2004a; Douglas et al., 2005). We have not measured contrast sensitivity in dystrophic RCS rats using the VWT because the length of time required to generate a curve precludes accurate measurements in animals with a degenerating retina. Using the VOS in the present study, we found that contrast

sensitivity of dystrophic RCS rats at 4 weeks of age was similar to that of adult non-dystrophic rats (Figure 16), indicating that when the retina is relatively intact, it supports normal function. As the retina degenerated contrast sensitivity decreased steadily at all spatial frequencies. Sensitivity at the two highest spatial frequencies tested (0.40 and 0.27 c/d) degenerated to immeasurable levels quickest (Figure 17), paralleling the results of the loss of spatial frequency sensitivity (Figure 18). Lower spatial frequencies appeared to lose contrast sensitivity in two phases: an early fast degenerating phase which lasted until ~20 weeks of age, followed by a slower phase. This may be because the loss of retinal circuits in the RCS rat is not linear, or that the visual system compensates for the loss of circuits in a non-linear way.

Another difference between the VOS and the VWT is that the VOS displays the sine-wave gratings on a rotating virtual cylinder, whereas the display stimulus in the VWT uses a static grating on one screen versus a grey screen of the same mean luminance. Therefore, we decided to evaluate the spatial frequency thresholds of Long-Evans rats using both standard visual stimuli (static grating) and moving visual stimuli. Spatial frequency thresholds measured using moving gratings were approximately 50% lower than using static gratings, and closely resembled OKR thresholds measured in the VOS. In the VWT, the animals did not appear to be generating and OKR to the moving stimuli, but rather making a perceptive choice between the oppositely moving stimuli. This is supported by the fact that each animal spent longer than usual periods at the choice point, and viewed each monitor repeatedly before making a decision (Prusky lab, unpublished observations). Granted, this is to be expected given that the moving visual stimulus was a more difficult stimulus to discriminate.

Perception of light (LaVail et al., 1974) and the pupillary light reflex (Trejo and Cicerone, 1982) are sustained until photoreceptor loss is near complete, however, when compared to the present study, these measures are not nearly as sensitive as the VOS. Previous studies using head tracking (Coffey et al., 2002) have shown that that non-dystrophic rats respond at better than 0.500 c/d and responses in the dystrophic RCS rats are lower at 23 weeks of age, and the present study confirms that indeed non-dystrophic rats have spatial frequency thresholds slightly above 0.500 c/d, and that dystrophic RCS rats are capable of responding to this stimulus early in life. However, the responses measured in the Coffey et al. study were not characterized in a psychophysical manner or longitudinally as in the present study, limiting the accuracy of the assessment of visual responses (Douglas et al., 2005). Moreover, the present study provides the necessary characterization of RCS rat OKR vision which should be used as background for studies which involve potential therapeutics.

When compared to photoreceptor survival, the extended period that RCS rats could generate an OKR to the stimuli in the VOS suggests that some phototransduction must occur. Because the light levels in the VOS are well within the photopic range, where any surviving rod photoreceptors are likely saturated, the extended timeframe of measurable vision is likely the effect of sporadic cone photoreceptor survival. Using a flicker ERG paradigm Pinilla et al. (Pinilla et al., 2005b; Pinilla et al., 2005a) have suggested that the photopic ERG b-wave is driven primarily by cones, and that cone function in the RCS rat can be measure up to ~200 days of age using this method. These results, along with the extensive loss of rod photoreceptor function and cell bodies at late

ages (LaVail et al., 1975; Girman et al., 2005; Wang et al., 2005a) suggests that that the behavioral response is in fact mediated by surviving cone photoreceptors.

The OKR is likely to be a subcortical response mediated by the Accessory Optic System (AOS; (Hoffmann, 1989; Hoffmann and Distler, 1989; Ilg and Hoffmann, 1996)). The Nucleus of the Optic Track (NOT) and the Dorsal Terminal Nucleus (DTN) of the AOS are the nuclei concerned with horizontal tracking (Schiff et al., 1988; Hoffmann, 1989; Hoffmann and Distler, 1989; Ilg and Hoffmann, 1996) and cells in these nuclei have large receptive fields (Hoffmann and Distler, 1989) which is consistent with a lower spatial frequency preference. It should be noted that the above studies were in primates, however it is probable that the AOS functions similarly in the rat (Reber et al., 1991; Schmidt et al., 1993).

Whether vision was measured in the VWT or the VOS, thresholds were measurable for up to 10-11 months of age, an age which in the RCS rat has been shown previously to exhibit significant retinal reorganization. By 9 months of age, there is Muller cell hypertrophy and displaced RPE cells embedded within the neural retina (Marc et al., 2003). Inner nuclear layer neurons migrate to the ganglion cell layer and some ganglion cells move towards the distal retina. In addition, there is massive focal loss of ganglion cells, bipolar cells, and amacrine cells even in central retina (Jones et al., 2003; Marc et al., 2003; Jones and Marc, 2005; Marc et al., 2007). Neurons of all classes, including horizontal, bipolar, amacrine and ganglion develop abnormal processes extending outside the normal lamination of the plexiform layers (Jones et al., 2003; Marc et al., 2003; Jones and Marc, 2005; Marc et al., 2007). Moreover, evidence of vascular invasion has also been well documented (Villegas-Perez et al., 1998) which leads to

compression of retinal structures and compromises of ganglion cell viability (Wang et al., 2003). Finally, myelinated processes have been observed in the RCS rats (Jones et al., 2003) raising the possibility that ganglion cells generate intra-retinal axonal fields that likely contribute to corruptive circuitry within the retina (Jones et al., 2003; Marc et al., 2003; Jones and Marc, 2005; Jones et al., 2005; Marc et al., 2007). The findings in the present study confirm that some of these retinal reorganization changes such as Muller cell activation and elongation of processes occur as early as P28 (Figure 22). These changes in Muller cells become more evident by P56 as these processes invade the inner nuclear layer, and by P149 significant Muller cell sprouting all the way into the sub-retinal space has occurred (Figure 22). Furthermore, changes in ganglion cells such as growth of filaments and migration of the cells themselves is evident by P56, and by P149 (Figure 21). Moreover, significant bipolar cell sprouting has occurred (Figure 23) by P149. Although we cannot parse the functional effects of photoreceptor loss from the effects of reorganization itself in this study, it is clear that with increasing reorganization of the retina there is increasing deficits in behaviorally measured visual function.

5. Summary

The results of this study support the visual adaptation model of visual system function. Photoreceptor degeneration in the RCS rat occurs over approximately 24 weeks whereas visual thresholds remained at ~40% of normal values at that time point. In addition, visual thresholds were measurable out to ~41 weeks, an age which could not be predicted by the established model. Furthermore, immunohistochemical analysis in this study shows that early retinal reorganization does occur in the RCS rat and as photoreceptor degeneration progresses, so does the degree of remodeling. The initiation

of photoreceptor degeneration and retinal remodeling begins at nearly the same age in conjunction with abnormalities in behaviorally measured visual thresholds. In addition, comparative data from a related study (McGill et al., 2004a) show that at ages with little photoreceptor loss (Figure 4), there is already a significant reduction in visual acuity which suggests that early retinal remodeling may be responsible for such loss of function.

Chapter IV – Schwann cell transplantation

1. Introduction

Retinal degenerative diseases (RDD's) are a leading cause of vision loss and blindness. One approach to treating RDDs is retinal cell transplantation which, when undertaken early in the course of degeneration in an animal model of RDD (McGill et al., 2004a), can limit the loss of vision (McGill et al., 2004b). McGill et al. (McGill et al., 2004b) reported that both human retinal pigment epithelial cell line (ARPE19) and human Schwann cell transplants delayed vision loss, and complementary studies have shown that both cell types preserve photoreceptors (Lawrence et al., 2000; Lund et al., 2001; Coffey et al., 2002; Lawrence et al., 2004; Wang et al., 2005b), electrophysiological responses (Lawrence et al., 2000; Lund et al., 2001; Coffey et al., 2002), and the duration of optokinetic tracking (Lawrence et al., 2000; Lund et al., 2001; Coffey et al., 2002; Lawrence et al., 2004). Collectively these studies support retinal cell transplantation as a treatment for RDD.

A major problem for translating the above studies into clinical practice is that the donor cells were derived from cell lines (Dunn et al., 1996) (ARPE19) or were harvested from xenogeneic stock (Casella et al., 1996) (human Schwann cells), leaving them vulnerable to immune system rejection. The specific need for immune suppression in cell transplantation studies has previously been demonstrated by showing that allogeneic cell grafts were rejected by the host immune system when transplanted into rat (Larsson et al., 1998) or mouse eyes (Jiang et al., 1995). As a consequence, the above studies used immune suppressants to maintain the viability of transplanted cells. Although immune

suppression is routine with major organ transplants, it is not desirable, particularly in the elderly population in which RDDs are most prevalent.

Syngeneic transplantation, in which the cells harvested and transplanted are genetically identical to the host, would in principle, not require immune-suppression because the transplanted cells should not be recognized by the host immune system as foreign. Larsson et al. (Larsson et al., 1998) previously confirmed that cells of syngeneic origin were not rejected when transplanted into rat eyes. Therefore, a possible approach in the RCS rat would be to harvest biopsied RPE, culture, genetic repair, and replace the cells back into the rat retina. However, this procedure is not practical because of the small eye of the rat, removal of all incompetent RPE would be near impossible, and this procedure would require multiple surgeries in an already compromised retina likely increasing retinal cell loss.

Schwann cells provide a promising source of cells for syngeneic transplantation because they can be harvested with relative ease from adult donors, can survive and proliferate in culture, and have previously been shown to limit the loss of vision in RCS rats (D'Cruz et al., 2000; McGill et al., 2004b) possibly through a paracrine effect (Faktorovich et al., 1990; Hammarberg et al., 1996). In the present study, we evaluated a model of syngeneic Schwann cell transplantation by harvesting Schwann cells from dystrophic RCS rats and transplanting them into dystrophic RCS rats. Because the RCS rat is highly inbred, cells transplanted within strain should not be recognized as foreign by the host immune system, however, allogeneic transplanted cells should be more vulnerable to rejection (Larsson et al., 1999). Jiang et al.,(Jiang et al., 1995) supported this assertion by showing that in mice, at 12 and 35 days post-injection, syngeneic

transplants thrived, however, allogeneic transplants appeared healthy at 12 days post-injection, but by 35 days post-injection the allogeneic grafts were significantly reduced in size, although not completely eradicated. The goal of the present study was to test whether immune-privileged (syngeneic) Schwann cells preserve vision in the RCS better than non-privileged (allogeneic) cells, without the use of immune system suppression, providing a model of autologous transplantation for the treatment of RDD.

Due to the previous success of Schwann cell transplants in preventing photoreceptor loss, and the increased syngeneic cell viability compared to allogeneic cells, the established model would predict that the syngeneic Schwann cells will prevent the loss of photoreceptors and the loss of vision to the same degree. Conversely, the visual adaptation model predicts that syngeneic Schwann cell transplantation will prevent vision loss, which will ultimately be the result of preventing retinal remodeling and photoreceptor degeneration, although the degree of photoreceptor preservation is not as directly relevant as in the established model.

2. Methods

2.1 Animals

Pigmented dystrophic RCS rats (*rdy*$^-$, *p*$^+$; n=30), non-dystrophic RCS rats (*rdy*$^+$, *p*$^+$; n=6), and Long-Evans rats (n=6) were used in this study. Animals were housed in rooms with a 12-hour dark/light cycle, a constant temperature of 22°C, and food and water were available *ad libitum*. Animals were housed and handled with the authorization of the Institutional Animal Care and Use Committee (IACUC) at the University of Utah, and the University of Lethbridge Animal Care Committee, which

only approve procedures that are in accordance with National Institute of Health (NIH), Canadian Council on Animal Care (CCAC) guidelines respectively. All procedures used in this study conform to the ARVO Statement for the Use of Animals in Ophthalmic and Vision Research.

2.2 Donor Cells

Sciatic nerves were dissected and transferred to Leibowitz's L15 medium. After removal of contaminating tissue, the nerves were cut into 100-µm pieces in a McIlwain tissue chopper and digested in a collagenase/trypsin mixture for 90 minutes at 37 ºC. The digestion was stopped with Dulbecco's modified Eagles medium plus 10% fetal calf serum. After cells were centrifuged at 1000 rpm for five minutes, they were re-suspended in medium and titrated through a glass capillary and a 25-gauge needle. Cells were plated onto poly-L-lysine coated 35 mm dishes in DMEMF, plus glutamine, pyruvate, and penicillin-streptomycin and incubated at 37ºC-5% CO_2. After 24 hours, the medium was changed to remove unattached cells and debris. One week later, cells were removed from the dish with trypsin-EDTA and suspended in DMEM without FCS. This suspension was penned by incubating at 37ºC in a 100mm dish previously coated with rabbit anti-rat IgG. Cells were ready for transplantation within 24-48 hours. After counting the number of contaminating fibroblasts (5-7%), cells were removed from the dish as before. Because Schwann cells are far less adherent to the dish than fibroblasts, and are morphologically distinct, it was possible to reduce further the number of contaminating cells by selecting only those cells that move into suspension rapidly while watching under a microscope. Once most cells have lifted, the medium was added to

stop the reaction. Syngeneic Schwann cells were derived from dystrophic RCS rats, and allogeneic Schwann cells from Long-Evans rats.

2.3 Transplantation

Transplantations were performed at the University of Utah. A modification of the procedure used by Keegan et al., (Keegan et al., 2003) was used in this experiment. Briefly, host rats (dystrophic RCS, n=18) were anesthetized with a ketamine/xylazine mixture and received monocular sub-retinal transplants of syngeneic Schwann cells (1 X 10^4 cells in 2μL of medium) or allogeneic Schwann cells (1 X 10^4 cells in 2μL of medium) at P21. Grafts were introduced trans-sclerally into the sub-retinal space in the dorso-temporal quadrant of the right eye with a glass micropipette (outer-diameter, ~150μm, inner diameter ~75μm) attached to a 10μL syringe (Hamilton, Reno, NV).

2.4 Behavioral Assessment of Vision

Following transplantation, the animals were shipped to the University of Lethbridge for behavioral evaluation. Previously, we used a visual perception task (Visual Water Task, VWT) (Prusky et al., 2000a) to measure grating acuity in dystrophic RCS rats following ARPE19 and human Schwann cell transplantations (McGill et al., 2004b). Although grating thresholds in rats measured in the VWT are probably the most comparable measure of vision to clinical assessments of acuity, the task requires a lengthy training and testing period for each threshold (on the order of weeks for each eye), limiting the number of thresholds that can be measured over the course of retinal degeneration in RCS rats. The repeated measurement of contrast sensitivity in dystrophic RCS rats is even more problematic when using the VWT, because significant retinal

degeneration occurs over the time it takes to measure a full contrast sensitivity curve (on the order of months). Recently, we developed a Virtual Optokinetic System (VOS; Douglas, 2005 #19; Prusky, 2004 #50}), which allows for rapid, repeated measurements of spatial frequency and contrast sensitivity thresholds of the optokinetic response (OKR). Using the VOS, spatial frequency thresholds and contrast sensitivity curves can be generated through each eye on a daily basis, enabling the longitudinal measurement of visual function in rats with retinal degeneration. In the present study, we took advantage of the strengths of each of the above tasks to evaluate over an extended period of time, the effects of retinal Schwann cell transplants on vision. In order to evaluate the effects of syngeneic and allogeneic Schwann cell transplants on preserving vision in the dystrophic RCS rat, we measured spatial frequency and contrast sensitivity of the optokinetic response through each eye weekly from 10 to 35 weeks of age. We separately measured grating acuity in the VWT binocularly at 16 weeks, and monocularly at 24 and 28 weeks.

2.4.1 Virtual Optokinetic System

Apparatus consists of four computer monitors positioned around a square testing arena. An unrestrained rat is placed on a platform in the center of the arena and a sine wave grating drawn on a virtual cylinder projected on the monitors in 3D coordinate space (OptoMotry©; CerebralMechanics). A video camera provides real-time video feedback from above, and the position of the head on each frame is used to continually center the hub of the cylinder at the rat's viewing position. On each trial the cylinder is rotated at a constant speed (12 °/s) and the experimenter judges whether the rat makes tracking movements with its head and neck to follow the drifting grating. The spatial frequency threshold, the point at which animals no longer tracked, was obtained by

incrementally increasing the spatial frequency of the grating at 100% contrast. Contrast sensitivity thresholds were measured at up to eight different spatial frequencies by systematically decreasing the contrast until no tracking was observed. Thresholds through each eye were measured separately by reversing the rotation of the cylinder (Douglas et al., 2005). Experimenters were blind to previously-recorded thresholds and treatment conditions whenever possible, and thresholds were regularly confirmed by more than one observer.

2.4.2 Visual Water Task

The VWT is a visual perception task previously described in detail (Prusky et al., 2000a; Prusky et al., 2002; McGill et al., 2004a; McGill et al., 2004b). Briefly, a trapezoidal-shaped pool with a midline divider at the wide end is filled with water to submerge a hidden escape platform. Two computer monitors face into the wide end of the pool. The platform is always placed directly below the monitor displaying the positive (grating) stimulus, and nothing is placed below the monitor displaying the negative (gray) stimulus of the same luminance. The left/right positions of the stimuli are alternated randomly over trials (Vista©; CerebralMechanics).

Training and testing procedures were the same as described elsewhere (McGill et al., 2004a; McGill et al., 2004b), except animals were tested with both eyes open at 16 weeks of age, and through each eye separately at 24 and 28 weeks. Monocular testing required placing a small occluder over one eye during each trial, which was removed immediately following the trial. In the event that the occluder became dislodged, that trial was disregarded and a new trial was run. When animals were no longer able to

distinguish between a single grating cycle and a gray screen in the un-operated eye, the stimuli were changed to a black screen (negative) and a white screen (positive), which together subtended ~0.015 cycles-per-degree (c/d). Animals were tested in blocks of trials at progressively incrementing spatial frequencies until they could no longer distinguish between the stimuli at a minimum of 7/10 correct. Accuracy for a given frequency was measured in blocks of 10 trials when near threshold and shorter blocks at the low spatial frequencies, thereby minimizing the number of trials far away from threshold. Acuity was calculated as the 70% correct point on a best-fit curve of the data. All testing was done early in the light phase of the circadian cycle. Thresholds through each eye were obtained in sequence.

2.5 Anatomical analysis

Animals were euthanized by lethal dose of euthansol (sodium pentabarbitol, 0.3 ml/kg) and perfused transcardially with phosphate buffered saline (PBS). Eyes were marked for orientation, removed, and immediately immersion fixed using a mixture of 4% paraformaldehyde in phosphate buffered saline before being cryoprotected in 10% sucrose for 1 h, 20% sucrose for 1 h and 30% sucrose overnight at 4 °C. The following day, eye cups were embedded in OCT and 10 μm thick sections were cut on a cryostat in a horizontal plane (to ensure that the area of retina containing the grafted cells was cut perpendicularly), and mounted on glass slides. Four sections were collected 50um apart in series of five. One series was used for cresyl violet staining to identify the injection site, lamination of the retina, and photoreceptor preservation, the rest were use for antibody staining. P75 antibody was used to label surviving Schwann cells, and for fluorescence microscopy DAPI was used as background for recoverin antibody which

was used to positively identify photoreceptors. Retinal sections were examined using both light and confocal microscopy. TIFF images were enhanced using Adobe Photoshop software.

2.6 Statistical Analysis

Data for OKR contrast sensitivity and spatial frequency thresholds and visual acuity thresholds are reported as group means. Differences between groups were analyzed by repeated measures ANOVA and Fishers post-hoc analysis using a $p<0.05$ level of significance.

3. Results

3.1 Effects of transplantation (VOS)

3.1.1 Spatial frequency thresholds

Spatial frequency thresholds measured through un-operated eyes, and through eyes with allogeneic Schwann cell transplants, were near 0.40 c/d at 10 weeks, and declined to ~0.1 c/d by 35 weeks of age (Figure 21). This deterioration in sensitivity followed the same trend as the background dystrophic controls (Figure 16). There was no significant difference between the allogeneic Schwann cell transplanted eyes, and un-operated eyes ($F_{(2,372)}=0.30$, $p=0.9704$; data not shown).

In contrast, spatial frequency thresholds measured through eyes that received syngeneic Schwann cell transplants were near normal (90-95%) at all ages tested (10-35 weeks; Figure 21). Compared to un-operated and allogeneic transplanted eyes, syngeneic transplanted eyes were significantly better at all ages ($F_{(3,384)}=5253.181$, $p<0.001$). The

most striking example of this difference is at 30 weeks of age: spatial frequency thresholds were near unmeasurable levels through un-operated eyes, whereas syngeneic transplanted eyes were near normal at ~0.500 c/d.

3.1.2 Contrast Sensitivity

At 30 weeks of age, un-operated eyes, and eyes that received allogeneic transplants exhibited a distinctly abnormal contrast sensitivity curve, with only the lowest spatial frequencies measurable (Figure 21, solid circle). Syngeneic transplanted eyes, on the other hand, displayed a typical inverted-U shaped contrast sensitivity curve, although the sensitivity was significantly lower ($F_{(1,7)}$=11433.883; $p<0.001$) than non-dystrophic eyes, with the largest differences at the low and middle range spatial frequencies (Figure 21, solid square). The contrast sensitivity of a dystrophic RCS rat at 14 weeks (Figure 17) is similar to the syngeneic transplanted eye at 0.1 c/d and lower, however, the spatial frequencies above 0.1 c/d are all preserved approximately the same as a dystrophic RCS rat eye at 10 weeks of age (data not shown). In addition, at 14 weeks, contrast sensitivity at 0.4 c/d is immeasurable in the background dystrophic controls, but the syngeneic transplanted eyes retained sensitivity near the levels recorded in non-dystrophic animals (Figure 22).

The contrast sensitivity profile of each spatial frequency measured longitudinally through both syngeneic and allogeneic transplanted eyes is shown in Figure 23 and Figure 24. Syngeneic-transplanted eyes exhibited a profile in which each spatial frequency remained intact until at least 30 weeks of age. Contrast sensitivity at low and middle spatial frequencies in the syngeneic transplanted eyes was variable and showed an

overall decline during the testing period (Figure 23). Allogeneic-transplanted eyes exhibited a profile in which the high spatial frequencies (0.4 c/d) were unmeasurable at 10 weeks of age, or became immeasurable early in testing (0.27 c/d). Allogeneic-transplanted eyes also showed a dramatic decline in contrast sensitivity at all spatial frequencies around 15 weeks of age, which declined until some spatial frequencies reached immeasurable levels (Figure 24). Although the preservation of contrast sensitivity in the syngeneic Schwann cell transplanted eyes was not complete, as it seemingly was with the spatial frequency threshold, it was significantly better than through allogeneic transplanted eyes.

3. 2 Effects of transplantation (VWT)

3.2.1 Training

All rats readily learned to associate swimming to the platform with escape from water. On average, about 200 trials (i.e. seven days of training) were required for animals to reach 90% accuracy over 40 trials, and there were no obvious behavioral differences in this ability. Animals performed the task as well for monocular testing as binocular testing.

3.2.2 Testing

Visual acuity of both syngeneic and allogeneic transplanted animals was measured binocularly at 16 weeks of age. Mean acuity obtained from animals with syngeneic Schwann cell transplants was 0.62 c/d, and 0.52 c/d from animals with allogeneic transplants. When we retested subsequently at 24 and 28 weeks, we measured the acuity thresholds from each eye separately (Figure 25). Eyes that received syngeneic

transplants had mean acuity of 0.61 c/d (24 weeks) and 0.63 c/d (28 weeks), approximately the same values as measured earlier with both eyes open. Allogeneic-transplanted eyes had acuities of 0.49 c/d (24 weeks) and 0.42 c/d (28 weeks), slightly lower than when measured binocularly, which may have been due to the effects of age on the degenerating retina. Un-operated eyes from syngeneic-transplanted animals had mean acuities of 0.15 at both 24 and 28 weeks, whereas un-operated eyes from allogeneic-transplanted animals had mean acuities of 0.24 (24 weeks) and 0.2 c/d (28 weeks). An ANOVA confirmed that syngeneic transplanted eyes had significantly higher thresholds than allogeneic transplanted eyes ($F_{(1,21)}$=9.673, p=0.0053). When compared with un-operated eyes at 24 and 28 weeks, the allogeneic transplanted eyes were significantly better than un-operated controls ($p<0.001$), and syngeneic transplanted eyes were better than all other groups (p=0.0067). These results also confirm that rats use the eye with the highest visual acuity when making discriminations binocularly in the VWT.

3.3 Histological analysis

Near the injection site, cresyl violet labeling revealed surviving groups of cell bodies which resembled photoreceptors. In addition, there was partial preservation of lamination in the inner nuclear layer when compared to areas of retina further from the injection site, although lamination was clearly not normal. Furthermore, away from the injection site, no surviving photoreceptor cell bodies were found. Recoverin antibody staining and DAPI nuclear marker double labeled cells (Figure 31) near the injection site correlating to the groups of cell bodies found with cresyl violet staining (Figure 29A), confirming the presence of photoreceptors. P75 antibody labeling revealed Schwann cells

surviving (Figure 32) near the injection site in syngeneically-transplanted animals although they were few, no allogeneic Schwann cells were found (data not shown).

4. Discussion

The results of this study show that syngeneic Schwann cell transplantation into the dystrophic RCS rat retina preserves OKR sensitivity and visual acuity, and did so without suppression of the host immune system. All animals performed competently in the tasks, indicating that only thresholds and not general behavioral proficiency changed over time, or with treatment condition. The ability to measure vision through each eye independently in each task allowed for the effects of the transplant, in a within-animal design, to be evaluated directly. In addition, the measurement of both optokinetic and perceptual forms of vision facilitated a more thorough evaluation of the effects of the transplants.

The central hypothesis tested in this study was that immune privileged (syngeneic) Schwann cells, transplanted into the RCS retina without the aid of immune-suppression, would be superior to transplanting allogeneic cells for preserving vision. Indeed, we found that this was the case. Spatial frequency thresholds through syngeneic cell transplanted eyes were near normal until 35 weeks of age, which is the best preservation of a visual function in RCS rats that has been reported. Function through allogeneic cell transplanted eyes, on the other hand, was far worse and no different than un-operated eyes (Figure 21). The difference between the effects of syngeneic and allogeneic transplants on contrast sensitivity, however, was not as dramatic (Figure 22). Sensitivity through syngeneically-transplanted eyes at 30 weeks of age was better than

that through allogeneically-transplanted eyes, however, it was not normal. Rather, it was comparable to that measured in 10-14 week-old un-operated dystrophic RCS rats, which was still markedly better than that measured through un-operated or allogeneic cell transplanted eyes. The difference between the two transplanted groups can be seen in more detail in Figure 23 & Figure 24, in that sensitivity degenerated only gradually through eyes that received syngeneic Schwann cell transplants, whereas, a rapid loss of sensitivity was apparent after 14 weeks of age through allogeneic-transplanted eyes.

Measures of grating acuity showed a similar profile of preservation (Figure 25) to that observed with contrast sensitivity: grating acuity measured through eyes that received syngeneic transplants was preserved, but not completely (~70% of threshold in un-operated animals). The level of preservation was still much better than that through allogeneically-transplanted eyes (~40% of un-operated animals), which in turn was better than in un-operated controls. Monocular testing in the VWT also confirmed that acuity through transplanted eyes had the highest thresholds. Given the near normal level of preservation of OKR sensitivity through syngeneic transplanted eyes, and the significant loss of OKR sensitivity in the allogeneic transplanted eyes, we expected to see a higher visual acuity in the animals with the syngeneic transplants, and lower thresholds in those with the allogeneic transplants. Clearly, measures of spatial frequency thresholds in the VOS are not the same as measures of acuity in the VWT. Using the two tasks in the same study, however, provides comprehensive evidence that syngenically-transplanted Schwann cells are superior to using allogeneically transplanted cells, when no immune suppressants are used.

The better preservation of visual function through syngeneically-transplanted eyes than through allogeneically-transplanted eyes might be explained by a differential response of the immune system to the transplant types. Jiang et al.,(Jiang et al., 1995) have reported that immune responses are mounted against transplanted allogeneic tissue, which will eventually destroy it, whereas the syngeneic tissue will survive. Another study (Larsson et al., 1999), which examined the expression of the major histocompatibility complex (MHC) following syngeneic and allogeneic transplants into rat retina (without immune suppression), showed that although both transplants can survive, there is significant up-regulation of MHC antigens in the allogeneically-transplanted animals and little, if any, up-regulation of antigens in syngeneically-transplanted animals. Collectively, these results are consistent with the explanation that our allogeneic transplants may have been compromised, which also may explain why allogeneically-transplanted cells provide better preservation than no transplant at all. In addition, this may explain why we found relatively good preservation of contrast sensitivity only up to 14 weeks of age in allogeneically-transplanted animals. Conversely, the modest preservation of visual acuity in animals with allogeneic transplanted Schwann cells may not be due to actions of the cells themselves, but rather, may be explained by transient sham effect induced by retinal damage unavoidably caused by the transplantation surgery (Silverman and Hughes, 1990; Sauve et al., 2002). This is further supported by the fact that some syngeneic Schwann cells were found when examined histologically, however allogeneic Schwann cells were not. Although there were few syngeneic cells surviving, this is not surprising as the animals were 9 months of age when sacrificed. This is an important finding as reports of cell transplantation in animals which have received

immune-suppression have not found grafted cells at time points later than this. None of the animals in this study were immune suppressed, and although the cells were likely not rejected by the immune system, it appears they have a "lifetime" in which they survive best.

Previously, we evaluated the effects of ARPE19 and human Schwann cells on preserving vision in the RCS rat. In that study, visual acuity was preserved for up to 7 months of age with the ARPE19 transplants, and up to 5 months of age with the human Schwann cells. Although the ARPE19 cell line may have an advantage in being homologous to the defective host RPE, and therefore potentially capable of replacing a number of physiological functions, there is no evidence that ARPE19 cells actually perform these functions, specifically phagocytosing photoreceptor outersegments. In addition, ARPE19 also has the drawback of not being syngeneic to the recipient and therefore required some level of immune-suppression, cyclosporine in the above study, again raising safety concerns that attend all cell lines. Although it has not been shown that Schwann cells phagocytose photoreceptor outersegments, they do, however, appear to survive without pathological manifestations in the subretinal space. In addition, Schwann cells have the advantage that they could be harvested from a peripheral nerve of a patient and introduced into the subretinal space of that same patient, autologous transplantation.

The process by which Schwann cells are working to preserve visual function is not known, but a likely candidate is via the release of trophic factors. Schwann cells have been shown to produce a number of growth factors, including bFGF, CNTF, and GDNF (Sendtner et al., 1992; Neuberger and De Vries, 1993), all of which have been shown to

preserve photoreceptors in the degenerating retina (Faktorovich et al., 1990; Carwile et al., 1998; Huang et al., 2004; Lawrence et al., 2004). Degenerating retinas are known to undergo atrophy and reorganization of inner retinal circuitry (Jones et al., 2003; Marc et al., 2003; Jones and Marc, 2005; Jones et al., 2005; Marc et al., 2007), and such trophic support may enable deafferented retinal neurons to respond relatively normally to their remaining inputs.

Our behavioral tasks used visual stimuli that were in well into photopic light levels (45cd/m^2 VOS; 36cd/m^2 VWT), suggesting that clinically relevant visual function is being measured, and preserved with Schwann cell transplantation. Girman et al. (Girman et al., 2005) showed, using multiunit recordings from superior colliculus, that following cell transplantation in the RCS rat, cone threshold responses (which normally deteriorate over time) are spared, whereas rod function is diminished early and never recovers. If cone function is responsible for the beneficial effects of the transplants, then measures of outer nuclear layer thickness or photoreceptor nuclei may not be appropriate for determining treatment effects in rodent models, because in the rat retina cone photoreceptors only comprise ~ 5% of the entire photoreceptor population. In addition, estimates of photoreceptor survival cannot predict visual performance as shown by McGill et al., (McGill et al., 2004a) where the amount of surviving photoreceptors in RCS rats is near normal early in life, but by one month of age, animals are already visually impaired (~80% of normal). Conversely, at late stages of retinal degeneration (six months of age) when almost no photoreceptors are surviving, RCS rats still had ~30% of normal visual acuity (McGill et al., 2004a).

In conclusion, the preservation of vision with syngeneic Schwann cell transplants in the RCS rat provides an incentive for future cellular-based experiments directed at developing practical treatments for human RDD.

5. Summary

The results of this study support the visual adaptation model. Syngeneic Schwann cell transplantation rescues two forms of behaviorally measured vision, and this preservation is coupled with a localized preservation of photoreceptors near the injection site, and an apparent partial preservation of inner retinal cells and lamination. The results of this study do not support the established model as there was not a complete preservation of the ONL as would be required to support the near normal OKR thresholds. Furthermore, the few photoreceptors which were preserved do not represent 60% of photoreceptors found in a normal retina, the degree to which visual acuity was preserved.

Chapter V – Transgenic rats with a rhodopsin mutation

1. Introduction

Evaluation of rodent visual function has focused primarily on anatomical and electrophysiological measures of visual centers such as the retina, lateral geniculate nucleus, and visual cortex, while less emphasis has been placed on behavioral measures of vision. Anatomical analysis focused primarily on the state of photoreceptors or thickness of the outer nuclear layer (ONL) adhering to the principles in the established model. In part, this bias was due to a lack of behavioral testing apparatus' which do not require extensive training procedures or nutritionally depriving animals. Lashley's jumping stand may have been the first method used to quantify rat vision (Lashley, 1930; Seymoure and Juraska, 1997), and it is still used to a limited extent. Y-mazes (Seymoure and Juraska, 1997), conditioned aversion (Dean, 1978) and operant tasks (Keller et al., 2000; Jacobs et al., 2001) have all been employed with some success, but in general, these methods require a considerable amount of time to train and test rats, which probably accounts for their limited popularity.

The relatively recent development of the VWT and VOS, has allowed for quicker and more efficient assessment of many visual capabilities of normally sighted rodents (Prusky et al., 2002; McGill et al., 2004a; Prusky et al., 2004a; Douglas et al., 2005). In addition, these new behavioral tasks have allowed for the visual capabilities of rodents with retinal degeneration to be examined. McGill et al., (McGill et al., 2004a) and McGill et al., (McGill et al., 2007a) characterized the visual degeneration of the RCS rat using both the VWT and the VOS, respectively. The RCS rat exhibits a progressive decline in visual capabilities over the first year of life (McGill et al., 2004a; McGill et al.,

2007a). Interestingly, at ~ 4 months of age in pigmented RCS rats, ERG b-wave amplitudes were no longer measurable (Pinilla et al., 2004), and ONL measurements showed 1 row or less of photoreceptors cell bodies surviving (Mullen and LaVail, 1976) with little to no outer-segments present, however, visual acuity in the VWT remained at ~ 1/3 of normal (McGill et al., 2004a), and spatial frequency thresholds of the optokinetic response (OKR) in the VOS were ~ 60% of normal (McGill et al., 2007a). At 6-7 months of age, less than one row of photoreceptor cell bodies remain (Mullen and LaVail, 1976), and luminance thresholds are no longer measurable in response to small spots (Girman S, et al. *IOVS* 2003;44;ARVO E-Abstract 482) from the superior colliculus. Visual acuity was still ~ 1/3 of normal and remained measurable until ~11 months of age (McGill et al., 2004a). OKR thresholds were ~40% of normal at 7 months, and remained measurable until ~10 months of age. Conversely, at an early stage of retinal degeneration when electrophysiological and histological measurements are near normal (postnatal day [P] 30), RCS rat visual acuity is already impaired (~80% of normal)(McGill et al., 2004a), and OKR thresholds have also begun to decline (McGill et al., 2007a). Thus, it is clear that the structural and functional relationship between anatomical measurements of the retina, ERG wave amplitudes, and visual thresholds is not always straight forward in animal models of retinal degeneration.

Although much knowledge about retinal degenerative disease has been gained through studies involving the RCS rat, only a small proportion of RP patients have the *Mertk* mutation. A much larger population of RP patients have mutations expressed in photoreceptors themselves, and within this group, rhodopsin mutations are the most prominent. In an attempt to understand the effects of human RP caused by rhodopsin

mutations, transgenic rats that express rhodopsin mutations have been developed and maintained (http://www.ucsfeye.net/mlavailRDratmodels.shtml). These mutations were P23H (single amino acid substitution at codon 23) and S334ter (a mouse opsin gene bearing a termination codon at residue 334), which results in a C-terminal truncated opsin protein lacking the last 15 amino acid residues and, thus, all of the phosphorylation sites of the molecule. Three lines of P23H and 5 lines of S334ter rats were identified that express retinal degeneration phenotypes of different rates.

Early studies using the fast degenerating line S334ter-3 have shown similar discrepancies between visual system measurements as seen in the RCS rat. For example, Sagdullaev et al., (Sagdullaev et al., 2003) reported that by P60-100, photoreceptor cell death is near complete and multi-unit recordings from the superior colliculus are non-responsive, however, Thomas et al. (Thomas et al., 2004) report measurable OKRs at both P135 and P205 using the same S334ter-3 rats. Therefore, the goal of the present study was to characterize the visual capabilities of 2 lines of P23H and 3 lines of S334ter rhodopsin transgenic rats throughout the course of retinal degeneration, and to correlate those measures with ERG amplitudes and morphologic assessment of the retina. The importance of this study lies in the notion that because the retina in each line degenerates at a different rate, each line effectively represents a different retinal disease, and thus, likely determines which treatment is most appropriate.

More generally, this experiment provided an opportunity in which the visual adaptation model could be evaluated using multiple animal models that exhibit different rates of photoreceptor degeneration. The established model of visual function predicts that there should be a linear relationship between each method of measuring function

regardless of strain. However, the visual adaptation model predicts that although a linear relationship between measurements is possible, it is more likely that behavioral measurements of vision are not predicted by ONL measurements or ERG wave amplitudes as seen in the RCS rat. In order to complete this experiment, we collaborated with Dr. Matthew Lavail and his laboratory, experts in electrophysiological and anatomical evaluations of the retina. Dr. Lavail has a long published history of such evaluations in animal models with retinal disease. In addition, we felt it appropriate to collaborate with Dr. LaVail as the animal models were developed in his laboratory.

2. Methods

2.1 Animals

This study was conducted in accordance with the ARVO Statement for the Use of Animals in Ophthalmic and Vision Research and the guidelines of the institutional animal care committees at the University of Lethbridge and the University of California, San Francisco. Anatomical and ERG data were used for comparison and were generated in Dr. Matthew Lavail's laboratory. The development of mutant rhodopsin transgenic rats on the albino Sprague-Dawley background is described elsewhere (http://www.ucsfeye.net/mlavailRDratmodels.shtml). To acquire the pigmented transgenic rats, homozygous albino transgenic rats were crossed with normal, pigmented Long-Evans animals and obtained all pigmented offspring, each carrying a single copy of the transgene, as described by Lowe et al., (*IOVS*, 2005; ARVO E-abstract 2300).

2.2 Behavioral measurements of vision

The VOS measures the threshold of optokinetic tracking response to moving gratings (Prusky et al., 2004a; Douglas et al., 2005; McGill et al., 2007a). The apparatus

consisted of four computer monitors positioned around a square testing arena. A sine wave grating was drawn on a virtual cylinder projected in 3D coordinate space on the monitors (OptoMotry©; CerebralMechanics), and the cylinder was rotated. Visual stimuli presented had a mean white level of 92.9975 cd/m^2 and mean black level of 0.0103 cd/m^2. An unrestrained rat was placed on a platform in the center of the arena. A video camera provided real-time video feedback from above, and the position of the head on each frame was used to continually center the hub of the cylinder at the rat's viewing position, and the cylinder was rotated at a constant speed (12 °/s). On each trial an experimenter judged whether the rat made tracking movements with its head and neck to follow the drifting grating. The spatial frequency threshold, the point at which animals no longer tracked, was obtained by incrementally increasing the spatial frequency of the grating at 100% contrast. Thresholds through each eye were measured separately by reversing the rotation of the cylinder (Douglas et al., 2005). Contrast sensitivity functions were measured by decreasing the percent contrast at fixed spatial frequencies until thresholds were generated. Percent contrast was converted into contrast sensitivity and plotted on a log scale. Animals were tested daily, at least initially, starting at eye opening (P15), and OKR thresholds were measured longitudinally until the animals no longer responded to the stimuli.

2.3 Experimental design

Electrophysiological and anatomical work was performed in Dr. LaVail's laboratory. ERG a- and b-waves and ONL measurements on P30, P60, P90 and P120 in pigmented transgenic rhodopsin mutant rats were characterized longitudinally. The

methods used to collect anatomical and electrophysiological data have been described previously (Lowe et al., *IOVS*, 2005; ARVO E-abstract 2300).

Behavioral evaluation of visual function was characterized longitudinally throughout the course of visual development and visual deterioration. Spatial frequency thresholds were examined from eye opening (P15) and whenever possible, experimenters were blind to previously-recorded results, and thresholds were regularly confirmed by more than one observer. A second group of animals were tested beginning on P25 to control for potential effects of testing. For comparison with behavioral data, selected animals were sacrificed at varying time points for anatomical analysis for consistency with the LaVail lab. Animals were euthanized via overdose of sodium pentabarbital, eyes were marked for orientation, removed, and the corneas punctured at the lateral margin using a 27g needle to allow the fixative to penetrate the eye. Eyes were immersion fixed in 2% paraformaldehyde and 2.5% glutaraldehyde in phosphate buffered saline, then bisected along the vertical meridian and embedded in an Epon-Araldite mixture and subsequently sectioned at 1 μm thickness as described (LaVail and Battelle, 1975). In cases of little or no correlation between behavioral data and anatomical and electrophysiological data, subsequent litters were used for re-evaluation and confirmation of previous behavioral testing results, and the eyes re-examined anatomically. For ease of comparison between measurements, data are represented in figures as % of normal, normal being the values given from a Long-Evans rat for each measurement, at each time-point.

3. Results

The results of this study showed that ERG a- and b-wave amplitudes, ONL thickness, and OKR thresholds do not exhibit a linear relationship between measures in transgenic rhodopsin rat models of RP. Specifically, P23H rats were more closely related on all 3 measures than the S334ter rats, however, the relationship was weak at best. Conversely, each of the S334ter lines showed major discrepancies between behavioral measurements of vision and the ERG and ONL measurements.

3.1 P23H-1

In normal, pigmented adult animals the OKR threshold is ~ 0.53 c/d (Douglas et al., 2005). OKR thresholds showed an early developmental increase from 40% on P15 to a maximum of 80% of normal by ~P23 (Figure 33). OKR thresholds and ERG photopic and scotopic b-waves were all sustained at around 80% of normal up to P60 (Figure 33). Thereafter, OKR thresholds persisted around 70% for up to at least P200, whereas ERG b-waves began to decline around P75 and were only 35% of normal by P180 (Figure 33). ONL thickness progressively declined from ~60% at P30 to 35% at P180, and scotopic a-waves deteriorated from ~30% to less than 10% over the same period.

The contrast sensitivity curve measured at eye opening (P15) closely resembled the contrast sensitivity curve of a non dystrophic rat (Figure 34; data not shown). At P100, the curve was still closely resembled that of a non-dystrophic rat, however, sensitivity at 0.400 c/d was significantly decreased. By P300, all spatial frequencies were not as sensitive to contrast as at P25, however, the curve still resembled an inverted-U shape (Figure 34), and all spatial frequencies except 0.400 c/d were still measurable.

3.2 P23H-3

OKR thresholds also showed an early developmental increase in thresholds however, thresholds were only ~ 20% on P15 and only increased to 70% by P19 (Figure 35). To our surprise, OKR thresholds then quickly declined to ~20% by P50, then slowed and further declined to ~10% by P100 (Figure 35). ERG photopic and scotopic b-waves and ONL measurements remained within 80-100% of normal from P30 to P180. Scotopic a-waves measured on P30 were ~75% of normal and progressively declined to ~45% by P180 (Figure 29).

Contrast sensitivity was significantly impaired by P25 and declined progressively thereafter. By P30, the highest spatial frequency was no longer measurable, and by P55, the top 2 spatial frequencies (0.272, 0.400 c/d) were no longer measurable (Figure 36).

3.3 S334ter-3

Much like the P23H line-1, the S334ter-3 rats had OKR thresholds that showed an early developmental increase in thresholds from from 40% on P15 to a maximum just under 80% of normal by ~P25 (Figure 37). OKR thresholds remained around 80% until P50 when OKR thresholds began to decline. By P65, OKR thresholds had declined to ~50% of normal (Figure 37), and by P230, the OKR thresholds had dropped to ~20%. Interestingly, no other measure maintained performance higher than 20% at any time (Figure 37).

Contrast sensitivity was graphed as spatial frequency “channels” against age (Figure 38). Animals measured beginning on P15 showed a slow progressive deterioration of sensitivity to contrast until ~9 weeks, followed by a sharp decline in

sensitivity (Figure 38). Thereafter, the highest spatial frequency (0.272 c/d) was no longer measurable, and all the remaining spatial frequencies maintained a near stable profile (Figure 38). Animals that were tested from P25 onward had a near identical profile (data not shown) to that of the animals tested from P15 onward.

3.4 S334ter-4

OKR thresholds increased from ~40% on P15 to ~80% on P18 (Figure 39). On P19, however, a dramatic drop in OKR thresholds to ~20% (Figure 39) of normal occurred. To be sure this unexpected event was not an artifact of breeding transgenic rats, we repeated the experiment 2 times, each finding the exact same results (data not shown). Photopic b-wave ranges from 80-100% of normal up to P90, ONL thickness and scotopic b-wave range from 50% to 70% up to P90, and the scotopic a-wave declined from ~30% to ~20% from P30 to P90, respectively (Figure 39).

Contrast sensitivity shows each spatial frequency channel increasing in sensitivity over the first 4 days of testing (Figure 40). On the 5^{th} day of testing, however, a significant drop in sensitivity occurred in which all spatial frequencies were reduced to near unmeasurable levels (Figure 40).

3.5 S334ter-9

OKR thresholds increased from ~40% on P15 to ~80% on P18 (Figure 41). A marked decline in OKR resulted thereafter, and the decline progressed to unmeasurable levels by P32 (Figure 41). Interestingly, all other measures (ERG a- and b-waves both photopic and scotopic and ONL measurements) maintained performance between 80% and 120% until at least P90 (Figure 41).

OKR thresholds from animals measured beginning on P25 were higher at each age tested than in animals tested from P15 onward (Figure 42). This result inspired a yoke-control experiment to evaluate the effects of testing on visual performance. Yoke control data (data not shown) mapped exactly onto the data presented in Figure 42, which suggested that the first few days of testing may increase the rate of functional degeneration in these animals.

Contrast sensitivity at each spatial frequency revealed a significant difference between the P15 and P25 tested groups. The P15 tested group's contrast sensitivity increased at all spatial frequencies over the first few days of testing, followed by progressive deterioration beginning on P25 (Figure 43). In contrast, the P25 tested group's contrast sensitivity at the low spatial frequencies remained stable, while the high spatial frequencies degenerated (Figure 44). Eventually, all spatial frequencies degenerated to unmeasurable levels in the P25 group.

3.6 Visual water task data

Visual acuity measured in the visual water task was performed using Long-Evans control rats (6 months of age) and P23H-1 transgenics (10 months of age) using both static and moving grating visual stimuli. Using static gratings, both the Long-Evans and P23H-1 rats had visual acuities near 1.0 c/d (Figure 45), comparable to previous reports (Prusky et al., 2000a; McGill et al., 2004a). Moving grating stimuli produced visual acuity thresholds slightly lower than 0.60 c/d (Figure 45), again comparable to what was measured previously (Figure 20).

3.7 Comparison between measures

The relationship between behavioral, anatomical, and electrophysiological measures of visual function in this study was not linear. However, in most instances the anatomical and electrophysiological measures were more closely related than the behavioral measures of vision. Specifically, S334ter-3 rats had relatively normal OKR thresholds for up to P50, whereas the anatomical and electrophysiological measures were less than 10% of normal. Conversely, S334ter-4 and S334ter-9 rats lost their ability to track the visual stimuli very early, almost even before the first electrophysiological or anatomical evaluation was performed. A similar yet less obvious discrepancy was seen using the P23H animals. At later ages (P100 or above) in P23H-1 rats, when anatomical and electrophysiological measures were decreasing, the behavioral responses remained intact, and conversely, P23H-3 rat OKR thresholds declined to non-measurable levels by ~P100, whereas ERG waves and ONL measurements persisted.

4. Discussion

The results of this study show that behavioral measurements of vision do not exhibit a linear relationship to ONL measurements and ERG amplitudes in transgenic rhodopsin mutant rats. Previous studies (Machida et al., 2000) (Lowe et al., *IOVS*, 2005; ARVO E-abstract 2300) have shown a strong correlation between anatomical and electrophysiological measures of the retina in the same animals, which is not surprising given that ERG a-wave responses elicited are directly dependent upon the number of surviving photoreceptors. However, the fact that behavioral measures of vision appeared independent of anatomical and electrophysiological responses of the retina suggests that the relationship between these 3 measurements in retinal degeneration models is less

synchronized than previously thought. Interestingly, none of the groups reached a maximum OKR threshold higher than 80% of normal, unlike the RCS rat (McGill et al., 2007a). The lower maximal thresholds are likely due to the rhodopsin mutation which is expressed in the rod photoreceptor cells themselves unlike the RCS rat where the *Mertk* mutation (Gal et al., 2000) is expressed in the RPE cell layer (Mullen and LaVail, 1976; Vollrath et al., 2001).

The unexpected thresholds generated through behavioral measures of vision may be explained by examining photopic (cone dominated) and scotopic (rod dominated) visual pathways. The light levels used for behavioral testing were within the photopic range, suggesting cone-dominated vision was being measured and therefore morphological analysis, which is biased towards rods, would not accurately predict visual performance due to the relatively small number of cones in the rodent retina (Girman et al., 2005). However, if only photopic vision driven by cone photoreceptors was assessed, one would then predict that photopic b-wave amplitudes would closely mimic the behavior. Unfortunately, the results here show no such relation. In addition, Goto et al.,(Goto et al., 1995) show in P23H mice that cone mediated ERG's remain near normal for up to ~5 months with progressive decline thereafter, which may account for the relatively long duration of OKR responses.

The variability between measures may also be due to inner retinal changes, which are evident in many models of retinal degenerative disease including the mutant rhodopsin transgenic rats used here (Jones et al., 2003; Marc et al., 2003; Jones and Marc, 2005; Jones et al., 2005; Marc et al., 2007). This hypothesis is supported by Cuenca et al., (Cuenca et al., 2005) who showed that before significant retinal degeneration in P23H

rats, processes of bipolar and horizontal cells show abnormalities. Cuenca et al. (Cuenca et al., 2004) also reported that retinal circuitry changes occur concurrently with impaired ERG amplitudes in these rats. Although it is clear that reorganization of the retina follows retinal degeneration, it is not clear how reorganization may affect visual performance. Clinically, people often experience temporary and sometimes permanent visual problems (Yorston et al., 2005) following retinal detachment (Erickson et al., 1992; Fisher et al., 2005) which has previously been shown to cause retinal reorganization (Lewis et al., 2002; Fisher et al., 2005). Experimental models of retinal detachment in cats suggest that the same cellular events that occur after detachment in humans are occurring in models of retinal degeneration suggesting that re-organization may be detrimental in both cases (Fisher et al., 2005). Therefore, the retinal detachment model may provide an avenue for examining the effects of retinal reorganization on vision, however, these studies have not yet been done.

Previous work by Lowe et al., (Lowe et al., *IOVS*, 2005; ARVO E-abstract 2300) showed that the rate of degeneration in pigmented rats, when compared with albino rats. In that study, the degeneration was slowed in P23H rats, but not in most S334ter rats, although one of the S334ter rat lines was slowed. This suggested that while some types of mutations in different lines of transgenic animals with different degrees of transgene expression may respond in a similar fashion, other types of mutations may not. The present study amplifies this point, that it may not be possible to draw generalizations based on mutation type, and that each line may need to be considered independently. Furthermore, in 4 of the 5 lines there appeared to be no effect of early testing. The simple act of testing the S334ter line 9 rats seemingly increased the progression of

functional deterioration, although retinal function (ERG) and retinal anatomy remained intact long after, the significance of which remains unclear.

5. Summary

The results of this study support the visual adaptation model. In each line of transgenic rats tested, there was no clear linear relationship between each measurement method, and in some cases, dramatic discontinuities between ONL thickness behaviorally measured visual thresholds existed. The most striking discord between behavioral measures of vision and ERG and ONL measurements is in the S334ter line 4 rats in which, functional vision was no longer measurable long before significant loss of ERG or photoreceptors. Therefore, this animal model provided an excellent opportunity to examine whether changes in retinal circuitry may account for such discrepancies between measures providing further evidence for the visual adaptation model of visual function.

Chapter VI – Immunohistochemical analysis of retinal remodeling

1. Introduction

Retinal remodeling is a relatively new concept and recently has been examined in aged humans (Eliasieh et al., 2007), in patients with Age-Related Macular Degeneration (Sullivan et al., 2007), in animal models with detached retinas (Fisher et al., 2005), and in models of human retinal degenerative disease (Marc et al., 2003). In each of the above examples, neuronal changes in retinal circuitry such as bipolar and horizontal cell sprouting, abnormal expression of retinal proteins such as mislocalization of rod opsin, and activation of glial and microglial cells (Jones et al., 2003; Marc et al., 2003) have been described. In the Marc et al. study (Marc et al., 2003), multiple models of RDD were examined, most of which at very late stages of degeneration. Although it is clear that reorganization occurs late in retinal degenerations, little evidence suggests when reorganization may commence. Evidence primarily from the rd1 mouse, although there is also some evidence in RCS rats, P347L transgenic pig, and others, suggests that even at early stages of photoreceptor stress and deconstruction, the neural retina reacts with bipolar and horizontal cell remodeling (Marc et al., 2003). In addition, cone-driven horizontal cells also exhibit neurite sprouting, and sometimes, as early as P15 (Strettoi et al., 2002). Furthermore, changes in intermediate filament expression appear to be the earliest evidence of Muller cell responses to retinal degeneration as GFAP signals increase during the acute phase of rod death in the rd1 mouse (Strettoi et al., 2002; Marc et al., 2003; Strettoi et al., 2003).

In a recent study, McGill et al., (McGill et al., *IOVS*, 2007; ARVO E-abstract #3448) reported that morphological (ONL thickness measurements) and electrophysiological (ERG) examinations of the retina did not predict behaviorally measured visual thresholds in multiple lines of rhodopsin transgenic rats (P23H and S334ter). In one specific line, S334ter-line 4, outer-nuclear layer measurements and scotopic and photopic b-wave amplitudes ranged between 60-100% of normal at 30 and 60 days of age, however, spatial frequency thresholds measured from P15 until P23, increased initially over the first 4 days of testing followed by a marked loss of function thereafter. Previous reports (Jones and Marc, 2005) of retinal remodeling in these same animals has been limited to late ages as it has been thought that the onset of remodeling did not occur until almost one year of age (Jones and Marc, 2005). Therefore, we performed an immunohistochemical evaluation of this model to determine whether early retinal remodeling may account for the abnormal visual function not predicted by the near normal ONL, to provide further support for the retinal adaptation model describe earlier. To perform this analysis, we began collaboration with Dr. Steve Fisher and Dr. Geoff Lewis who are well known experts in the field of immunohistochemical analysis of retinal remodeling.

This study was designed to provide confirmation that neuronal remodeling does occur in early stages of retinal degeneration and that these changes occur concomitantly with significant decline in visual thresholds. In addition, the results will confirm further that the degree of photoreceptors does not predict visual outcome providing support for the visual adaptation model.

2. Methods

2.1 Animals

This study was conducted in accordance with the ARVO Statement for the Use of Animals in Ophthalmic and Vision Research and the guidelines of the institutional animal care committees at the University of Lethbridge and University California at Santa Barbara. For the purposes of this study, S334ter line 4 rats (n=12; 4 at P15, P30, and P40, respectively) were used, and age-matched Long-Evans rats (n=6) served as controls. The development of mutant rhodopsin transgenic rats on the albino Sprague-Dawley background is described elsewhere (http://www.ucsfeye.net/mlavailRDratmodels.shtml). To acquire the pigmented transgenic rats, we crossed homozygous albino transgenic rats by normal, pigmented Long-Evans animals and obtained all pigmented offspring, each carrying a single copy of the transgene, as described by Lowe et al., (IOVS, 2005; ARVO E-abstract 2300).

2.2 Tissue preparation

Animals were euthanized by lethal dose of euthansol (sodium pentabarbitol; 340 mg/ml; 0.3 ml/kg), eyes were marked for orientation, removed, and immediately immersion fixed using a mixture of 4% paraformaldehyde in phosphate buffered saline. The eyes were then transported to Dr. Lewis where the cornea and lens were then removed, and the eyecup was cut in half. One half of the eye was stored in the fixative solution. From this sample, small areas of retina were excised and embedded in low-melting-point agarose then sectioned at 100 μm. Sections were then labeled with various antibodies to photoreceptors, second and third order neurons, synaptic vesicles and

ribbons, and glial and microglial proteins: Their distribution was determined using an Olympus FluoView confocal microscope.

2.3 Immunohistochemistry

For confocal analysis, 100-um-thick agarose-embedded sections were cut on a microtome (Vibratome; Technical Products International, Polysciences, Warrington, PA) and blocked overnight at 4°C in normal donkey serum (1:20) containing 0.1 M phosphate-buffered saline (PBS), 0.5% bovine serum albumin (BSA; Fisher Scientific, Pittsburgh, PA), 0.1% Triton X-100 (Roche Molecular Biochemicals, Indianapolis, IN), and 0.1% sodium azide (Sigma, St. Louis, MO), together referred to as PBTA. The next day, the sections were incubated in primary antibodies overnight at 4°C on a rotator. The sections were then rinsed in PBTA and incubated in donkey anti-mouse or anti-rabbit IgG conjugated to the fluorochrome Cy2, Cy3, or Cy5 (Jackson ImmunoResearch Laboratories, Inc., West Grove, PA) overnight at 4°C on a rotator. Finally, the sections were mounted in 5% n-propyl gallate in glycerol and viewed on a laser scanning confocal microscope (model 1024; Bio-Rad, Hercules, CA). All antibody solutions were made in PBTA.

The primary antibodies used in this study were a mouse monoclonal antibody to rod opsin (Rho4D2, 1:50; provided by Robert Molday, University of British Columbia, Vancouver, British Columbia, Canada), a rabbit polyclonal antibody to synaptophysin (1:100; Dako, Carpinteria, CA), a rabbit polyclonal antibody to glial fibrillary acidic protein (GFAP, 1:400; Dako), a goat polyclonal antibody to Chat (1:50; Chemicon), a rabbit polyclonal antibody to PKC-beta (1:100; Biomol. Res. Labs). In addition, some

sections were stained with biotinylated peanut agglutinin (PNA) lectin (400 g/mL; Vector Laboratories, Burlingame, CA) and Isolectin B4 (0.5mg; Vector Laboratories, Burlingame, CA; 1:50).

3. Results

3.1 Photoreceptors

In normal animals, both rods and cones appeared normal at all ages examined. In the S334ter rats, neither rod nor cone photoreceptors appeared to undergo significant degeneration throughout the ages examined. Both the Long-Evans and the S334ter-4 rats on P15 expressed initially elevated levels of rod opsin throughout the ONL, however, in the LE rats this expression but became restricted to the outer segments, whereas continuous rod opsin expression was found throughout the ONL in the S334ter-4 rats (Figure 46). Cone photoreceptors appeared normal at P15 and P30 (PNA; Figure 47) in both LE and S334ter-4's, and although an outright loss of cones does not occur, by P40 in the S334ter-4 rats, there are some structural abnormalities (slanting and twisting, data not shown) which are possibly caused by a loss of adjacent rod photoreceptors.

3.2 Inner retinal neurons

Long-Evans rats exhibited a typical developmental shift in ribbon formation: synaptic ribbons in the OPL changed from a rounded appearance to their normal crescent shape. In addition, bipolar cells labeled with PKC beta appeared to have normal processes extending from the ONL to the ganglion cell layer. Horizontal cells were restricted to the outer plexiform layer, and did not appear to support neurite sprouting. Finally, ganglion cells and their dendrites were limited to the ganglion cell layer. No

microneuromas were evident in the LE rats. S334ter rats, on the other hand, exhibited persistent abnormal synaptic terminals (anti-synaptophysin and -CtbP2; data not shown). In addition, ganglion cell filaments are found in the inner nuclear layer by P30 (Figure 46D), and horizontal cell neurite outgrowth was not evident until detected (anti-neurofilament) in the ONL by P40 (Figure 48), whereas these events were not detected in the LE controls. Synaptophysin labeling in the OPL appears normal at P15 (Figure 47C) but started to become disrupted by P30 (Figure 47D), and by P40, there was significant disruption of synaptic vesicles in the inner nuclear layer, which suggested there may also be complications with neurotransmission in the S334ter-4 animals.

3.3 Muller glia and microglial cells

Long-Evans rats showed no abnormalities in Muller glial or microglial cells at all time points examined (data not shown). Muller glial cells extended processes from their end feet into the INL and microglia appear to be at normal levels. S334ter-4 rats also appeared normal at P15, however by P30 evidence of Muller glial cell growth (anti-GFAP and vimentin) into the subretinal space which caused significant glial scarring was detected (Figure 49). In addition, although microglial activation (Isolectin B4; Figure 50) was not detected at P15 and P30, multiple examples were evident by P40 (Figure 50) where microglial cells were found in the inner retina.

4. Discussion

The results of this study show that significant events of retinal remodeling such as abnormal rod opsin expression, persistent abnormal synaptic terminals, and extensive Muller cell reactivity which resulted in subretinal scar formations, occur in S334ter

transgenic rats early in life. The results found here also suggest that impairments found in the behavioral measurements of vision cannot be explained by the rapid loss of rod or cone photoreceptors. Although rod opsin expression is found throughout the ONL in these animals, there appears to be a slow loss of rod outersegments, however, the rate of loss suggests consistency with previous gross morphological measures (McGill et al., *IOVS*, 2007; ARVO E-abstract #3448). At the present time, it is unclear whether the expression of rod opsin throughout the ONL is a direct effect of transgene expression, or whether it is a consequence of early abnormal photoreceptor function. Cones, although they appear more tortuous than in control animals, do not appear to generate over the time period tested here. Moreover, scotopic a- and b-wave and photopic b-wave amplitudes, although not normal, can be measured for up to at least 90 days in these animals (McGill et al., *IOVS*, 2007; ARVO E-abstract #3448), again suggesting that the early deficits in visual behavior are not a result of non-functional, or the outright loss of rod or cone photoreceptors.

Previous reports of retinal remodeling have suggested that horizontal and bipolar cell outgrowth may contribute to the development of microneuromas. Microneuromas are collections of outgrowths from various retinal neurons which appear to form synapses creating an abnormal neuronal circuit. In the present study, we found no evidence of formed microneuromas, however, the constituents of neurite outgrowth were found in multiple samples. The lack of formation of microneuromas in these animals is because they require significant numbers of inner retinal neurons to extend processes which typically doesn't occur without the outright loss of photoreceptor cells or at late stages of reorganization. Microneuromas are evident in rhoDeltaCTA mice that express the same

gene mutation as the S334ter rats, but even in these mice, microneuromas do not develop until near 18 months of age. In the present study, animals were young, and the degree of remodeling was not extensive, suggesting that the formation of potential microneuromas in these animals is in the infant stage. Therefore, it is unlikely that abnormal retinal circuitry caused by microneuromas is the source causing deficits in behaviorally measured vision.

It has been shown previously, that when Muller cells grow beyond the ONL into the subretinal space and are present between the outer segments and the RPE, the outer segments can't interdigitate with the RPE (Lewis et al., 2002) resulting in progressive photoreceptor loss and eventual loss of vision. The formation of the distal glial seal is common to human (Milam et al., 1996) and animal (Jones et al., 2003) retinal degenerations, and occurs in every instance where the sensory retina becomes significantly depleted of rods. It is difficult to prove that the seal represents completely new processes, because the collapse of the outer nuclear layer leaves behind a great mass of Muller cell distal processes, however, in the present study there was not a significant loss of rods yet Muller glia nevertheless grew such processes. The effects on visual function of Muller glial cell changes is largely unknown, however, a recent study (Franze et al., 2007) suggests that in addition to regulating neurotrophic support, and providing structural support to the retina, Muller cells may also act as “optical fibers” funneling light to photoreceptors to mediate image transfer with little distortion. Therefore, in the present study, given significant disruption of Muller cells in response to the inherent photoreceptor defect, the Muller cells are likely to change their image mediation properties potentially resulting in poor visual outcomes (Franze et al., 2007).

Successful, cell transplantation can prevent remodeling of the retina for long periods of time (Wang et al., 2005a; Pinilla et al., 2007). The preservation appears to be best at or near the injection site, which is also the location of best photoreceptor preservation. Although the present study shows that the presence of photoreceptors themselves can be independent of the effects from reorganization, this suggests that a fundamental feature of the transplantation procedure is preventing retinal remodeling. A possible mechanism of this benefit is through neurotrophic support as transplanted cells, particularly ones transfected to overproduce growth factors, show significant benefit to the retina. These diffusible factors are thought to be regulated primarily by Muller glial cells (Beltran et al., 2005). Therefore, in the present study, the early activation of retinal remodeling may be promoted by abnormal concentrations of growth factors. Unfortunately, the application of exogenous growth factors to prevent this remodeling has intrinsic complications as injection of CNTF into the vitreous, and delivered sub-retinally via AAV transfection has been shown to cause photoreceptor death (Wen et al., 2006), Muller glial mobility (Wen et al., 2006), and decreases in behaviorally measured vision (McGill et al., 2007b).

5. Summary

The results of this study provide further evidence supporting the visual adaptation model. Early retinal reorganization in S334ter line 4 rats is evident shortly before behavioral deficits are observed suggesting that significant cellular and molecular changes occur before gross anatomical changes are evident, and that these changes may non-adaptively affect visual function. Given that more than 60% of photoreceptor cell bodies are surviving and ERG wave amplitudes are measurable in the S334ter line 4 rats

long after the loss of behaviorally measured vision (Figure 39), the results of this study suggest that neural remodeling is functionally non-adaptive

Chapter VII - Discussion

1. General Discussion

The current treatments for RDD's are inadequate, and the theoretical framework behind the design of most emerging experimental treatments is fundamentally flawed. The established model, which utilizes a theoretical photoreceptors equal vision construct, has significant limitations when evaluating emerging therapies for retinal degenerative disease. The results of the studies reported here provide empirical support for a new model to guide future vision research and therapy development: the visual adaptation model. Based on this model, behavioral measures of vision were used as the primary measure of the visual system, and these were supported with anatomical and sometimes electrophysiological measures of the retina. The use of this approach facilitated the development of new hypotheses and insights into visual system function, which could not have been predicted using the established model.

2. Established photoreceptor equals vision model

The established photoreceptors equal vision model for treatment of RDD focuses on preventing the premature death of photoreceptors with the hopes of preventing consequent vision loss as well. The model is predicated on a photoreceptor structure equals functional vision relationship, which implies there is a linear relationship between the physical state of photoreceptors and the function of the visual system. In other words, with a full complement of healthy photoreceptors visual function should be normal, degeneration in photoreceptors should predict a decline in visual function, and where no photoreceptors are present, visual function should not be measurable. One reason the

established model may be inaccurate is because behavioral measurements of vision are an output of the visual *system* rather than an output of a selected component of the visual system such as photoreceptors. For example: following intravitreal delivery of CNTF into the eye of Long-Evans rats, the degree of photoreceptor cell death was not equal to the degree of visual decline. Furthermore, the detrimental effects on visual thresholds far outlasted those on morphological measures of the retina. In another example, visual thresholds of RCS rats declined in a similar fashion to photoreceptor depletion, however, upon closer examination, the time course of visual decline extended much further than photoreceptor degeneration. Moreover, following syngeneic Schwann cell transplantation, OKR thresholds were maintained near normal levels and visual acuity was significantly preserved, however, anatomical evaluation revealed limited photoreceptor preservation, and this preservation was limited to close proximity to the injection site. Finally, visual thresholds and photoreceptor degeneration in rats that express transgenic rhodopsin mutations declined at varying rates, however, visual performance of these animals could not have predicted from the rate photoreceptor degeneration. Clearly, the work in this thesis provides multiple examples which cannot be directly accounted for by the established model.

3. Visual adaptation model

The visual adaptation model requires that vision is measured first, and that vision is the primary measure of function. The visual adaptation model also suggests that the retina is capable of significant neural remodeling, the retina undergoes these changes in models of RDD, and that these changes are likely non-adaptive. The experiments in this thesis provide empirical evidence for the visual adaptation model.

3.1 Effects of CNTF

Transient CNTF levels did not promote significant retinal remodeling. This was to be expected as it has been shown previously that growth factors introduced into disease retinas, either by direct injection or through emission by transplanted cells, prevent retinal remodeling in addition to preventing photoreceptor degeneration (Faktorovich et al., 1990; Wang et al., 2005a). Following sustained delivery of CNTF into the eye of Long-Evans rats, glial cell remodeling paralleled reduced visual performance, a similar finding to that reported by Rhee et al. (Rhee et al., 2007). Although it is unclear exactly how the introduction of CNTF resulted in decreased visual capabilities, it is clear that with sustained expression of CNTF, retinal changes such as Muller cell proliferation increases. The fact that CNTF, when injected intravitreally, is metabolized relatively quickly (on the order of days) suggests that the delayed recovery of visual thresholds are likely due to retinal changes similar to those found in the AAV injected group, although no overt retinal changes were seen with the histological analysis. Collectively, the results of this study show that CNTF causes significant retinal remodeling and visual deficits that are not directly correlated with photoreceptor death. These results also support the visual adaptation model and suggest that growth factors may regulate remodeling in the diseased retina.

3.2 RCS rats

RCS rats undergo remodeling of inner retinal neurons, which progresses concomitantly with the progression of photoreceptor degeneration. Furthermore, the integrity of inner retinal layers in near proximity to the site of injection of Schwann cells

also paralleled the preservation of OKR thresholds and visual acuity, suggesting that prevention retinal remodeling has serious implications for visual function. Although microneuromas were not explicitly identified in the work here, the neuronal changes observed in the studies in this thesis are characteristic of those in retinas that develop microneuromas. Aged RCS rat retinas show evidence of microneuromas that include bipolar, amacrine, and ganglion cell processes with abundant synapses (Jones and Marc, 2005). All types of neurons can contribute terminal processes to a microneuroma, but it is clear that the synaptic assemblies they form are clearly unlike those of the normal retina. Modeling the synaptic circuitry suggests that such circuits are highly unstable and exhibit resonant activity (Jones et al., 2003). These microneuromas connect to the inner plexiform layer, suggesting that they are not confined to small areas within particular layers of the retina nor do neurons intrinsically know how to rewire (Jones et al., 2003; Marc et al., 2003; Jones and Marc, 2005; Marc et al., 2007). Because progressive retinal degeneration eventually leads to the development of microneuromas, and because cell transplantation apparently delays remodeling of the retina, preventative cell transplantation should be performed as early as possible to prevent such retinal changes.

3.3 Transgenic rats with rhodopsin mutations

Transgenic rats that express rhodopsin mutations presented multiple lines in which, the retina degenerates at different rates. It is this expression of the gene mutation that defines the disease and will likely define the treatment. The results of the studies done here demonstrated that anatomical and electrophysiological measurements of the retina did not show a clear linear relationship to the visual thresholds measured behaviorally. In one line, the S334ter-line 4 rats exhibited early inner retinal remodeling

and Muller cell gliosis that paralleled significant visual decline. Again, although microneuromas were not explicitly identified in the studies done here, the implications of remodeling suggest that microneuromas exist in these animals. For example, immunohistological markers for horizontal and bipolar cells revealed significant changes early in life in the S334ter line 4 rat, suggesting that microneuromas may be developed or are in the process of developing. This also suggests that microneuromas may account for the lack of correlation between retinal anatomy and functional vision in the transgenic rhodopsin mutated rats and possibly in all retinal degenerations.

The characterization of visual function and retinal degeneration in the transgenic rats provides the retinal degeneration field the valuable background information required for a comprehensive analysis of potential treatment regimens in another model of RDD other than the RCS rat. The RCS rat has been regarded as the primary model for RP for many years, yet the mutation in the RCS rats that is also found in the human population represents only a fraction of the total RP population. Rhodopsin mutations account for a much larger population of RP patients and therefore it is vitally important to examine whether treatments found to be successful in the RCS rat are also examined in other models of RP.

3.4 Retinal remodeling

Retinal reorganization has been found in multiple models of retinal degenerative disease including the models used in the studies presented here (Jones et al., 2003). In addition, remodeling has also been well characterized in other circumstances of challenge to the retina such as detachment (Fisher et al., 2005). There is an increasing body of

evidence that biochemical and or significant small scale changes in the retina occur without effecting the overall gross morphology. That is, changes in ion buffering of Muller glia, or Muller glia extending processes into the subretinal space, although potentially harmful, they go undetected in a standard histological analysis of photoreceptor cell body survival. The studies done here confirm that inner retinal structural changes are widespread (except where preserved by cell transplantation), these changes can occur without significant photoreceptor degenerations as seen in the S334ter line 4 transgenic rats, and these changes appear to have significant functional consequences.

3.5 Photoreceptors

Each experiment in this thesis raises the question of which photoreceptors are regulating visual function? In the first experiment, a high dose CNTF was delivered to the retina either intravitreally or subretinally and it appeared that the effects of the CNTF on the ERG and behavioral responses are greater for the cone pathways, or the cones themselves, than for the rods. Behavioral testing using the VOS and VWT was in the photopic illuminance range (30-40 cd/m^2), and the photopic b-wave showed the greatest and longest suppression following a high-dose CNTF injection. The photopic b-wave ERG response reflects cone function, but is thought to be generated primarily by depolarizing bipolar cells in the rat (Xu et al., 2003). In *rcd-1* and normal dog retinas, higher doses of CNTF released from encapsulated cells resulted in reduced immunohistochemical staining with antibody to human cone arrestin, and the effect was greater than that on rhodopsin (in rods; (Zeiss et al., 2006)). Similarly, in AAV-vectored

CNTF in *rds*$^{+/-P216L}$ mouse retinas, both s-opsin and m-opsin normally expressed in cones was greatly reduced, but rhodopsin expression was not significantly affected (Rhee et al., 2007).

Behavioral evaluation of RCS rat OKR thresholds and their degeneration with age, and previous characterization of the progressive degeneration of RCS rat visual acuity was also done in photopic conditions where the light levels used would likely saturate rods suggesting that cone photoreceptors mediated the behavioral response. In addition, in the RCS rat where the primary defect is in the RPE cell layer, the rod photoreceptors have been shown to be non-functional from as early as P21 (Girman et al., 2005; Rubin and Kraft, 2007). It is unfortunate that the rodent photopic a-wave is so difficult to measure through ERG as it would aid in confirming the function of cone photoreceptors, the presence of which has previously been confirmed by anatomical analysis up to 200 days of age in RCS rats (Pinilla et al., 2005b).

Cell transplantation appears to prevent the loss of rods and cones although cone function appears to be preserved better in such studies. For example, one study (Sauve et al., 2006) that used transplantation of human RPE cells (APRE19) into the retina appeared to preserve function of both rods and cones measured electrophysiologically, however, cone function (photopic b-wave) was preserved up to at least P120 whereas rods were preserved only up to 90 days. In addition, cortically mediated responses, measured by single unit recordings in the visual cortex of RCS rats following cell transplantation into the retina, showed that cortical responses can be preserved for up to and beyond 7 months of age, an age at which responses in untreated RCS rats are no longer elicited (Coffey et al., 2002). The mean luminance of the screens used in Coffey

et al., (Coffey et al., 2002) was roughly the same luminance as the computer screens used in McGill et al., (McGill et al., 2004b; McGill et al., 2007a) which showed that behavioral measures of cone vision can be preserved for up to at least 7 months of age, suggesting that the Coffey et al. study likely measured cone responses. Collectively, these studies suggest that cone function is primarily responsible for the behaviorally measured visual thresholds, and because of the heavy bias towards rods in the rodent retina, a gross morphological evaluation of the ONL will not accurately predict visual function.

The argument of which photoreceptor system is regulating the behaviorally measured visual function is limited by the fact that the VOS is not currently equipped to function in scotopic light levels. For this to occur, there are some serious technical issues that would require addressing. For example, computer monitors emit large quantities of light, and because there are 4 monitors used for the display of visual stimuli in this task, removing nearly all the light from each of them is not an easy task. Once light levels within the testing arena are reduced to scotopic levels, specialized video equipment is required to then view the animal as it is required that the operator can view the animals behavior. In addition, the viewing monitor would require having its light emission also decreased significantly. Aside from the technical issues, such a device equipped to examine scotopic vision would greatly increase our knowledge of retinal degenerations and treatments for these diseases.

3.6 Discontinuities in measurements of visual function

Other discontinuities between measures of visual function in animals with a degenerating retina have been identified: Kovaleski et al., (Kovalevsky et al., 1995) found no correlation between pupillary light reflex and photoreceptor number in RCS rats, again providing more support for the visual adaptation model. Using S334ter-3 rats that degenerate very quickly, Sagdullaev (Sagdullaev et al., 2003) and Thomas (Thomas et al., 2004) have reported discrepancies between OKR visual thresholds, morphological analysis of the retina, and electrophysiological responses of the superior colliculus, although none of these studies closely examined retinal remodeling.

3.7 Potential mechanism of remodeling induced visual impairments

One potential mechanism which may account for the difference in measurements of visual function is small scale cellular and molecular events which are not represented at the level of analysis currently used. For example, although Muller glial cell structural changes are evident in the experiments in this thesis, the possibility remains that a down-regulation or closure of K^+ channels in Muller cells may occur, which should have deleterious consequences for retinal function because the K^+ channels of Muller cells are crucially involved in the maintenance of the extracellular K^+ homeostasis (Newman and Reichenbach, 1996). A decreased uptake by Muller cells of neuronally released K^+ in the outer retina may cause over-excitation and intracellular Ca^{2+} overload of photoreceptor cells, resulting in eventual apoptosis of the photoreceptors. In addition, this over-excitation could potentially deplete neurotransmitter stores in the photoreceptors causing excess release of glutamate into the synaptic cleft. Pannicke et al.,(Pannicke et al., 2000)

suggested that extracellular K^+ significantly decreases Muller glial cell ability to uptake neurotransmitter, thereby causing neuronal dysfunction and apoptosis (Barnett and Pow, 2000). Furthermore, extracellular neurotransmitter (glutamate) can become toxic to neurons even in low concentrations (Kashii et al., 1996). Although all the neuronal changes and their mechanism in the current studies were not identified, it is clear that such changes have dire consequences on visual function.

3.8 Neurotrophic factors

Neurotrophins control neuronal survival via two types of receptors: the Trk family of high-affinity tyrosine kinase receptors transmit prosurvival signals, while the low affinity p75 neurotrophin receptor transmits anti-survival signals (Casaccia-Bonnefil et al., 1999a), both of which are located on Muller cells. Muller cells are implicated in either photoreceptor cell death or rescue, in dependence on the receptor activated (Casaccia-Bonnefil et al., 1999b). Neurotrophin-3 mediates its protective effect on photoreceptor cells by binding on the TrkC receptors of photoreceptors and of Muller cells, the latter of which results in an increased release of bFGF from Muller glia (Harada et al., 2002). On the other hand, nerve growth factor reduces the bFGF production in Muller cells via binding on the p75 receptors, the reduced bFGF release by Muller cells may contribute to increased photoreceptor apoptosis (Harada et al., 2002). Additional (previous) retinal injuries like mechanical stress (Faktorovich et al., 1990; Silverman and Hughes, 1990) or preconditioning with bright light (Liu et al., 1998) may protect photoreceptors from degeneration because these stimuli cause an up-regulation of bFGF and CNTF expression in Muller cells (Wen et al., 1995; Liu et al., 1998). Likewise, argon laser photocoagulation slows photoreceptor degeneration in the RCS rat which correlates

with an induction of bFGF in retinal blood vessels, Muller cells and astrocytes (Chu et al., 1998). Collectively, these studies confirm that neurotrophins, depending on dose and receptor system activated, are responsible for some aspects of photoreceptor cell survival, and these effects are mediated largely through the function of retinal Muller cells.

3.9 Cell transplantation

Cell transplantation appears to be the most promising method for the treatment of human retinal disease. There are two avenues one can take when using cell transplantation as a therapy: replacement or prevention. The replacement method is designed for patients with advanced cases of retinal disease in which some, most, or all photoreceptors have died. Ideally, sheets of cells (Seiler and Aramant, 1998; Aramant and Seiler, 2002; Seiler and Aramant, 2005) or cells in suspension are injected into the eye between the retinal pigment epithelium and what remains of the neural retina. Typically, this procedure requires the use of stem cells (Maclaren and Pearson, 2007), progenitor cells (Seiler and Aramant, 2005) or sheets of fetal retinal cells (Seiler and Aramant, 1998). Thus far, this method has yielded both promising and disappointing results. Most reports state that the transplanted cells live following transplantation and that retinal function is restored (Woch et al., 2001; Sagdullaev et al., 2003; Seiler and Aramant, 2005) to some degree, and at least one study has reported restoration of visual function (Seiler et al., 2007). Recent attempts at retinal sheet transplantation into the human eye have provided some evidence of functional improvement (Kaplan et al., 1997; Radtke et al., 2004) and phase II clinical trials are expected to be complete by March 2010 (clinicaltrials.gov). Although the replacement approach is a promising technique, it is also faced with major complications. The first major complication is a source of cells.

Historically, fetal stem cells are not easily accessible due to legal and ethical reasons, and other stem cells such as bone-marrow derived or olfactory ensheathing cells are difficult to obtain if they are to be used for autologous transplantation. The second major complication is integration of the graft into a retina which has undergone significant reorganization. Simply put, transplantation of stem cells into the retina at a late stage of degeneration, which has likely undergone significant reorganization, in the hopes the graft will integrate and synapse appropriately to the reorganized neural retina and restore vision, is a very tall order. Some authors (Seiler and Aramant, 2005; Seiler et al., 2007) claim functional integration of the grafts, although it remains unclear whether it is the graft itself supporting function, or whether the graft is supporting the function of remnants of the host retina. In addition, there are technical complications with sub-retinal transplantation at late stages of degeneration as retinal puncture, efflux of cells, etc., are all of major concern.

Prevention of the progression of retinal disease avoids each of these complications by having multiple sources of potential cell types and transplants are performed in the early stages of the disease when little to no reorganization has occurred. Reports of early cell transplantation have utilized many different cells types, which have been shown to be of benefit to the retina, and some have also been shown to prevent the loss of vision (McGill et al., 2004b; McGill et al., 2007a). Early transplantation is of great advantage as studies (Wang et al., 2005a; Pinilla et al., 2007) have shown that early sub-retinal transplantation can prevent most of the changes seen in the outer retina. Unfortunately, cell transplantation in humans has not been encouraging (Kaplan et al., 1997) likely due to limitations with experimental design. In clinical trials thus far, the

patients who received transplants were at an advanced stage of photoreceptor degeneration. Because the intended use of these cells was for prevention of cell loss, and not replacement, it understandable why poor results have been obtained. Justifiably, FDA restrictions require safety concerns to be addressed first, and therefore it will be some time before we see these methods used for prevention of the progression of the retinal disease as they are intended. Only one study has examined late-stage preventative cell transplantation in animal models (Wang et al., 2008) and found that both functional and morphological rescue can be obtained limiting the progression of degeneration to the same degree at which the transplant was performed. In that study, there was no evidence of improvement of function, nor was there any indication that the transplanted cells restored retinal cells. These results suggest that in order to achieve maximum functional rescue from preventative cell transplantation, the procedure must be performed as early as possible following diagnosis of retinal disease (Wang et al., 2008).

3.10 Growth factors versus Cells

The use of growth factors as a potential method of treatment is not without complication. Delivery via intravitreal or subretinal injection limits the volume of injectate and because growth factors only remain in the vitreous for short periods of time, it may be required to use either one large dose or multiple injections of lower doses for long term maintenance. However, some reports (Wen et al., 2006; McGill et al., 2007b) as described in Chapter II suggest that a single large doses of some neurotrophic factors (eg specifically CNTF), may be toxic and cause more harm than benefit, and multiple intraocular injections is not very practical in a clinical setting. Viral mediated delivery of growth factors is a method that could be employed for continuous release of

neurotrophins and would require only a single injection, however, viral infection in vivo remains a controversial issue due to safety concerns and an unclear understanding of viral action following transfection into the retina. For example, there have been a few deaths in human patients following this procedure cautioning the use of this method (Lehrman, 1999). However, in 2001, Rasmussen (Rasmussen et al., 2001) and colleagues completed the first clinical trial of gene therapy for human age-related macular degeneration (AMD). This was primarily a safety study directed towards tolerance, feasibility, and dose, and not designed for prevention of the disease. More recently, Campochiaro et al., (Campochiaro et al., 2006) used adenoviral vectors to deliver pigment epithelium-derived factor for neovascular AMD. The results of this study showed no significant detriment to the patient supporting further use and experimentation with this technique.

The use of cell transplantation as a method of continual delivery of neurotrophic factors avoids complications with multiple injections, doses, recycling of the vitreous, and potential safety issues involved with viral vectors. In addition, many cell lines have wide availability, have been well established (e.g. ARPE19 (Dunn et al., 1996)), and the properties of such cells are well known. Furthermore, many cell types can be generated which express larger than normal amounts of growth factors (Lawrence et al., 2004), and some cell types are reported to be compatible with the host immune system (Jiang et al., 1995; Larsson et al., 1999). Recently, a technology termed Encapsulated Cell Therapy (ECT) has been developed which takes advantage of each of the strengths of cell transplantation and neurotrophin delivery. Currently, ECT uses engineered RPE cells which produce copious amounts of CNTF, thereby providing a continuous release of neurotrophin in the vitreous. However, the current device is relatively large, making

surgical procedures difficult, and the device has the potential to cause significant refractive interference if it is not isolated to a peripheral location within the eye. Although someday ECT will no doubt be a powerful technique for treating RDD, currently, the advantages of cell transplantation alone promote its use over other methodologies.

3.11 Summary

Collectively, these studies suggest that visual system function in retinal disease is dependent upon 2 main factors: 1) the presence of photoreceptors, and 2) limitation of remodeling of inner retinal neurons and retinal glial cells. The work done here also suggests that the latter may be more important than the former. The established model has been used with great success to further our knowledge of visual system function with close attention paid to photoreceptors specifically. However, using the visual adaptation model in these studies allowed for new insights into visual system function, and proved to be a valuable change as little attention has previously been paid to preventing the loss of vision first followed by preventing neuronal changes in the retina and the loss of photoreceptors. In addition, the experiments in this thesis show unequivocally that vision must be measured when evaluating experimental therapies for retinal degenerative disease. The results of this thesis also has serious clinical implications as vision loss is the primary indicator of visual disease, and rescuing vision loss is the primary goal of therapy for RDD. Furthermore, preventing vision loss and its causes (e.g. retinal remodeling) in humans may require a different therapeutic procedure than what is currently used for photoreceptor preservation.

Clearly, the retina is capable of various forms of adaptation including, but not exclusively, Muller cell gliosis, horizontal and bipolar cell neurite sprouting, changes in the regulation of pathways controlled by neurotrophic factors, and all of these appear to affect visual function. Again, the studies done here provide added support for the visual adaptation model of visual system function, suggesting a careful re-examination of the current experimental methods of treating RDD is required. Thus, the visual adaptation model provides a framework for future research directed at developing therapies for RDD, while accounting for inconsistencies in previous theoretical models.

4. Animal Model

The rat proved to be a valuable model system for studying visual system function. Although the rat visual system evolved to specialize in low light and low resolution vision, visual functions such as acuity and contrast sensitivity were characterized using behavioral measures in a similar fashion as is done clinically. For the present studies, behavioral evaluations of vision provided the primary output measure which is most important when treating a diseased retina. In addition, behavioral measures of vision are extremely sensitive to small changes in the retina and therefore, these measures provided insight into abnormalities of cellular function which were previously not known to exist (i.e. long period of recovery after intraocular CNTF; S334ter line 4). In addition, the specific gene mutation in the retinal disease models used (RCS rat and rhodopsin mutated transgenic rats) are well known and have been identified in the human population of Retinitis Pigmentosa (RP). This is of particular advantage as knowing the specific cause of the disease allows of more specific selection of treatment parameters to increase the likelihood of treatment success. In addition, expressivity of gene mutations can differ

even within a single mutation. Here, we confirmed that different morphological phenotypes resulted in different visual performance, suggesting that each line within the S334ter mutation could be considered a different form of retinal disease. Furthermore, characterization of behaviorally measured visual thresholds from animal models of human retinal disease provides insight into the phenotypic expression of such diseases in the human condition, as well as providing a background for evaluation of potential therapeutic interventions.

5. Future directions and final thoughts

The specific effects of reorganization of the retina on visual function are not fully known. Examining this problem in animals with a degenerating retina in the past has been difficult because the effects of photoreceptor loss are difficult to separate from the effects of reorganization. In addition, the focus of treatment for RDD has been slightly misdirected in that although photoreceptors are important to some degree, other significant retinal events such as remodeling also play a major role in visual outcome. To complicate issues further, current clinical and experimental treatments for retinal degenerative disease are not designed to prevent reorganization, which would likely decrease the treatments potential efficacy, although some evidence provided here suggests that cell transplantation may coincidentally limit some of these changes. Ironically, cell transplantation is performed via sub-retinal injection which necessarily causes retinal detachment consequently resulting in retinal remodeling (Lewis et al., 2002; Fisher et al., 2005). The studies in this thesis show that Muller glial cell activation and migration occur in multiple models of retinal degeneration, and in a normal laboratory rat following the injection of CNTF. In each of these cases there is

concomitant reduction in the visual performance of these animals suggesting that reducing reorganization in the retina should be regarded as a major concern when treating clinical retinal diseases such as RP or AMD. Although it is not clear why inner retinal neurons or Muller glial cells extend uncommon processes, there are a few possible explanations. Inner retinal neurons likely extend neurites in an attempt to re-establish the lost photoreceptor input by developing new synapses with remaining retinal cells. Evidence of the microneuromas in diseased retinas suggests that these neurons do not inherently know where to grow implying that microneuromas are the product of random collections of growing neurons. Muller glial cells however are thought to have specific roles that explain the gliosis found in diseased retinas. Gliosis is thought to be an attempt by the Muller cells to restore potential breaks in the blood-brain barrier by scar formation, and to modulate cytokines and growth factors that are up-regulated in diseased retinas, and Muller cells may also phagocytose retinal degeneration by-products (Bringmann et al., 2006).

It is clear that Muller glial cells are significant regulators of neurotrophic factors in the retina, and may play a significant role in maintaining behaviorally measured visual performance. To clarify the role of Muller glial cell proliferation on visual function, one must thoroughly examine Muller cell gliosis and its effect on visual performance without photoreceptor abnormalities. Unfortunately, the only current reliable method of inducing Muller cell gliosis is through retinal detachment, however, photoreceptor outersegment abnormalities ensue, thereby confounding the results of visual performance testing. Another potential avenue is to use an animal with a naturally occurring gene mutation in Muller cells which causes gliosis, yet does not exhibit photoreceptor degeneration until

well after gliosis has started. This model may very well exist, however examining hundreds of potential animal models in search of such events would be a daunting task. Finally, inducing gliosis through the use of gene therapy may be a potential avenue for examining Muller cell changes, however, there is currently no evidence selective Muller gliosis is achievable. With respect to retinal degeneration, Muller cells are well suited as tartgets for therapeutic intervention because they span the entire thickness of the retina, and are in contact with all retinal cells. Therefore, adenovirus-mediated gene therapy, cell transplant therapy, or neurotrophin delivery based therapy for retinal degenerative disease, which is targeted to Muller cells, may have extra advantages in that these cells may be able stimulate the survival of retinal neurons and photoreceptors independent of the mutation or underlying cause of retinal cell death.

Cell transplantation remains one of the premier methods for treating retinal disease. Numerous cell types are available and have been shown to preserve retinal cells, limit retinal reorganization, preserve visual responses such as ERG and measures from recorded superior colliculus and cortex, as well as preserve optomotor responses and spatial vision. There remains a major obstacle to the cell therapy procedure which is immune rejection of the grafted cells. The work done here suggests that if cells are harvested from syngeneic, or potentially another autologous source, the grafted cells may not be rejected, suggesting long-term prevention of retinal disease is possible. A very exiting recent development is the engineering of cells which resemble embryonic stem cells from adult human and primate somatic sources (Byrne et al., 2007; Yu et al., 2007). Incredibly, these cells have the potential to avoid immune rejection while holding the promise of replenishing lost retinal cells and producing neurotrophic factors believed to

be the source of rescue cell transplants provide. However, these technologies are in their infancy and much is yet to be learnt about them.

Historically, neurotrophic delivery has been limited to intraocular injections of the factor itself, or of AAV-associated expression. Recently, a new technology has been developed which allows cells (RPE, but in theory any cell type could be used) to survive within a capsule which is made of permeable membrane and allows the overproduced growth factors to diffuse into the eye. This technology has recently been used in phase I clinical studies with some success (Sieving et al., 2006). Although one study in this thesis suggests high concentrations of CNTF may be harmful to the normal retina, the effects of high doses to the human diseased eye are yet to be elucidated. It is likely the case that cell transplantation and ECT therapy will be applied selectively for different circumstances. For example, RP patients who suffer severe loss of rod photoreceptors across the entire retina require a widespread preservation of these cells, which is more easily achieved using ECT than sub-retinal cell delivery. However, in a cone-rod dystrophy or in dry AMD (and maybe wet AMD too), cell transplantation is likely to be the treatment of choice as local preservation (macular or foveal) is achieved easier through cell transplants and doesn't hold the complication of delivering toxic levels of neurotrophic factors to remaining normal retinal cells within the same diseased eye.

It is important to make a clear distinction between visual function and functional vision. Visual function has become a term in the cell transplantation literature that encompasses ERG wave recordings, superior colliculus recordings, visual cortex recordings, and the pupillary light reflex. In many reports, visual function is equated with functional vision, this is simply not true and as the experiments in this thesis show,

often times visual function and functional vision do not directly map onto one another. Furthermore, vision being defined as the perceptual experience of seeing, requires that behavioral evaluation is performed to assess it. The experiments in this thesis place heavy emphasis on behavioral assessment of vision for 2 specific and very important reasons: First, in the human condition, progressive visual dysfunction such as loss of night vision, blurry spots etc., are used as the diagnostic measure for retinal degenerative disease. That is, degeneration in vision rather than degeneration of the retina is what defines many diseases such as RP or AMD. Secondly, as patients with these diseases inevitably lose sight, the ultimate measure of treatment success is restoration, or prevention of the loss of eye-sight.

The work in this thesis pleads for the continuation of multiple aspects of these studies. For example, although we know cell transplantation preserves retinal cells, retinal function, and vision in animals with retinal disease, it is currently unknown what the specific mechanism is by which this effect is mediated. The current hypothesis is that diffusible growth factors released from the grafted cells are sufficient for this preservation for varying lengths of time. A potential avenue for confirming this hypothesis is by evaluating the levels of growth factors such as CNTF, BDNF, and GDNF in animals that have undergone cell transplantation versus untreated controls using techniques such as in situ hybridization and polymerase chain reaction (PCR). Done properly, this would be a lengthy study as behavioral measures of vision, standard histological analysis of the retina, immunohistochemical analysis of the retina, and the molecular biological analysis would all be required on the same animals (as much as possible), and using multiple time points would thereby require a very large initial cohort

of animals. However, the results of such a study would be significant as it would highlight the crucial factors involved in maintaining vision and potentially photoreceptor survival, and it is likely these same factors are involved to some extent in maintaining the structural integrity of the INL, IPL, ganglion cell layer, and Muller cells. Furthermore, the results of such a study would provide a biochemical basis for further examination into the cellular and molecular events in retinal remodeling. Moreover, this study would also provide insight into dosages as in one study presented here, delivery of CNTF in high concentrations caused impairments in photoreceptor structure and functional deficiencies as measured by ERG and optokinetic response. However, lower doses (which we did in a dose dependent logarithmic fashion) exist, which are thought to prevent photoreceptor cell death in diseased retinas, and yet do not appear to have serious consequences for photoreceptors or vision in the normal eye. Therefore, clarification into the specific factors and dosages will be a vital piece to solving RDD treatment puzzle.

Brain plasticity has the potential to compensate for significant visual impairments due to damage in the retina. However, we did not directly examine brain plasticity in the studies performed here for a couple of reasons: 1) manipulation of brain plasticity when treating the human condition of RDD is not an option, 2) as the retina begins degenerating early in the animals models used in these studies, developmental plasticity would be the most logical culprit, however, in the human condition, most RDD's do not develop until long after developmental periods of plasticity are over. Having said that, it is a very interesting and exciting idea that a potential manipulation to the brain may increase its tolerance for lost input thereby decreasing the effects of retinal degeneration,

however, this was not the goal of the experiments in this thesis and would require an extensive set of experiments to address the issue properly.

6. Summary

In summary, the work in this thesis is exciting because it demonstrates, for the first time, that remodeling of the retina is in fact a non adaptive process. These studies provide empirical support for the visual adaptation model which should be used as a template for the design of experiments involving visual function and retinal disease. In addition, the work done here urges that 2 important principles be highlighted. First, visual function is clearly the most important output measure when examining retinal degenerative diseases and their respective treatments, and therefore it is imperative that vision be measured in some capacity. Second, prevention of retinal remodeling is likely as important as preventing photoreceptor loss, and preventing both simultaneously is likely to be the most effective method of treating retinal dystrophies.

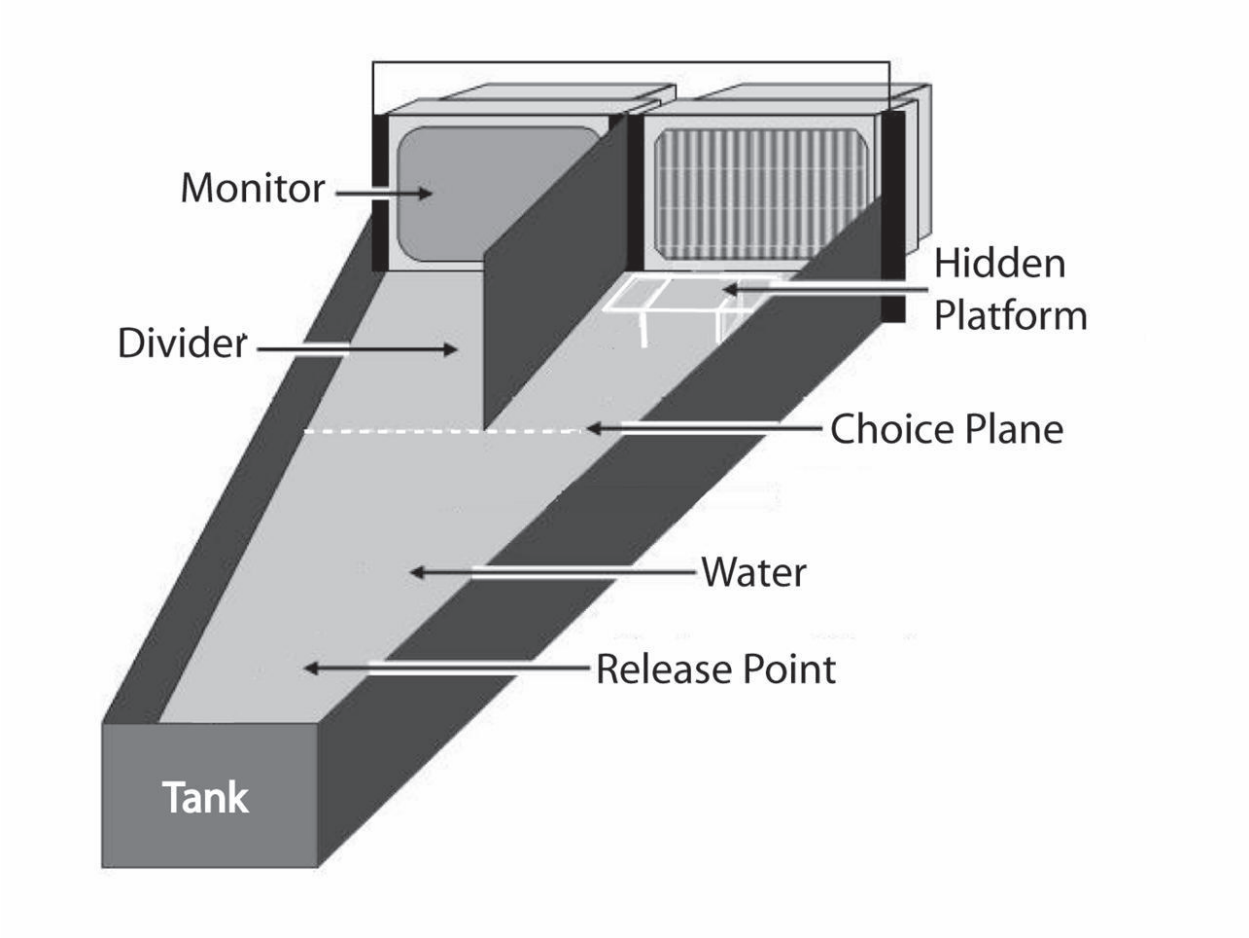

Figure 1. The Visual Water Task; a task which can be used to evaluate the visual perception of rodents.

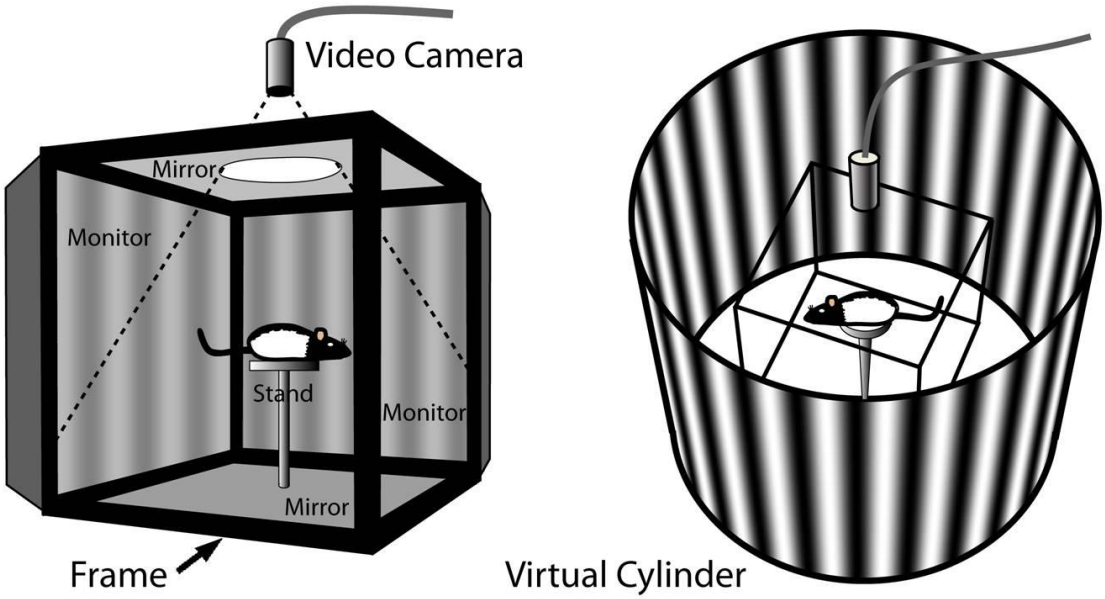

Figure 2. The Virtual Optomotor System (VOS). Left: Side view of apparatus which consists of 4 computer monitors facing inward (2 removed for ease of viewing) into an arena. An animal is placed on a platform located in the middle of the arena and a video camera viewing from above provides real-time feedback of animals' behavior. Right: The virtual cylinder displaying sine-wave gratings with the testing arena and animal highlighted within.

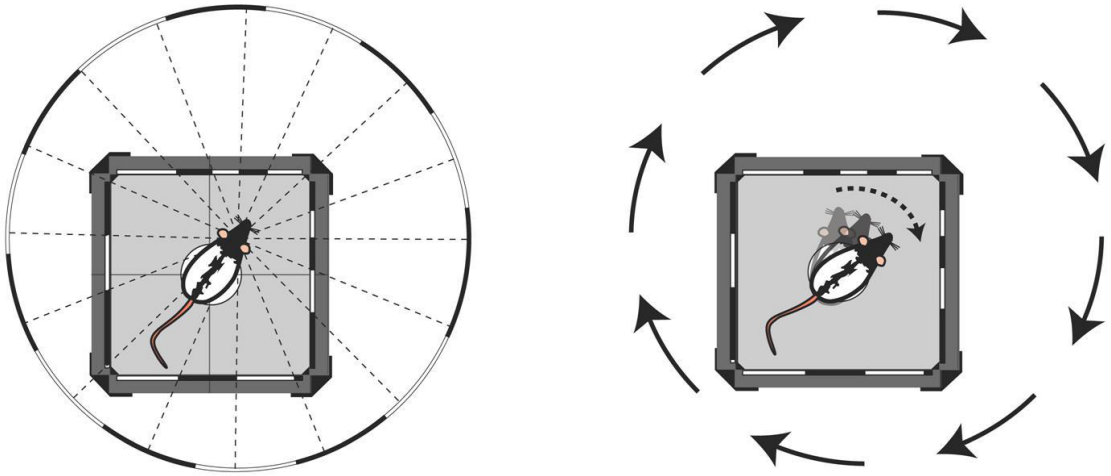

Figure 3. The Virtual Optomotor System (VOS). Left: Diagram depicts the animals viewing angle of the the visual stimuli. The sine-wave gratings are displayed as different sizes on the monitors in order to keep the virtual cylinder homogenous throughout the testing arena. Right: Arrows showing direction of rotation of the virtual cylinder and the corresponding movement of an animal performing the optokinetic tracking behavior. Figure adapted from Prusky et al., 2004.

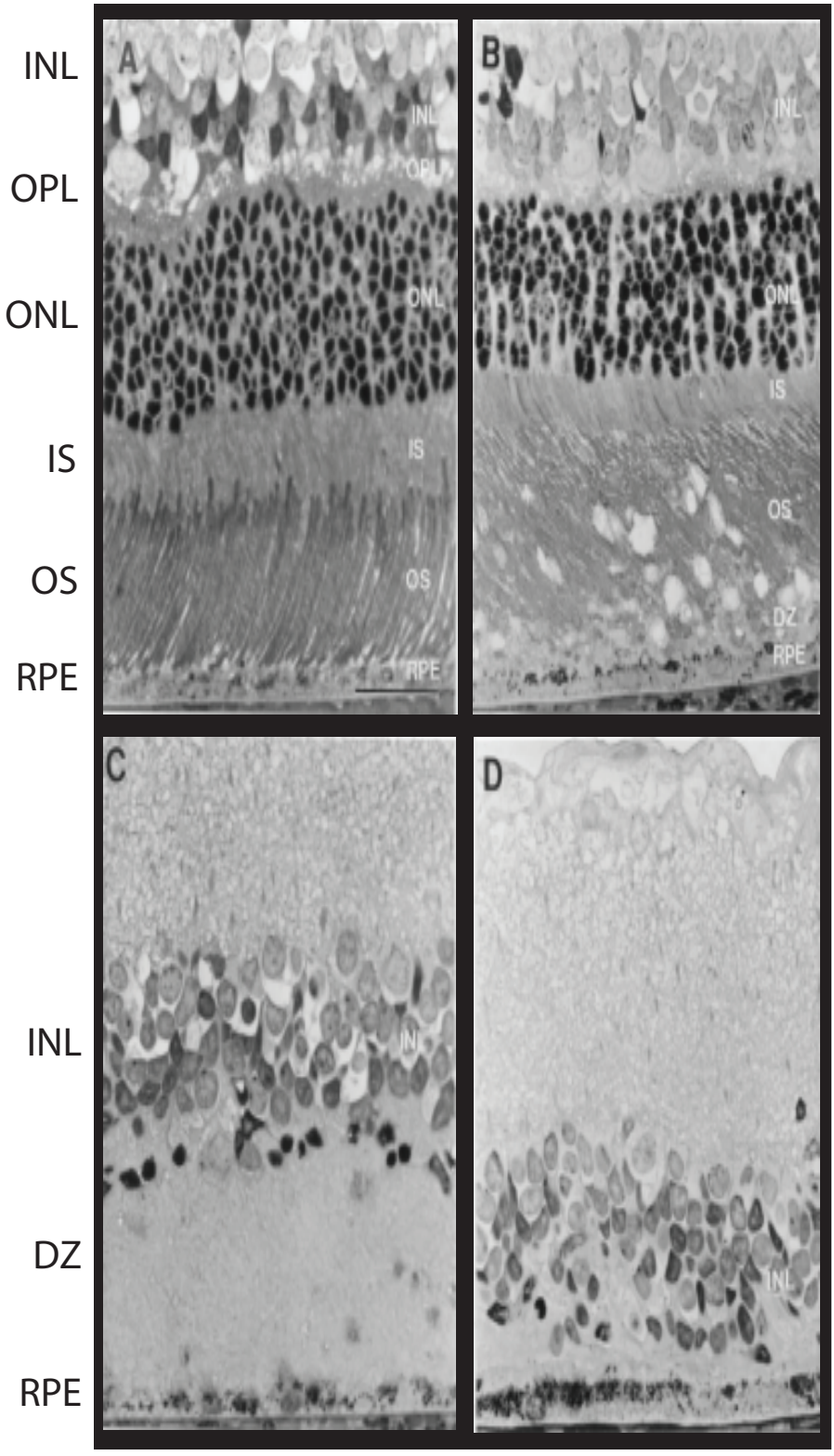

Figure 4. Retinal anatomy of the RCS rat at 21 days (A), 45 days (B), 90 days (C), and 180 days of age (D). (INL-inner nuclear layer; OPL-outer plexiform layer; ONL-outer nuclear layer; IS-inner segment; OS-outersegment; RPE-retinal pigment epithelium). Reprinted with perission from Dr. Ray Lund. Scale bar 100 um.

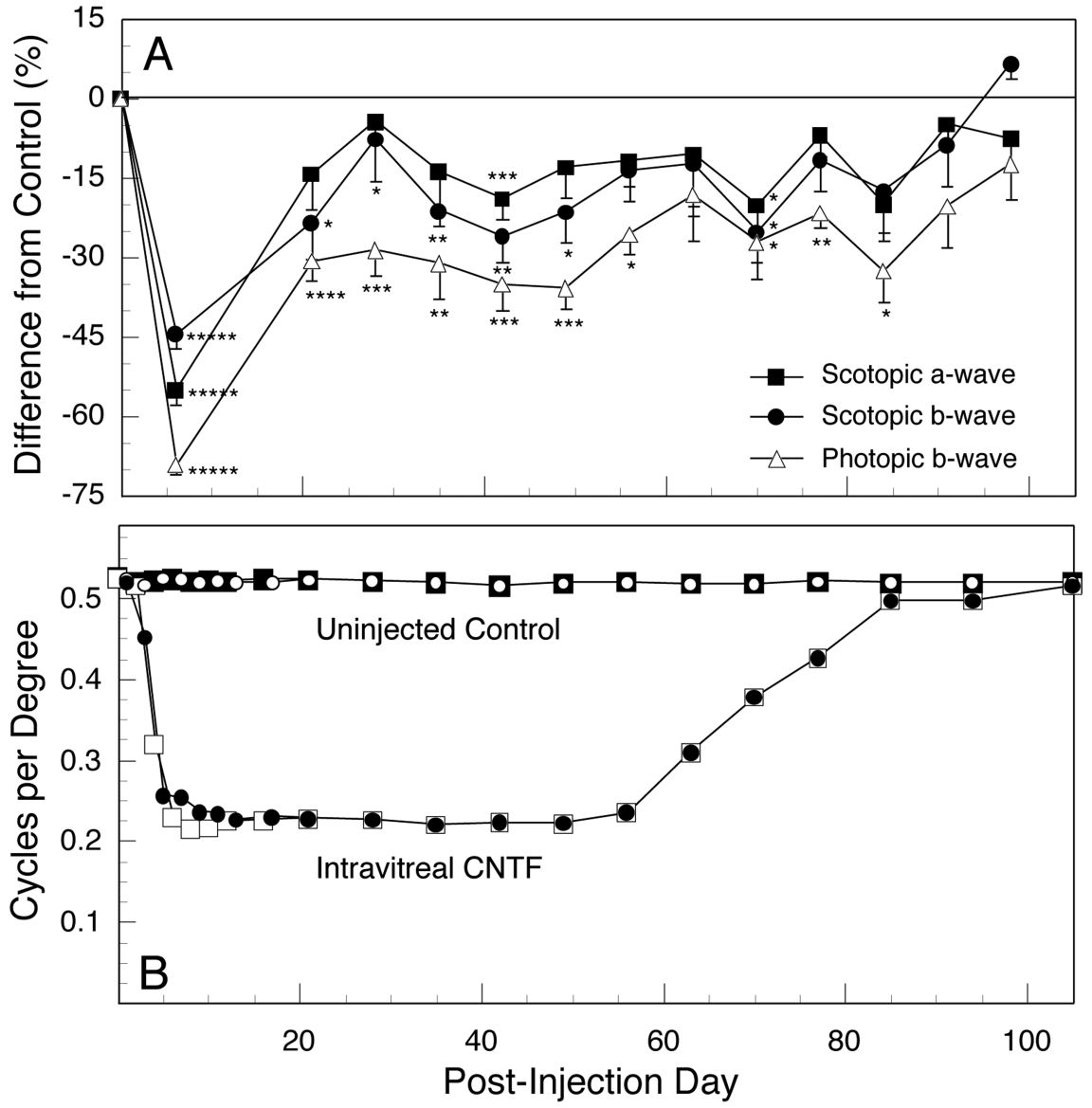

Figure 5. Changes in the ERG and spatial frequencies thresholds of the optomotor response (OKR) following intravitreal injection of 10 ug of CNTF. (A) Maximal ERG amplitudes of injected eyes compared with control eyes measured simultaneously. At 6 days postinjection (PI), all three waves are 45-70% lower than those of control eyes. The maximal amplitudes of each of the ERG waves remain lower than those of control eyes through 91 day PI, with variable degrees of statistical significance. The scotopic a-waves mostly recover to near normal by 21 days PI, while the photopic b-waves recover the slowest, still significantly different from control values at 81 days PI. At 6 days PI, n = 11 rats; thereafter n = 5-7 rats, except at 91 days (n = 4) and 98 days (n = 3). Each value = mean ± S.E.M. *$p < 0.05$; **$p < 0.01$; ***$p < 0.005$; ****$p < 0.001$; *****$p < 10^{-5}$; those values not marked are not significantly different from control

values. (B) OKR spatial frequency thresholds measured through eyes injected intravitreally with 10 µg of CNTF compared to uninjected control eyes. By 3 days PI, the thresholds decline to about 0.450 cycles per degree (cpd), where they are already significantly different ($p < 0.001$) from control values of 0.53 cpd (n=11). By 8 days thresholds reach 0.210 cpd, where they remain until day 56. Thereafter, the thresholds begin to recover, and while they are near control values at 85 and 94 days PI, they still differ statistically ($p < 0.05$). At 105 and 119 (not shown) days PI, thresholds in injected eyes no longer differ from those in control values. Eleven rats were studied, initially in two groups (n=5 and 6, solid dots and open squares, respectively). These groups were examined on alternate days until day 21 PI; thereafter, the rats of both groups were examined at the same PI intervals. The spatial frequency thresholds at any given age are extremely consistent from animal to animal resulting in little variance, and therefore the error bars on the graph are hidden by the symbols of the data points.

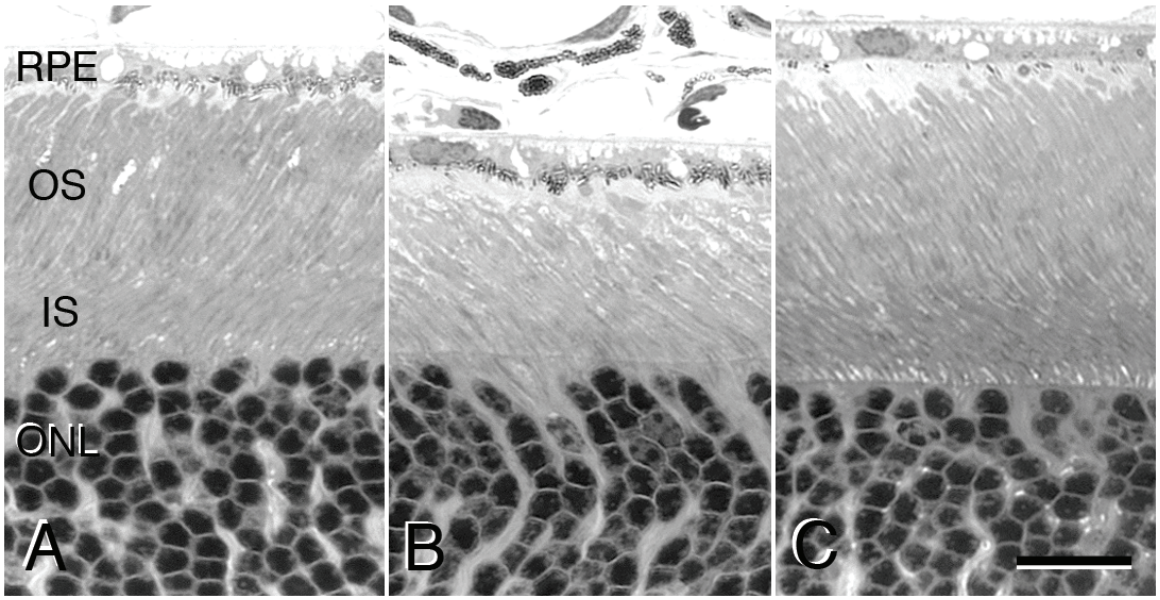

Figure 6. Light micrographs of retinas of normal Long-Evans rats. (A) Uninjected eye. (B) 6 days following intravitreal injection of 10ug of CNTF, and (C) 22 days post-injection (PI). At 6 days PI (B), the photoreceptor outer segments (OS) are somewhat tattered and are only about half the length of those before the injection (A). By 21 days PI (C), the OS have fully recoverend in structural integrity and length,. IS, inner segment; ONL, outer nuclear layer; RPE, retinal pigment epithelium. Scale bar, 25um.

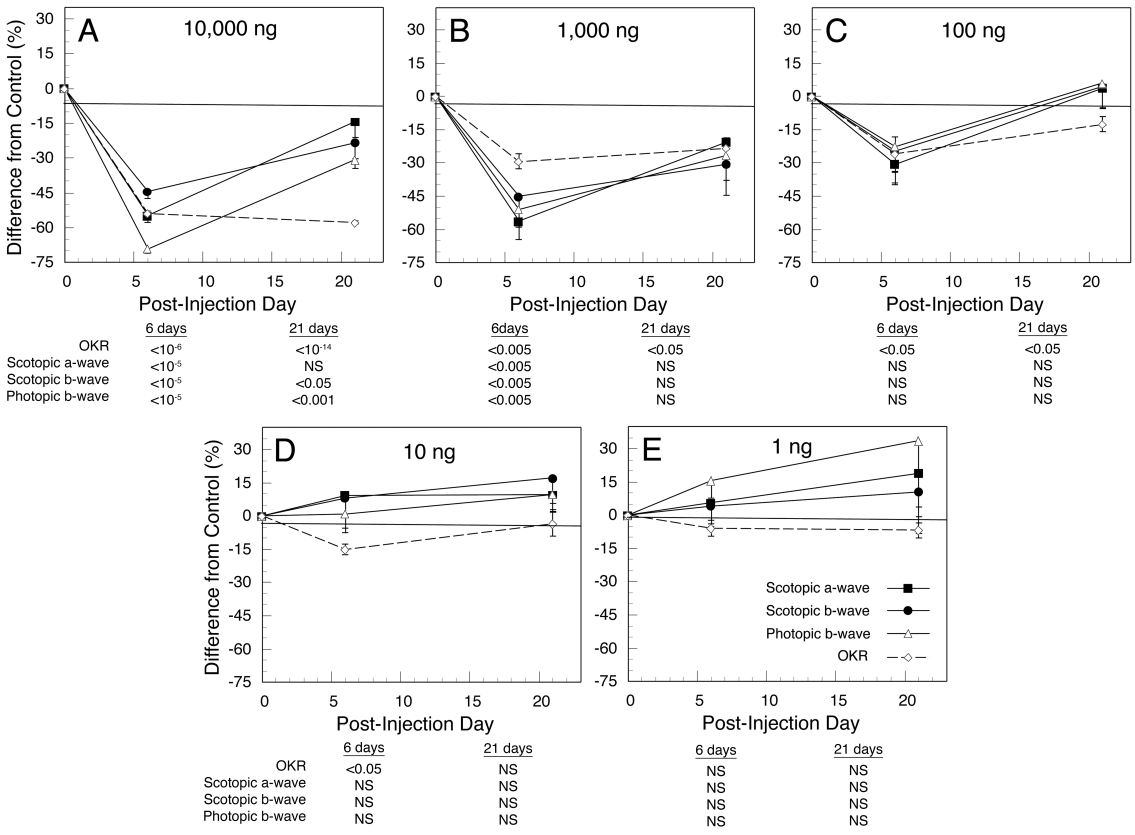

Figure 7. Dose-response analysis of ERG responses and OKR thresholds following monocular intravitreal injection of CNTF at 6 and 21 days PI. The results of paired Student's t-test are shown beneath the graph of each dose; injected eyes are compared with uninjected eyes of the same rat. (A) 10,000 ng (10 µg), data from the same animals shown in Fig. 1 (n=11). (B and C) 1,000 and 100 ng, respectively (n=5). (D and E) 10 and 1 ng, respectively (n=3). The suppression of ERG amplitudes of all three waveforms is significant with 10,000 ng at 6 and 21 days PI, and at 6 days PI with 1,000 ng, but not thereafter. A significant reduction in OKR thresholds occurs at even lower doses, at 6 days PI with 100 ng, and with a very small reduction at 21 days PI with 100 ng, and 6 days PI with 10 ng. There was no measurable effect on the OKR thresholds at 21 days PI with 10 ng, or at either PI interval with 1 ng.

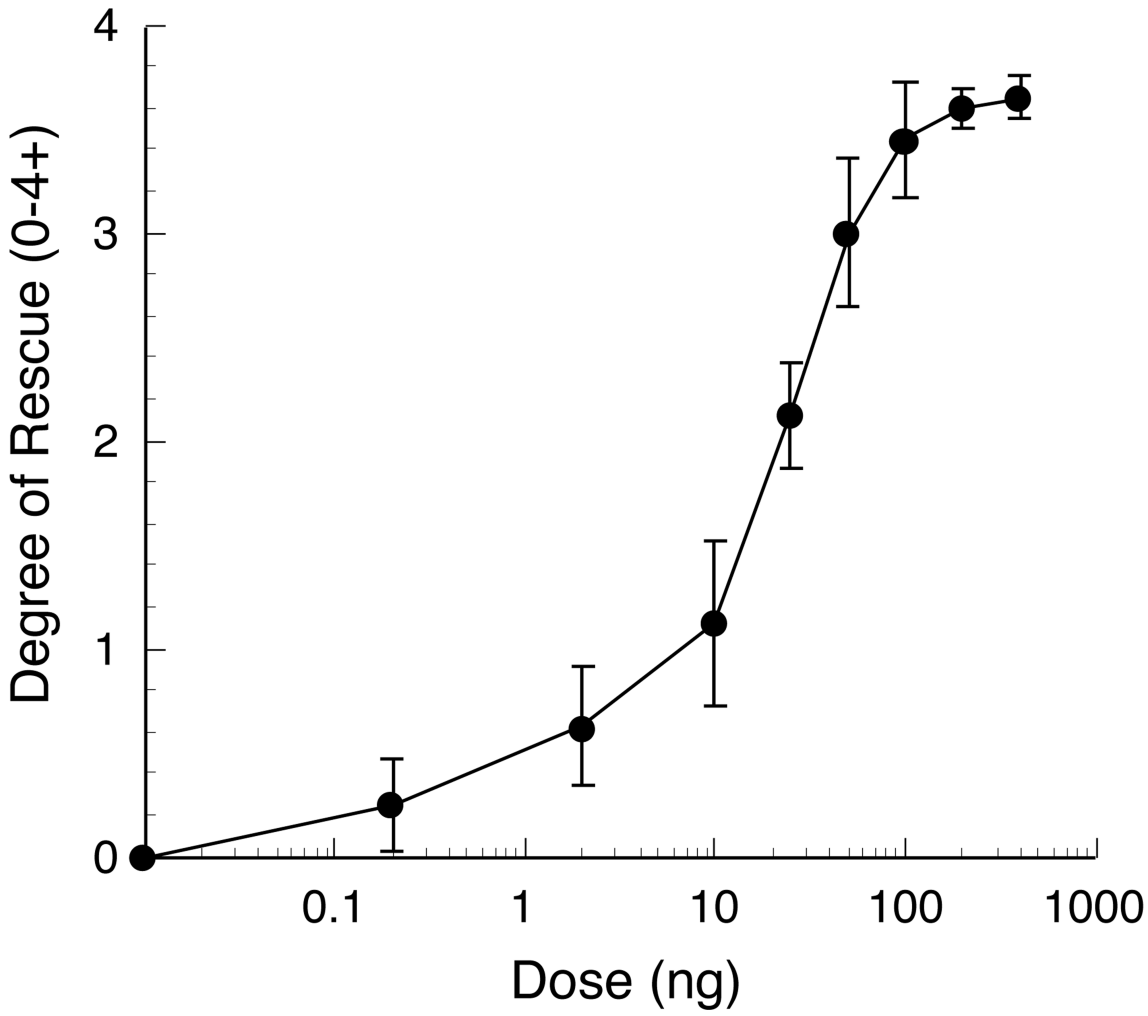

Figure 8. Dose-response analysis of protection of the retina of albino Sprague-Dawley rats from constant light damage due to intravitreal injection of rat CNTF. CNTF was injected 2 days before a 7-day light exposure. Doses of 50, 100 and 200 ng were not statistically different from the highest dose of 400 ng, and thus all gave maximal protection. A dose of 25 ng gave moderate protection, but was significantly less effective than the maximal dose ($p<0.005$). Doses of 10 ng and lower gave progressively less protection, but protection from the 10-ng dose was significantly greater than the 0.2-ng dose ($p<0.05$). For each dose n=5 or 6.

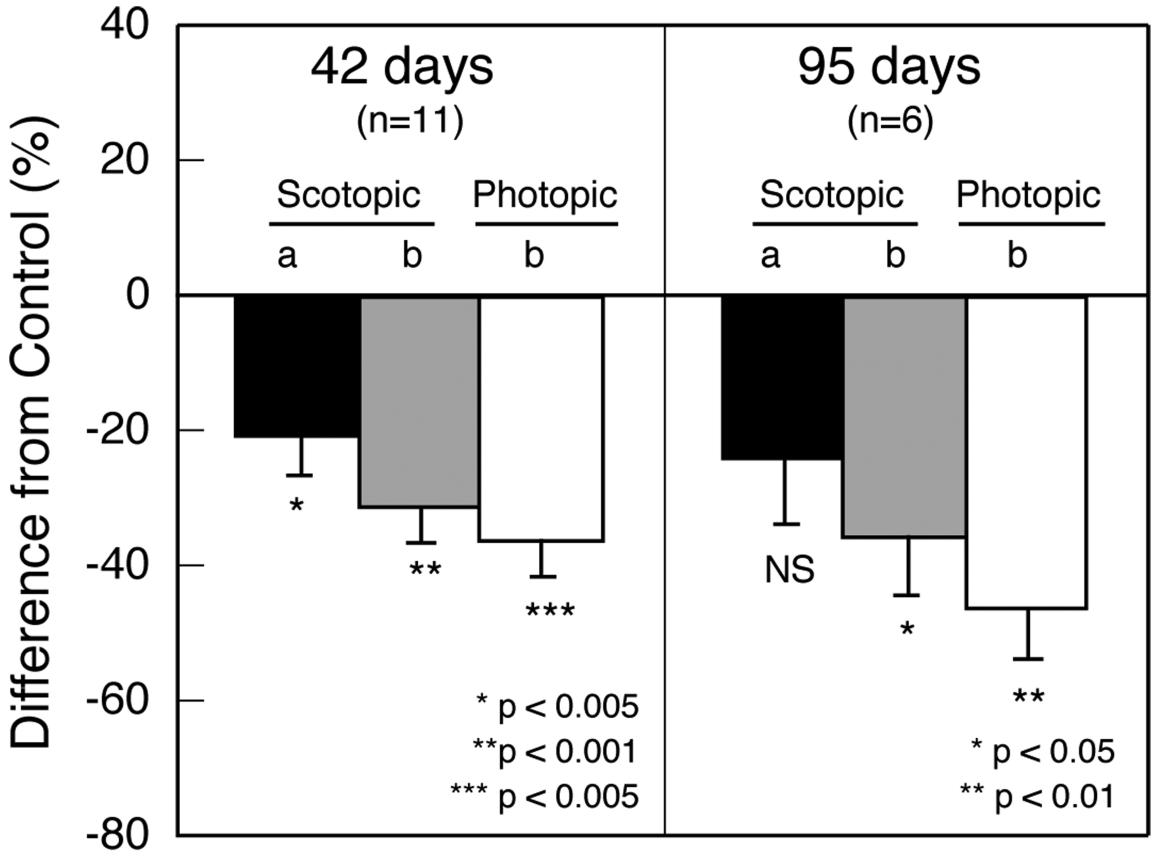

Figure 9. Changes in the ERG following subretinal injection of AAV-CNTF. Maximal ERG amplitudes of injected eyes compared with control eyes measured simultaneously. At 42 and 95 days PI, all of the ERG waves in the injected eyes are reduced from those of control eyes, although scotopic a-waves are not statistically different (NS) at 95 days.

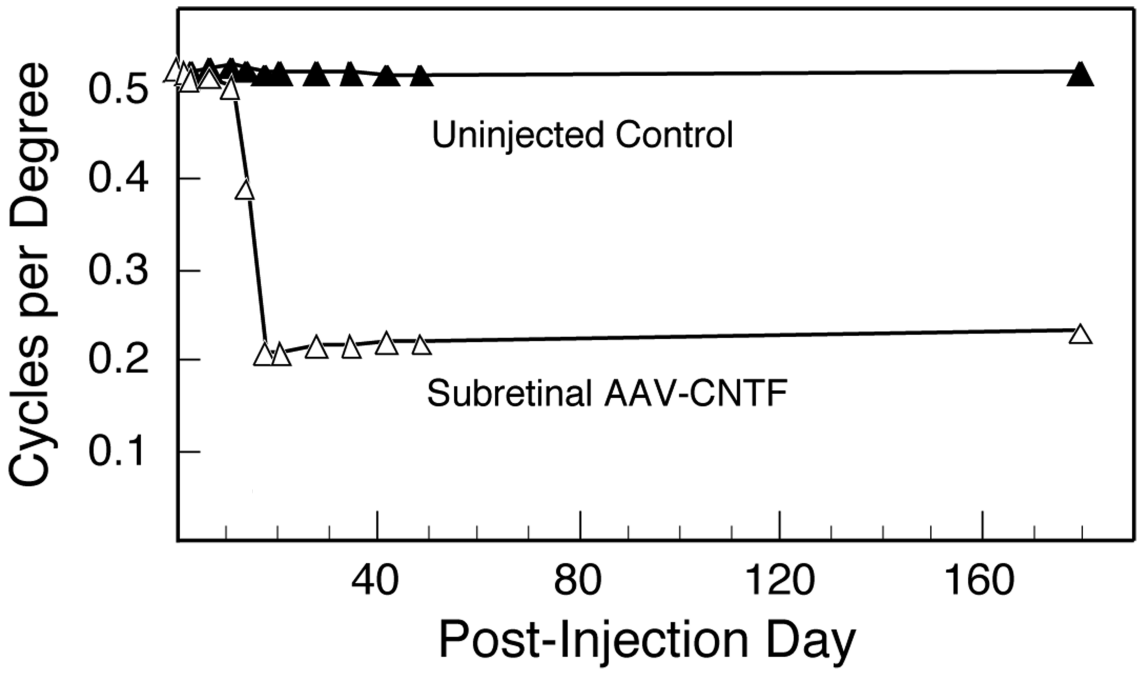

Figure 10. OKR spatial frequency thresholds measured through eyes injected subretinally with AAV-CNTF compared to uninjected control eyes. The thresholds of the injected eyes appear almost normal until 11 days PI, although they are already statistically lower than normal ($p < 0.01$), and drop rapidly between 11 and 18 days PI, after which they remain consistently at about 0.210-0.233 cpd for up to 180 days PI. The measurements up to 49 days PI are from a group of 9 rats, and the measurements at 180 days are from 5 different rats. At 18 days PI and thereafter, the injected eyes differ from control values with a high level of significance (see text for details).

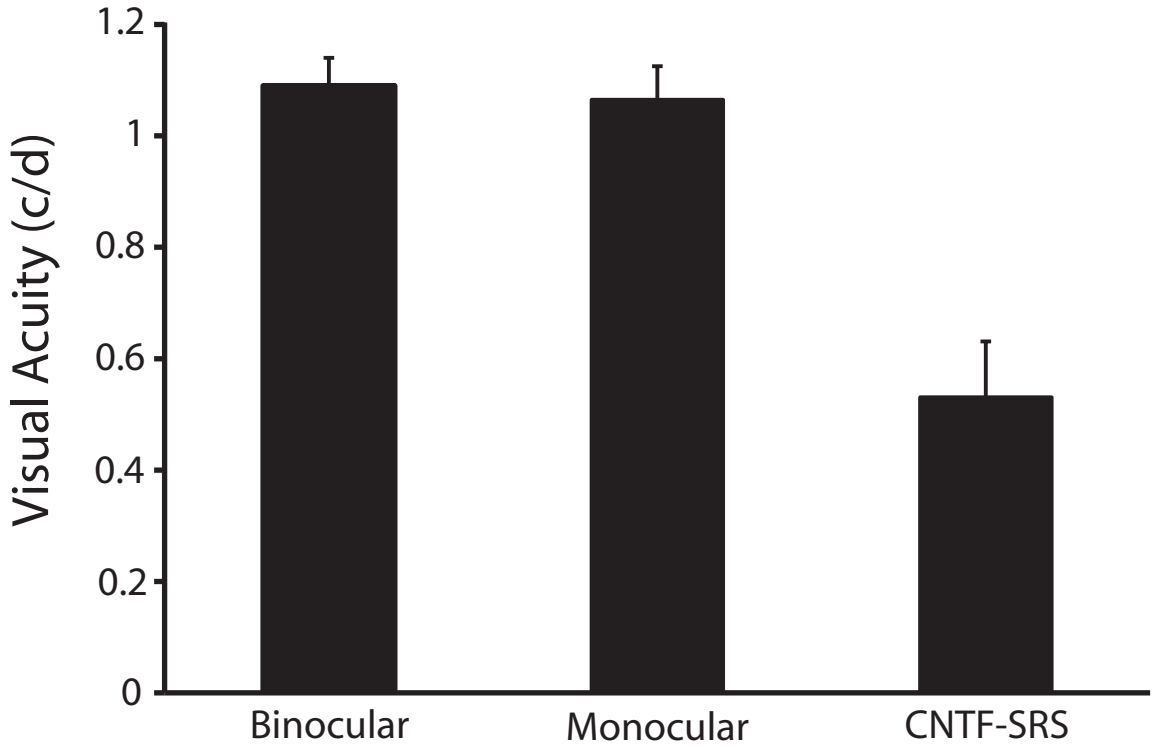

Figure 11. Change in perceptual visual acuity measured using the visual water task 6 months following subretinal injection of AAV-CNTF. Animals measured binocularly show acuity values of approximately 1.0 c/d, normal for pigmented rats. Similarly, acuity measured monocularly through the uninjected control eye is the same as that measured binocularly, whereas the acuity measured through the eyes injected with AAV-CNTF is reduced to about half that of normal eyes ($p < 0.003$).

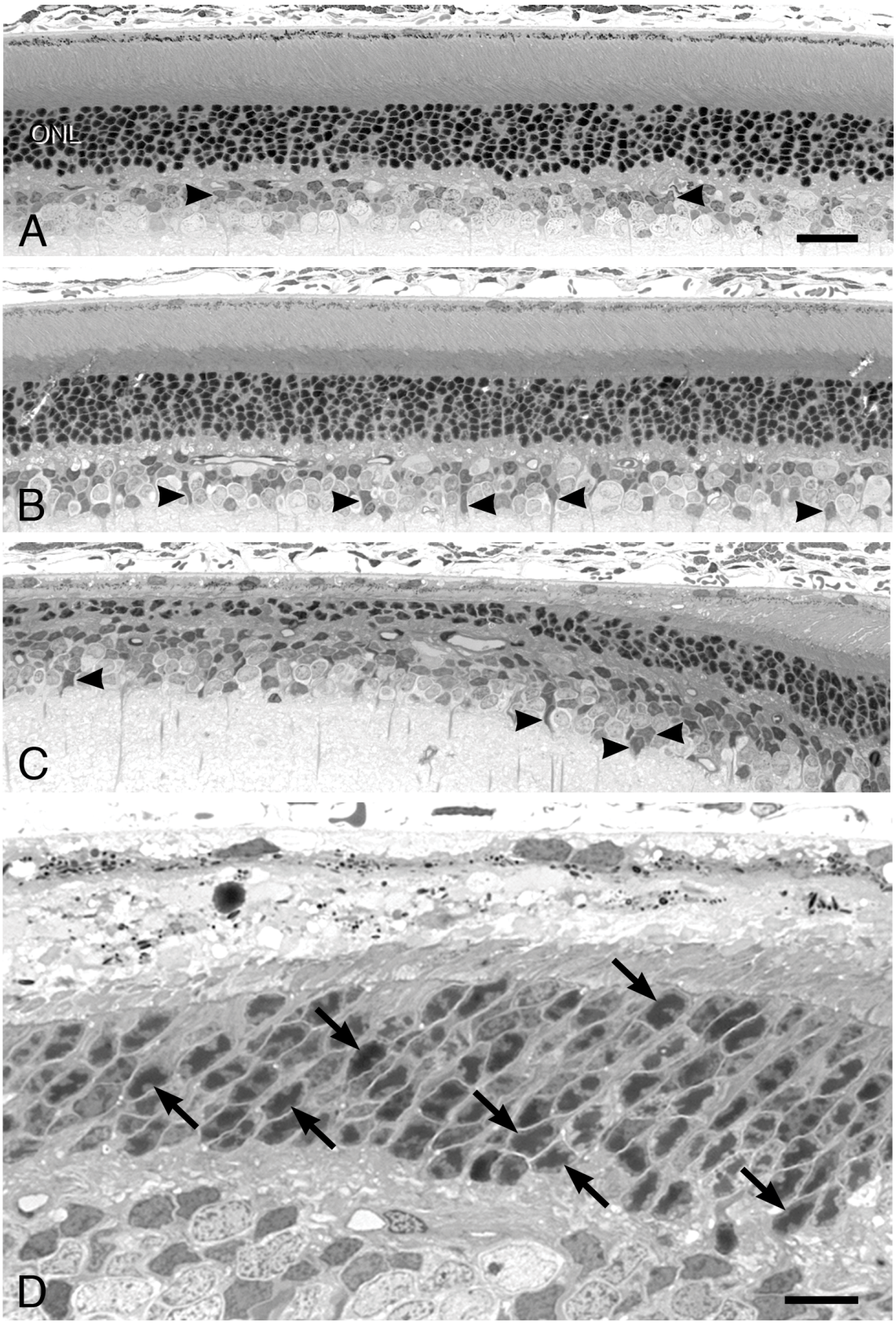
ONL
A
B
C
D

Figure 12. Light micrographs of the retinas of Long-Evans rats at P194 that were either normal, uninjected eyes (A) or following subretinal injection of AAV-CNTF into the superior hemisphere of the eye (B-D). (A) The control retina has the normal complement of photoreceptor nuclei in the outer nuclear layer (ONL), and most of the densely staining Müller cell nuclei that typically conform to the shape of the other nuclei of the inner nuclear layer are located in the middle or middle-to-outer part of the inner nuclear layer (arrowheads). (B) Example of one of the AAV-CNTF-injected retinas that had no apparent loss of photoreceptors, but some of the Müller cell nuclei are located in the inner aspect of the inner nuclear layer (arrowheads). (C) Retina that has lost most of the photoreceptors (left side) with a transition to almost normal retina (right side) and which shows atypical distribution of Müller cell nuclei (arrowheads). (D) Higher magnification of a transition zone where some rod photoreceptors have the typical single large clump of heterochromatin with "moth-eaten" edges and densely staining euchromatin (arrows), but where most rod photoreceptor nuclei have dispersed heterochromatin giving a spotty, cone-like appearance. True cones comprise only about 1.5% of the photoreceptor population in the normal rat. Quantitative measures and distribution of photoreceptor loss are presented in Figure 13. Scale bar in A represents 25 um, and 15 um in D.

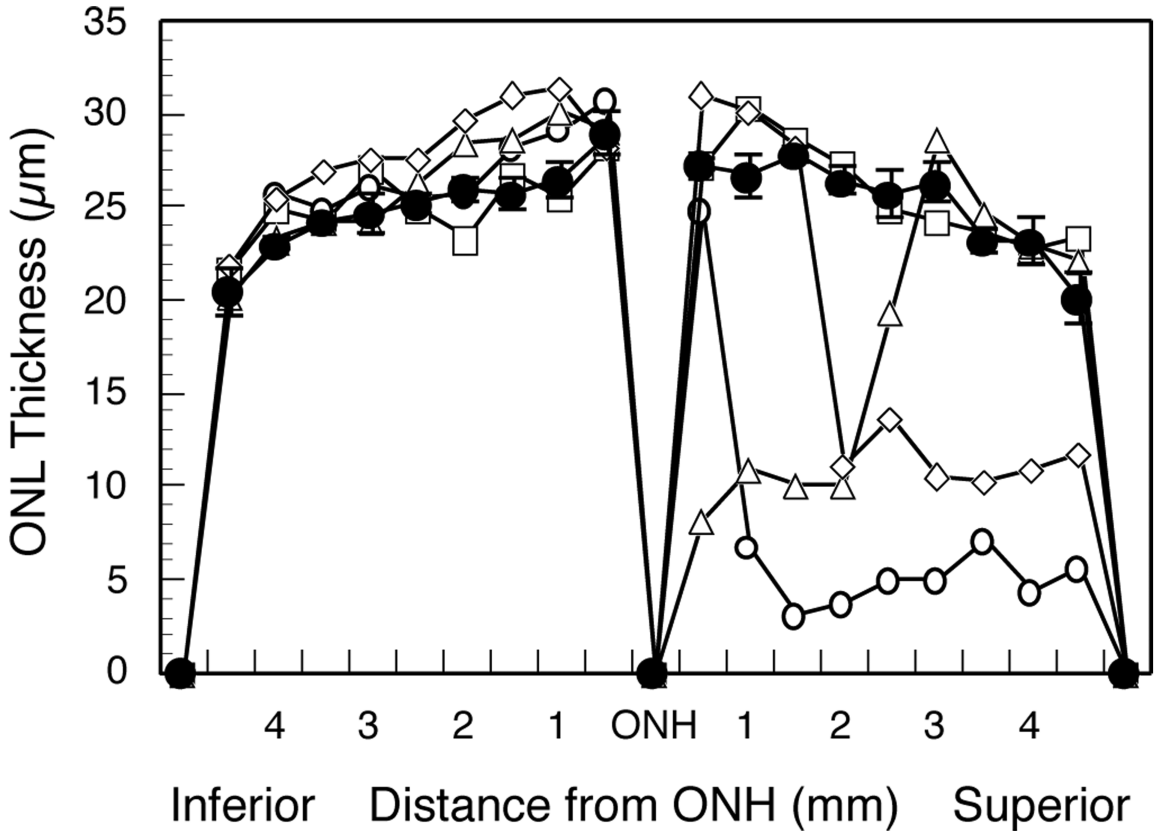

Figure 13. Quantitative measures and distribution of photoreceptor loss represented from Figure 12. Outer nuclear layer (ONL) thickness is shown across individual retinal sections through the vertical meridian of one normal, uninjected control eye (solid symbols) and 4 eyes injected subretinally with AAV-CNTF. One of the retinas shows no reduction in ONL thickness across the retina (open squares), and the retina from another rat in this cohort had a similar pattern (data not shown), despite having reduced ERG amplitudes and behavioral responses. The injected retinas from 3 of the rats had regions of reduced ONL thickness (i.e., loss of photoreceptors) for variable lengths of retina in the superior hemisphere (open circles, triangles and diamonds).

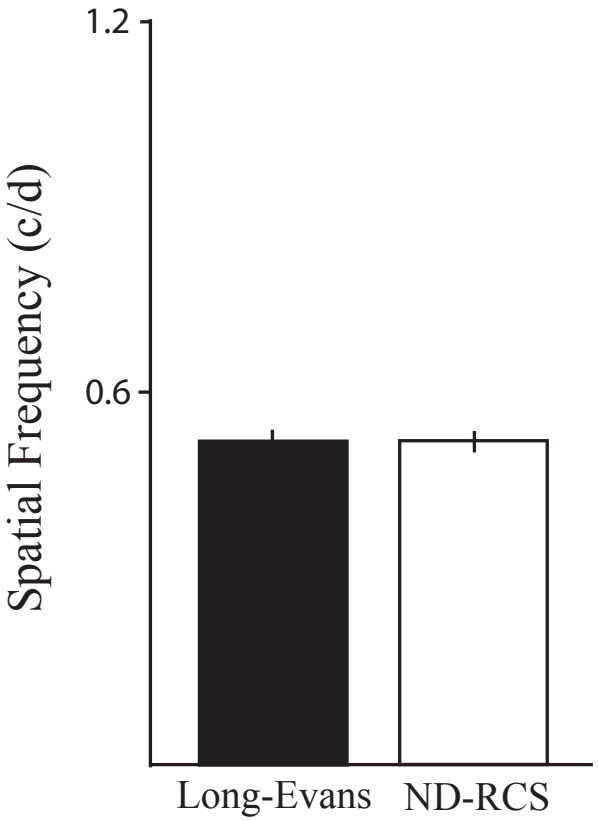

Figure 14. Spatial frequency thresholds of the optokinetic response. Both adult Long-Evans and Non-Dystrophic RCS rats had thresholds ~ 0.530 cycles-per-degree.

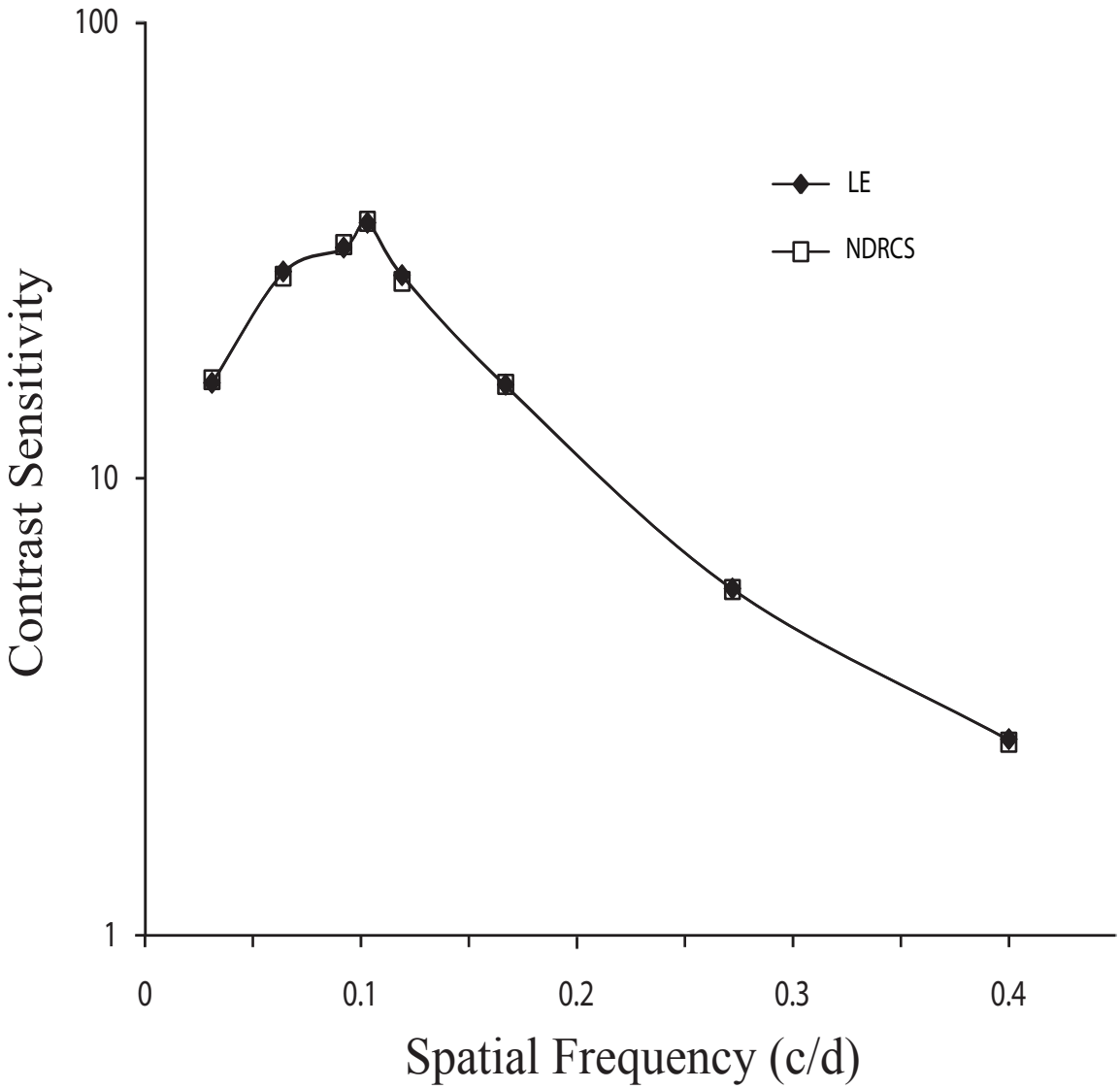

Figure 15. Contrast sensitivity function of Long-Evans and Non-Dystrophic RCS rats. Both groups had near identical inverted-U shaped curves typical of mammalian visual systems.

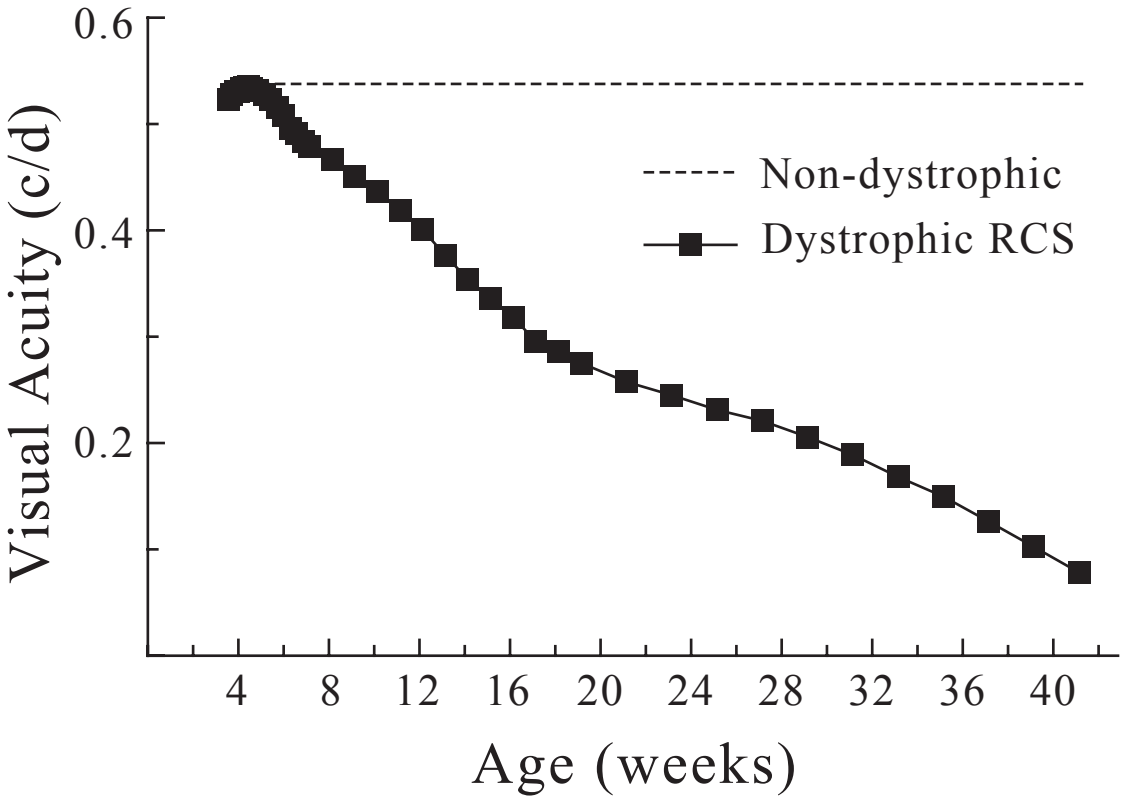

Figure 16. Progression of visual decline in dystrophic Royal College of Surgeons rat compared with a non-dystrophic (Long-Evans) rat. Visual thresholds were measured using optokinetic tracking response in the Virtual Optomotor System.

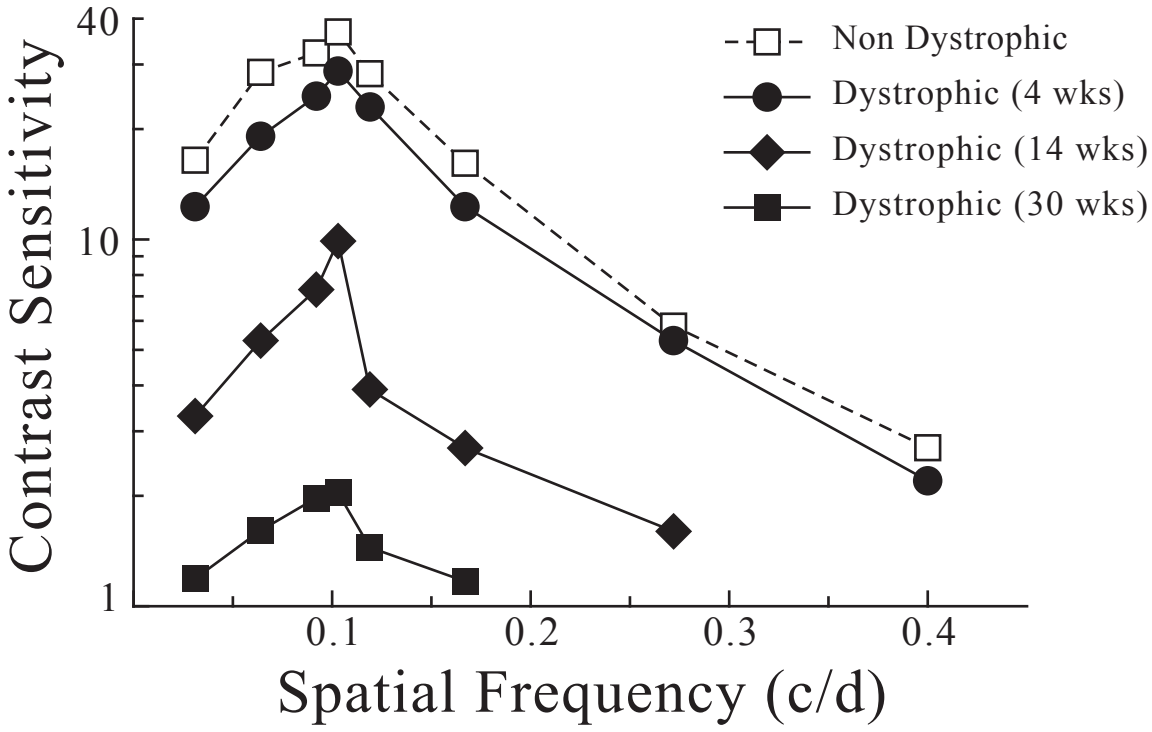

Figure 17. Contrast sensitivity curves of non-dystrophic (Long-Evans) rats and dystrophic RCS rats at 4, 14, and 30 weeks of age.

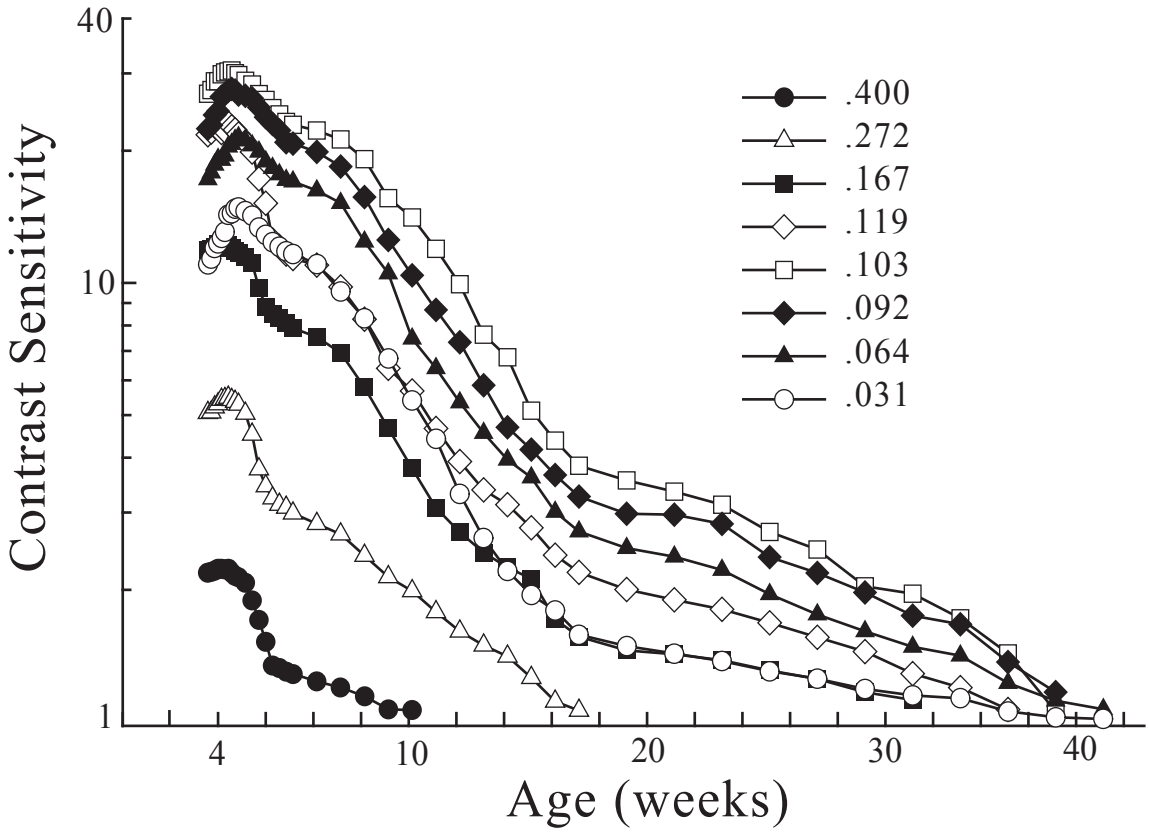

Figure 18. Contrast sensitivity of dystrophic Royal College of Surgeons rats with age. Each spatial frequency is plotted as an individual line and symbol emphasizing the effect of retinal degeneration on various receptive field sizes.

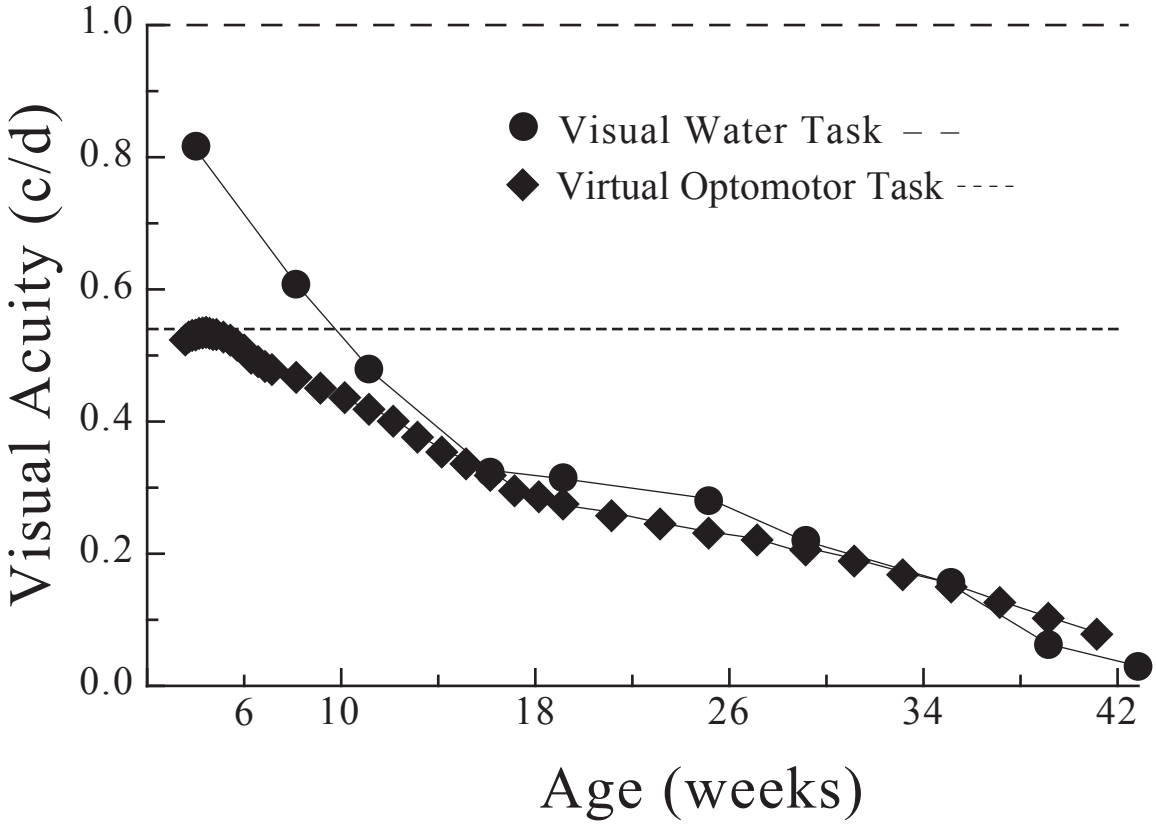

Figure 19. Comparison between the visual thresholds obtained from the dystrophic RCS rats by using both the Visual Water Task (VWT) and the Virtual Optomotor Task (VOS). Dotted lines represent thresholds measured from non-dystrophic rats in the VWT (top) and the VOS (bottom).

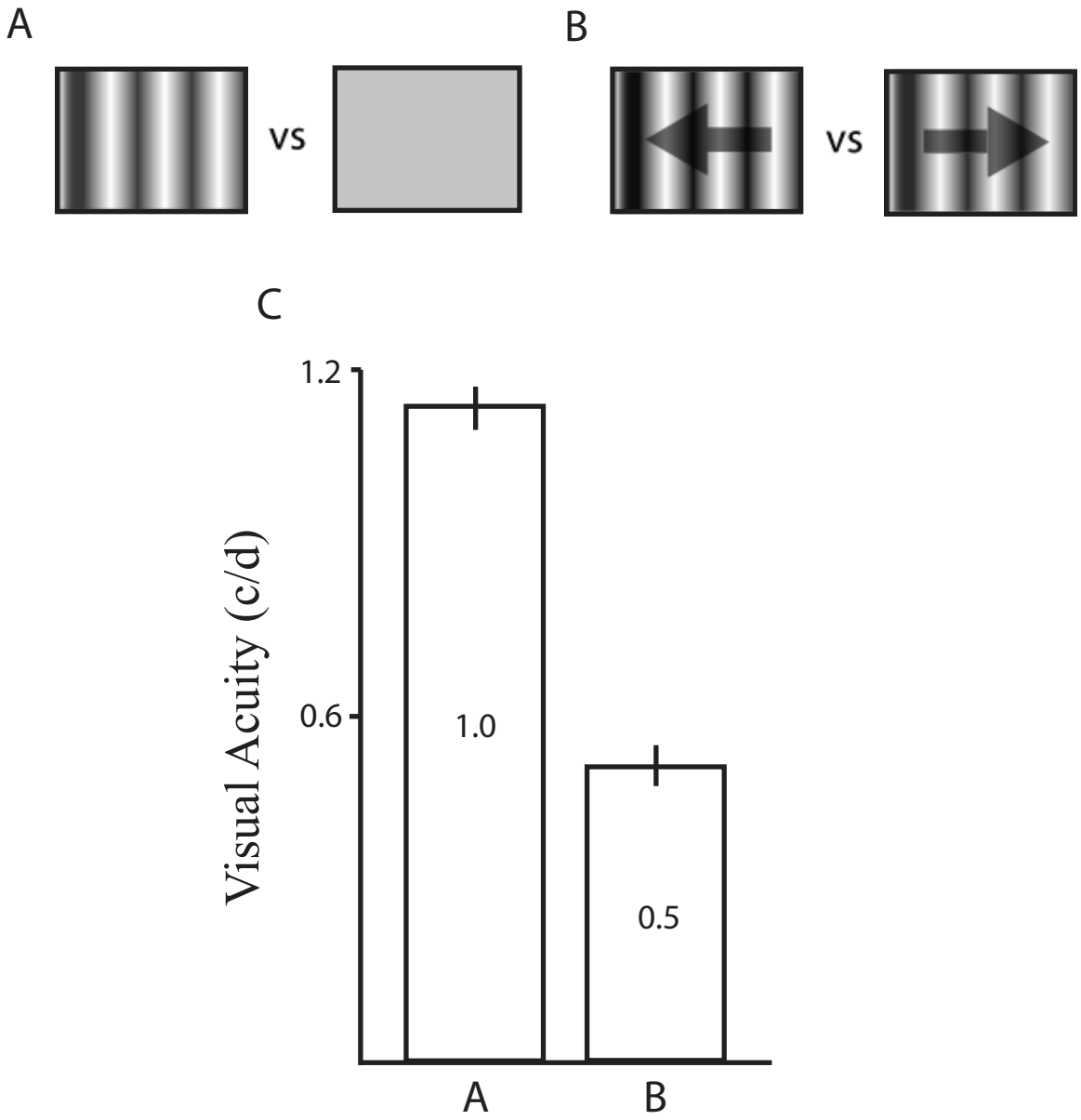

Figure 20. Visual acuity of Long-Evans rats measured in the Visual Water Task. (A) Static stimuli: one screen displays a static sine-wave grating and the other a grey screen of the same mean luminance. (B) Moving stimuli: each screen displays a moving sine-wave grating moving in opposite directions.

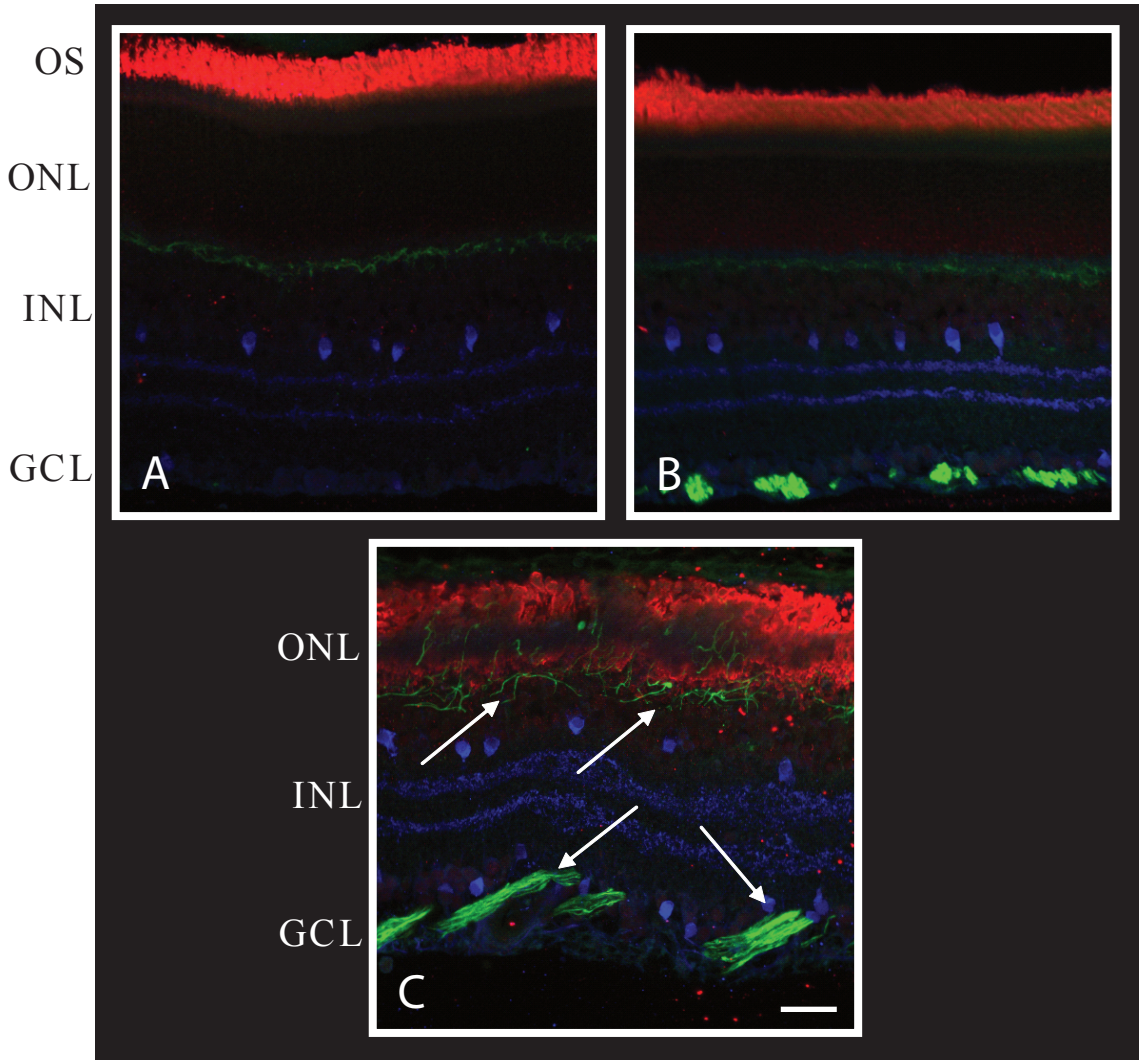

Figure 21. Immunohistochemical staining of RCS rat retinas at P28 (A), P56 (B), and P149 (C). Ganglion cell growth of filaments and migration occurs in B and C, as well as growth of horizontal cells in the outer retina. Markers used were neurofilament protein (green) which stains ganglion cell axons and horizontal cells, rod opsin which labels rod outer segments (red), and Chat which labels amacrine cells (blue). At P28, the RCS rat retina appears near normal exhibiting proper lamination of the retina, rod opsin localized in the rod outer segments, and little evidence of abnormalities within horizontal or ganglion cells (A). By P56 (B), however, evidence of degeneration has is noticable and ganglion cell activation is evident. By P149 (C) severe photoreceptor degeneration has occured, horizontal cells have nerutie sprouting into the ONL, and ganglion cell axons are extending into the INL. Scale bar 50 um.

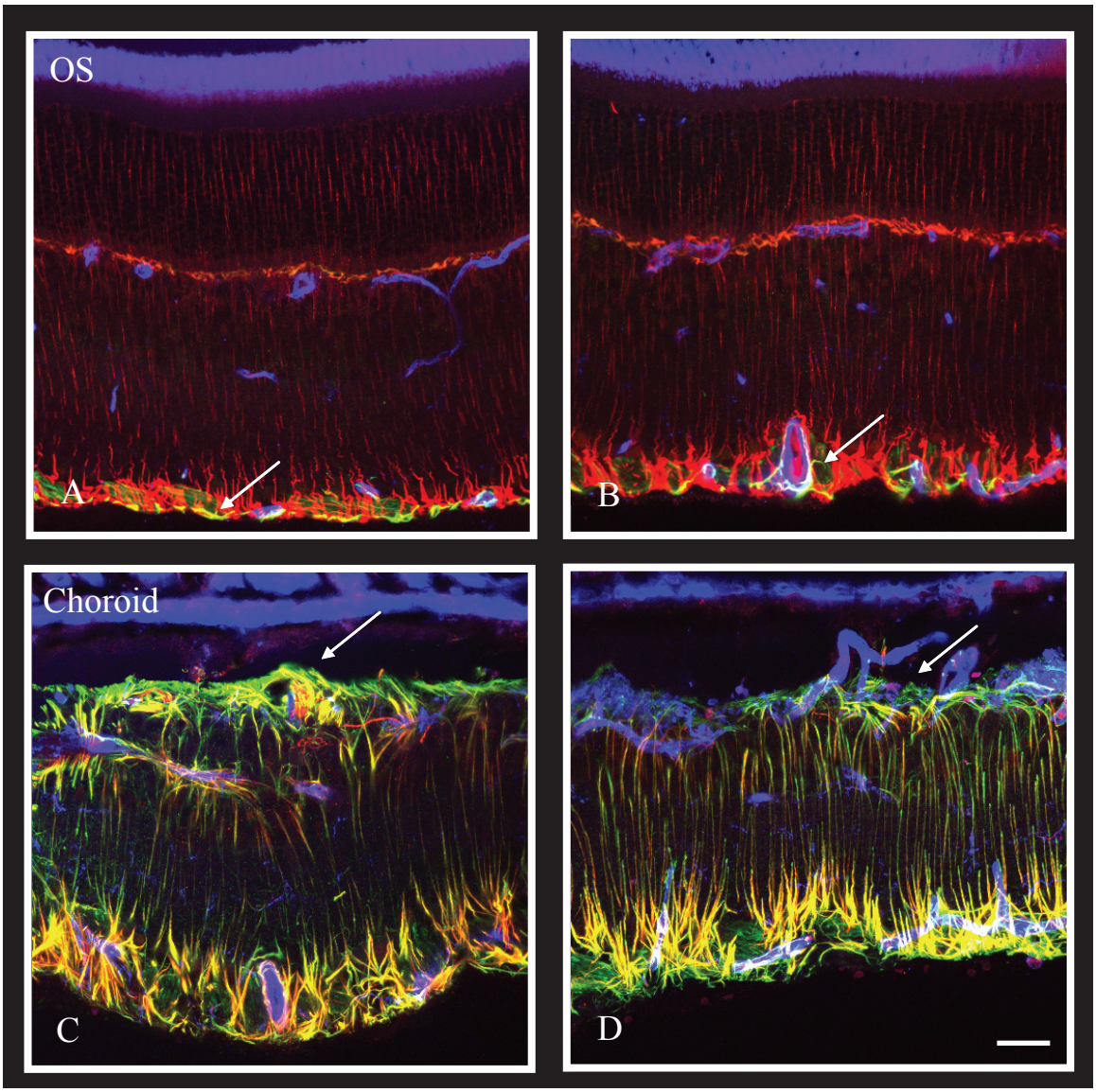

Figure 22. Immunohistochemical staining of RCS rat retinae at P28 (A), P56 (B), and P149 (C & D) using markers GFAP (green), which stains astrocytes and Muller glial cells in a degenerating retina, Vimentin (red) which labels Muller cells, and Isolectin B4 (blue) which lables blood vessels and microglia found in the inner retina. At P28 (A) and P56 (B), Muller cells have mostly normal processes through the retina, however, there are some Muller cell changes as indicated by the arrow. Significant Muller cell sprouting into in the subretinal space is evident by P149 (C & D: white arrows). Scale bar 50 um.

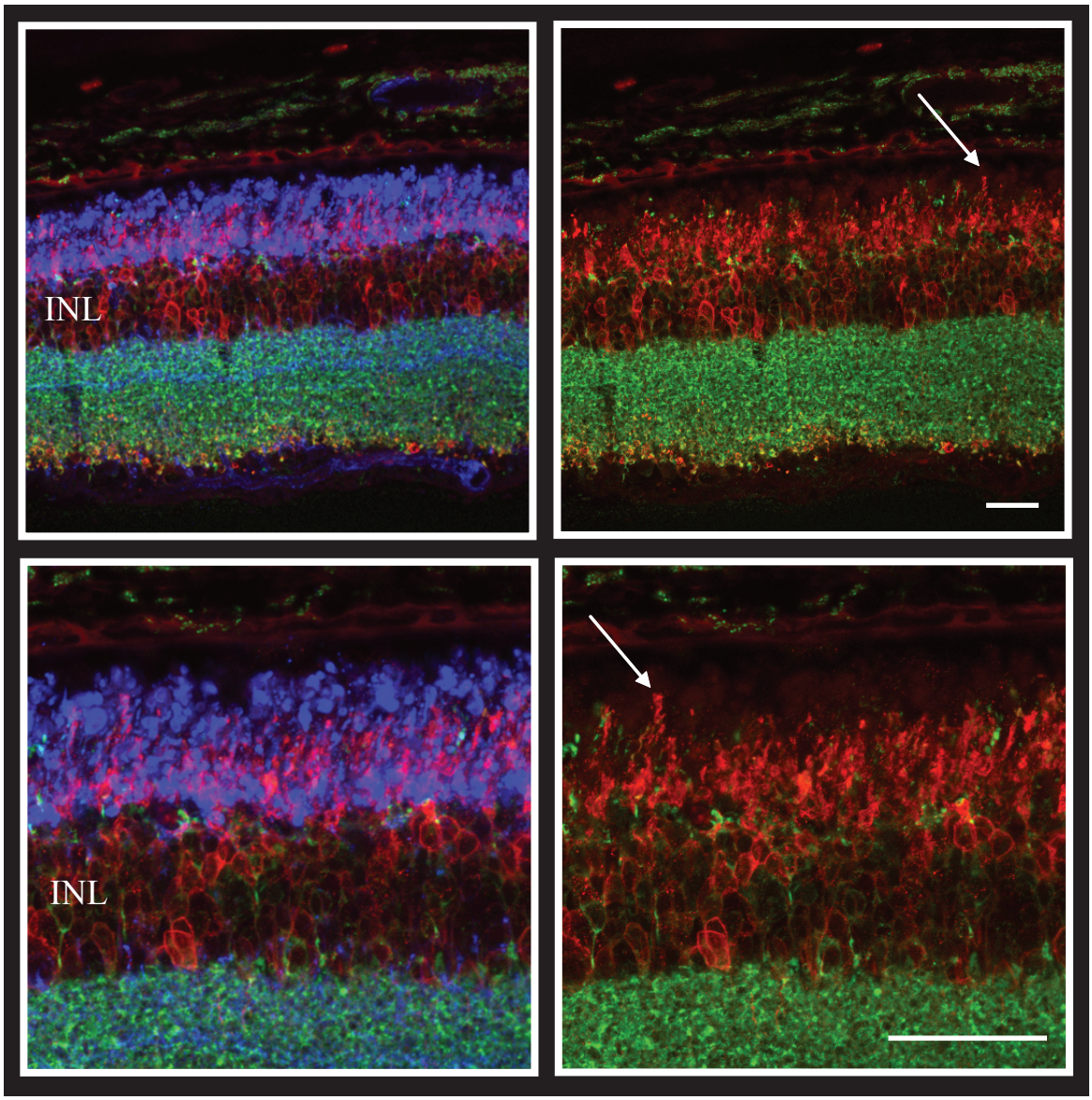

Figure 23. Immunohistochemical staining of RCS rat retinas at P149 showing bipolar cell neurite sprouting. The images on the right are the same as images on the left with blue removed. Images on the bottom are higher magnification of the top images. Sections were stained with labels for synaptophysin (green), PKC (red), and PNA (blue). Scale bars, 50 um.

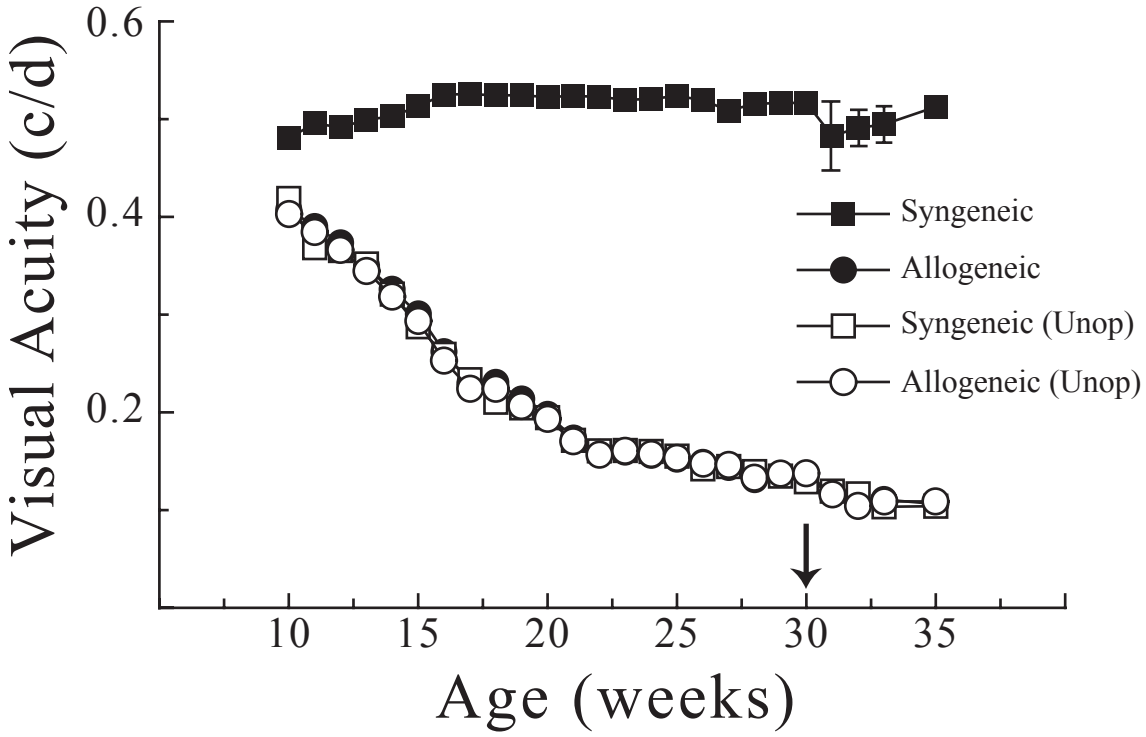

Figure 24. Visual thresholds of RCS rats following transplantation of either syngeneic Schwann cells or allogeneic Schwann cells. Arrow indicates age of representative contrast sensitivity curves in Figure 25.

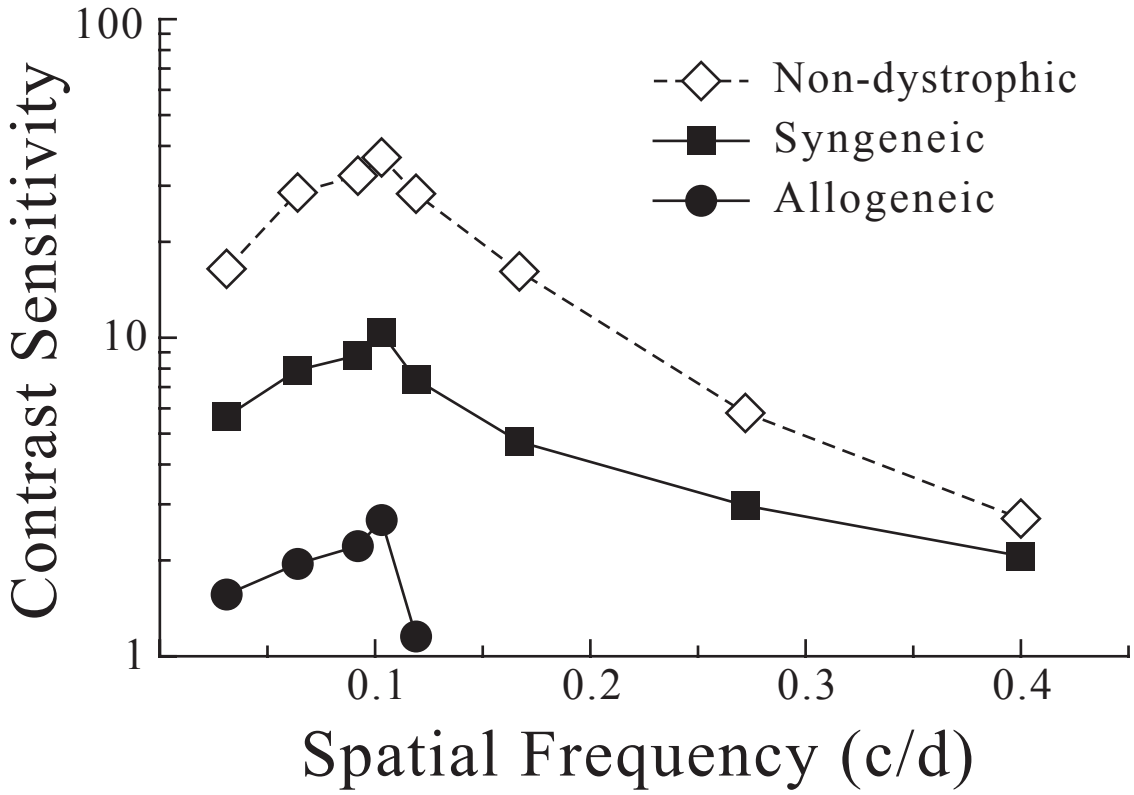

Figure 25. Contrast sensitivity function of non-dystrophic, syngeneic transplanted, and allogeneic transplanted eyes at 30 weeks of age. The allogeneic contrast sensitivity function is severely impaired, with no measurable values at the higher spatial frequencies. The syngeneic contrast sensitivity function is significantly better than allogeneic, and is comparable to that of dystrophic RCS rats at 14 weeks of age; however, they are not at normal (non-dystrophic) values.

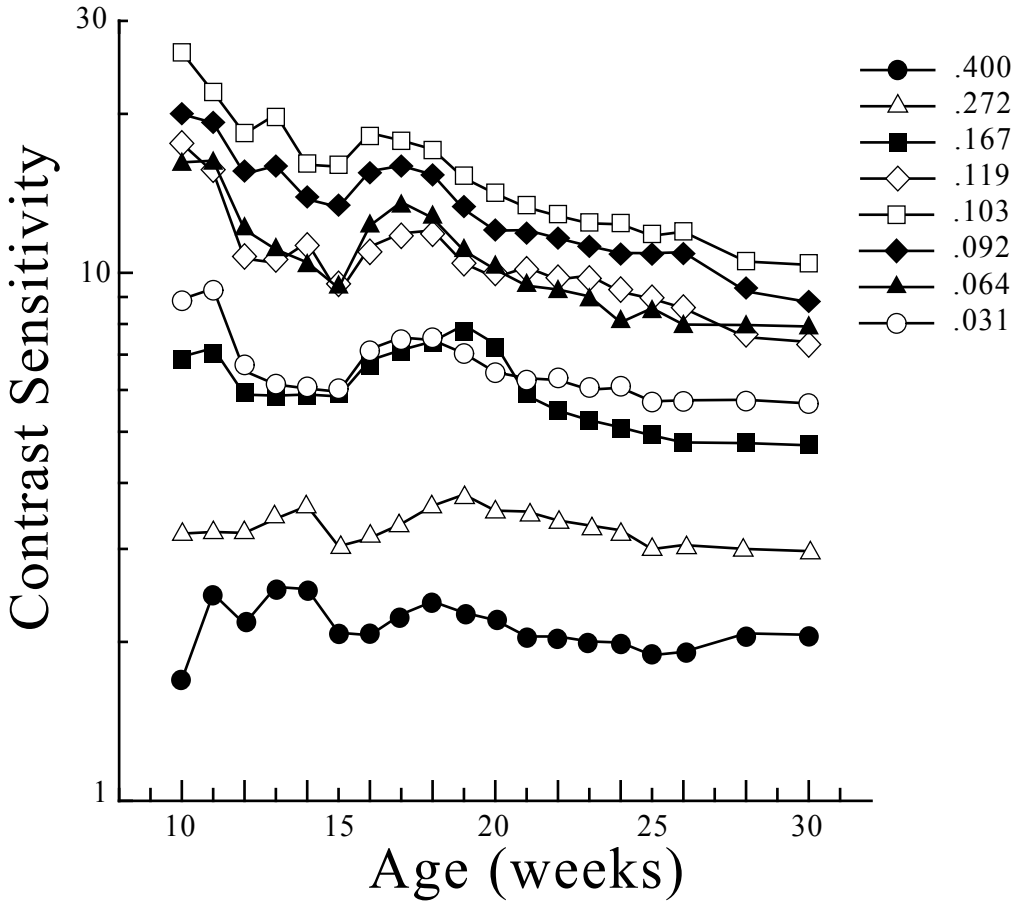

Figure 26. Contrast sensitivity profile of syngeneic transplanted animals over time. While there is a small decline with most spatial frequencies, all spatial frequencies remain intact, and the highest two spatial frequencies are least affected by the course of degeneration.

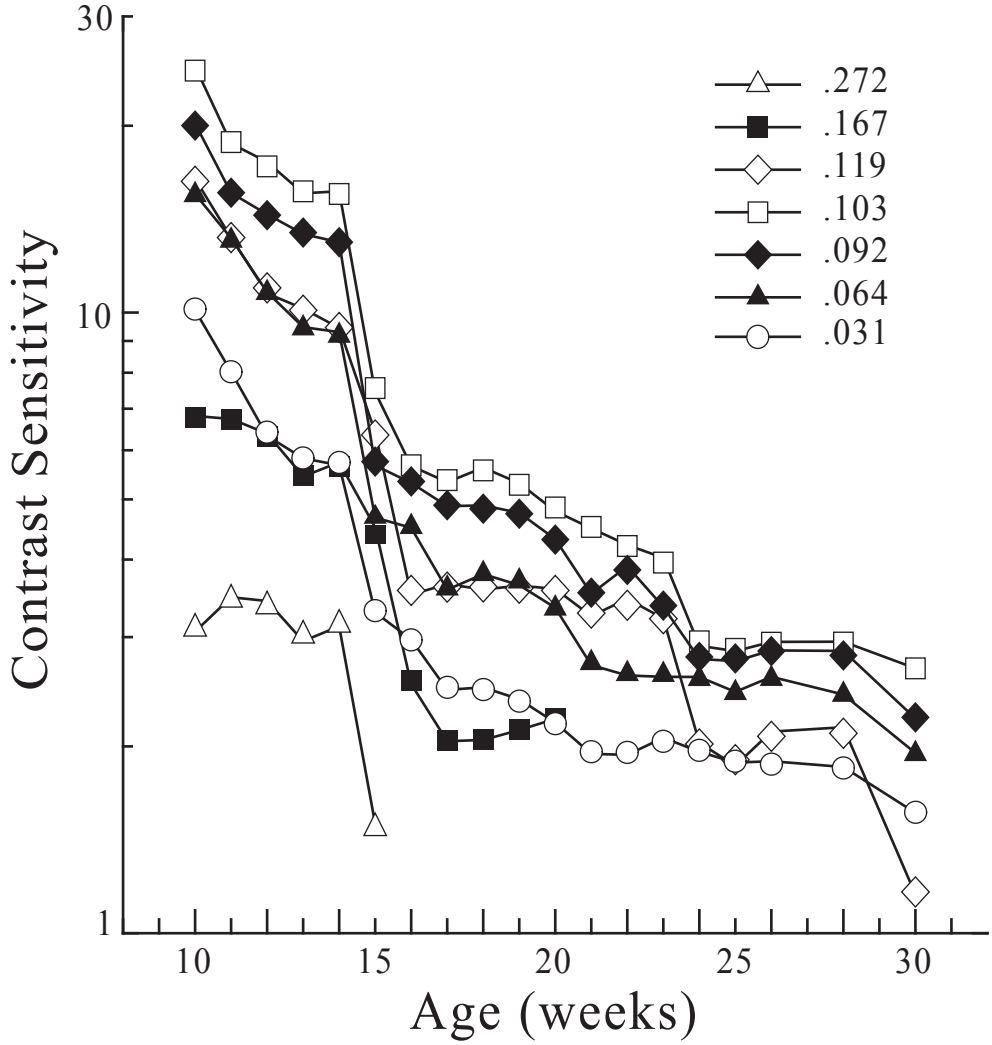

Figure 27. Contrast sensitivity profile of allogeneic transplanted animals over time. All spatial frequencies' contrast sensitivity values are severely impaired by 15 weeks of age, and continue to decline thereafter.

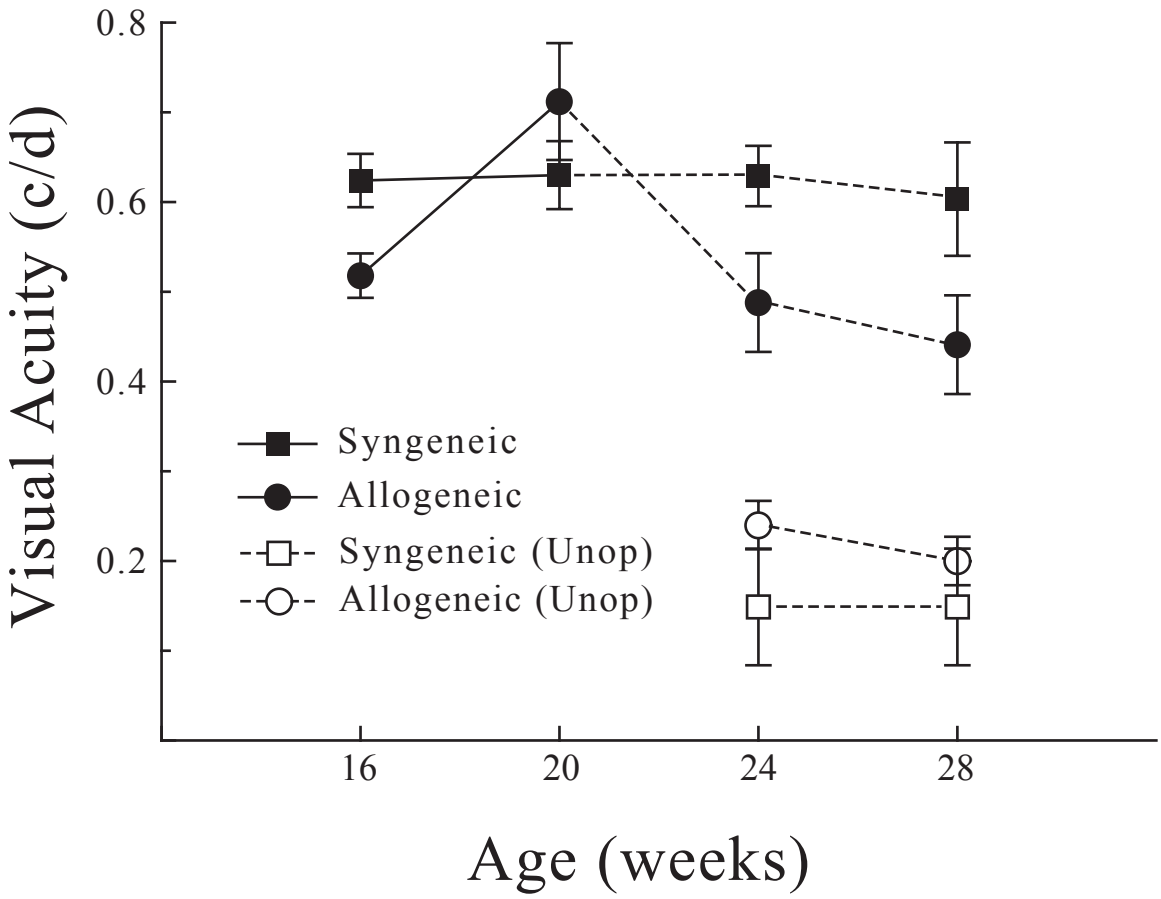

Figure 28. Grating acuity thresholds measured through syngeneic Schwann cell transplanted, allogeneic Schwann cell transplanted, and un-operated eyes. Thresholds were measured binocularly at 16 weeks, and monocularly at 24 and 28 weeks of age. Allogeneic transplanted eyes had higher acuity thresholds than un-operated controls; however, syngeneic transplanted eyes had thresholds higher than all other groups.

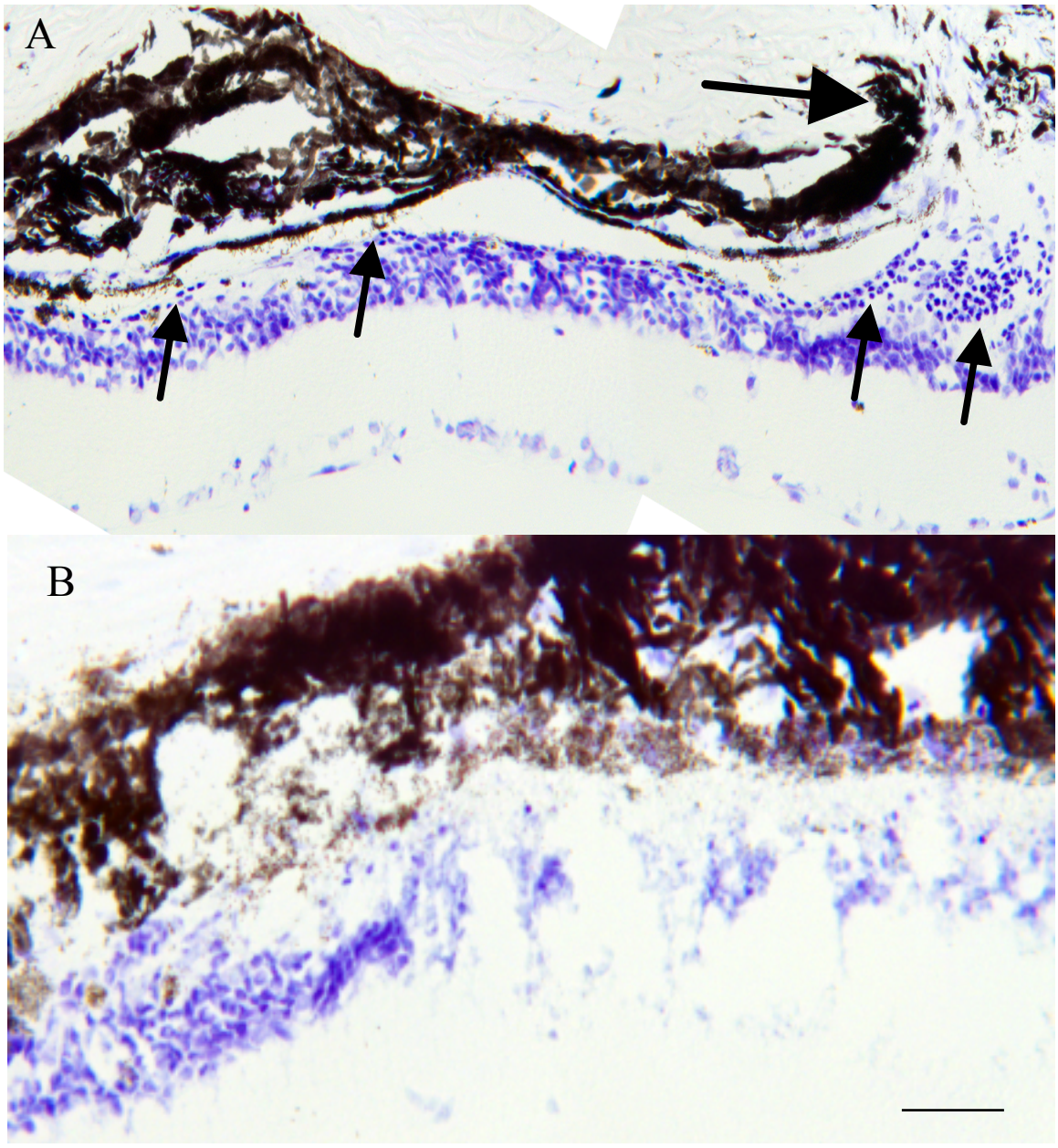

Figure 29. Cresyl violet staining of 36 week old RCS rats following syngeneic Schwann cell transplantation; near injection site (A) and away from injection site (B). Note the presence of a single layer of photoreceptor cell bodies (small arrows) near injection site (A) as indicated by the large arrow, as well as a partial maintenance of the laminar organization of the retina. Away from the injection site, there are no photoreceptors present, is significant loss of lamination, and significant loss of inner retinal neurons. Scale bar 50 um.

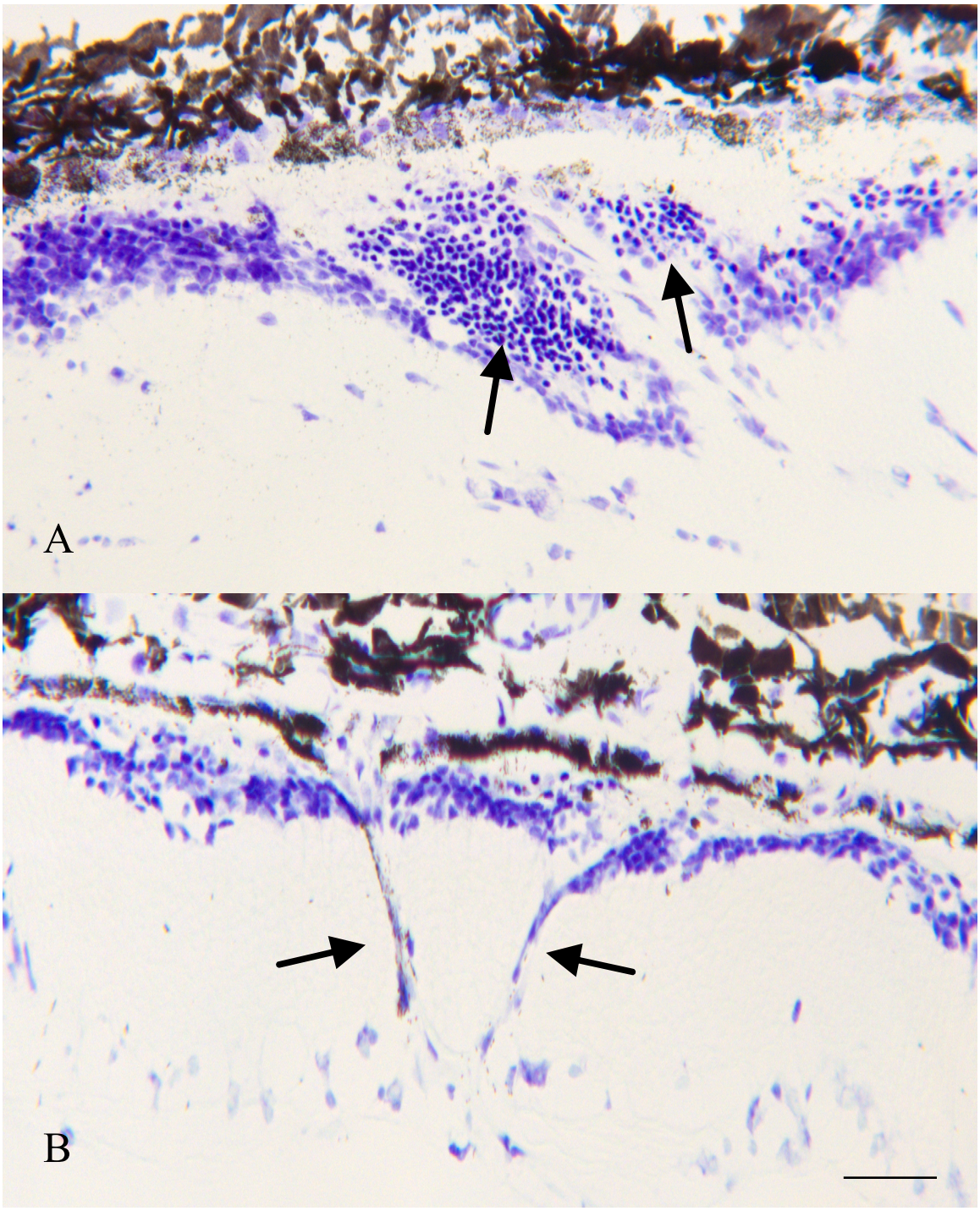

Figure 30. Cresyl violet staining of 36 week old RCS rat retinas following syngeneic Schwann cell transplantation. (A) is taken from near the injection site. Note the large collection of photoreceptor cell bodies surviving. (B) was taken away from the injection site and shows a distinct vascularization of the retina. Some inner nuclear cells are surviving in this area. Scale bars 50 um.

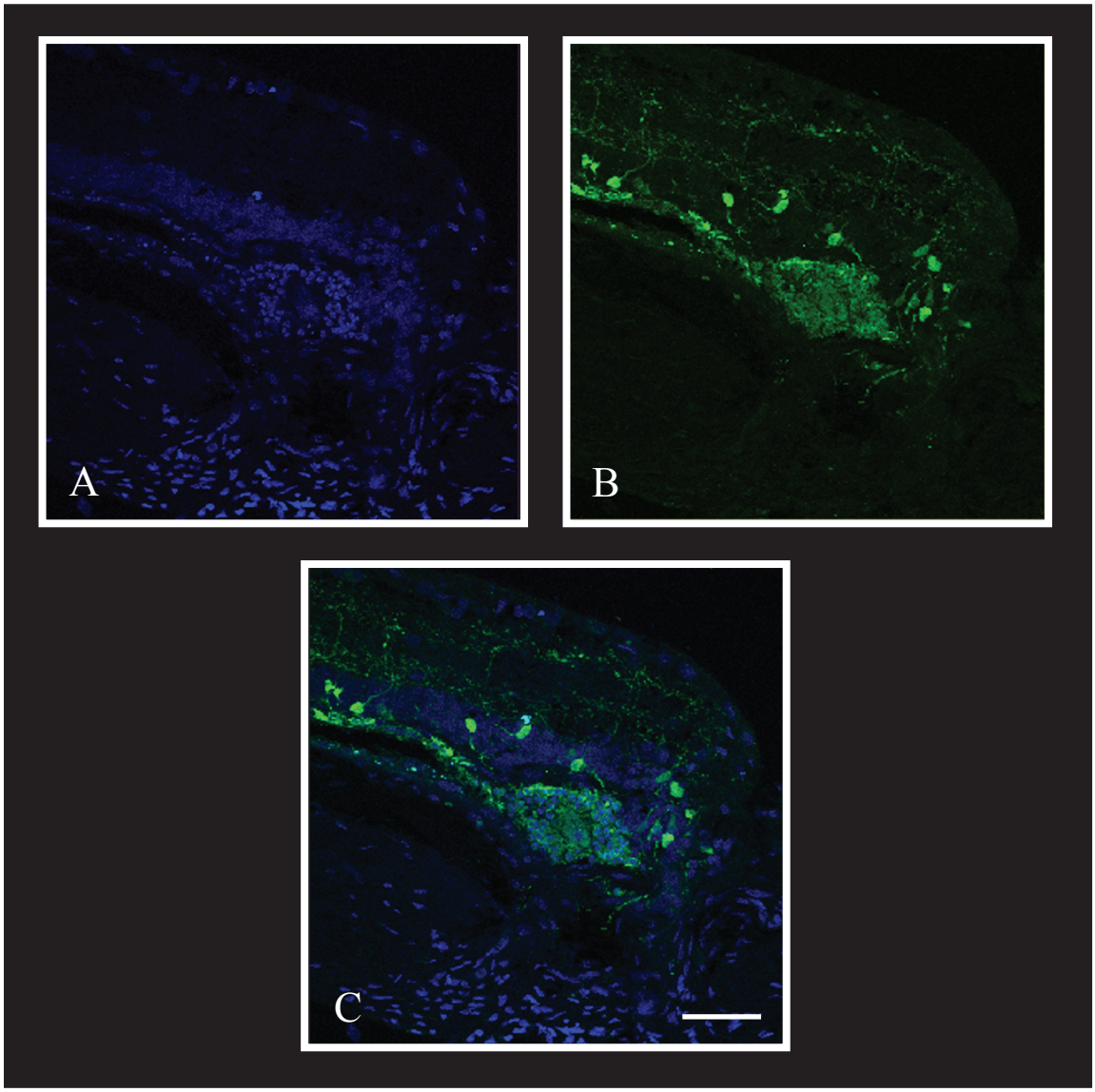

Figure 31. DAPI (A; blue) and recoverin (B; green) labelling of 9 month old RCS rat retinas. Collections of cell bodies near the injection site double labelled with both DAPI and recoverin (C) confirming that the surviving cell bodies near the injection site are photoreceptors. Scale bar 50 um.

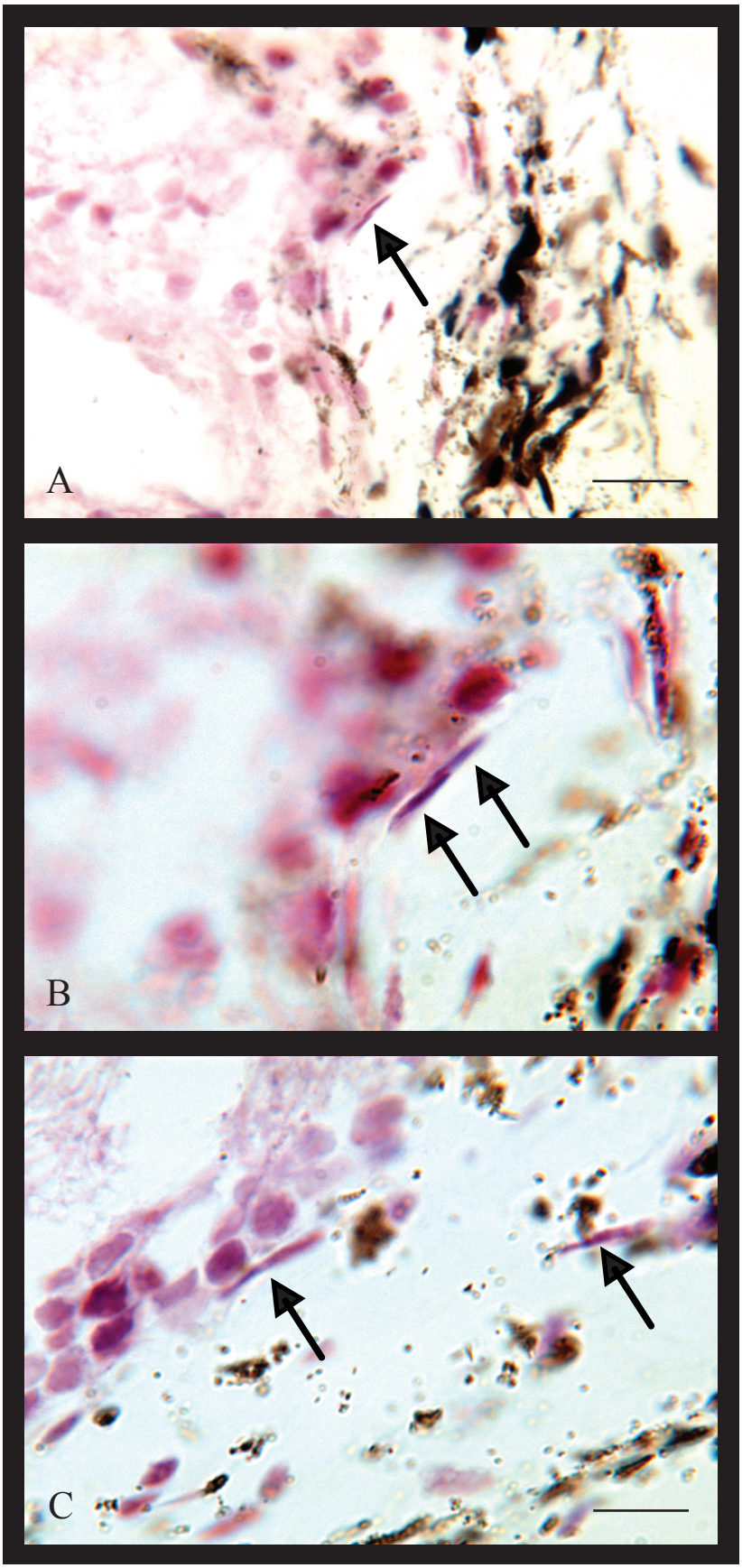
A
B
C

Figure 32. RCS rat retinas at 9 months of age following syngeneic Schwann cell transplantation, viewed at 50x (A) and 100x (B & C) magnification stained with an antibody to P75 receptors. Syngeneic Schwann cells have a characterisitic morphology which is long and cylindrical in nature. Schwann cells were only found near the injection site in both cases. B is the same as A, viewed at 100x.
Scale bars 20 um (A) and 10 um (C).

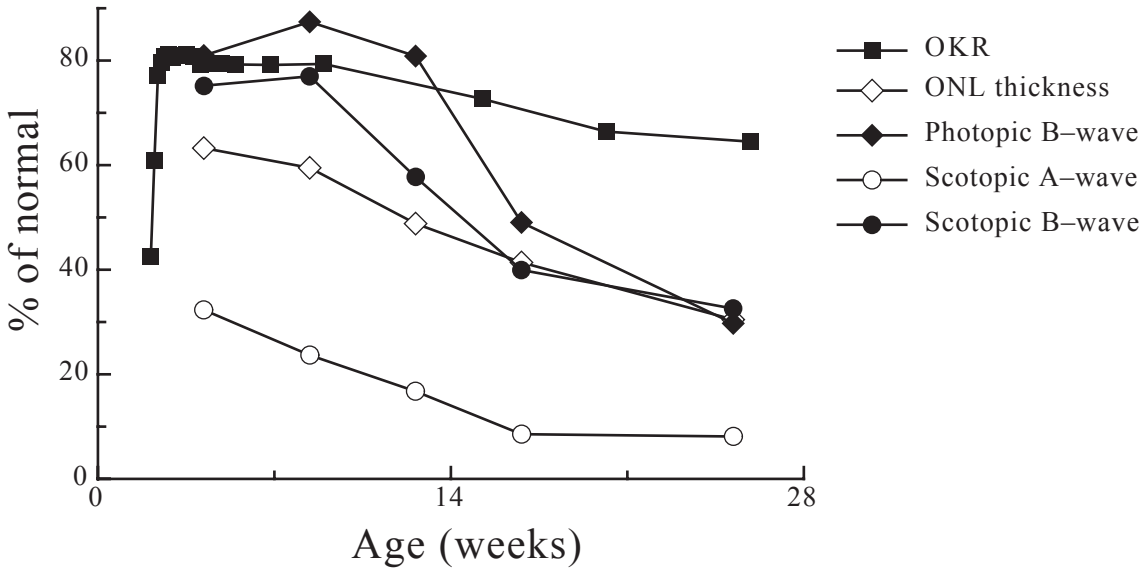

Figure 33. Comparison of OKR thresholds, ERG, and ONL thickness measurements in the P23H-1 rat.

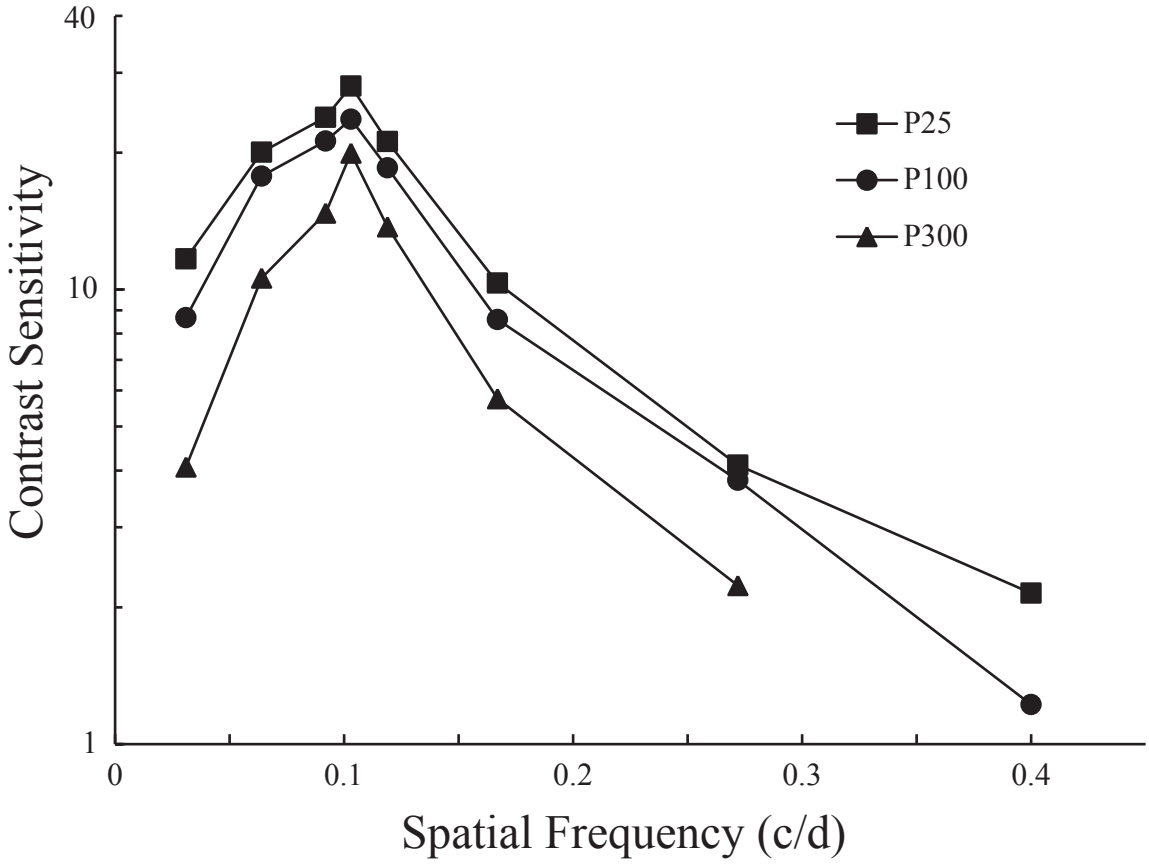

Figure 34. Contrast sensitivity functions of P23H line-1 rats at 25, 100, and 300 days of age. Contrast sensitivity curves at P25 and P100 closely resemble that of non-dystrophic rats (data not shown), and although sensitivity at P300 is not as high as previous measures, a distinct inverted-U shaped curve remains.

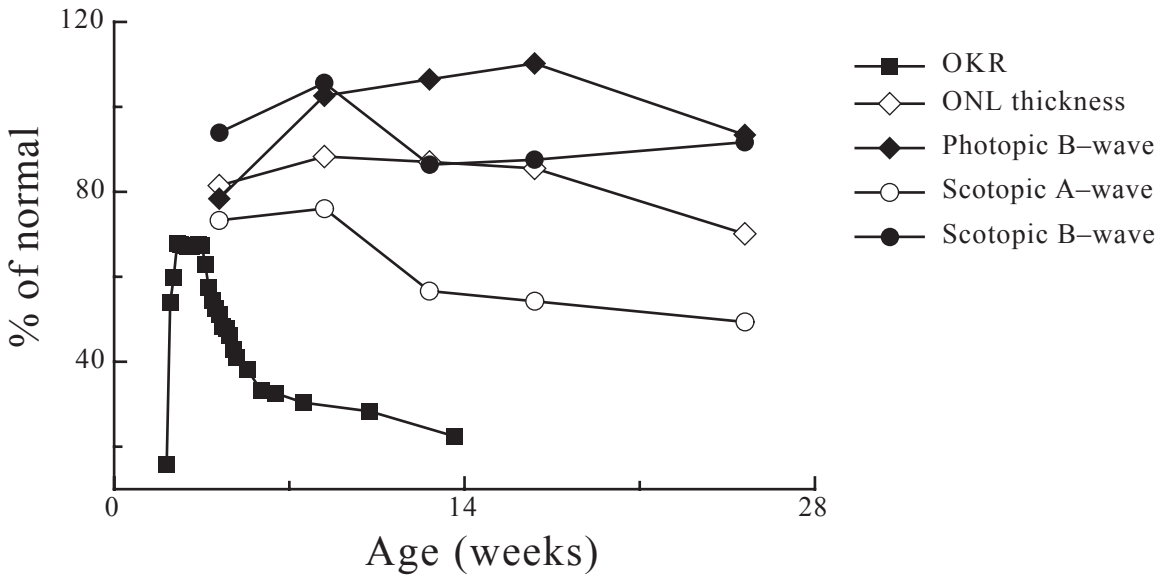

Figure 35. Comparison of OKR thresholds, ERG, and ONL thickness measurements in the P23H-3 rat.

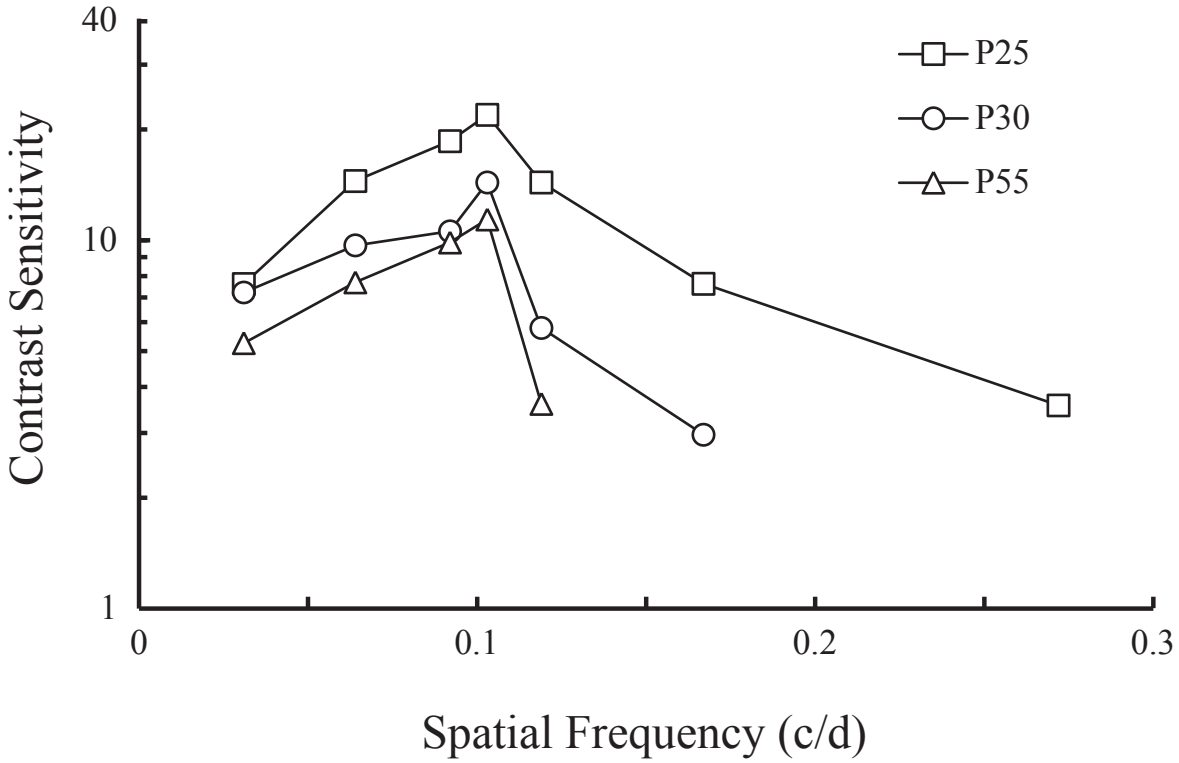

Figure 36. Contrast sensitivity functions of P23H line 3 rat at 25, 30 and 55 days of age. The contrast sensitivity function at P25 closely resembles that of a non-dystrophic rat (data not shown), however, the curve quickly degenerates over the next few weeks time.

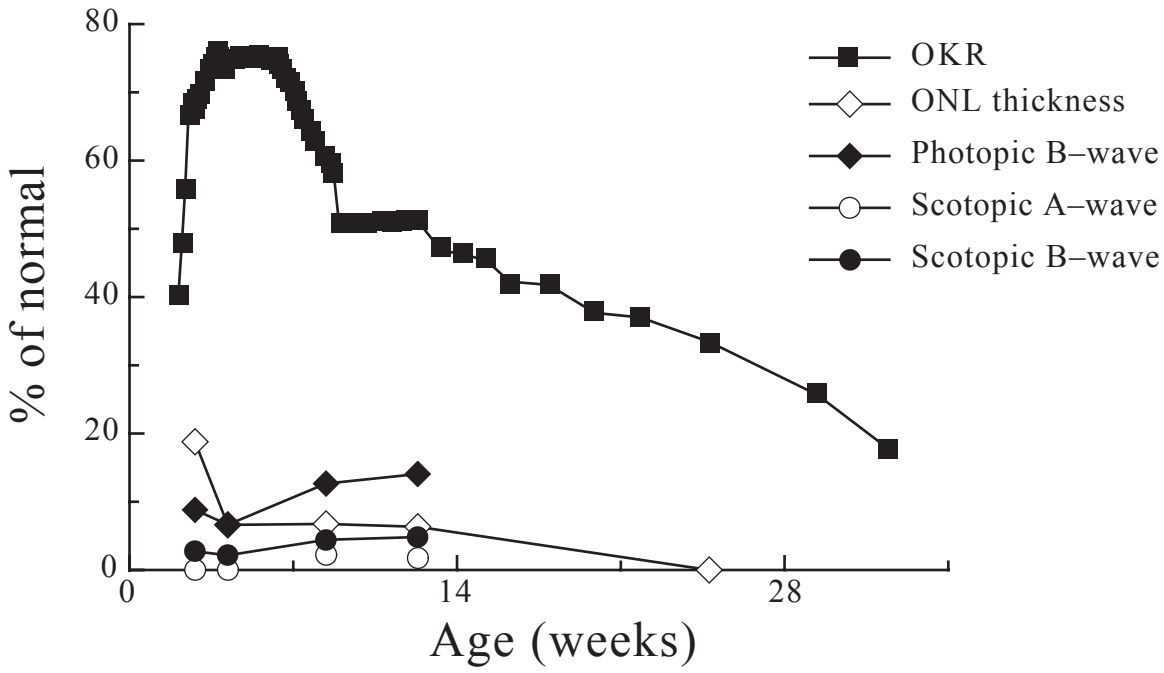

Figure 37. Comparison of OKR thresholds, ERG, and ONL thickness measurements in the S334ter-3 rat.

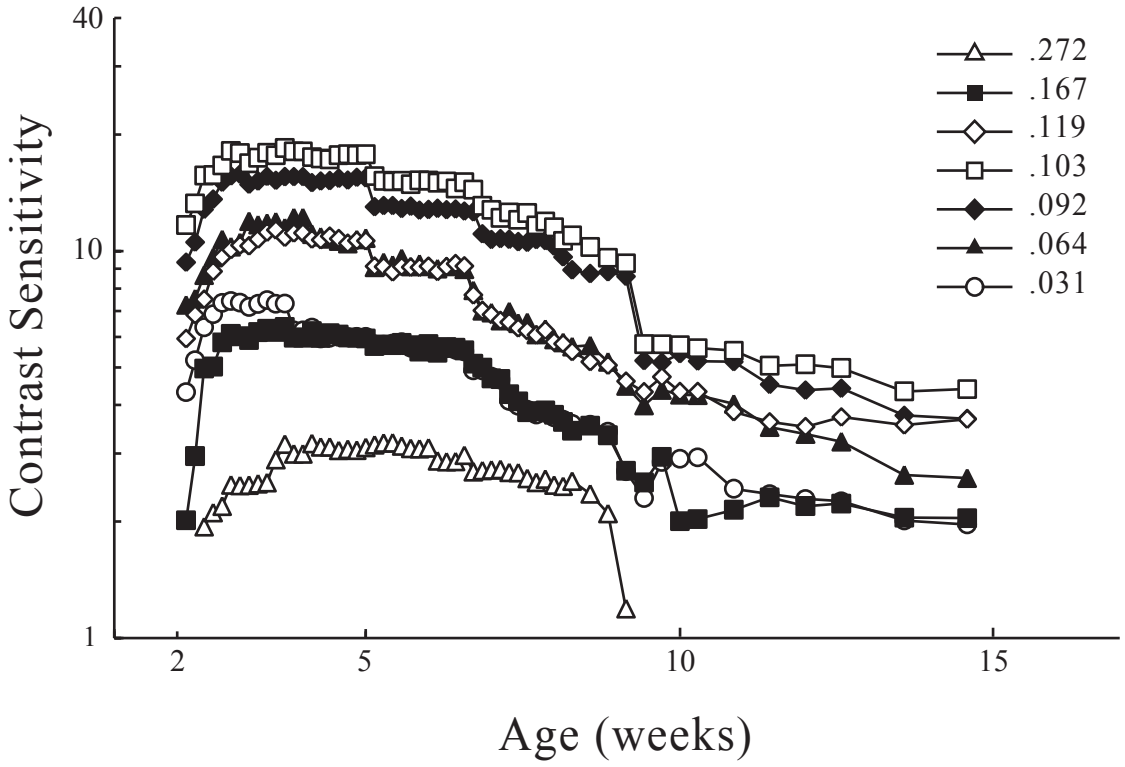

Figure 38. Each spatial frequency channel is plotted against age of animal in the S334ter line-3 rat. The contrast sensitivity of all spatial frequencies' increased over the first week of testing, followed by a slow yet steady decline up to 9 weeks of age. At this point select spatial frequency channels lost a significant proportion of sensitivity. Past 10 weeks of age, the remaining spatial frequency channels maintained near stable sensitivity.

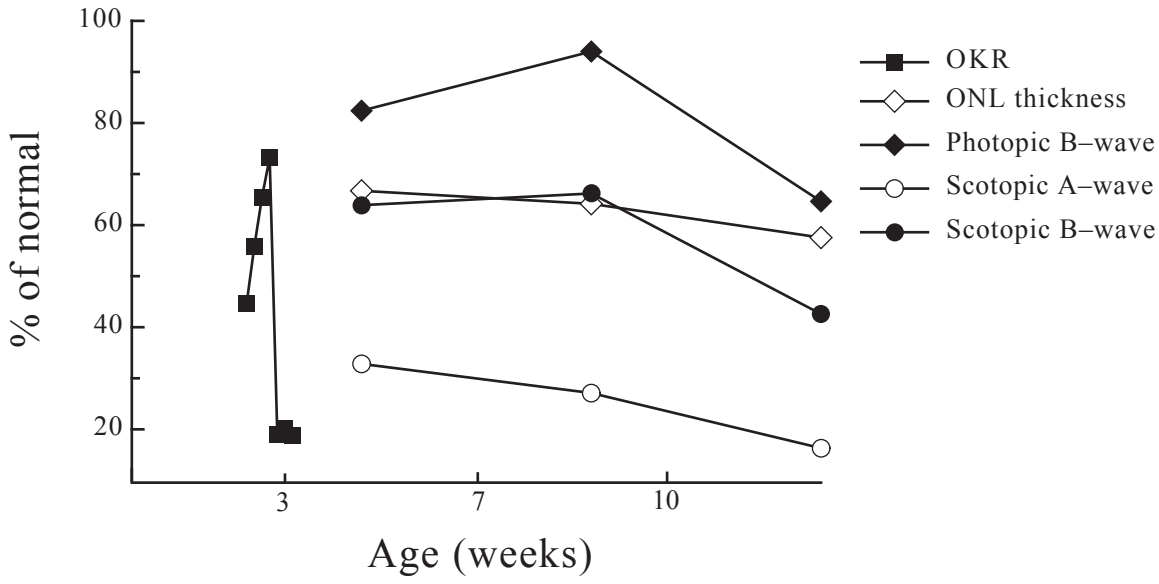

Figure 39. Comparison of OKR thresholds, ERG, and ONL thickness measurements in the S334ter-4 rat.

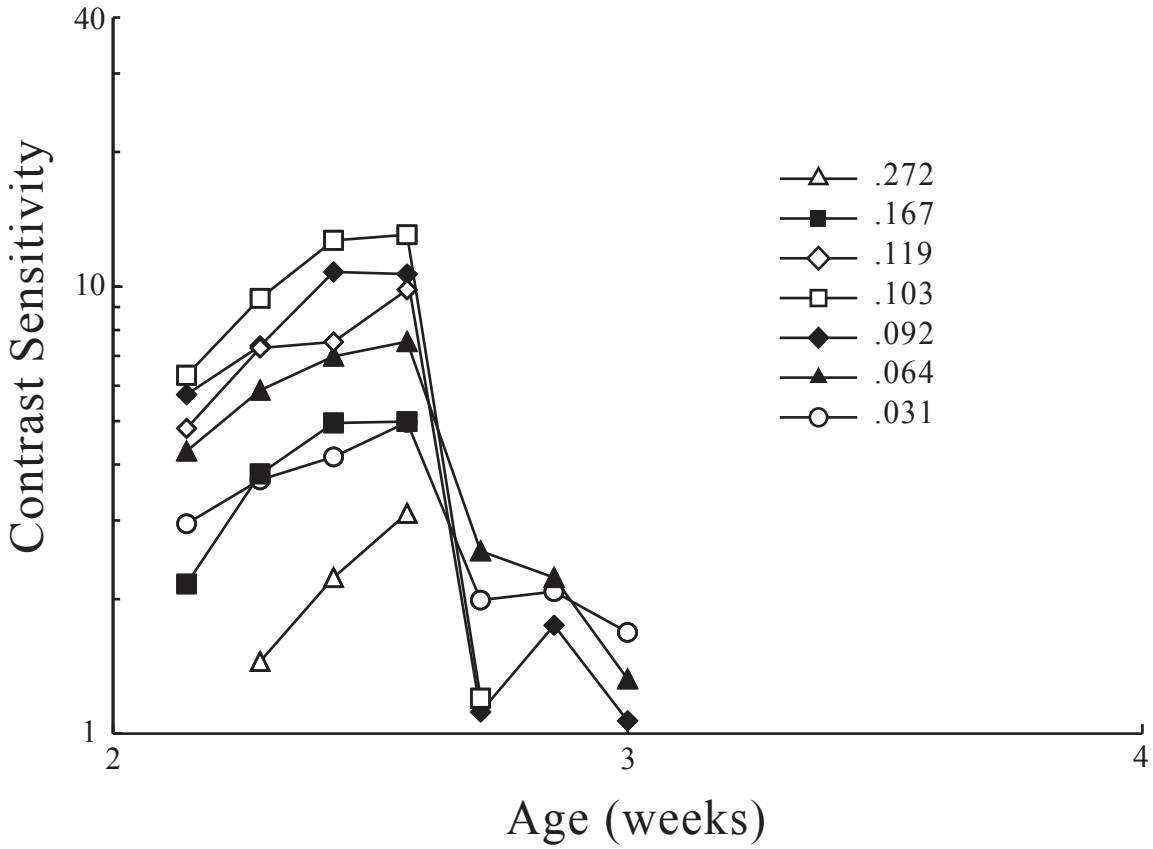

Figure 40. Contrast sensitivity of each spatial frequency channel in the S334ter line 4 rat was plotted against age. The first 4 days of testing resulted in near normal development of contrast sensitivity; however, on the 5th day of testing all spatial frequency channels lost significant sensitivity to contrast to immeasurable levels by 3 weeks of age.

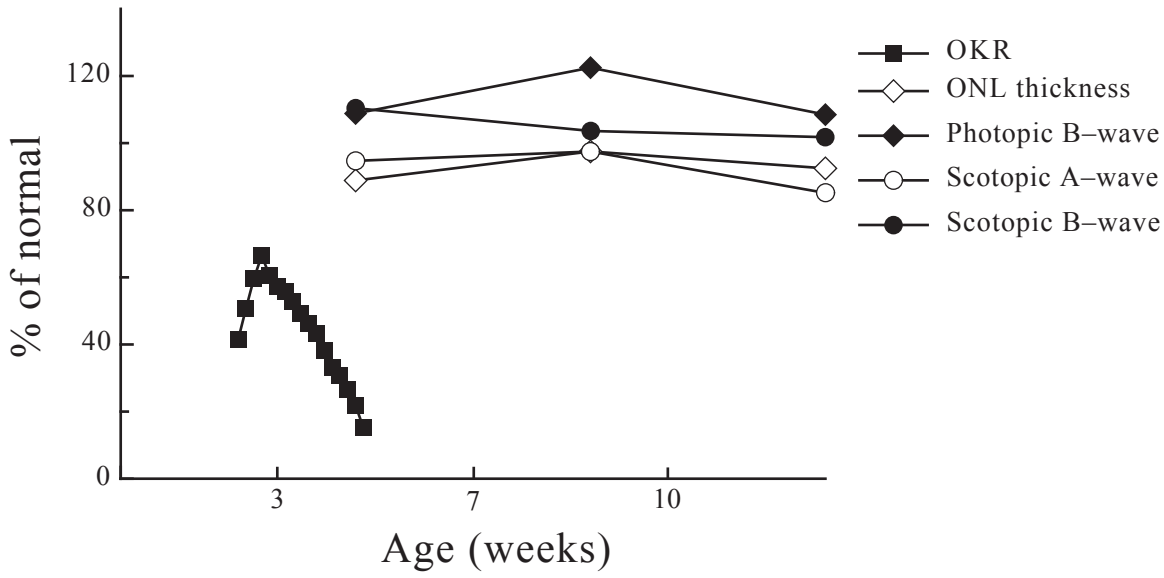

Figure 41. Comparison of OKR thresholds, ERG, and ONL thickness measurements in the S334ter-9 rat.

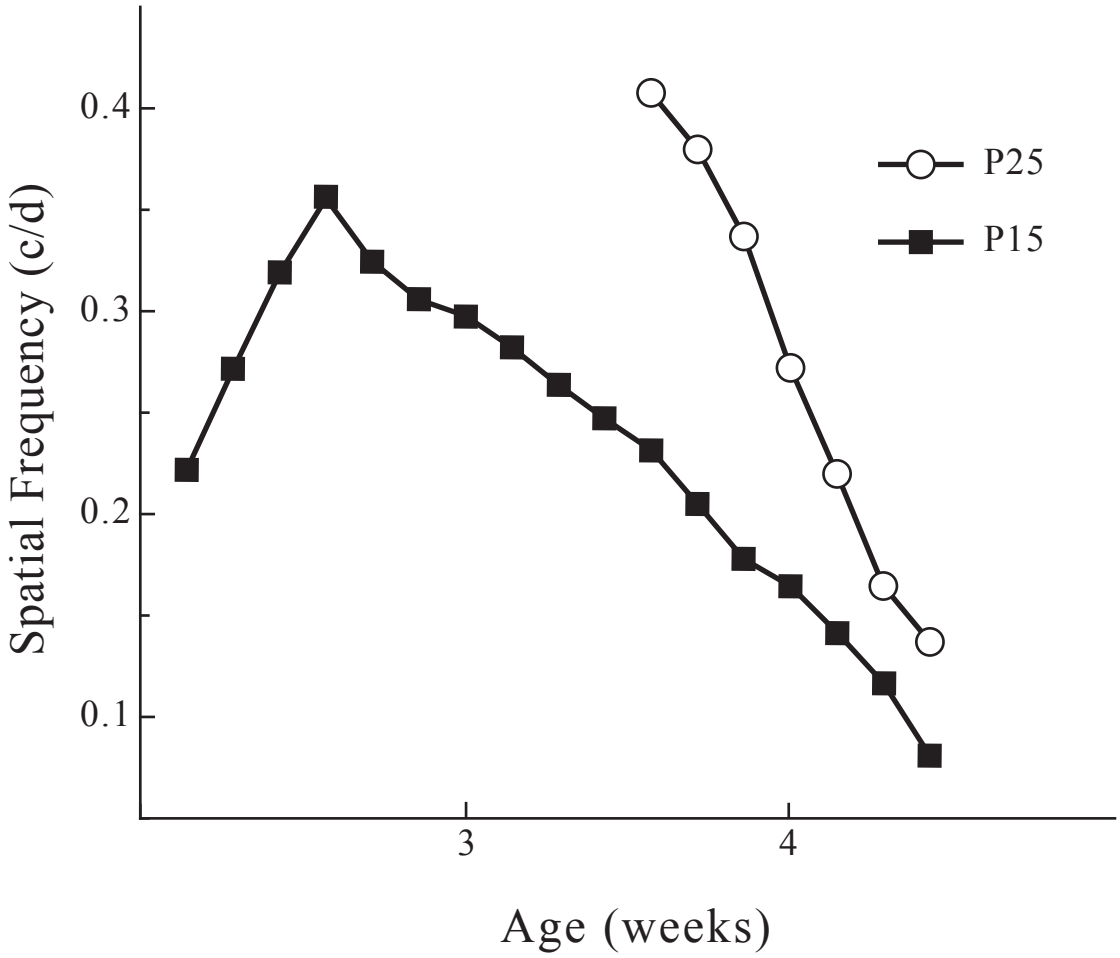

Figure 42. Spatial frequency thresholds of the optomotor response of S334ter line 9 rats from P15 and P25 until thresholds could no longer be measured. Thresholds measured beginning on P25 were higher than at any other time, although the thresholds in this group declined faster than in the P15 group.

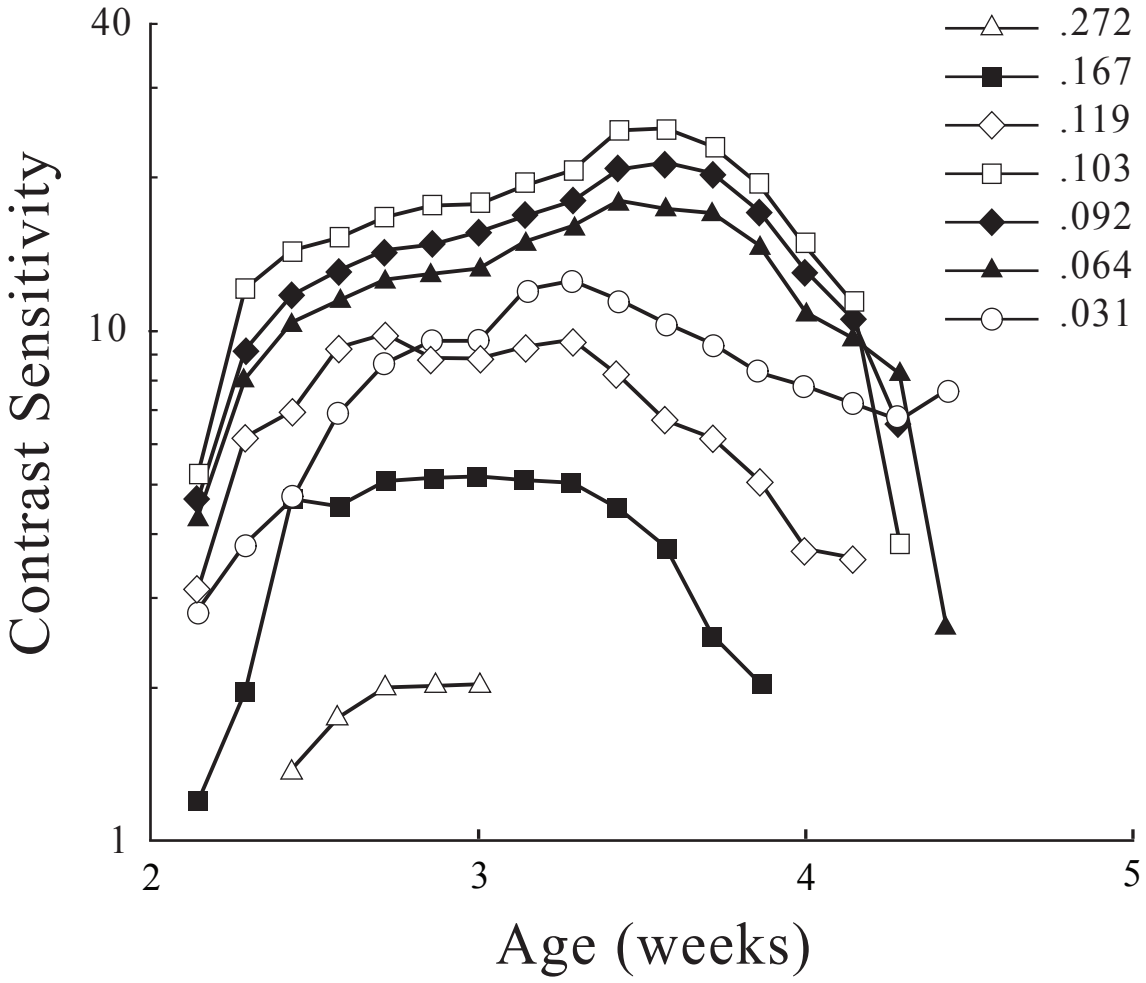

Figure 43. Contrast sensitivity of each spatial frequency channel plotted against age in the S334ter line-9 rat. Sensitivity increased prom P15 up to ~P25, followed by significant decline. Thresholds were no longer measurable after P31.

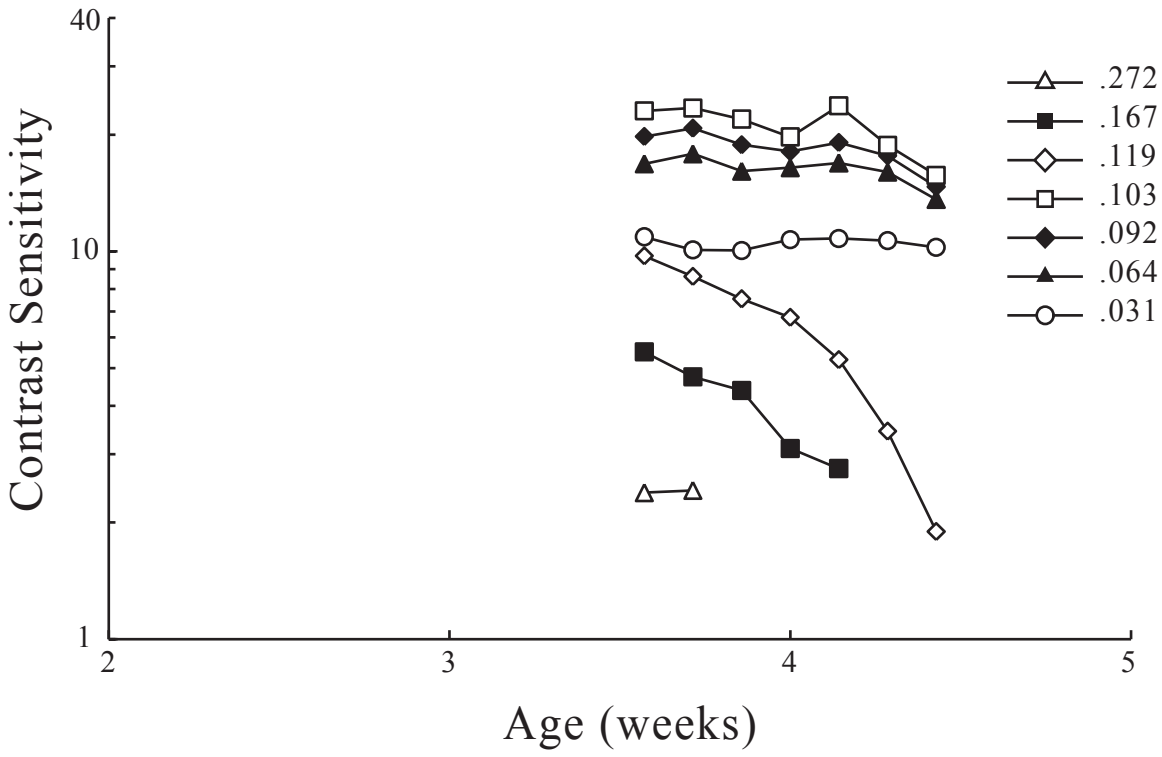

Figure 44. Contrast sensitivity of each spatial frequency channel in S334ter line 9 rats plotted against age. Thresholds were measured from animals beginning on P25. Thresholds at the higher spatial frequencies declined fastest with the low spatial frequencies remaining intact until declining to below measurable levels by P32.

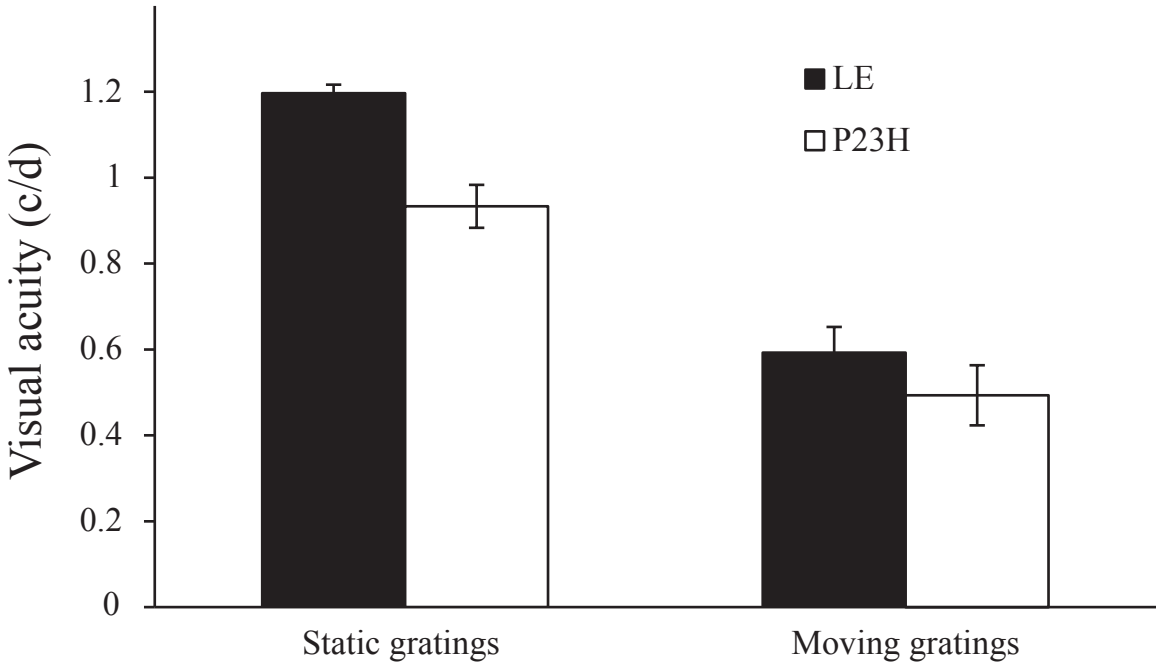

Figure 45. Comparison of visual thresholds of Long-Evans and P23H-1 rats measured in the Visual Water Task using both static grating and moving grating visual stimuli at 10 months of age.

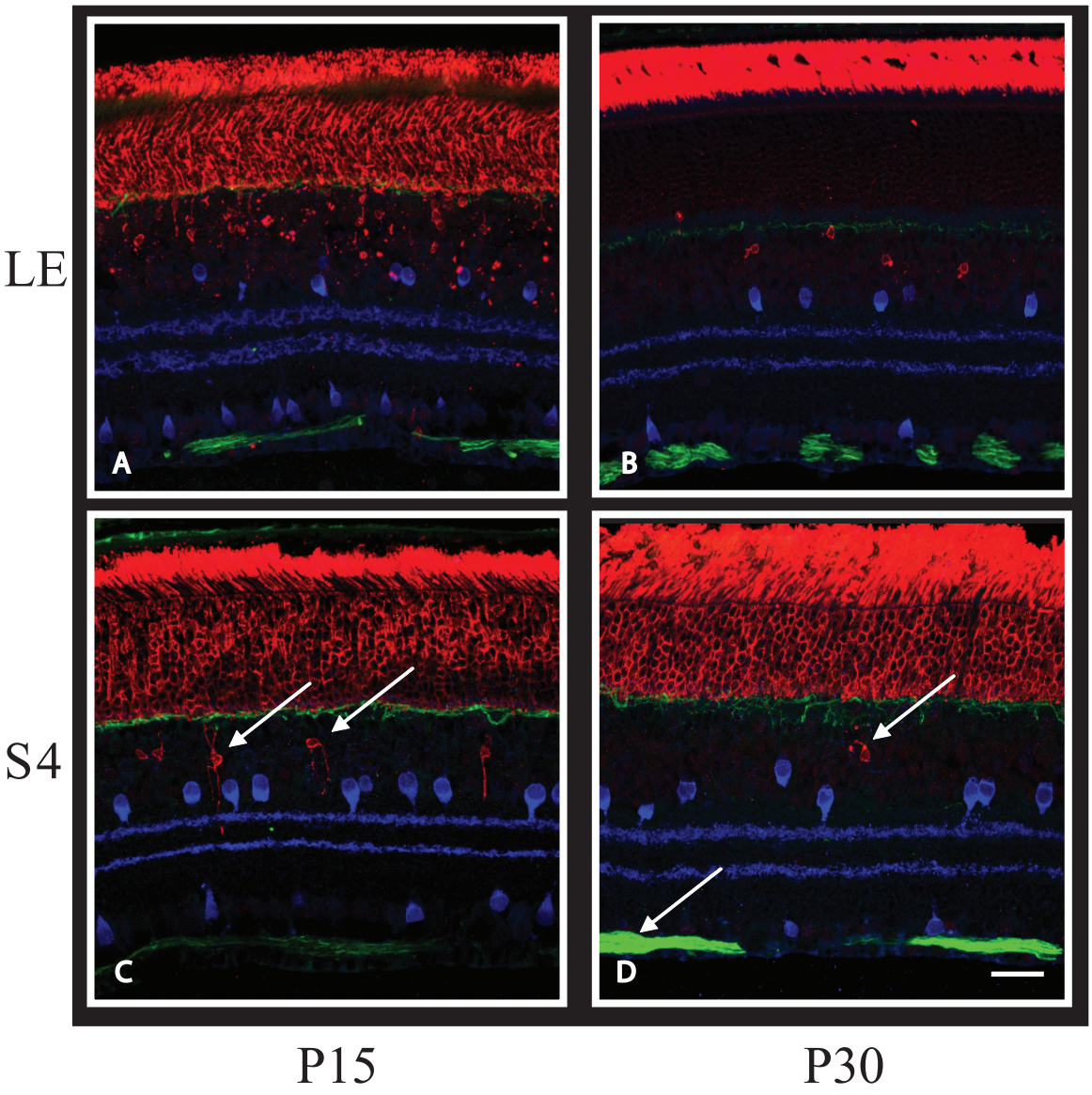

Figure 46. Immunohistochemical staining of the retinas of Long-Evans (LE) and S334ter line-4 (S4) rats at postnatal day (P) 15 and 30. Markers used were neurofilament protein (green) which stains ganglion cell axons and horizontal cells, rod opsin (red) which labels rod outer segments, and Chat (blue) which labels amacrine cells. Long-Evans rats show a typical developmental profile with rod opsin becoming localized to the outersegments over the first few weeks after eye opening (A,B). S4 rats also have mislocalized rod opsin at P15 (C); however, the rod opsin remains as such past 40 days of age (D). In addition, S4 rats have upregulated ganglion cell filaments evident by P30(D). Scale bar 50 um.

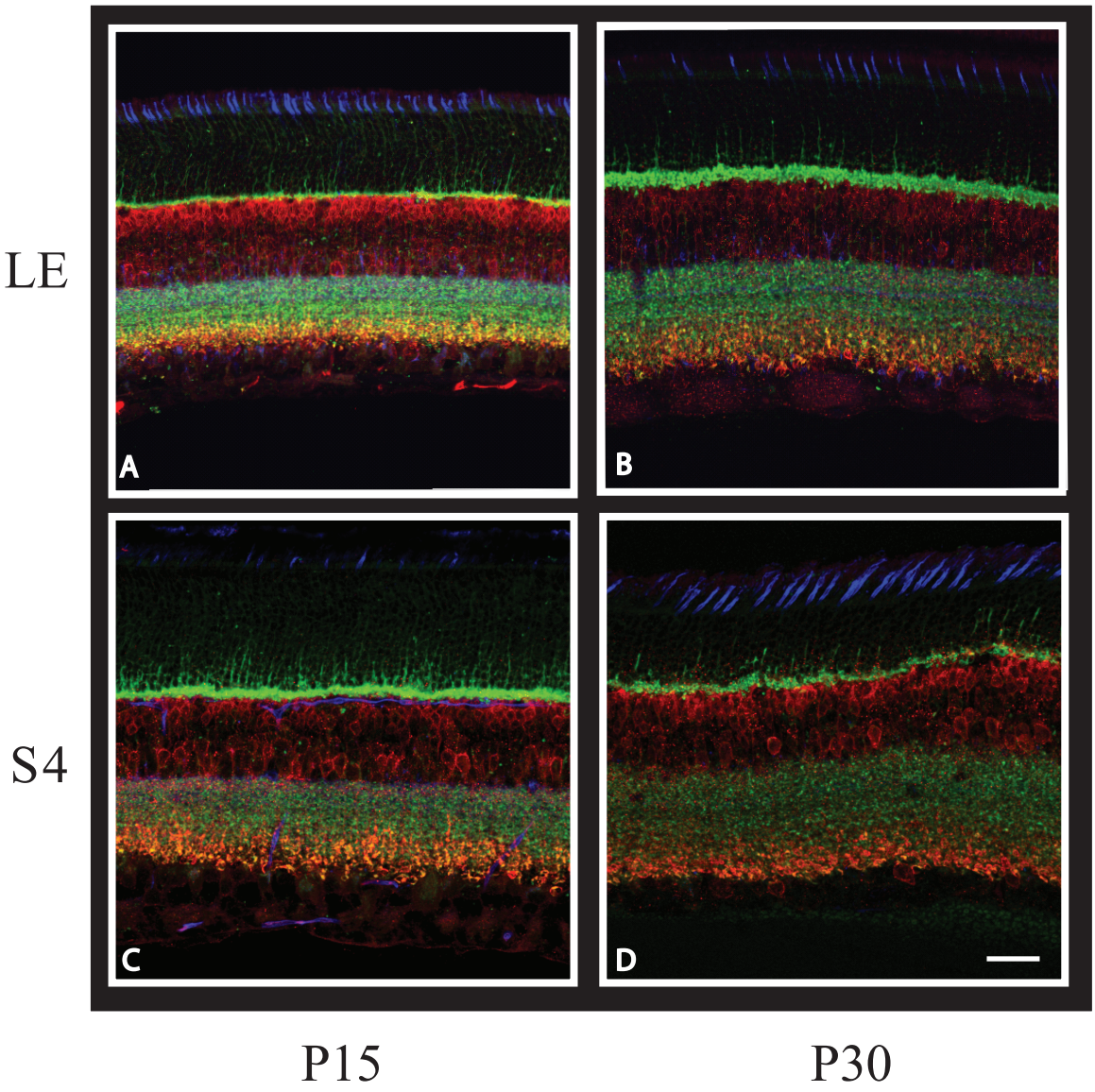

Figure 47. Immunohistochemical staining of the retinas of Long-Evans (LE) and S334ter line-4 (S4) rats at postnatal day (P) 15 and 30. Markers used were Synaptophysin (green) which stains synaptic vessicles in the OPL and IPL, PKC beta (red) which labels bipolar cells, and PNA (blue) which labels cone matrix sheaths. There does not appear to be an outright loss of cone photoreceptors in the S334 rats, although by P30 (D) the cone outersegments appear slanted and partially tortuous. Scale bar 50 um.

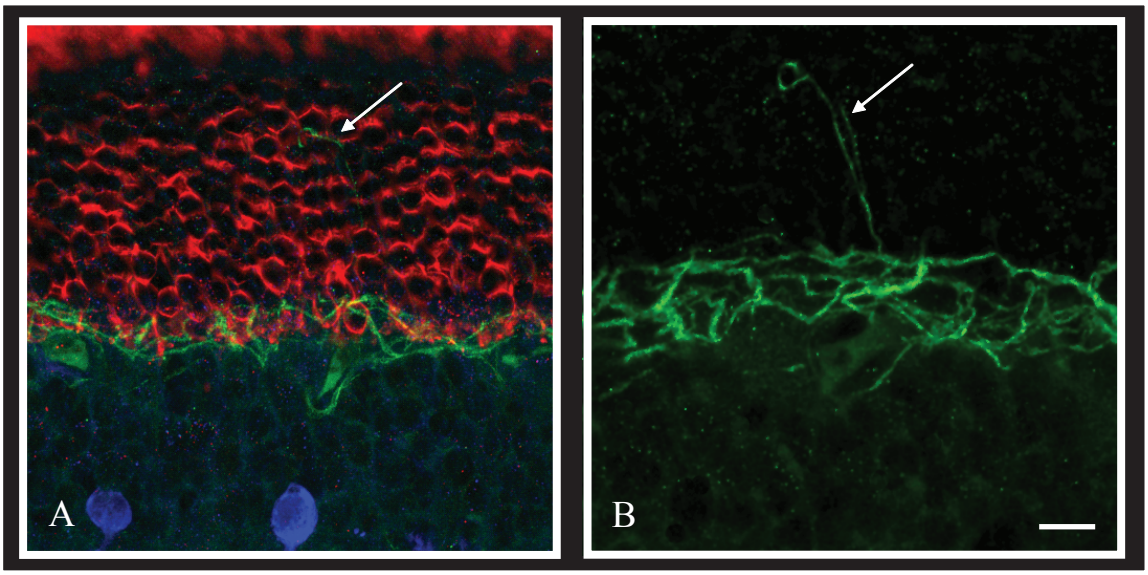

Figure 48. Immunohistochemical staining of S334ter line-4 rat retina at P40. Markers used were neurofilament protein (green) which stains ganglion cell axons and horizontal cells, rod opsin (red) which labels rod outer segments, and Chat (blue) which labels amacrine cells. At this age, horizontal cell outgrowth is evident as indicated by the arrows. B is a similar image to A with blue and red removed. Scale bar 50um.

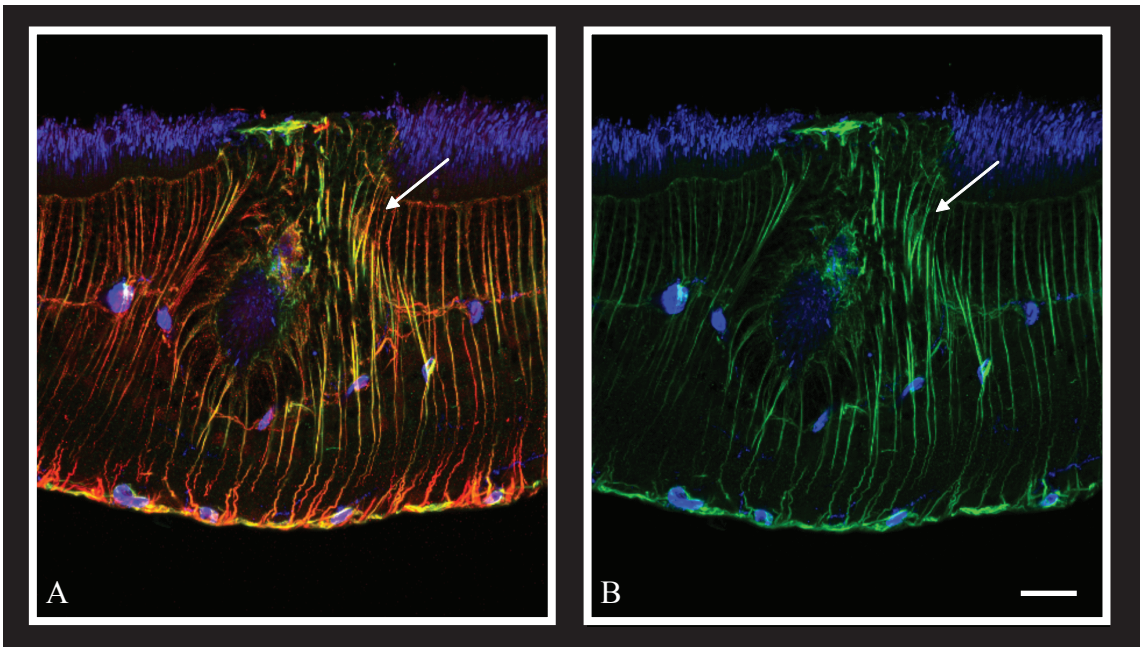

Figure 49. Immunohistochemical staining of S334ter line-4 rats at P30. Markers used were GFAP (green) which stains astrocytes and Muller glial cells in a degenerating retina, Vimentin (red) which labels Muller cells, and Isolectin B4 (blue) which lables blood vessels and microglia found in the inner retina. The glial scar, as indicated by the arrows, is a common event in degenerating retinas. B is the same image as A without red. Scale bar 50 um.

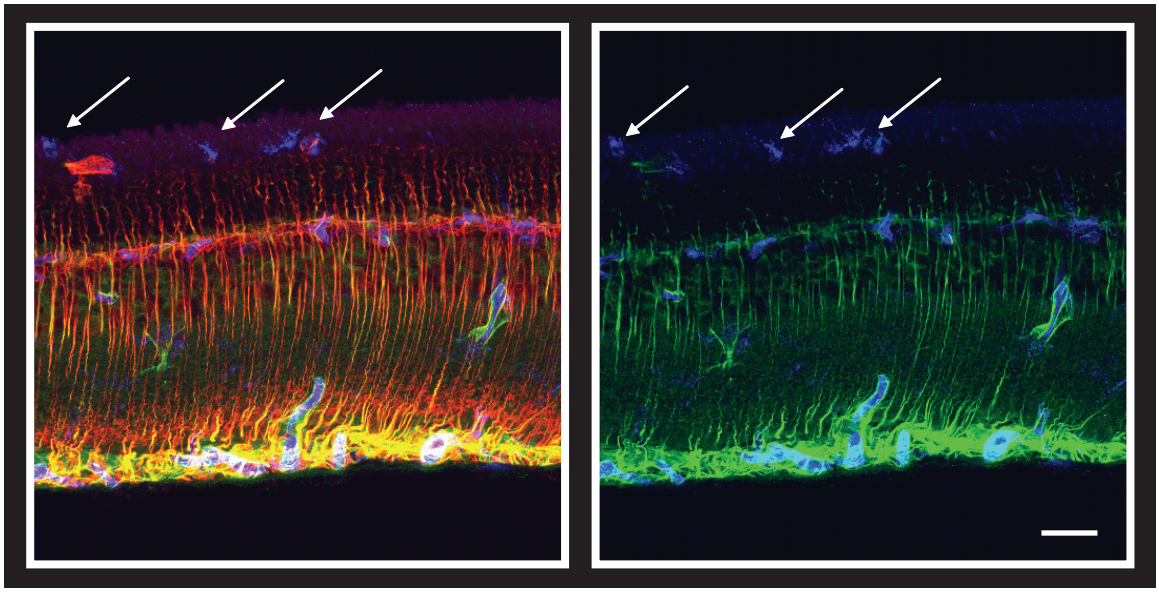

Figure 50. Immunohistochemical staining of S334ter line-4 retinas at P40 showing activation of microglia in the subretinal space. Markers used were GFAP (green) which stains astrocytes and Muller glial cells in a degenerating retina, Vimentin which labels Muller cells, and Isolectin B4 which lables blood vessels and microglia found in the inner retina. Scale bar 50 um.

Antibody	Source	Cat #	Concentration
Chat (goat)	Chemicon	AB144P	1 to 50
GFAP (r)	DAKO	Z0334	1 to 400
Isolectin B4	Vector	B1205 (0.5mg)	1 to 50
Neurofilament-biotin	Vector	V1079	1 to 100
PKC beta1 (m)	Santa Cruz	SC8049(200ug)	1 to 50
PNA-biotin	Vector	B1075 (5mg)	1 to 10,000
Recoverin (r)	Alexander Dizhoor	Univ Washington	1 to 500
Rod opsin (m)	R. Molday	Univ B.C.	1 to 500
Synaptophysin (r)	DAKO	A-0010	1 to 100
Vimentin (m)	DAKO	mo725(clone V9)	1 to 500

Table 1. List of antibodies used including the source, catagory number and dilution used for each.

References

Agarwal N, Martin E, Krishnamoorthy RR, Landers R, Wen R, Krueger S, Kapin MA, Collier RJ (2002) Levobetaxolol-induced up-regulation of retinal bFGF and CNTF mRNAs and preservation of retinal function against a photic-induced retinopathy. Experimental Eye Research 74:445-453.

Akimoto M, Miyatake S, Kogishi J, Hangai M, Okazaki K, Takahashi JC, Saiki M, Iwaki M, Honda Y (1999) Adenovirally expressed basic fibroblast growth factor rescues photoreceptor cells in RCS rats. Investigative Ophthalmology & Visual Science 40:273-279.

Andrieu-Soler C, Aubert-Pouessel A, Doat M, Picaud S, Halhal M, Simonutti M, Venier-Julienne MC, Benoit JP, Behar-Cohen F (2005) Intravitreous injection of PLGA microspheres encapsulating GDNF promotes the survival of photoreceptors in the rd1/rd1 mouse. Molecular Vision 11:1002-1011.

Aramant RB, Seiler MJ (2002) Retinal transplantation--advantages of intact fetal sheets. Progress in Retinal and Eye Research 21:57-73.

Arnhold S, Heiduschka P, Klein H, Absenger Y, Basnaoglu S, Kreppel F, Henke-Fahle S, Kochanek S, Bartz-Schmidt KU, Addicks K, Schraermeyer U (2006) Adenovirally transduced bone marrow stromal cells differentiate into pigment epithelial cells and induce rescue effects in RCS rats. Investigative Ophthalmology & Visual Science 47:4121-4129.

Barnett NL, Pow DV (2000) Antisense knockdown of GLAST, a glial glutamate transporter, compromises retinal function. Investigative Ophthalmology & Visual Science 41:585-591.

Bayer AU, Mittag T, Cook P, Brodie SE, Podos SM, Maag K-P (1999) Comparisons of the amplitude size and the reproducity of three different electrodes to record the corneal flash electroretinogram in rodents. Documenta Ophthalmologica 98:233-246.

Beltran WA, Rohrer H, Aguirre GD (2005) Immunolocalization of ciliary neurotrophic factor receptor alpha (CNTFRalpha) in mammalian photoreceptor cells. Molecular Vision 11:232-244.

Beltran WA, Wen R, Acland GM, Aguirre GD (2007) Intravitreal injection of ciliary neurotrophic factor (CNTF) causes peripheral remodeling and does not prevent photoreceptor loss in canine RPGR mutant retina. Experimental Eye Research 84:753-771.

Bennett J, Duan D, Engelhardt JF, Maguire AM (1997) Real-time, noninvasive in vivo assessment of adeno-associated virus-mediated retinal transduction. Investigative Ophthalmology & Visual Science 38:2857-2863.

Birch D, Jacobs GH (1979) Spatial contrast sensitivity in albino and pigmented rats. Vision Research 19:933-937.

Bok D, Yasumura D, Matthes MT, Ruiz A, Duncan JL, Chappelow AV, Zolutukhin S, Hauswirth W, LaVail MM (2002) Effects of adeno-associated virus-vectored ciliary neurotrophic factor on retinal structure and function in mice with a P216L rds/peripherin mutation. Experimental Eye Research 74:719-735.

Bourne MC, Grüneberg H (1939) Degeneration of the retina and cataract, a new recessive gene in the rat. The Journal of Heredity 30:130-136.

Bourne MC, Campbell DA, Tansley K (1938a) Retinitis pigmentosa in rats.Trans Am Ophthalmol Soc. 58:234-245.

Bourne MC, Campbell DA, Tansley K (1938b) Hereditary degeneration of the rat retina. British Journal of Ophthalmology 22:613-623.

Bringmann A, Pannicke T, Grosche J, Francke M, Wiedemann P, Skatchkov SN, Osborne NN, Reichenbach A (2006) Muller cells in the healthy and diseased retina. Progress in Retinal and Eye Research 25:397-424.

Bush RA, Lei B, Tao W, Raz D, Chan CC, Cox TA, Santos-Muffley M, Sieving PA (2004) Encapsulated cell-based intraocular delivery of ciliary neurotrophic factor in normal rabbit: dose-dependent effects on ERG and retinal histology. Investigative Ophthalmology & Visual Science 45:2420-2430.

Byrne JA, Pedersen DA, Clepper LL, Nelson M, Sanger WG, Gokhale S, Wolf DP, Mitalipov SM (2007) Producing primate embryonic stem cells by somatic cell nuclear transfer. Nature 450:497-502.

Campochiaro PA, Nguyen QD, Shah SM, Klein ML, Holz E, Frank RN, Saperstein DA, Gupta A, Stout JT, Macko J, DiBartolomeo R, Wei LL (2006) Adenoviral vector-delivered pigment epithelium-derived factor for neovascular age-related macular degeneration: results of a phase I clinical trial. Human Gene Therapy 17:167-176.

Carwile ME, Culbert RB, Sturdivant RL, Kraft TW (1998) Rod outer segment maintenance is enhanced in the presence of bFGF, CNTF and GDNF. Experimental Eye Research 66:791-805.

Casaccia-Bonnefil P, Gu C, Chao MV (1999a) Neurotrophins in cell survival/death decisions. Advances in Experimental Medicine and Biology 468:275-282.

Casaccia-Bonnefil P, Gu C, Khursigara G, Chao MV (1999b) p75 neurotrophin receptor as a modulator of survival and death decisions. Microscopy Research and Technique 45:217-224.

Casella GT, Bunge RP, Wood PM (1996) Improved method for harvesting human Schwann cells from mature peripheral nerve and expansion in vitro. Glia 17:327-338.

Cayouette M, Gravel C (1997) Adenovirus-mediated gene transfer of ciliary neurotrophic factor can prevent photoreceptor degeneration in the retinal degeneration (*rd*) mouse. Human Gene Therapy 8:423-430.

Cayouette M, Smith SB, Becerra SP, Gravel C (1999) Pigment epithelium-derived factor delays the death of photoreceptors in mouse models of inherited retinal degenerations. Neurobiology of Disease 6:523-532.

Cayouette M, Behn D, Stendtner M, Lachapelle P, Gravel C (1998) Intraocular gene transfer of ciliary neurotrophic factor prevents death and increases responsiveness of rod photoreceptors in the retinal degeneration slow mouse. Journal of Neuroscience 18:9282-9293.

Chader GJ (2002) Animal models in research on retinal degenerations: past progress and future hope. Vision Research 42:393-399.

Chang B, Hawes NL, Pardue MT, German AM, Hurd RE, Davisson MT, Nusinowitz S, Rengarajan K, Boyd AP, Sidney SS, Phillips MJ, Stewart RE, Chaudhury R, Nickerson JM, Heckenlively JR, Boatright JH (2007) Two mouse retinal degenerations caused by missense mutations in the beta-subunit of rod cGMP phosphodiesterase gene. Vision Research 47:624-633.

Chklovskii DB, Mel BW, Svoboda K (2004) Cortical rewiring and information storage. Nature 431:782-788.

Chong NH, Alexander RA, Waters L, Barnett KC, Bird AC, Luthert PJ (1999) Repeated injections of a ciliary neurotrophic factor analogue leading to long-term photoreceptor survival in hereditary retinal degeneration. Investigative Ophthalmology & Visual Science 40:1298-1305.

Chong NHV, Waters L, Barnett KC, Bird AC, Luthert PJ (1997) Axokine delays photoreceptor cell death in rdy cats. Investigative Ophthalmology & Visual Science 39:S310.

Chu Y, Humphrey MF, Alder VV, Constable IJ (1998) Immunocytochemical localization of basic fibroblast growth factor and glial fibrillary acidic protein after laser photocoagulation in the Royal College of Surgeons rat. Australian and New Zealand Journal of Ophthalmology 26:87-96.

Cibis GW, Fitzgerald KM (2001) The negative ERG is not synonymous with nightblindness. Trans Am Ophthalmol Soc 99:171-175; discussion 175-176.

Cibis GW, Fitzgerald KM, Harris DJ, Rothberg PG, Rupani M (1993) The effects of dystrophin gene mutations on the ERG in mice and humans. Investigative Ophthalmology & Visual Science 34:3646-3652.

Coffey PJ, Girman S, Wang SM, Hetherington L, Keegan DJ, Adamson P, Greenwood J, Lund RD (2002) Long-term preservation of cortically dependent visual function in RCS rats by transplantation. Nature Neuroscience 5:53-56.

Cuenca N, Pinilla I, Sauve Y, Lund R (2005) Early changes in synaptic connectivity following progressive photoreceptor degeneration in RCS rats. The European Journal of Neuroscience 22:1057-1072.

Cuenca N, Pinilla I, Sauve Y, Lu B, Wang S, Lund RD (2004) Regressive and reactive changes in the connectivity patterns of rod and cone pathways of P23H transgenic rat retina. Neuroscience 127:301-317.

D'Cruz PM, Yasumura D, Weir J, Matthes MT, Abderrahim H, LaVail MM, Vollrath D (2000) Mutation of the receptor tyrosine kinase gene Mertk in the retinal dystrophic RCS rat. Human Molecular Genetics 9:645-651.

Dean P (1978) Visual acuity in hooded rats: effects of superior collicular or posterior neocortical lesions. Brain Research 156:17-31.

Dean P (1981) Visual pathways and acuity hooded rats. Behavioral Brain Research 3:239-271.

DiLoreto DA, Jr., del Cerro C, Cox C, del Cerro M (1998) Changes in visually guided behavior of Royal College of Surgeons rats as a function of age: a histologic, morphometric, and functional study. Investigative Ophthalmology & Visual Science 39:1058-1063.

Douglas RM, Neve A, Quittenbaum JP, Alam NM, Prusky GT (2006) Perception of visual motion coherence by rats and mice. Vision Research 46:2842-2847.

Douglas RM, Alam NM, Silver BD, McGill TJ, Tschetter WW, Prusky GT (2005) Independent visual threshold measurements in the two eyes of freely moving rats and mice using a virtual-reality optokinetic system. Visual Neuroscience 22:677-684.

Dowling JE, Sidman RL (1962) Inherited retinal dystrophy in the rat. The Journal of Cell Biology 14:73-109.

Dunn KC, Aotaki-Keen AE, Putkey FR, Hjelmeland LM (1996) ARPE-19, a human retinal pigment epithelial cell line with differentiated properties. Experimental Eye Research 62:155-169.

Edwards RB, Szamier RB (1977) Defective phagocytosis of isolated rod outer segments by RCS rat retinal pigment epithelium in culture. Science 197:1001-1003.

Effron JT, Szamier RB, Edwards RB (1981) Selective phagocytosis of liposomes by cultured RCS rat pigment epithelium. Investigative Ophthalmology & Visual Science 21:611-616.

Eliasieh K, Liets LC, Chalupa LM (2007) Cellular reorganization in the human retina during normal aging. Investigative Ophthalmology & Visual Science 48:2824-2830.

Erickson PA, Feinstein SC, Lewis GP, Fisher SK (1992) Glial fibrillary acidic protein and its mRNA: ultrastructural detection and determination of changes after CNS injury. Journal of Structural Biology 108:148-161.

Faktorovich EG, Steinberg RH, Yasumura D, Matthes MT, LaVail MM (1990) Photoreceptor degeneration in inherited retinal dystrophy delayed by basic fibroblast growth factor. Nature 347:83-86.

Faktorovich EG, Steinberg RH, Yasumura D, Matthes MT, LaVail MM (1992) Basic fibroblast growth factor and local injury protect photoreceptors from light damage in the rat. Journal of Neuroscience 12:3554-3567.

Farber DB, Lolley RN (1977) Light-induced reduction in cyclic GMP of retinal photoreceptor cells in vivo: abnormalities in the degenerative diseases of RCS rats and rd mice. Journal of Neurochemistry 28:1089-1095.

Fariss RN, Li ZY, Milam AH (2000) Abnormalities in rod photoreceptors, amacrine cells, and horizontal cells in human retinas with retinitis pigmentosa. American Journal of Ophthalmology 129:215-223.

Felsenfeld G, Boyes J, Chung J, Clark D, Studitsky V (1996) Chromatin structure and gene expression. Proceedings of the National Acadamy of Sciences U S A 93:9384-9388.

Fisher SK, Lewis GP (2003) Muller cell and neuronal remodeling in retinal detachment and reattachment and their potential consequences for visual recovery: a review and reconsideration of recent data. Vision Research 43:887-897.

Fisher SK, Lewis GP, Linberg KA, Verardo MR (2005) Cellular remodeling in mammalian retina: results from studies of experimental retinal detachment. Progress in Retinal and Eye Research 24:395-431.

Franze K, Grosche J, Skatchkov SN, Schinkinger S, Foja C, Schild D, Uckermann O, Travis K, Reichenbach A, Guck J (2007) Muller cells are living optical fibers in the vertebrate retina. Proceedings of the National Acadamy of Sciences U S A 104:8287-8292.

Frasson M, Picaud S, Leveillard T, Simonutti M, Mohand-Said S, Dreyfus H, Hicks D, Sahel J (1999) Glial cell line-derived neurotrophic factor induces histologic and functional protection of rod photoreceptors in the rd/rd mouse. Investigative Ophthalmology & Visual Science 40:2724-2734.

Gaillard F, Sauve Y (2007) Cell-based therapy for retina degeneration: the promise of a cure. Vision Research 47:2815-2824.

Gal A, Li Y, Thompson DA, Weir J, Orth U, Jacobson SG, Apfelstedt-Sylla E, Vollrath D (2000) Mutations in MERTK, the human orthologue of the RCS rat retinal dystrophy gene, cause retinitis pigmentosa. Nature Genetics 26:270-271.

Gamm DM, Wang S, Lu B, Girman S, Holmes T, Bischoff N, Shearer RL, Sauve Y, Capowski E, Svendsen CN, Lund RD (2007) Protection of visual functions by human neural progenitors in a rat model of retinal disease. PLoS ONE 2:e338.

Gartner S, Henkind P (1982) Pathology of retinitis pigmentosa. Ophthalmology 89:1425-1432.

Gehlbach P, Hose S, Lei B, Zhang C, Cano M, Arora M, Neal R, Barnstable C, Goldberg MF, Zigler JS, Jr., Sinha D (2006) Developmental abnormalities in the Nuc1 rat retina: a spontaneous mutation that affects neuronal and vascular remodeling and retinal function. Neuroscience 137:447-461.

Girman SV, Lund RD (2007) Most superficial sublamina of rat superior colliculus: neuronal response properties and correlates with perceptual figure-ground segregation. Journal of Neurophysiology 98:161-177.

Girman SV, Sauve Y, Lund RD (1999) Receptive field properties of single neurons in rat primary visual cortex. Journal of Neurophysiology 82:301-311.

Girman SV, Wang S, Lund RD (2005) Time course of deterioration of rod and cone function in RCS rat and the effects of subretinal cell grafting: a light- and dark-adaptation study. Vision Research 45:343-354.

Gorbatyuk M, Justilien V, Liu J, Hauswirth WW, Lewin AS (2007) Preservation of photoreceptor morphology and function in P23H rats using an allele independent ribozyme. Experimental Eye Research 84:44-52.

Goto Y, Peachey NS, Ripps H, Naash MI (1995) Functional abnormalities in transgenic mice expressing a mutant rhodopsin gene. Investigative Ophthalmology & Visual Science 36:62-71.

Green ES, Rendahl KG, Zhou S, Ladner M, Coyne M, Srivastava R, Manning WC, Flannery JG (2001) Two animal models of retinal degeneration are rescued by recombinant adeno-associated virus-mediated production of FGF-5 and FGF-18. Molecular Therapy 3:507-515.

Hammarberg H, Piehl F, Cullheim S, Fjell J, Hokfelt T, Fried K (1996) GDNF mRNA in Schwann cells and DRG satellite cells after chronic sciatic nerve injury. Neuroreport 7:857-860.

Harada T, Harada C, Kohsaka S, Wada E, Yoshida K, Ohno S, Mamada H, Tanaka K, Parada LF, Wada K (2002) Microglia-Muller glia cell interactions control neurotrophic factor production during light-induced retinal degeneration. Journal of Neuroscience 22:9228-9236.

Hasegawa Y, Yamagishi S, Fujitani M, Yamashita T (2004) p75 neurotrophin receptor signaling in the nervous system. Biotechnology Annual Review 10:123-149.

Hoffmann KP (1989) Control of the optokinetic reflex by the nucleus of the optic tract in primates. Progress in Brain Research 80:173-182; discussion 171-172.

Hoffmann KP, Distler C (1989) Quantitative analysis of visual receptive fields of neurons in nucleus of the optic tract and dorsal terminal nucleus of the accessory optic tract in macaque monkey. Journal of Neurophysiology 62:416-428.

Hosomi S, Yamashita T, Aoki M, Tohyama M (2003) The p75 receptor is required for BDNF-induced differentiation of neural precursor cells. Biochemical and Biophysical Research Communications 301:1011-1015.

Huang SP, Lin PK, Liu JH, Khor CN, Lee YJ (2004) Intraocular gene transfer of ciliary neurotrophic factor rescues photoreceptor degeneration in RCS rats. Journal of Biomedical Science 11:37-48.

Ilg UJ, Hoffmann KP (1996) Responses of neurons of the nucleus of the optic tract and the dorsal terminal nucleus of the accessory optic tract in the awake monkey. The European Journal of Neuroscience 8:92-105.

Inoue Y, Iriyama A, Ueno S, Takahashi H, Kondo M, Tamaki Y, Araie M, Yanagi Y (2007) Subretinal transplantation of bone marrow mesenchymal stem cells delays retinal degeneration in the RCS rat model of retinal degeneration. Experimental Eye Research 85:234-241.

Jacobs GH, Fenwick JA, Williams GA (2001) Cone-based vision of rats for ultraviolet and visible lights. The Journal of Experimental Biology 204:2439-2446.

Jacobson SG, Boye SL, Aleman TS, Conlon TJ, Zeiss CJ, Roman AJ, Cideciyan AV, Schwartz SB, Komaromy AM, Doobrajh M, Cheung AY, Sumaroka A, Pearce-Kelling SE, Aguirre GD, Kaushal S, Maguire AM, Flotte TR, Hauswirth WW (2006a) Safety in nonhuman primates of ocular AAV2-RPE65, a candidate treatment for blindness in Leber congenital amaurosis. Human Gene Therapy 17:845-858.

Jacobson SG, Acland GM, Aguirre GD, Aleman TS, Schwartz SB, Cideciyan AV, Zeiss CJ, Komaromy AM, Kaushal S, Roman AJ, Windsor EA, Sumaroka A, Pearce-Kelling SE, Conlon TJ, Chiodo VA, Boye SL, Flotte TR, Maguire AM, Bennett J, Hauswirth WW (2006b) Safety of recombinant adeno-associated virus type 2-RPE65 vector delivered by ocular subretinal injection. Molecular Therapy 13:1074-1084.

Jiang LQ, Jorquera M, Streilein JW, Ishioka M (1995) Unconventional rejection of neural retinal allografts implanted into the immunologically privileged site of the eye. Transplantation 59:1201-1207.

Jones BW, Marc RE (2005) Retinal remodeling during retinal degeneration. Experimental Eye Research 81:123-137.

Jones BW, Watt CB, Marc RE (2005) Retinal remodelling. Clinincial & Experimental Optomotry 88:282-291.

Jones BW, Watt CB, Frederick JM, Baehr W, Chen CK, Levine EM, Milam AH, Lavail MM, Marc RE (2003) Retinal remodeling triggered by photoreceptor degenerations. The Journal of Comparative Neurology 464:1-16.

Kalloniatis M, Fletcher EL (2004) Retinitis pigmentosa: understanding the clinical presentation, mechanisms and treatment options. Clinincial & Experimental Optomotry 87:65-80.

Kaplan HJ, Tezel TH, Berger AS, Wolf ML, Del Priore LV (1997) Human photoreceptor transplantation in retinitis pigmentosa. A safety study. Archives of Ophthalmology 115:1168-1172.

Karlsson M, Mayordomo R, Reichardt LF, Catsicas S, Karten H, Hallbook F (2001) Nerve growth factor is expressed by postmitotic avian retinal horizontal cells and

supports their survival during development in an autocrine mode of action. Development (Cambridge, England) 128:471-479.

Kashii S, Mandai M, Kikuchi M, Honda Y, Tamura Y, Kaneda K, Akaike A (1996) Dual actions of nitric oxide in N-methyl-D-aspartate receptor-mediated neurotoxicity in cultured retinal neurons. Brain Research 711:93-101.

Keegan DJ, Kenna P, Humphries MM, Humphries P, Flitcroft DI, Coffey PJ, Lund RD, Lawrence JM (2003) Transplantation of syngeneic Schwann cells to the retina of the rhodopsin knockout (rho(-/-)) mouse. Investigative Ophthalmology & Visual Science 44:3526-3532.

Keller J, Strasburger H, Cerutti DT, Sabel BA (2000) Assessing spatial vision - automated measurement of the contrast-sensitivity function in the hooded rat. Journal of Neuroscience Methods 97:103-110.

Kolb H, Gouras P (1974) Electron microscopic observations of human retinitis pigmentosa, dominantly inherited. Investigative Ophthalmology & Visual Science 13:487-498.

Kovalevsky G, DiLoreto D, Jr., Wyatt J, del Cerro C, Cox C, del Cerro M (1995) The intensity of the pupillary light reflex does not correlate with the number of retinal photoreceptor cells. Experimental Neurology 133:43-49.

Laeng P, Molthagen M, Yu EG, Bartsch U (1996) Transplantation of oligodendrocyte progenitor cells into the rat retina: extensive myelination of retinal ganglion cell axons. Glia 18:200-210.

Larsson J, Juliusson B, Ehinger B (1998) Survival and MHC-expression of embryonic retinal transplants in the choroid. Acta Ophthalmologica Scandinavica 76:417-421.

Larsson J, Juliusson B, Holmdahl R, Ehinger B (1999) MHC expression in syngeneic and allogeneic retinal cell transplants in the rat. Graefe's Archive for Clinical and Experimental Ophthalmology 237:82-85.

Lashley KS (1930) The mechanism of vision: I. A method for rapid analysis of pattern vision in the rat. Journal of General Psychology 37:453-460

Lau D, McGee LH, Zhou S, Rendahl KG, Manning WC, Escobedo JA, Flannery JG (2000) Retinal degeneration is slowed in transgenic rats by AAV-mediated delivery of FGF-2. Investigative Ophthalmology & Visual Science 41:3622-3633.

LaVail MM (1981) Photoreceptor characteristics in congenic strains of RCS rats. Investigative Ophthalmology & Visual Science 20:671-675.

LaVail MM, Battelle BA (1975) Influence of eye pigmentation and light deprivation on inherited retinal dystrophy in the rat. Experimental Eye Research 21:167-192.

LaVail MM, Sidman RL, Gerhardt CO (1975) Congenic strains of RCS rats with inherited retinal dystrophy. The Journal of Heredity 66:242-244.

LaVail MM, Pinto LH, Yasumura D (1981) The interphotoreceptor matrix in rats with inherited retinal dystrophy. Investigative Ophthalmology & Visual Science 21:658-668.

LaVail MM, Sidman M, Rausin R, Sidman RL (1974) Discrimination of light intensity by rats with inherited retinal degeneration: a behavioral and cytological study. Vision Research 14:693-702.

Lavail MM, Li L, Turner JE, Yasumura D (1992a) Retinal pigment epithelial cell transplantation in RCS rats: normal metabolism in rescued photoreceptors. Experimental Eye Research 55:555-562.

LaVail MM, Matthes MT, Yasumura D, Faktorovich EG, Steinberg RH (1997) Histological method to assess photoreceptor light damage and protection by survival factors. In: Degenerative Retinal Diseases (LaVail MM, Hollyfield JG, Anderson RE, eds), pp 369-384. New York: Plenum Press.

LaVail MM, Unoki K, Yasumura D, Matthes MT, Yancopoulos GD, Steinberg RH (1992b) Multiple growth factors, cytokines and neurotrophins rescue photoreceptors from the damaging effects of constant light. Proceedings of the National Acadamy of Sciences U S A 89:11249-11253.

LaVail MM, Yasumura D, Matthes MT, Lau-Villacorta C, Unoki K, Sung C-H, Steinberg RH (1998) Protection of mouse photoreceptors by survival factors in retinal degenerations. Investigative Ophthalmology & Visual Science 39:592-602.

Lawrence JM, Keegan DJ, Muir EM, Coffey PJ, Rogers JH, Wilby MJ, Fawcett JW, Lund RD (2004) Transplantation of Schwann cell line clones secreting GDNF or BDNF into the retinas of dystrophic Royal College of Surgeons rats. Investigative Ophthalmology & Visual Science 45:267-274.

Lawrence JM, Sauve Y, Keegan DJ, Coffey PJ, Hetherington L, Girman S, Whiteley SJ, Kwan AS, Pheby T, Lund RD (2000) Schwann cell grafting into the retina of the dystrophic RCS rat limits functional deterioration. Royal College of Surgeons. Investigative Ophthalmology & Visual Science 41:518-528.

Lehrman S (1999) Virus treatment questioned after gene therapy death. Nature 401:517-518.

Leveillard T, Mohand-Said S, Lorentz O, Hicks D, Fintz AC, Clerin E, Simonutti M, Forster V, Cavusoglu N, Chalmel F, Dolle P, Poch O, Lambrou G, Sahel JA (2004) Identification and characterization of rod-derived cone viability factor. Nature Genetics 36:755-759.

Lewin AS, Drenser KA, Hauswirth WW, Nishikawa S, Yasumura D, Flannery JG, LaVail MM (1998) Ribozyme rescue of photoreceptor cells in a transgenic rat model of autosomal dominant retinitis pigmentosa. Nature Medicine 4:967-971.

Lewis GP, Charteris DG, Sethi CS, Fisher SK (2002) Animal models of retinal detachment and reattachment: identifying cellular events that may affect visual recovery. Eye (London, England) 16:375-387.

Li LX, Turner JE (1988) Transplantation of retinal pigment epithelial cells to immature and adult rat hosts: short- and long-term survival characteristics. Experimental Eye Research 47:771-785.

Liang FQ, Aleman TS, Dejneka NS, Dudus L, Fisher KJ, Maguire AM, Jacobson SG, Bennett J (2001a) Long-term protection of retinal structure but not function using RAAV.CNTF in animal models of retinitis pigmentosa. Molecular Therapy 4:461-472.

Liang FQ, Dejneka NS, Cohen DR, Krasnoperova NV, Lem J, Maguire AM, Dudus L, Fisher KJ, Bennett J (2001b) AAV-mediated delivery of ciliary neurotrophic factor prolongs photoreceptor survival in the rhodopsin knockout mouse. Molecular Therapy 3:241-248.

Liu C, Peng M, Laties AM, Wen R (1998) Preconditioning with bright light evokes a protective response against light damage in the rat retina. Journal of Neuroscience 18:1337-1344.

Liu C, Li Y, Peng M, Laties AM, Wen R (1999) Activation of caspase-3 in the retina of transgenic rats with the rhodopsin mutation S334ter during photoreceptor degeneration. Journal of Neuroscience 19:4778-4785.

Lolley RN, Farber DB (1976) A proposed link between debris accumulation, guanosine 3', 5' cyclic monophosphate changes and photoreceptor cell degeneration in retina of RCS rats. Experimental Eye Research 22:477-486.

Lopez R, Gouras P, Brittis M, Kjeldbye H (1987) Transplantation of cultured rabbit retinal epithelium to rabbit retina using a closed-eye method. Investigative Ophthalmology & Visual Science 28:1131-1137.

Lowenstein DH, Seren MS, Longo FM (1993) Prolonged increases in neurotrophic activity associated with kainate-induced hippocampal synaptic reorganization. Neuroscience 56:597-604.

Lue CL (1994) Rod cell activity in retinal degenerative rats. Journal of the Formosan Medical Association = Taiwan yi zhi 93:605-610.

Lund RD, Wang S, Klimanskaya I, Holmes T, Ramos-Kelsey R, Lu B, Girman S, Bischoff N, Sauve Y, Lanza R (2006) Human embryonic stem cell-derived cells rescue visual function in dystrophic RCS rats. Cloning and Stem Cells 8:189-199.

Lund RD, Adamson P, Sauve Y, Keegan DJ, Girman SV, Wang S, Winton H, Kanuga N, Kwan AS, Beauchene L, Zerbib A, Hetherington L, Couraud PO, Coffey P, Greenwood J (2001) Subretinal transplantation of genetically modified human cell lines attenuates loss of visual function in dystrophic rats. Proceedings of the National Acadamy of Sciences U S A 98:9942-9947.

Machida S, Kondo M, Jamison JA, Khan NW, Kononen LT, Sugawara T, Bush RA, Sieving PA (2000) P23H rhodopsin transgenic rat: correlation of retinal function with histopathology. Investigative Ophthalmology & Visual Science 41:3200-3209.

Machida S, Chaudhry P, Shinohara T, Singh DP, Reddy VN, Chylack LT, Jr., Sieving PA, Bush RA (2001) Lens epithelium-derived growth factor promotes photoreceptor survival in light-damaged and RCS rats. Investigative Ophthalmology & Visual Science 42:1087-1095.

Maclaren RE, Pearson RA (2007) Stem cell therapy and the retina. Eye (London, England) 21:1352-1359.

Marc RE, Jones BW, Watt CB, Strettoi E (2003) Neural remodeling in retinal degeneration. Progress in Retinal and Eye Research 22:607-655.

Marc RE, Jones BW, Anderson JR, Kinard K, Marshak DW, Wilson JH, Wensel T, Lucas RJ (2007) Neural reprogramming in retinal degeneration. Investigative Ophthalmology & Visual Science 48:3364-3371.

Masiakowski P, Liu H, Radziejewski C, Lottspeich F, Oberthuer W, Wong V, Lindsay RM, Furth ME, Panayotatos N (1991) Recombinant human and rat ciliary neurotrophic factors. Journal of Neurochemistry 57:1003-1012.

McGee Sanftner LH, Abel H, Hauswirth WW, Flannery JG (2001) Glial cell line derived neurotrophic factor delays photoreceptor degeneration in a transgenic rat model of retinitis pigmentosa. Molecular Therapy 4:622-629.

McGill TJ, Douglas RM, Lund RD, Prusky GT (2004a) Quantification of spatial vision in the Royal College of Surgeons rat. Investigative Ophthalmology & Visual Science 45:932-936.

McGill TJ, Lund RD, Douglas RM, Wang S, Lu B, Prusky GT (2004b) Preservation of vision following cell-based therapies in a model of retinal degenerative disease. Vision Research 44:2559-2566.

McGill TJ, Lund RD, Douglas RM, Wang S, Lu B, Silver BD, Secretan MR, Arthur JN, Prusky GT (2007a) Syngeneic Schwann cell transplantation preserves vision in RCS rat without immunosuppression. Investigative Ophthalmology & Visual Science 48:1906-1912.

McGill TJ, Prusky GT, Douglas RM, Yasumura D, Matthes MT, Nune G, Donahue-Rolfe K, Yang H, Niculescu D, Hauswirth W, Girman S, Lund R, Duncan JL, LaVail MM (2007b) Intraocular CNTF Reduces Vision in Normal Rats in a Dose-Dependent Manner. Investigative Ophthalmology & Visual Science 48:5756-5766.

Michon JJ, Li ZL, Shioura N, Anderson RJ, Tso MOM (1991) A comparative study of methods of photoreceptor morphometry. Investigative Ophthalmology & Visual Science 32:280-284.

Milam AH, Li ZY, Fariss RN (1998) Histopathology of the human retina in retinitis pigmentosa. Progress in Retinal and Eye Research 17:175-205.

Milam AH, Li ZY, Cideciyan AV, Jacobson SG (1996) Clinicopathologic effects of the Q64ter rhodopsin mutation in retinitis pigmentosa. Investigative Ophthalmology & Visual Science 37:753-765.

Min SH, Molday LL, Seeliger MW, Dinculescu A, Timmers AM, Janssen A, Tonagel F, Tanimoto N, Weber BH, Molday RS, Hauswirth WW (2005) Prolonged recovery of retinal structure/function after gene therapy in an Rs1h-deficient mouse model of x-linked juvenile retinoschisis. Molecular Therapy 12:644-651.

Mullen RJ, LaVail MM (1976) Inherited retinal dystrophy: primary defect in pigment epithelium determined with experimental rat chimeras. Science (New York, NY 192:799-801.

Neuberger TJ, De Vries GH (1993) Distribution of fibroblast growth factor in cultured dorsal root ganglion neurons and Schwann cells. II. Redistribution after neural injury. Journal of Neurocytology 22:449-460.

Newman E, Reichenbach A (1996) The Muller cell: a functional element of the retina. Trends in Neurosciences 19:307-312.

Ogilvie JM, Speck JD, Lett JM (2000) Growth factors in combination, but not individually, rescue rd mouse photoreceptors in organ culture. Experimental Neurology 161:676-685.

Pang JJ, Chang B, Kumar A, Nusinowitz S, Noorwez SM, Li J, Rani A, Foster TC, Chiodo VA, Doyle T, Li H, Malhotra R, Teusner JT, McDowell JH, Min SH, Li Q, Kaushal S, Hauswirth WW (2006) Gene therapy restores vision-dependent behavior as well as retinal structure and function in a mouse model of RPE65 Leber congenital amaurosis. Molecular Therapy 13:565-572.

Pannicke T, Fischer W, Biedermann B, Schadlich H, Grosche J, Faude F, Wiedemann P, Allgaier C, Illes P, Burnstock G, Reichenbach A (2000) P2X7 receptors in Muller glial cells from the human retina. Journal of Neuroscience 20:5965-5972.

Paskowitz DM, Nune G, Yasumura D, Yang H, Bhisitkul RB, Sharma S, Matthes MT, Zarbin MA, LaVail MM, Duncan JL (2004) BDNF reduces the retinal toxicity of verteporfin photodynamic therapy. Investigative Ophthalmology & Visual Science 45:4190-4196.

Pavlidis M, Fischer D, Thanos S (2000) Photoreceptor degeneration in the RCS rat attenuates dendritic transport and axonal regeneration of ganglion cells. Investigative Ophthalmology & Visual Science 41:2318-2328.

Pearce-Kelling S, Acland G, Laties A, Cedarbaum J, Aguirre G (1998) Survival factors slow inherited retinal degeneration in the *RCD1* and *ERD* dog models. Investigative Ophthalmology & Visual Science 39:S571.

Perlman I (1978a) Dark-adaptation in abnormal (RCS) rats studied electroretinographically. The Journal of Physiology 278:161-175.

Perlman I (1978b) Kinetics of bleaching and regeneration of rhodopsin in abnormal (RCS) and normal albino rats in vivo. The Journal of Physiology 278:141-159.

Peterson WM, Wang Q, Tzekova R, Wiegand SJ (2000) Ciliary neurotrophic factor and stress stimuli activate the Jak-STAT pathway in retinal neurons and glia. Journal of Neuroscience 20:4081-4090.

Pinilla I, Lund RD, Sauve Y (2004) Contribution of rod and cone pathways to the dark-adapted electroretinogram (ERG) b-wave following retinal degeneration in RCS rats. Vision Research 44:2467-2474.

Pinilla I, Lund RD, Sauve Y (2005a) Cone function studied with flicker electroretinogram during progressive retinal degeneration in RCS rats. Experimental Eye Research 80:51-59.

Pinilla I, Lund RD, Lu B, Sauve Y (2005b) Measuring the cone contribution to the ERG b-wave to assess function and predict anatomical rescue in RCS rats. Vision Research 45:635-641.

Pinilla I, Cuenca N, Sauve Y, Wang S, Lund RD (2007) Preservation of outer retina and its synaptic connectivity following subretinal injections of human RPE cells in the Royal College of Surgeons rat. Experimental Eye Research 85:381-392.

Prusky GT, Douglas RM (2003) Developmental plasticity of mouse visual acuity. The European Journal of Neuroscience 17:167-173.

Prusky GT, Douglas RM (2004) Characterization of mouse cortical spatial vision. Vision Research 44:3411-3418.

Prusky GT, West PW, Douglas RM (2000a) Behavioral assessment of visual acuity in mice and rats. Vision Research 40:2201-2209.

Prusky GT, Reidel C, Douglas RM (2000b) Environmental enrichment from birth enhances visual acuity but not place learning in mice. Behavioral Brain Research 114:11-15.

Prusky GT, West PW, Douglas RM (2000c) Reduced visual acuity impairs place but not cued learning in the Morris water task. Behavioral Brain Research 116:135-140.

Prusky GT, West PW, Douglas RM (2000d) Experience-dependent plasticity of visual acuity in rats. The European Journal of Neuroscience 12:3781-3786.

Prusky GT, Alam NM, Douglas RM (2006) Enhancement of vision by monocular deprivation in adult mice. Journal of Neuroscience 26:11554-11561.

Prusky GT, Harker KT, Douglas RM, Whishaw IQ (2002) Variation in visual acuity within pigmented, and between pigmented and albino rat strains. Behavioral Brain Research 136:339-348.

Prusky GT, Alam NM, Beekman S, Douglas RM (2004a) Rapid quantification of adult and developing mouse spatial vision using a virtual optomotor system. Investigative Ophthalmology & Visual Science 45:4611-4616.

Prusky GT, Douglas RM, Nelson L, Shabanpoor A, Sutherland RJ (2004b) Visual memory task for rats reveals an essential role for hippocampus and perirhinal cortex. Proceedings of the National Acadamy of Sciences U S A 101:5064-5068.

Prusky GT, Silver BD, Tschetter WW, Alam NM, Douglas RM (2008) Experience-dependent enhancement of vision from eye opening is maintained with iterative critical period experience. . Jounal of Neuroscience (in press).

Radtke ND, Aramant RB, Seiler MJ, Petry HM, Pidwell D (2004) Vision change after sheet transplant of fetal retina with retinal pigment epithelium to a patient with retinitis pigmentosa. Archives of Ophthalmology 122:1159-1165.

Rasmussen H, Chu KW, Campochiaro P, Gehlbach PL, Haller JA, Handa JT, Nguyen QD, Sung JU (2001) Clinical protocol. An open-label, phase I, single administration, dose-escalation study of ADGVPEDF.11D (ADPEDF) in neovascular age-related macular degeneration (AMD). Human Gene Therapy 12:2029-2032.

Reber A, Sarrau JM, Carnet J, Magnin M, Stelz T (1991) Horizontal optokinetic nystagmus in unilaterally enucleated pigmented rats: role of the pretectal commissural fibers. The Journal of Comparative Neurology 313:604-612.

Represa A, Ben-Ari Y (1992) Long-term potentiation and sprouting of mossy fibers produced by brief episodes of hyperactivity. Epilepsy Research 7:261-269.

Rhee KD, Goureau O, Chen S, Yang XJ (2004) Cytokine-induced activation of signal transducer and activator of transcription in photoreceptor precursors regulates rod differentiation in the developing mouse retina. Journal of Neuroscience 24:9779-9788.

Rhee KD, Ruiz A, Duncan JL, Hauswirth WW, LaVail MM, Bok D, Yang X-J (2007) Molecular and cellular alterations induced by sustained expression of ciliary neurotrophic factor in a mouse model of retinitis pigmentosa. Investigative Ophthalmology & Visual Science 48:1389-1400.

Rivolta C, Sharon D, DeAngelis MM, Dryja TP (2002) Retinitis pigmentosa and allied diseases: numerous diseases, genes, and inheritance patterns. Human Molecular Genetics 11:1219-1227.

Rubin GR, Kraft TW (2007) Flicker assessment of rod and cone function in a model of retinal degeneration. Documenta Ophthalmologica 115:165-172.

Sagdullaev BT, Aramant RB, Seiler MJ, Woch G, McCall MA (2003) Retinal transplantation-induced recovery of retinotectal visual function in a rodent model of retinitis pigmentosa. Investigative Ophthalmology & Visual Science 44:1686-1695.

Saggio I, Gloaguen I, Poiana G, Laufer R (1995) CNTF variants with increased biological potency and receptor selectivity define a functional site of receptor interaction. EMBO Journal 14:3045-3054.

Sauve Y, Lu B, Lund RD (2004) The relationship between full field electroretinogram and perimetry-like visual thresholds in RCS rats during photoreceptor degeneration and rescue by cell transplants. Vision Research 44:9-18.

Sauve Y, Pinilla I, Lund RD (2006) Partial preservation of rod and cone ERG function following subretinal injection of ARPE-19 cells in RCS rats. Vision Research 46:1459-1472.

Sauve Y, Girman SV, Wang S, Lawrence JM, Lund RD (2001) Progressive visual sensitivity loss in the Royal College of Surgeons rat: perimetric study in the superior colliculus. Neuroscience 103:51-63.

Sauve Y, Girman SV, Wang S, Keegan DJ, Lund RD (2002) Preservation of visual responsiveness in the superior colliculus of RCS rats after retinal pigment epithelium cell transplantation. Neuroscience 114:389-401.

Schiff D, Cohen B, Raphan T (1988) Nystagmus induced by stimulation of the nucleus of the optic tract in the monkey. Experimental Brain Research 70:1-14.

Schlichtenbrede FC, MacNeil A, Bainbridge JW, Tschernutter M, Thrasher AJ, Smith AJ, Ali RR (2003) Intraocular gene delivery of ciliary neurotrophic factor results in significant loss of retinal function in normal mice and in the $Prph2^{Rd2/Rd2}$ model of retinal degeneration. Gene Therapy 10:523-527.

Schmidt M, Zhang HY, Hoffmann KP (1993) OKN-related neurons in the rat nucleus of the optic tract and dorsal terminal nucleus of the accessory optic system receive a direct cortical input. The Journal of Comparative Neurology 330:147-157.

Schraermeyer U, Kociok N, Heimann K (1999) Rescue effects of IPE transplants in RCS rats: short-term results. Investigative Ophthalmology & Visual Science 40:1545-1556.

Schraermeyer U, Kayatz P, Thumann G, Luther TT, Szurman P, Kociok N, Bartz-Schmidt KU (2000) Transplantation of iris pigment epithelium into the choroid slows down the degeneration of photoreceptors in the RCS rat. Graefe's archive for Clinical and Experimental Ophthalmology 238:979-984.

Seiler MJ, Aramant RB (1998) Intact sheets of fetal retina transplanted to restore damaged rat retinas. Investigative Ophthalmology & Visual Science 39:2121-2131.

Seiler MJ, Aramant RB (2005) Transplantation of neuroblastic progenitor cells as a sheet preserves and restores retinal function. Seminars in Ophthalmology 20:31-42.

Seiler MJ, Sagdullaev BT, Woch G, Thomas BB, Aramant RB (2005) Transsynaptic virus tracing from host brain to subretinal transplants. The European Journal of Neuroscience 21:161-172.

Seiler MJ, Thomas BB, Chen Z, Arai S, Chadalavada S, Mahoney MJ, Sadda SR, Aramant RB (2007) BDNF-treated retinal progenitor sheets transplanted to degenerate rats: Improved restoration of visual function. Experimental Eye Research.

Sendtner M, Stockli KA, Thoenen H (1992) Synthesis and localization of ciliary neurotrophic factor in the sciatic nerve of the adult rat after lesion and during regeneration. The Journal of Cell Biology 118:139-148.

Sethi CS, Lewis GP, Fisher SK, Leitner WP, Mann DL, Luthert PJ, Charteris DG (2005) Glial remodeling and neural plasticity in human retinal detachment with

proliferative vitreoretinopathy. Investigative Ophthalmology & Visual Science 46:329-342.

Seymoure P, Juraska JM (1997) Vernier and grating acuity in adult hooded rats: the influence of sex. Behavioral Neuroscience 111:792-800.

Sieving PA, Caruso RC, Tao W, Coleman HR, Thompson DJ, Fullmer KR, Bush RA (2006) Ciliary neurotrophic factor (CNTF) for human retinal degeneration: phase I trial of CNTF delivered by encapsulated cell intraocular implants. Proceedings of the National Academy of Sciences U S A 103:3896-3901.

Silverman MS, Hughes SE (1990) Photoreceptor rescue in the RCS rat without pigment epithelium transplantation. Current Eye Research 9:183-191.

Steinberg RH, Flannery JG, Naash MI, Chen J, Matthes MT, Yasumura D, LaVail MM (1996) Transgenic rat models of inherited retinal degeneration caused by mutant opsin genes. Investigative Ophthalmology & Visual Science 37.

Strettoi E, Pignatelli V (2000) Modifications of retinal neurons in a mouse model of retinitis pigmentosa. Proceedings of the National Academy of Sciences U S A 97:11020-11025.

Strettoi E, Porciatti V, Falsini B, Pignatelli V, Rossi C (2002) Morphological and functional abnormalities in the inner retina of the rd/rd mouse. Journal of Neuroscience 22:5492-5504.

Strettoi E, Pignatelli V, Rossi C, Porciatti V, Falsini B (2003) Remodeling of second-order neurons in the retina of rd/rd mutant mice. Vision Research 43:867-877.

Sullivan R, Penfold P, Pow DV (2003) Neuronal migration and glial remodeling in degenerating retinas of aged rats and in nonneovascular AMD. Investigative Ophthalmology & Visual Science 44:856-865.

Sullivan RK, Woldemussie E, Pow DV (2007) Dendritic and synaptic plasticity of neurons in the human age-related macular degeneration retina. Investigative Ophthalmology & Visual Science 48:2782-2791.

Tao W, Wen R, Goddard MB, Sherman SD, O'Rourke PJ, Stabila PF, Bell WJ, Dean BJ, Kauper KA, Budz VA, Tsiaras WG, Acland GM, Pearce-Kelling S, Laties AM, Aguirre GD (2002) Encapsulated cell-based delivery of CNTF reduces photoreceptor degeneration in animal models of retinitis pigmentosa. Investigative Ophthalmology & Visual Science 43:3292-3298.

Thomas BB, Seiler MJ, Sadda SR, Coffey PJ, Aramant RB (2004) Optokinetic test to evaluate visual acuity of each eye independently. Journal of Neuroscience Methods 138:7-13.

Trejo LJ, Cicerone CM (1982) Retinal sensitivity measured by the pupillary light reflex in RCS and albino rats. Vision Research 22:1163-1171.

Trejo LJ, Cicerone CM (1987) Changes in visual sensitivity with age in rats with heredity retinal degeneration. Vision Research 27:915-918.

Villegas-Perez MP, Lawrence JM, Vidal-Sanz M, Lavail MM, Lund RD (1998) Ganglion cell loss in RCS rat retina: a result of compression of axons by contracting intraretinal vessels linked to the pigment epithelium. The Journal of Comparative Neurology 392:58-77.

Vollrath D, Feng W, Duncan JL, Yasumura D, D'Cruz PM, Chappelow A, Matthes MT, Kay MA, LaVail MM (2001) Correction of the retinal dystrophy phenotype of the

RCS rat by viral gene transfer of Mertk. Proceedings of the National Academy of Sciences U S A 98:12584-12589.

Wahlin KJ, Campochiaro PA, Zack DJ, Adler R (2000) Neurotrophic factors cause activation of intracellular signaling pathways in Muller cells and other cells of the inner retina, but not photoreceptors. Investigative Ophthalmology & Visual Science 41:927-936.

Wang F, Xia X, Hu H, Li L, Tian Y, Chen X, Huang Q (2002) Liposome-mediated gene transfer into retina. Zhonghua Yan Ke Za Zhi 38:520-522.

Wang S, Lu B, Lund RD (2005a) Morphological changes in the Royal College of Surgeons rat retina during photoreceptor degeneration and after cell-based therapy. The Journal of Comparative Neurology 491:400-417.

Wang S, Lu B, Wood P, Lund RD (2005b) Grafting of ARPE-19 and Schwann cells to the subretinal space in RCS rats. Investigative Ophthalmology & Visual Science 46:2552-2560.

Wang S, Lu B, Girman S, Holmes T, Bischoff N, Lund R (2008) Morphological and functional rescue in RCS rats after RPE cell line transplantation at a later stage of degeneration. in press.

Wang S, Villegas-Perez MP, Holmes T, Lawrence JM, Vidal-Sanz M, Hurtado-Montalban N, Lund RD (2003) Evolving neurovascular relationships in the RCS rat with age. Current Eye Research 27:183-196.

Wecker JR, Ison JR (1986) Visual function measured by reflex modification in rats with inherited retinal dystrophy. Behavioral Neuroscience 100:679-684.

Wen R, Song Y, Cheng T, Matthes MT, Yasumura D, LaVail MM, Steinberg RH (1995) Injury-induced upregulation of bFGF and CNTF mRNAS in the rat retina. Journal of Neuroscience 15:7377-7385.

Wen R, Song Y, Kjellstrom S, Tanikawa A, Liu Y, Li Y, Zhao L, Bush RA, Laties AM, Sieving PA (2006) Regulation of rod phototransduction machinery by ciliary neurotrophic factor. Journal of Neuroscience 26:13523-13530.

Whiteley SJ, Klassen H, Coffey PJ, Young MJ (2001) Photoreceptor rescue after low-dose intravitreal IL-1beta injection in the RCS rat. Experimental Eye Research 73:557-568.

Williams GA, Daigle KA, Jacobs GH (2005) Rod and cone function in coneless mice. Visual Neuroscience 22:807-816.

Woch G, Aramant RB, Seiler MJ, Sagdullaev BT, McCall MA (2001) Retinal transplants restore visually evoked responses in rats with photoreceptor degeneration. Investigative Ophthalmology & Visual Science 42:1669-1676.

Xu L, Ball SL, Alexander KR, Peachey NS (2003) Pharmacological analysis of the rat cone electroretinogram. Visual Neuroscience 20:297-306.

Yamashita T, Tucker KL, Barde YA (1999) Neurotrophin binding to the p75 receptor modulates Rho activity and axonal outgrowth. Neuron 24:585-593.

Ying S, Jansen HT, Lehman MN, Fong SL, Kao WW (2000) Retinal degeneration in cone photoreceptor cell-ablated transgenic mice. Molecular Vision 6:101-108.

Yorston D, Yang YF, Sullivan PM (2005) Retinal detachment following surgery for congenital cataract: presentation and outcomes. Eye (London, England) 19:317-321.

References

Yu J, Vodyanik MA, Smuga-Otto K, Antosiewicz-Bourget J, Frane JL, Tian S, Nie J, Jonsdottir GA, Ruotti V, Stewart R, Slukvin, II, Thomson JA (2007) Induced Pluripotent Stem Cell Lines Derived from Human Somatic Cells. Science (New York, NY.

Zeiss CJ, Allore HG, Towle V, Tao W (2006) CNTF induces dose-dependent alterations in retinal morphology in normal and rcd-1 canine retina. Experimental Eye Research 82:395-404.

Appendix A: Published graduate work

Papers:

6) T.J. McGill, M.M. LaVail, D. Yasumura, K.M. Donohue-Rolfe, M.T. Matthes, R.J. Lowe, R.M. Douglas, J.L. Duncan, G.T. Prusky (2007). Discrepant anatomical, electrophysiolgical, and behavioral profiles of retinal degeneration in rat models of retinal degenerative disease. In Preparation.

5) T.J. McGill, G.T. Prusky, R.M. Douglas, D. Yasumura, M.T. Matthes, G. Nune, K. Donohue-Rolf, H. Yang, D. Niculescu, W.W. Hauswirth, J.L. Duncan, M.M. LaVail. Intraocular CNTF Reduces Vision in Normal Rats in a Dose Dependent Manner. Invest Ophthalmol Vis Sci. 2007. Dec. 48: 5756-5766.

4) McGill TJ, Lund RD, Douglas RM, Wang S, Lu B, Silver BD, Secretan MR, Arthur JN, Prusky GT. Syngeneic Schwann cell transplantation preserves vision in the RCS rat without immune suppression. Invest Ophthalmol Vis Sci. 2007 Apr;48(4):1906-12.

3) Douglas RM, Alam NM, Silver BD, McGill TJ, Tschetter WW, Prusky GT. Independent visual threshold measurements in the two eyes of freely-moving rats and mice using a virtual-reality optokinetic system. Visual Neurosience. 2005;22(5): 677-684.

2) T.J. McGill, R.D. Lund, B.Lu, S. Wang, R.M. Douglas, G.T. Prusky. Preservation of Vision Following Cell-Based Therapies in an Model of Retinal Degenerative Disease.(2004) Vision Research 44, 2559-2566.

1) T.J. McGill, B.Lu, R.M. Douglas, R.D. Lund,G.T. Prusky. Quantification of spatial vision in the RCS rat. Investigative Ophthalmology and Visual Science. (2004) 45, 932-936.

Abstracts:

10) T.J. McGill, G.T. Prusky, M.M. LaVail, G. Luna, S.K. Fisher, G.P. Lewis. (2008). Early Retinal Reorganization may Cause Visual Abnormalities in Rhodopsin Transgenic Rats. ARVO program number 2987/A328.

9) T.J. McGill, M.M. LaVail, D. Yasumura, K.M. Donohue-Rolfe, M.T. Matthes, R.J. Lowe, R.M. Douglas, J.L. Duncan, G.T. Prusky (2007). Discrepant anatomical, electrophysiolgical, and behavioral profiles of retinal degeneration in rat models of retinal degenerative disease. ARVO program 382/B712.

8) T.J. McGill, G.T. Prusky, D. Yasumura, K.M. Donohue-Rolfe, M.T. Matthes, G.C. Nune, D. Niculescu, W.W. Hauswirth, J.L. Duncan, M.M. LaVail (2006). Visual Thresholds and ERG Amplitudes are Impaired by Intraocular Delivery of CNTF. ARVO program 4815/B73.

7) T.J.McGill; R.D.Lund; R.M.Douglas; L.Bin; S.Wang; B.D.Silver; G.T.Prusky. (2005) Subretinal Syngeneic and Allogeneic rat Schwann Cell Transplants Preserve Vision in Dystrophic RCS rat. SFN program 977.5.

6) McGill, TJ. & Prusky, GT. (2005). Preservation of vision following retinal Schwann cell transplants in a model of retinal degenerative disease. Spring Conference on Behaviour and Brain, Fernie, B.C., Canada, February 24-26.

5) T.J.McGill; N.M.Alam; B.D.Silver; R.M.Douglas; G.T.Prusky. (2005) Independant Measures of Visual Function in each eye of the Rat and Mouse using Directional Optomotor Responses. SFN program 866.13.

4) McGill, TJ. & Prusky, GT. (2004). Schwann cell transplants delay blinding in RCS rat. Spring Conference on Behaviour and Brain, Fernie, B.C., Canada February 12-14.

3) T.J. McGill; G.T. Prusky; B. Lu; R.M. Douglas; R.D. Lund. (2003) Preservation of Vision in Dystrophic RCS Rats with Human Schwann cell Retinal Transplants. SFN Program 5046

2) G.T. Prusky, T.J. McGill, B.Lu, R.M. Douglas, R.D. Lund. Retinal Pigment Epithelial Cell Transplantation Limits the Loss of Vision Resulting From Retinal Degeneration. (2003) ARVO Program 512/B487.

1) McGill, T. & Prusky, G.T. (2003). Retinal transplantation limits the loss of visual function in a rat model of human retinal degenerative disease. Spring Conference on Behaviour and Brain, Fernie, B.C, Canada, February 18-20.